



UNIVERSITÀ DEGLI STUDI DI SALERNO



UNIVERSITÀ DEGLI STUDI DI SALERNO
Dipartimento di Farmacia

PhD Program
in **Drug Discovery and Development**
XXXI Cycle — Academic Year 2018/2019

PhD Thesis in

*Valorization of typical agricultural
productions and related biomasses as
sources of bioactive compounds*

Candidate

Alfredo Bottone

Supervisor

Prof. *Sonia Piacente*

PhD Program Coordinator: Prof. Dr. *Gianluca Sbardella*

Index

Introduction	1
Chapter 1	
Metabolite profiling of PDO <i>Opuntia ficus indica</i> Mill. flowers	11
1.1 Introduction	13
1.2 Results and discussion	16
1.2.1 Antioxidant activity and LC-ESI/LTQOrbitrap/MS/MS analysis	16
1.2.2 Isolation and characterization of phenolics from the EtOH/H ₂ O extract of <i>O. ficus indica</i> flowers	18
1.2.3 Quantitative analysis of the EtOH/H ₂ O extract of <i>O. ficus indica</i> Mill. cv. Sulfarina flowers	26
1.3 Conclusions	28
1.4 Experimental section.....	29
1.5 References	31
Chapter 2	
Phytochemical investigation of PDO <i>Ficus carica</i> L. cv. Dottato leaves	35
2.1 Introduction	37
2.2 Results and discussion	39
2.2.1 LC-ESI/LTQOrbitrap/MS/MS metabolite profiling of the MeOH extract of <i>F. carica</i> cv. Dottato leaves.....	39
2.2.2 Isolation and characterization.....	43
2.2.3 Coumarins	51
2.2.4 “Eco-friendly” extractions and comparison of their chemical composition by LC-ESI/LTQOrbitrap/MS experiments	53
2.2.5 Total phenolic content and radical scavenging activity of the different extracts of <i>F. carica</i> cv. Dottato leaves	55
2.3 Conclusions	56
2.4 Experimental section.....	56
2.5 References	59
Chapter 3	
Polar constituents, multi-class polar lipids and free fatty acids profiling of almonds (<i>Prunus dulcis</i> Mill. cvs. Toritto and Avola) by LC-ESI/HRMS/MS and GC-FID	65
3.1 Introduction	67
3.2 LC-ESI/LTQOrbitrap/MS/MS based approach for a quick and exhaustive metabolite screening of the polar constituents of the <i>P. dulcis</i> cv. Toritto seeds.....	69
3.2.1 Results and discussion	69
3.2.1.1 LC-ESI/HRMS/MS profiling of almond kernels	69
3.2.1.2 “Eco-friendly” extractions of <i>P. dulcis</i> cv. Toritto seeds.....	73
3.2.1.3 Catechins and proanthocyanidins	74

3.2.1.4 Almond peeling main product and by-products metabolite profiling	78
3.2.1.5 Comparison of the MeOH extracts chemical composition of <i>P. dulcis</i> seeds cvs. Toritto and Avola	80
3.2.1.6 Peeling process by-products showed good phenolic content and radical scavenging activity	82
3.3 LC-ESI/QToF/MS/MS multi-class polar lipids profiling of <i>P. dulcis</i> seeds (cvs. Toritto and Avola)	84
3.3.1 Results and discussion	84
3.3.1.1 Polar lipids: a brief overview	84
3.3.1.2 LC-HRMS/MS in lipidomics	84
3.3.1.3 LC-ESI/QToF/MS/MS analysis of the polar lipids of “Mandorla di Toritto” and “Mandorla d’Avola”	85
3.3.1.4 Phospholipids identification	87
3.3.1.5 Diacylglycerols and triacylglycerols identification	90
3.3.1.6 Free fatty acids identification	93
3.3.1.7 Multivariate data analysis	94
3.4 Free fatty acids GC-FID quali-quantitative analysis of <i>P. dulcis</i> seeds (cvs. Toritto and Avola)	97
3.4.1 Results and discussion	97
3.4.1.1 GC-FID analysis	97
3.4.1.2 Fatty acids extraction and fatty acid methyl esters (FAMES) synthesis	98
3.4.1.3 Identification and quantification of the major free fatty acids	98
3.5 Conclusions	101
3.6 Experimental procedures	103
3.7 References	106
Chapter 4	
<i>Prunus dulcis</i> Mill. (cvs. Toritto and Avola) biomasses (leaves, husks and shells) as potential source of bioactives	115
4.1 Introduction	117
4.2 Metabolite profiling of the polar fraction of (<i>Prunus dulcis</i> Mill.) leaves, cvs. Toritto and Avola	118
4.2.1 Results and discussion	118
4.2.1.1 Qualitative analysis of the MeOH extract of <i>P. dulcis</i> , cv Toritto leaves	118
4.2.1.2 LC-ESI/LTQOrbitrap/MS analysis and comparison of eco-friendly extracts	132
4.2.1.3 Comparison among the Apulian (cv. Toritto) and the Sicilian (cvs. Fascionello, Pizzuta and Romana) <i>P. dulcis</i> leaves by LC-ESI/LTQOrbitrap/MS experiments	134
4.2.1.4 Multivariate data analysis	136
4.2.1.5 Total phenolic content and antioxidant activity evaluation	140

4.3 LC-ESI/LTQOrbitrap/MS based metabolite profiling of <i>Prunus dulcis</i> Mill. (Italian cvs. Toritto and Avola) husks and evaluation of antioxidant activity	142
4.3.1 Results and discussion	142
4.3.1.1 <i>Qualitative analysis of the MeOH extract of P. dulcis cv. Toritto husks</i>	142
4.3.1.2 <i>LC-ESI/LTQOrbitrap/MS based comparison of different extraction procedures</i>	154
4.3.1.3 <i>Metabolite profile comparison of P. dulcis husks originating from different geographical areas</i>	155
4.3.1.4 <i>Total phenolic content and antioxidant activity of P. dulcis husks cvs. Toritto, Fascionello, Pizzuta and Romana</i>	157
4.4 LC-ESI/LTQOrbitrap/MS/MS profiling highlights <i>P. dulcis</i> (cv. Toritto and Avola) shells as a rich source of phenolics with multiple biological activities	158
4.4.1 Results and discussion	158
4.4.1.1 <i>Liquid chromatography high resolution mass spectrometry based putative identification of the MeOH of P. dulcis cv. Toritto shells</i>	158
4.4.1.2 <i>Lignans</i>	162
4.4.1.3 <i>Neolignans</i>	166
4.4.1.4 <i>“Eco-friendly” extracts comparison by LC-ESI/LTQOrbitrap/MS experiments</i>	172
4.4.1.5 <i>LC-ESI/LTQOrbitrap/MS analysis of MeOH extracts obtained from the shells of different cultivars (Toritto and Avola)</i>	173
4.4.1.6 <i>Total phenolic content and radical scavenging activity of the different extract typologies of P. dulcis shells (cvs. Toritto and Avola)</i>	174
4.5 Conclusions	175
4.6 Experimental section	176
4.7 References	183
Chapter 5	
Polar constituents, multi-class polar lipids and free fatty acids profiling of pistachios (<i>Pistacia vera</i> cv. <i>Napoletana</i>) by LC-ESI/HRMS/MS and GC-FID	193
5.1 Introduction	195
5.2 LC-ESI/HRMS/MS analysis of the polar fraction of <i>P. vera</i> cv. <i>Napoletana</i> seeds	197
5.2.1 Results and discussion	197
5.2.1.1 <i>LC-ESI/HRMS/MS profiling of pistachios</i>	197
5.2.1.2 <i>“Eco-friendly” extractions</i>	202
5.2.1.3 <i>Total phenolic content and radical scavenging activity</i>	203
5.2.1.4 <i>Quantification of anacardic acids by Multiple Reaction Monitoring (MRM) approach</i>	204

5.3 LC-ESI/QToF/MS/MS multi-class polar lipids profiling of <i>P. vera</i> seeds	205
5.3.1 Results and discussion	205
5.3.1.1 LC-ESI/QToF/MS/MS analysis of the polar lipids of “ <i>Pistacchio di Bronte</i> ”	205
5.3.1.2 Phospholipids identification	205
5.3.1.3 Diacylglycerols and triacylglycerols identification	207
5.3.1.4 Free fatty acids identification	207
5.4 Free fatty acids GC-FID quali-quantitative analysis of <i>P. vera</i> seeds	208
5.4.1 Results and discussion	208
5.4.1.1 Fatty acids extraction and fatty acid methyl esters (FAMES) synthesis	208
5.4.1.2 Identification and quantification of the major free fatty acids	208
5.5 Conclusions	210
5.6 Experimental section	211
5.6 References	213
Chapter 6	
Analysis of polar constituents of <i>Pistacia vera</i> (cv. <i>Napoletana</i>) biomasses	219
6.1 Introduction	221
6.2 Analysis of the leaves of <i>P. vera</i> polar fraction	223
6.2.1 Results and discussion	223
6.2.1.1 LC-ESI/LTQOrbitrap/MS/MS metabolite profiling of the MeOH extract of <i>P. vera</i> “non-fruiting year” leaves	223
6.2.1.2 Isolation and characterization	226
6.2.1.3 Extraction of <i>P. vera</i> “non-fruiting year” leaves by employing “green” solvents and protocols, with subsequent LC-ESI/LTQOrbitrap/MS analysis	230
6.2.1.4 Anacardic acids	231
6.2.1.5 Comparison of the “non-fruiting year” and “fruiting year” <i>P. vera</i> leaves	233
6.2.1.6 <i>P. vera</i> leaves as promising source of antioxidants	234
6.3 Phenolic constituents of <i>P. vera</i> cv. <i>Napoletana</i> husks	236
6.3.1 Results and discussion	236
6.3.1.1 Preliminary LC-ESI/LTQOrbitrap/MS/MS analysis of the MeOH extract of <i>P. vera</i> husks	236
6.3.1.2 Isolation and characterization	239
6.3.1.3 “Eco-friendly” extraction methods show class-specific selectivity	248
6.3.1.4 Antioxidant activity of the extracts of <i>P. vera</i> husks	249
6.4 Phenolic-based metabolite profile of <i>P. vera</i> shells extracts	251
6.4.1 Results and discussion	251
6.4.1.1 LC-ESI/LTQOrbitrap/MS/MS of the MeOH extract of <i>P. vera</i> shells	251
6.4.1.2 Isolation and characterization	253

6.4.1.3 “Eco-friendly” extracts and comparison by LC-ESI/LTQOrbitrap/MS	260
6.4.1.4 Phenolic content and radical scavenging activity of <i>P. vera</i> shells extracts.....	261
6.5 LC-ESI/QTrap/MS/MS quantitative determination of the main anacardic acids by Multiple Reaction Monitoring (MRM) analysis.....	262
6.6 Conclusions	265
6.7 Experimental section.....	267
6.8 References	273
General experimental procedures	281
Conclusion.....	295
Publications.....	299

Introduction

The rapid growth of world population, jointly with better life conditions, caused an increasing food request over the last years, also promoted by the latest technological improvements which allowed a higher amount of available viands. This phenomenon led to a consequent increasing production of waste material deriving from the manufacturing processes, of which disposal expenses directly encumber on the industries or farmers, and may considerably affect the price of the final products.

By-products of agroalimentary productions typical of Southern Italy: "Ficodindia dell'Etna", "Fico bianco del Cilento", "Mandorla di Toritto" and "Mandorla d'Avola", "Pistacchio di Bronte".

Southern Italy is characterized by an intensive agricultural manufacture, which represents one of the major economic resources. Due to the peculiar climatic conditions, as well as to former commercial trades, each region is distinguished for its typical products, featured by a remarkable number of varieties, deep-rooted in local culinary traditions and also in folklore spectacles.

Among the umpteen typical productions, mainly represented by fruits and vegetables, noteworthy are "Ficodindia dell'Etna" (*Opuntia ficus indica* Mill.), "Fico bianco del Cilento" (*Ficus carica* L.), "Mandorla di Toritto" and "Mandorla d'Avola" (*Prunus dulcis* Mill.), "Pistacchio di Bronte" (*Pistacia vera* L.).



"Ficodindia dell'Etna".

Such denomination refers to three of the most widespread

nopal cactus varieties cultivated in Sicily, which are "Sulfarina", "Muscaredda" and "Sanguigna", differentiated by the color of their fruits,

yellow, white and red, respectively, awarded with the Protected Designation of Origin (PDO) label in 2003. Even if highly adaptable and pervasive, nopal cactus found an ideal habitat on Etna vulcan slopes, thanks to the warm climate and fertile soil. The fruits are juicy, sweet and larger if compared to those obtained elsewhere, this because of a process known as “scozzolatura”, consisting in chopping off the flowers of the first blooming (falling between the end of May and the beginning of June), in order to induce a second blooming (falling during August) affording larger fruits available during the winter.

Prickly pears are mostly consumed fresh, sometimes dried, but also employed for the production of juices, jams and liquors.



“Fico bianco del Cilento”.

Achieving the Protected Designation of Origin (PDO) in 2006, the fig

variety Dottato is cultivated in the Cilento area, which represents the Southern part of Campania region. It shows a smaller size if compared to the common red fig, and even if the external peel appears green as usual for the red variety, the internal edible part is light brown, converging to white, feature responsible of its denomination (“bianco”, which in Italian means white).

Generally figs are consumed fresh or dried, or used for the production of marmelade; in Cilento area this peculiar fig variety is mostly employed sun-dried, prior peel, for the production of traditional preparations, like the “Capocollo di fichi”, consisting in several dried figs pressed to form a cylinder reminiscent of the homonymic sausage, or to produce dried fig

skewers by tucking them on wooden sticks and occasionally covered with bitter chocolate.



“Mandorla di Toritto” and “Mandorla d’Avola”. The two most renowned almond breeds in Italy.

The former is represented by the cultivar Filippo Cea, of which still subsists the mother plant, and is cultivated in the outskirts of Toritto, a small city located in the central area of Apulia region. The latter is cultivated in the most Southern area of Sicilia region, close to Avola city, and is represented by the cultivars Fascionello, Pizzuta and Romana. Although growing in the meridional area of the Italian boot, their harvesting periods are rather different, since in Apulia almonds are collected in late August or September, while in Sicily harvesting occurs in June; such difference might be due to the different climatic conditions. Even if they are often consumed as they are, fresh or roasted, these almond varieties are plenty employed in confectionery and pastry, more in industrial processes than in homemade preparations.



“Pistacchio verde di Bronte”. Probably the most appreciated pistachio in Italy, the

variety *Napoletana* is cultivated on the Western slopes of Etna vulcan, in the cities of Bronte, Adrano and Biancavilla, and was awarded in 2009 with the Protected Designation of Origin (PDO) label, characterized by rich aroma and flavor, an intense green color of the seed and a lively violet color of the integument. It is a very profitable economic source, so that it is called “green

gold” by the local farmers, since its cultivation generates a profit of more than 20 millions euro/production year, with the trees fruiting occurring in alternating years.

Even if widely consumed fresh, or better roasted and salted, pistachios represent the main ingredient of numerous typical desserts, especially Sicilian, and thanks to the recent food trends they are more and more employed in cookery for the preparation of innovative dishes.

The above mentioned agroalimentary products are part of the local culinary traditions of Southern Italy, and play a key role in the economic maintenance of agricultural companies and farmers. Their peculiar features, like their taste and flavor, made them to be widely known all over the Italian territory; in addition, international trades allowed these products to be experienced abroad. Thus, over the last years it has been attended to a growing demand of such products on the national and international markets, in particular by food industries, where they are mainly employed for mass productions. This resulted in the yield of a considerable amount of collateral waste material with no commercial value, of which disposal costs encumber on companies and farmers, and therefore affecting the price of the finished products.

Moreover, even if much is known about their nutritional properties and benefits exerted on human health, a lack of information about their metabolome still persists in some cases. A deeper knowledge of their chemical composition may give rise to a higher value, asserting the quality of the “Made in Italy” brand and supporting these products in the treacherous struggle against uncontrolled importations from non-European countries, which threaten local economy because of lower prices often associated to lower quality, as well as representing a potential risk for the health of consumers due to not exhaustive inspections.

Furthermore, in the frame of a “green economy” development, aiming at awarding an economic value and reducing, or even better nullifying their disposal costs, research has paid great attention to agricultural industry wastes, focusing on the main vegetable and fruit manufacturing by-products. They might be employed for several secondary scopes, like animal fodder or as compost, as well as for the production of bio-fuel.

In particular, the leaves of the “Fico bianco del Cilento”, the early flowers of the “Ficodindia dell’Etna”, the leaves, husks and shells of the “Mandorla di Toritto”, “Mandorla d’Avola” and “Pistacchio di Bronte” have no useful applications, albeit in the past years several attempts assayed to find out secondary scopes for these biomasses.

Main target of the present PhD project was to define the metabolome of the main by-products, and edible parts in certain cases, of the selected agroalimentary productions, focusing the attention on valorizing waste materials as potential sources of bioactives, pointing out their perspective employment in nutraceuticals, for the production of dietary supplements, in cosmetics, for the manufacture of formulations possessing peculiar properties, or even in medical therapies, for the treatment of diseases related to certain onset conditions like oxidative stress.

Particularly, the targets achieved during the PhD are the following:

- chemical profile definition of the different parts of the selected plant species *Opuntia ficus indica* Mill. cv. Sulfarina, *Ficus carica* L. cv. Dottato, *Prunus dulcis* Mill. cvs. Filippo Cea, Fascionello, Pizzuta, Romana and *Pistacia vera* L. cv. Napoletana;
- development of methods for qualitative and quantitative analysis of extracts obtained from the different parts of the selected plant species;
- preliminary evaluation of the obtained extracts bioactivity, focusing the attention on the antioxidant properties.

Experimental plan

Extraction of the selected plant parts

Due to the countless typologies of metabolites found in plant tissues, the choice of an extraction method is a critical step for the subsequent analyses. Many are the parameters that must be considered, such as solvent polarity, extraction time, temperature, solvent/drug ratio and the extraction mechanisms. In particular, the most appropriate solvent must be chosen according to the targeted metabolites planned to be extracted and investigated. Moreover, a further issue to be considered is the environmental impact of the selected chemicals, because of the pollution related to their production and disposal. Therefore, targeted extraction protocols were developed for each plant material, by employing standard laboratory methods, as well as traditional homemade processes by using “eco-friendly” solvents, in the frame of a “green” and sustainable research.

Qualitative and quantitative analysis

Aiming at defining their chemical composition, the sundry typologies of extracts obtained from the different parts of the investigated plant species were explored by liquid chromatography coupled to mass spectrometry (LC-MS), following an untargeted metabolomics approach. LC-MS proved over the last years to be a powerful tool in phytochemistry and food chemistry, able to detect in a single analysis a high number of metabolites of a plant matrix; furthermore, structural information can be achieved by performing appropriate fragmentation experiments. Best results are obtained by employing modern Ultra High Pressure Liquid Chromatographs (UHPLC) coupled to ElectroSpray Ionization sources (ESI) with multicollisional Ion Traps (IT) or Quadrupole-Time of Flight (QToF) analyzers, resulting in a quick separation, fragmentation and detection of a wide range of analytes. The above mentioned analyzers are able to perform tandem mass

spectrometry experiments, enhancing the number of obtained information as well as to determine the accurate mass of the detected ions with a higher reliability, if compared to instruments of past generations. Hence, in accordance to this, high resolution mass spectrometers (QToF and Orbitrap) were employed.

However, for an irrefutably structural characterization of the main constituents, in most cases crude extracts were submitted to sequential fractionating steps, selected according to the complexity and the chemical characteristics of the extracts, and to the compounds of interest as well. Mainly preparative and semi-preparative techniques were approached, sometimes preceded by clean-up operations, exploiting their capability to lead to a rapid isolation of pure compounds.

Structural elucidation of isolated compounds was principally performed by NMR spectroscopy and mass spectrometry.

NMR spectroscopy showed to be an essential analytical method for an unambiguous structural elucidation of small molecules, also because of the broad selection of available experiments, able to return a very high amount of structural information. In particular, monodimensional experiments ($^1\text{H-NMR}$) were performed to achieve preliminary information, plenty satisfactory to assess the class of the analyzed molecules; subsequently, two-dimensional experiments were carried out in order to acquire heteronuclear spectra (HMBC, HSQC), to identify the molecule functional groups and moieties, together with scalar coupling homonuclear spectra (COSY), to establish the spin systems.

In addition, for a further confirmation of the assigned identities, the characterized molecules were analyzed by high resolution mass spectrometry experiments with direct injection in the ESI source (ESI/HRMS/MS), to determine their accurate mass and evaluate the matching of their fragmentation patterns with the attributed structure.

Along with Liquid Chromatography (LC), Gas Chromatography (GC) proved to be a versatile analytical method in phytochemical and food analysis, as well as in cosmetic, pharmaceutical and environmental fields, thanks to its capacity to separate in very short times a huge number of molecules; such capacity has improved after the introduction of capillary columns, leading to a High Resolution Gas Chromatography (HRGC). Usually gaschromatographs are coupled to universal or selective detectors, like Flame Ionization Detector (FID) and Electron Capture Detector (ECD), respectively, but for more advanced applications mass spectrometers are employed, especially in food quality and environmental controls.

According to these considerations, GC-FID was used to investigate the non-polar fraction of the edible parts of selected plant species, due to the reduced analysis times if compared to its liquid counterpart and the uncomplete appropriateness of this last method. The analyses were carried out adopting a targeted approach, aimed at the identification of specific metabolites, easily detected by FID and identified by comparison with reference standards.

Where possible, quantitative analyses were performed after metabolite profiling analyses. For the polar identified metabolites, quantification was carried out by LC-ESI/QTrap/MS/MS experiments by a Multiple Reaction Monitoring (MRM) approach, a very selective mass tandem experiment; on the other hand, non-polar constituents were quantified by GC-FID experiments on the basis of the peak areas using integration data.

Evaluation of antioxidant activity of the selected plant extracts

Aiming at valorizing by-products as a potential source of bioactives to be employed for secondary scopes, like nutraceutics and cosmetics, preliminary chemical assays were carried out on the obtained extracts, in order to assess eventual properties of interest, focusing the attention on highlighting their antioxidant activity. Therefore, the total phenolic content was determined at first,

by performing the Folin-Ciocalteu assay. Successively, on the basis of the obtained results, radical scavenging activity was evaluated by performing DPPH \cdot and ABTS \cdot^+ assays.

Chapter 1
Metabolite profiling of PDO *Opuntia ficus indica*
Mill. flowers

1.1 Introduction

Nopal cactus (*Opuntia ficus indica* Mill.) is a Cactacea native of Mexico, widely spread all over the world thanks to its capability to adapt itself to almost all types of climates. The stem is constituted by several cladodes covered by thorns, which are structurally modified leaves. During the blooming period, yellow flowers appear on the cladodes, successively producing the fruits commonly named prickly pears. These are juicy and sweet, and of various colours depending on the different varieties.

A noteworthy application of nopal cactus plantations is the breeding of *Dactylopius coccus*, a scale insect better known as cochineal, employed for the production of a red pigment identified with the label E120, and approved by Food and Drug Administration (FDA) as food colorant thanks to its safety for human consumption.

However, the main purpose of its extensive cultivation, even if spontaneous, is the production of the sweet and juicy fruits, consumed mostly fresh, very appreciated by the local population and deep-rooted in the traditional cookery for the manufacture of jams and juices. In Sicily three are the main cultivars: Sulfarina, Sanguigna and Muscaredda, characterized by yellow-orange, red and white colored berries, respectively; thanks to their unique taste and flavor, probably due to the peculiar climate and the growing location, such cvs. were awarded with the Protected Designation of Origin (PDO) label, and named “Ficodindia dell’Etna”.

The natural blooming period occurs starting from the last decade of May till the first half of June, leading to the production during August of fruits named “Agostani”. Nevertheless, the number and the size of such fruits are trifling. To overcome these problems, in Sicily local farmers perform a technique named “scozzolatura”, consisting in chopping off the flowers of the first blooming period, to induce a second and more abundant blooming in August, returning a higher number of fruits available in winter, characterized by a bigger size, named

“Bastardoni”. Notwithstanding, the “scozzolatura” technique clearly shows a disadvantage: the plant wastes generated by this process, represented by the chopped off flowers, must be disposed of, resulting in additional costs for the producers.

The flowers are used in traditional medicine as infusions for their depurative and diuretic effects, as well as in the treatment of urological affections and kidney colics, and also for their ability to promote renal calculus expulsion (Pitrè G., 1949). Moreover, flowers showed to possess antimicrobial activity and wound healing properties (¹Ammar et al., 2015).

Although the metabolite profile of *O. ficus indica* flowers has been already explored, most part of the existing reports focused the attention on Tunisian, Moroccan and Mexican varieties; hence, a lack of information about the Italian varieties, especially Sicilian, still persists (²Ammar et al., 2015; Benayada et al., 2014).

Therefore, in order to achieve a deepest knowledge about the chemical composition of the Sicilian *O. ficus indica* cv. Sulfarina flowers deriving from the first blooming, main by-products of the chopping off process, and to valorize such biomass as a potential source of bioactives, the EtOH/H₂O extract of the trimmed flowers was investigated.

The phytochemical investigation of the h EtOH/H₂O extract of Sicilian *O. ficus indica* cv. Sulfarina flowers led to the isolation and characterization of two phenylbutanoic acids, several flavonoids reported for their antioxidant and antiinflammatory activities (Pietta P., 2000), and a glycosylated phenolic derivative never reported before in *Opuntia* genus. In this chapter the following topics are reported:

- evaluation of the total phenolic content by Folin-Ciocalteu assay, followed by determination of the radical scavenging activity by performing DPPH• and ABTS•⁺ assays;

- isolation, by chromatographic techniques, and characterization, by NMR experiments, of the main constituents detected by LC-ESI/LTQOrbitrap/MS/MS analyses;
- quantification of the main constituents by UHPLC-ESI/QTrap/MS/MS experiments, exploiting the advantages of the MRM approach.

***Opuntia ficus indica* Mill. flowers**

The flowers are large and solitary, with a perianth made up of spirally arranged yellow-orange tepals.

1.2 Results and discussion**1.2.1 Antioxidant activity and LC-ESI/LTQOrbitrap/MS/MS analysis**

To evaluate the phenolic content of the EtOH/H₂O extract of the Sicilian nopal cactus flowers, Folin-Ciocalteu assay was performed. The results showed a phenolic content of 246.24 ± 4.17 mg GAE/g of dried extract. Successively, on the basis of the obtained promising results, the radical scavenging activity of the extract was tested by DPPH· ($IC_{50} = 88.51 \pm 2.11$ µg/mL) and ABTS^{•+} (TEAC value = 1.54 mM \pm 0.09) assays.

On the basis of the preliminary assays results, with the aim of correlating the phenolic content and the antioxidant activity with the chemical composition of the tested EtOH/H₂O extract, a LC-ESI/HRMS/MS analysis was carried out to achieve a first overview on the chemical composition of the extract. In particular, a high performance liquid chromatograph coupled to a linear ion-trap and a high resolution analyzer, with electrospray ionization source, was employed. Experiments were performed in negative ion mode and in data dependent scan mode, in which the most intense peaks in the LC-MS spectrum are selected as precursor ions and fragmented.

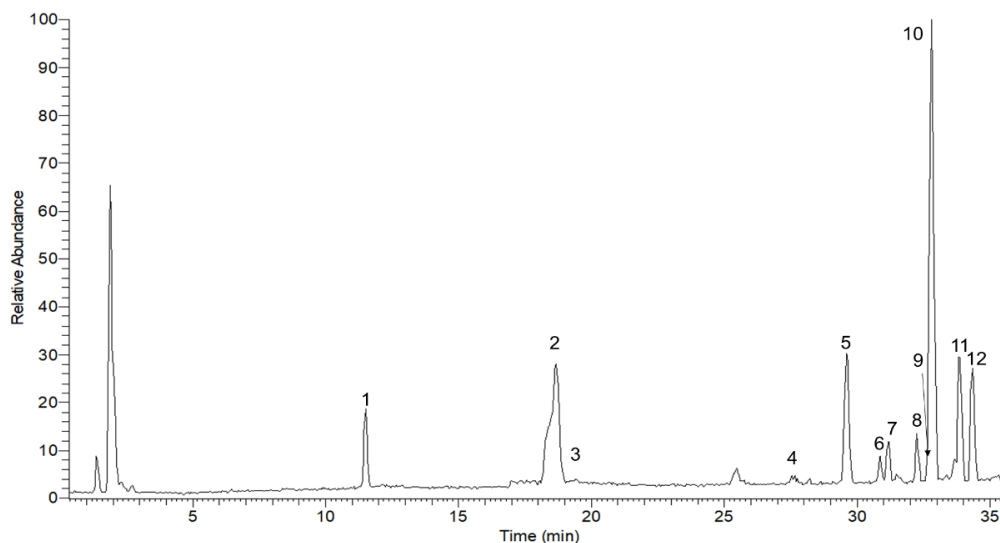


Figure 1.1 LC-HRMS profile in negative ion mode of the EtOH/H₂O extract of *O. ficus indica* flowers

The LC-HRMS/MS spectrum analysis of the EtOH/H₂O extract showed peaks with m/z values ascribable to phenolics, with fragmentation patterns typical of glycosylated flavonoids (**4-12**) and phenylbutanoic acids (**1-2**), as well as a glycosylated phenolic derivative (**3**) (Table 1.1).

Table 1.1 Compounds identified in the EtOH/H₂O extract of *O. ficus indica* flowers

N°	R _t	Calculated Mass	[M-H] ⁻	Δppm	MS ² (%)	Molecular Formula	Compound
1	11.9	256.0583	255.0508	1.68	209(5), 193(30), 179(12), 165(100)	C ₁₁ H ₁₂ O ₇	piscidic acid ²
2	18.68	240.0633	239.0561	1.70	221(24), 195(20), 179(100), 177(71), 149(64)	C ₁₁ H ₁₂ O ₆	eucomic acid ²
3	19.04	330.0950	375.0894 ¹	1.69	329(100), 167(21)	C ₁₄ H ₁₈ O ₉	woodorien ²
4	28.2	770.2269	769.2201	1.05	605(75), 315(50), 314(100)	C ₃₄ H ₄₂ O ₂₀	isorhamnetin-3-O-β-D-(di-2'',6''-α-L-rhamnosyl)-glucopyranoside ²
5	29.59	610.1533	609.1467	1.82	301(100), 300(41)	C ₂₇ H ₃₀ O ₁₆	quercetin-3-O-β-D-rutinoside ²
6	30.85	464.0954	463.0881	1.30	301(100), 300(54)	C ₂₁ H ₂₀ O ₁₂	quercetin-3-O-β-D-galactopyranoside ²
7	31.17	464.0954	463.0883	1.75	301(100), 300(46)	C ₂₁ H ₂₀ O ₁₂	quercetin-3-O-β-D-glucopyranoside ²
8	32.25	624.1690	623.1620	1.22	315(100), 300(24)	C ₂₈ H ₃₂ O ₁₆	isorhamnetin-3-O-β-D-robinobioside ²

9	32.62	594.1584	593.1513	1.27	285(100)	C ₂₇ H ₃₀ O ₁₅	kaempferol-3-O-β-D-rutinoside ²
10	32.81	624.1690	623.1621	1.20	315(100), 300(27)	C ₂₈ H ₃₂ O ₁₆	isorhamnetin-3-O-β-D-rutinoside ²
11	33.83	478.1111	477.1034	1.54	357(22), 315(34), 314(100)	C ₂₂ H ₂₂ O ₁₂	isorhamnetin-3-O-β-D-galactopyranoside ²
12	34.34	478.1111	477.1031	1.52	357(19), 315(32), 314(100)	C ₂₂ H ₂₂ O ₁₂	isorhamnetin-3-O-β-D-glucopyranoside ²

¹Observed as formate adduct. ² The identification of this compound was corroborated by isolation and NMR spectra analysis

1.2.2 Isolation and characterization of phenolics from the EtOH/H₂O extract of *O. ficus indica* flowers

With the aim to univocally identify the detected compounds, the EtOH/H₂O extract was submitted to purification by size-exclusion chromatography, the profiles of the collected fractions were monitored by Thin Layer Chromatography (TLC) and further purified by Reverse Phase High Pressure Liquid Chromatography with Refractive Index detector (RP-HPLC-RI), yielding two phenylbutirric acids (**1**, **2**), one glycosylated phenol (**3**) and nine glycosylated flavonoids (**4-12**). The structural elucidation of the isolated compounds was carried out by comparing their experimental NMR spectroscopic data with literature (Jiang et al., 2002; Maier et al., 2015; Xu et al., 1993; Kazuma et al., 2003); moreover, as confirmation of the assigned identity, ESI/HRMS experiments were performed to determine the accurate masses, as well as ESI/HRMS/MS experiments to acquire the fragmentation spectra of each isolated compound.

On the basis of the information obtained from the performed experiments, it was possible to identify the isolated flavonoids as isorhamnetin 3-*O*-(di-2",6"-*O*-α-L-rhamnosyl)-β-D-glucopyranoside (**4**), quercetin 3-*O*-β-D-rutinoside (**5**), quercetin 3-*O*-β-D-galactopyranoside (**6**), quercetin 3-*O*-β-D-glucopyranoside (**7**), isorhamnetin 3-*O*-β-D-robinobioside (**8**), kaempferol 3-*O*-β-D-rutinoside (**9**), isorhamnetin 3-*O*-β-D-rutinoside (**10**), isorhamnetin 3-*O*-β-D-galactopyranoside (**11**) and isorhamnetin 3-*O*-β-D-glucopyranoside (**12**) (Fig. 1.1).

Flavonoids are widespread in plant kingdom, playing a key role in several mechanisms like phytoalexins, inhibiting the growth of pathogenic microorganisms, seed germination, promoting buds sprouting, UV-filters, protecting the plant from dangerous radiations, and pollinators attractants, promoting seeds dispersion operated by lured insects or animals (Amalesh et al., 2011). This phenolic phytoconstituents are daily assimilated through diet, and a growing number of scientific reports highlighted their beneficial effects exerted on human health, mainly due to their antioxidant properties, accountable of inhibiting lipid peroxidation and as consequence counteracting atherosclerosis origination; moreover, flavonoids proved to be strong radical scavengers, useful to prevent potential damages originated by oxidative stress events (Atmani et al., 2009), as demonstrated by *in vitro* and *in vivo* tests, highlighting their capacity to prevent cell damage induced by free radicals, as well as to prevent the onset of several hearth diseases (Matias et al., 2014; Pietta P., 2000). Moreover, some flavonoids showed to possess antimicrobial activity against *Staphylococcus*, *Streptococcus* and *Pseudomonas* species, and promising anticancer properties too (Cushnie et al., 2005; Kandaswami et al., 2005).

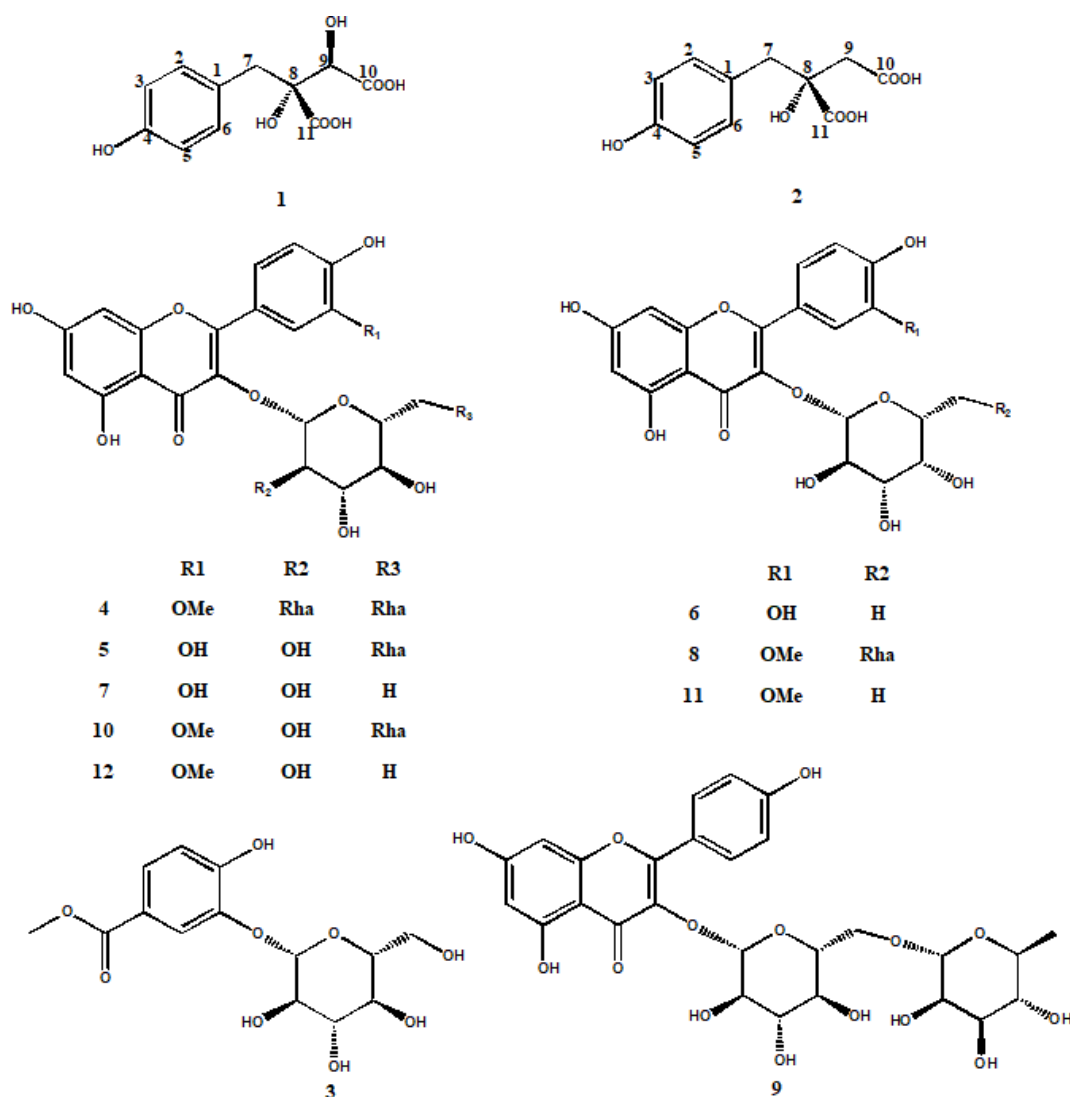


Figure 1.1 Compounds isolated from the EtOH:H₂O extract of *O. ficus indica* flowers

The occurrence of flavonoids in the flowers of the Sicilian nopal cactus may suggest their potential employment in the production of dietary supplements, with remarkable benefits for human health, or in the manufacture of cosmetic formulations rich in phenolics, able to counteract skin damage induced by oxidative agents. However, the listed flavonoids have been exhaustively reported in the flowers of the Tunisian and Portuguese varieties of *O. ficus indica*, with the only

exception of compound **4**, exclusively reported in the cladodes, evidencing a persisting lack of information about the metabolite profile of varieties originating from different areas (²Ammar et al., 2015; De Leo et al., 2010).

Besides flavonoids, a glycosylated phenolic compound was isolated and identified as 3-*O*-(β -D-glucopyranosyloxy)-4-hydroxybenzoic acid methyl ester, most commonly known as woodorien (**3**), named after the plant species *Woodwardia orientalis*, from which it was firstly isolated and identified (Xu et al., 1993). It showed a noteworthy *in vitro* activity against herpes simplex virus 1 (HSV-1), suggesting a potential employment of *O. ficus indica* flowers for the treatment of Herpes labialis, better known as cold sores, reducing the recovery period usually lasting 10 days. Moreover, to the best of our knowledge, woodorien (**3**) has never been reported before in *Opuntia* species (Xu et al., 1993).

Finally, the purification of the EtOH:H₂O extract of *O. ficus indica* cv. Sulfarina flowers led to the isolation of two phenylbutirric acid derivatives, identified as piscidic acid (**1**) and eucomic acid (**2**). For both compounds *in vitro* interesting antiinflammatory activity, in particular against intestinal inflammatory states, has been reported (Simmler et al., 2011). In addition, for piscidic acid (**1**) antioxidant activity, mainly due to its capacity to chelate iron, has been demonstrated (Mata et al., 2016).

Below the structural elucidation of compounds **1** and **2** by interpretation of their ¹H-NMR (Fig. 1.2 for **1**, Fig. 1.5 for **2**), HSQC (Fig. 1.3 for **1**, Fig. 1.6 for **2**) and HMBC (Fig. 1.4 for **1**, Fig. 1.7 for **2**) spectra will be briefly discussed.

The ¹H-NMR spectrum of compound **1** (Fig. 1.2) showed two signals at δ 6.67 (d, $J = 8.6$ Hz) and 7.11 (d, $J = 8.6$ Hz), attributed respectively to H-3,5 and H-2,6 of a 1,4-disubstituted aromatic ring. Moreover, a signal at δ 4.32 (s), and two signals at δ 3.00 (d, $J = 14.2$ Hz) and 3.03 (d, $J = 14.2$ Hz) typical of geminal protons, were evident. The signal at δ 4.32 exhibited in the HMBC spectrum (Fig. 1.4) a correlation with the carbon resonances at δ 42.3 (C-7), at δ 174.6 (C-10) and 175.3

(C-11), and at δ 81.3 (C-8); this last one also showed HMBC correlations with the proton signals at δ 3.00 (d, $J = 14.2$ Hz) and 3.03 (d, $J = 14.2$ Hz), attributed to H-2,7, and the signals at δ 7.11 (d, $J = 8.6$ Hz) attributed to H-2,6. Thus, the structure of compound **1** was identified as piscidic acid (Maier et al., 2015).

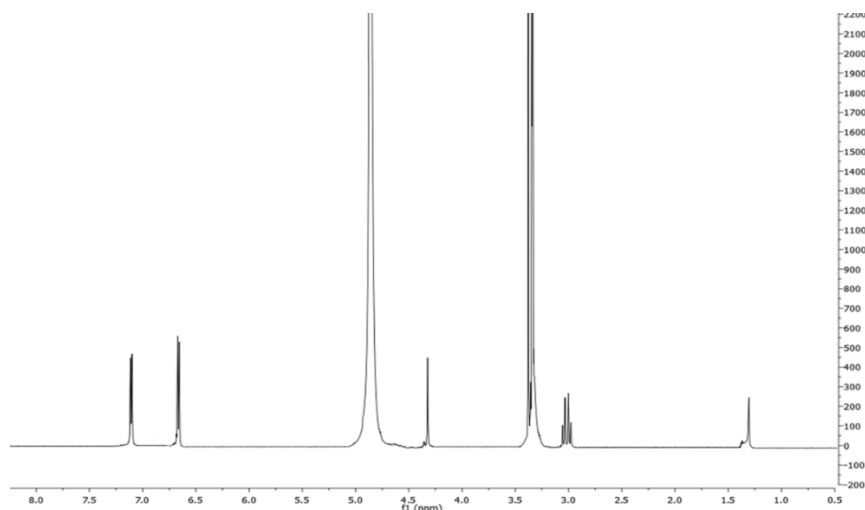


Figure 1.2 ^1H -NMR spectrum of compound **1**

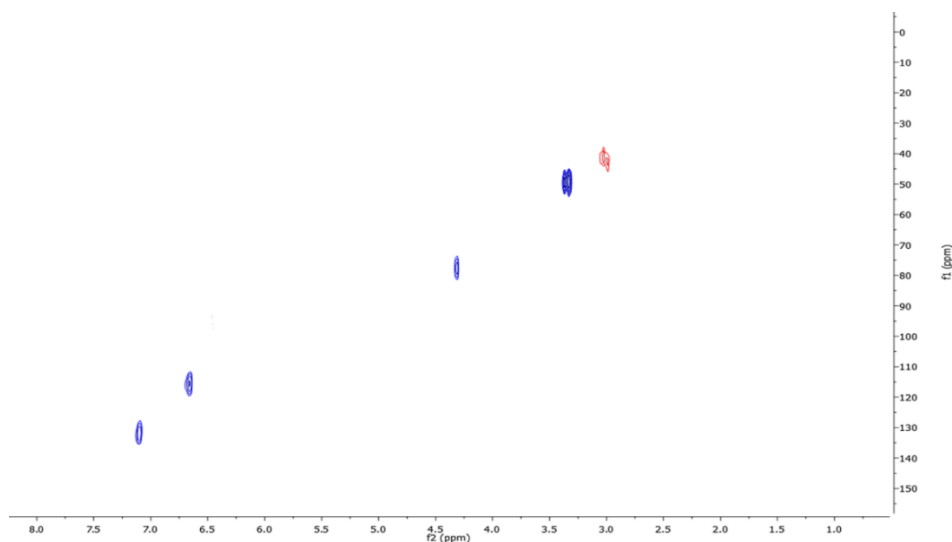


Figure 1.3 HSQC spectrum of compound **1**

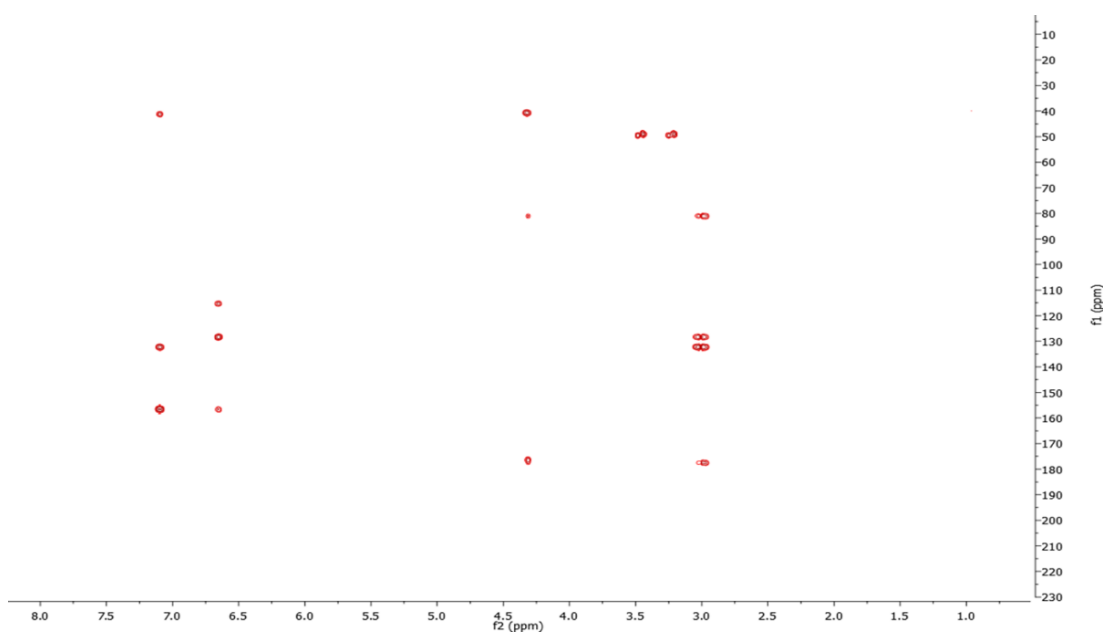


Figure 1.4 HMBC spectrum of compound **1**

In the ¹H-NMR spectrum of compound **2** (Fig. 1.5) signals ascribable to H-2,6 at δ 7.11 (d, $J = 8.6$ Hz), to H-3,5 at δ 6.67 (d, $J = 8.6$ Hz) and to H₂-7 at δ 2.81 (d, $J = 11.2$ Hz) and 3.18 (d, $J = 11.2$ Hz) were once again observed; two signals ascribable to H₂-9 at δ 2.64 (d, $J = 13.2$ Hz) and at δ 2.93 (d, $J = 13.2$ Hz) showed in the HMBC spectrum (Fig. 1.7) correlations with the carbon resonances at δ 45.2 (C-7), 76.2 (C-8) 177.1 (C-10) and 180.3 (C-11). On the basis of the above evidences compound **2** was identified as eucomic acid (Simmler et al., 2011).

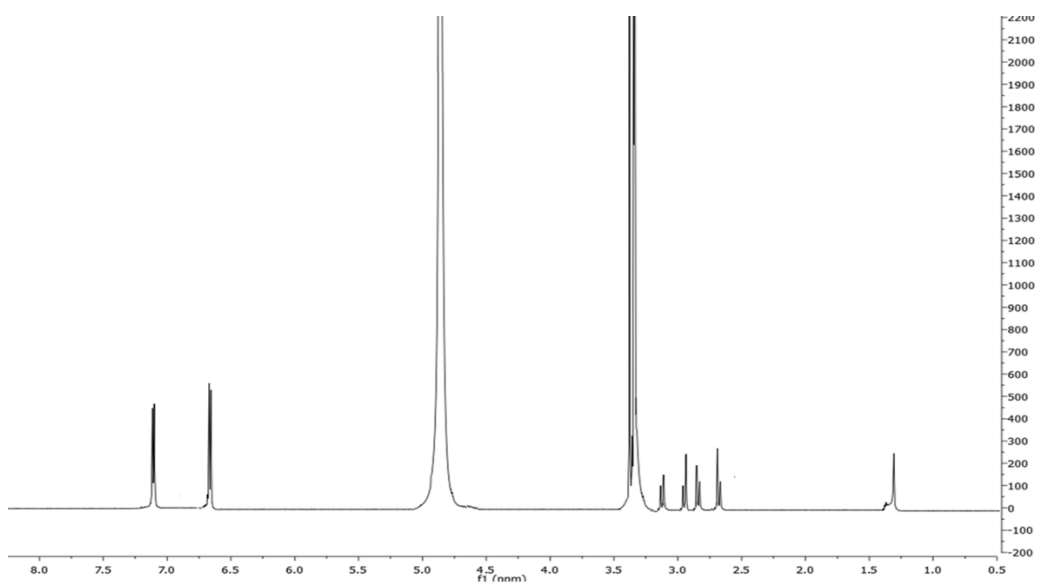


Figure 1.5 ^1H -NMR spectrum of compound 2

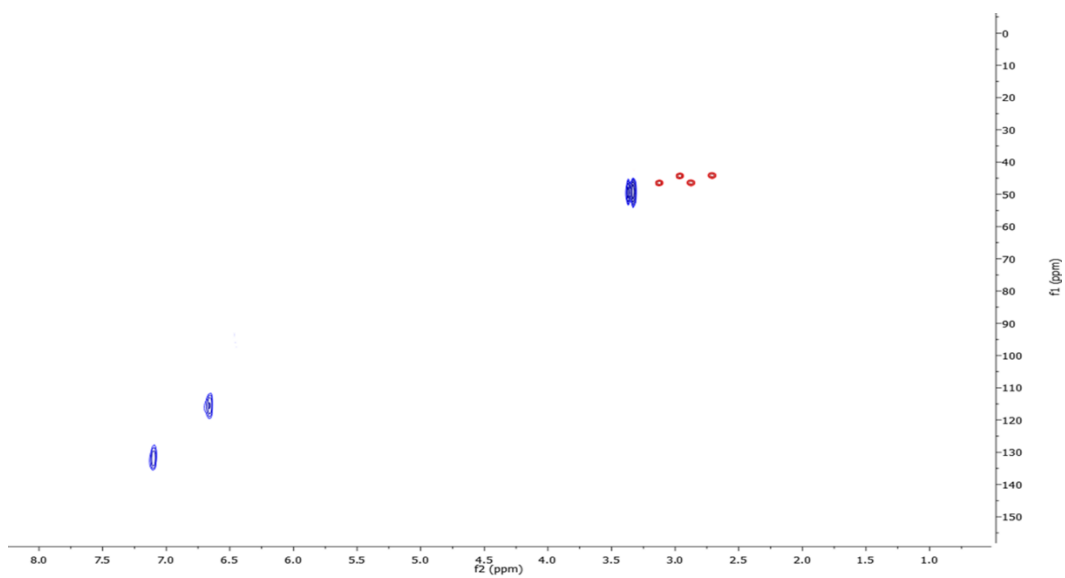


Figure 1.6 HSQC spectrum of compound 2

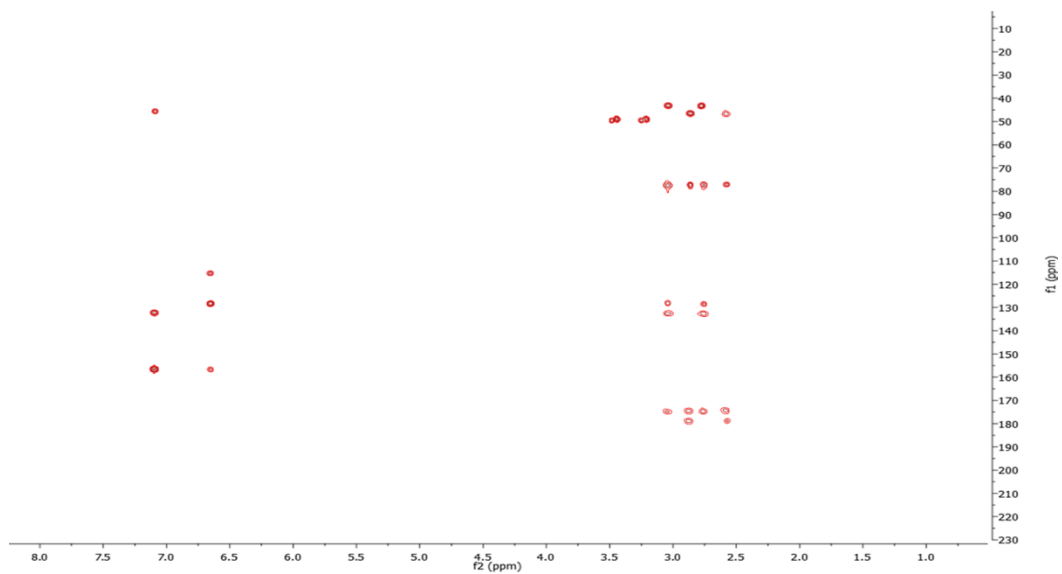


Figure 1.7 HMBC spectrum of compound 2

Table 1.2 ^1H (600 MHz) and ^{13}C (150 MHz) NMR spectral data of compounds 1 and 2

	1		2	
	δ_{C}	δ_{H} (J in Hz)	δ_{C}	δ_{H} (J in Hz)
1	128.2	-	128.3	-
2	131.3	7.11, d(8.6)	131.3	7.11, d(8.6)
3	115.1	6.67, d(8.6)	115.2	6.67, d(8.6)
4	157.6	-	157.5	-
5	115.1	6.67, d(8.6)	115.2	6.67, d(8.6)
6	131.3	7.11, d(8.6)	131.3	7.11, d(8.6)
7	42.3	3.00, d(14.2) 3.03, d(14.2)	45.2	2.81, d(11.2) 3.18, d(11.2)
8	81.3	-	76.2	-
9	76.1	4.32, s	44.1	2.64, d(13.2) 2.93, d(13.2)
10-COOH	174.6	-	177.1	-
11-COOH	175.3	-	180.3	-

In MeOH- d_4

1.2.3 Quantitative analysis of the EtOH:H₂O extract of *O. ficus indica* Mill. cv. *Sulfarina* flowers

To evaluate the content of the major constituents identified in the EtOH:H₂O extract of the Sicilian nopal cactus flowers, a quantitative analysis was performed by UHPLC-ESI/QTrap/MS/MS experiments by a MRM approach.

To achieve accurate results, a UHPLC-ESI/QTrap/MS/MS method was developed; standard solutions of the compounds of interest were submitted to ESI/MS and ESI/MS/MS experiments by direct infusion in the ESI source of the mass spectrometer, and the main transitions observed during the MS/MS analyses were used to optimize the instrument tuning settings for each analyzed standard, allowing to develop a selective MRM method (Table 1.3). Successively, standard solutions were used to produce standard mixtures at different concentrations, and analyzed by LC-ESI/MS/MS experiments in order to assess the calibration curves for each compound of interest. The results were expressed as mean of three experiments, and the calibration curves were generated by plotting the peaks areas in function of the reported concentrations. Finally, a diluted solution of the EtOH:H₂O extract was analyzed in triplicate in the same operating conditions.

Table 1.3 Instrument settings used for the quantitative analysis of the major compounds of *O. ficus indica* flowers EtOH:H₂O extract

Compound	[M-H] ⁻	MS/MS	DP	EP	CE	CXP
piscidic acid (1)	255	165	-70 V	-8 V	-30 V	-16 V
eucomic acid (2)	239	149	-70 V	-8 V	-30 V	-16 V
quercetin 3-O-β-D-rutinoside (5)	609	301	-45 V	-9.4 V	-40 V	-37 V
quercetin 3-O-β-D-galactopyranoside (6)	463	301	-167 V	-11 V	-30 V	-37 V
quercetin 3-O-β-D-glucopyranoside (7)	463	301	-167 V	-11 V	-30 V	-37 V
isorhamnetin-3-O-β-D-robinobioside (8)	623	313.9	-165 V	-12 V	-35 V	-37 V
isorhamnetin 3-O-β-D-rutinoside (10)	623	313.9	-165 V	-12 V	-35 V	-37 V
isorhamnetin 3-O-β-D-galactopyranoside (11)	477	313.9	-165 V	-12 V	-35 V	-37 V
isorhamnetin 3-O-β-D-glucopyranoside (12)	477	313.9	-165 V	-12 V	-35 V	-37 V

DP Declustering Potential, EP Entrance Potential, CE Collision Energy, CXP Collision Cell Exit Potential

To ensure a correct workflow, along with the reproducibility of the experiments and of the obtained results, the UHPLC-ESI/QTrap/MS/MS method employed for the quantitative analyses was validated according to the European Medicine Agency guidelines (EMA Quality guidelines ICH Q2). In particular, all experiments were performed in triplicate; accuracy was determined by analyzing random standard solutions after calibration curves were assessed, while precision was evaluated by analyzing the same concentration in standard in triplicate, and repeating the experiments in different days. Moreover, a satisfactory linearity was observed in the quantification concentrations range of all the analytes, with a correlation coefficient (R^2) between 0.995 and 0.999 (Table 1.4).

Table 1.4 Quantitative data of *O. ficus indica* flowers EtOH:H₂O extract, (MRM, negative ion mode). Five-point calibration, with nine standards. LOQ (Limit of quantification) and LOD (Limit of detection) expressed as ng/mL

Compound	R^2	Regression line	LOQ (ng/mL)	LOD (ng/mL)
piscidic acid (1)	0.9989	y=590x-10100	16.0	3.0
eucomic acid (2)	0.9994	y=342x+603	19.0	4.0
quercetin 3-O-β-D-rutinoside (5)	0.9995	y=1420x-14900	16.0	2.0
quercetin 3-O-β-D-galactopyranoside (6)	0.9993	y=541x+18000	15.0	4.0
quercetin 3-O-β-D-glucopyranoside (7)	0.9993	y=541x+18000	16.0	3.0
isorhamnetin-3-O-β-D-robinobioside (8)	0.9950	y=1250x-10000	21.0	5.5
isorhamnetin 3-O-β-D-rutinoside (10)	0.9996	y=786x-6410	12.0	2.0
isorhamnetin 3-O-β-D-galactopyranoside (11)	0.9991	y=5060x+9550	11.0	2.5
isorhamnetin 3-O-β-D-glucopyranoside (12)	0.9987	y=5400x +31600	12.0	2.5

The obtained results (Table 1.5) highlighted the EtOH:H₂O extract of *O. ficus indica* flowers as a rich source of phenolics reported for their antioxidant and anti-inflammatory properties; in particular, piscidic acid (1) and eucomic acid (2) resulted among the most abundant constituents, while isorhamnetin 3-O-β-D-robinobioside (8), also known as narcissin and extensively reported for its radical scavenging activity, resulted the most abundant flavonoid (Hyun et al., 2006).

These promising results suggested a potential use of the EtOH:H₂O extract for applications in cosmetics and nutraceuticals.

Table 1.5 Concentrations ($\mu\text{g}/\text{mg}$ of dried extract) of the major compounds identified in the flowers extract of *O. ficus indica* obtained by employing an UHPLC system coupled to a Sciex (Foster City, CA, USA) 6500 Q-Trap instrument.

Compound	Concentration	SD
piscidic acid (1)	30.7	± 1.28
eucomic acid (2)	36.55	± 0.84
quercetin 3- <i>O</i> - β -D-rutinoside (5)	22.55	± 0.61
quercetin 3- <i>O</i> - β -D-gal (6)	29.65	± 1.62
quercetin 3- <i>O</i> - β -D-glc (7)	22.15	± 0.77
isorhamnetin-3- <i>O</i> - β -D-(6''- α -L-rha)-gal (8)	36.15	± 2.16
isorhamnetin 3- <i>O</i> - β -D-rut (10)	24.5	± 1.03
isorhamnetin 3- <i>O</i> - β -D-gal (11)	12.5	± 0.42
isorhamnetin 3- <i>O</i> - β -D-glc (12)	17.55	± 0.68

Mean in $\mu\text{g}/\text{mg}$ of dried extract (n=3). Standard Deviation of three independent experiments.

1.3 Conclusions

The EtOH:H₂O extract of *Opuntia ficus indica* Mill. cv. Sulfarina flowers showed to possess a considerable phenolic content, and a noteworthy antioxidant activity as well. The LC-ESI/LTQOrbitrap/MS/MS analysis evidenced the occurrence of phenolics, mainly represented by glycosylated flavonoids and phenylbutanoic acids, together with a minor glycosylated phenolic derivative. The subsequent multiple-steps purification of the crude extract confirmed the results obtained from the LC-HRMS/MS analysis, leading to the isolation of two phenylbutanoic acids, namely piscidic acid (1) and eucomic acid (2), reported for their anti-inflammatory properties (Simmler et al., 2011), a glycosylated phenol known as woodorien (3), with interesting anti-HSV-1 activity, and nine flavonoids with different glycosylation levels. Quantitative analyses carried out by UHPLC-ESI/QTrap/MS/MS experiments confirmed the EtOH:H₂O extract of the Sicilian nopal cactus flowers as a source of phenolics with renowned antioxidant properties.

1.4 Experimental section

Plant Material

EtOH:H₂O flowers extract of *Opuntia ficus indica* cv. Sulfarina was provided by Bionap s.r.l. (Belpasso, CT, Italy), stored by arrival at 4°C, until its usage for the analyses.

Chromatographic purification

Column chromatography was performed on Sephadex LH-20 (Pharmacia). HPLC-RI separations were performed on instrument described in general experimental procedures, using a Knauer Eurospher 100-10 C-18 column (300 x 8 mm, 10 µm).

LC-ESI/LTQOrbitrap/MS/MS and LC-ESI/LTQOrbitrap/MS procedures

LC-HRMS experiments were carried out on instrument reported in general experimental procedures. LC separation was performed on a Waters (Milford, MA, USA) X-Select RP C18 column (150 mm x 2.1 mm, 3.5 µm), at a flow rate of 0.2 mL/min. Employed mobile phases were (A) water and (B) acetonitrile, both acidified at 0.1% formic acid. Elution gradient was: 0 min 5% B (held for 3 minutes), 28 min 23% B (held for 3 minutes), 52 min 26% B, 77 min 40% B, 82 min 80% B, 84 min 100% B (held for 6 minutes), returning to start conditions in 7 min. Injection volume was 10 µL, keeping the column at room temperature.

The ESI source parameters were set as following: source voltage at 5.0 kV, capillary voltage at -12 V, tube lens offset at -121.47 V, capillary temperature at 280°C, sheath gas at 30 (arbitrary unit) and auxiliary gas flow at 10 (arbitrary unit).

Isolation

100 mL of the liquid extract were dried in vacuo; 2.87 g of crude extract were obtained. The dried extract was submitted to a liquid/liquid extraction (BuOH:H₂O), yielding 1.04 g of BuOH extract. Solvent was dried in vacuo and the withered extract dissolved in 8 mL of MeOH and fractionated on a Sephadex LH-20 column (100 x 5 cm), using MeOH as mobile phase, affording 50 fractions (8 mL each), monitored by TLC. Fractions 15 and 16 (44.9 mg) were chromatographed by semipreparative HPLC using MeOH:H₂O (2:3) as mobile phase (flow rate 2.0 mL/min) to yield compound **3** (0.4 mg, R_t = 14.0 min). Fractions 19 and 20 (22.0 mg) were chromatographed by semipreparative HPLC using MeOH:H₂O (12:13) as mobile phase (flow rate 2.0 mL/min) to yield compound **4** (0.5 mg, R_t = 8.4 min). Fractions 22-23 (58.2 mg) were chromatographed by semipreparative HPLC using MeOH:H₂O (12:13) as mobile phase (flow rate 2.0 mL/min) to yield compound **10** (2.3 mg, R_t = 27.0 min). Fractions 24-26 (91.7 mg) were chromatographed by semipreparative HPLC using MeOH:H₂O (12:13) as mobile phase (flow rate 2.0 mL/min) to yield compounds **5** (5.0 mg, R_t = 18 min), **7** (1.5 mg, R_t = 13.5 min) and **9** (3.3 mg, R_t = 25.1 min). Fractions 27 and 28 (25.0 mg) were chromatographed by semipreparative HPLC using MeOH:H₂O (12:13) as mobile phase (flow rate 2.0 mL/min) to yield compound **8** (0.8 mg, R_t = 25.1 min). Fractions 32-33 (15.7 mg) were chromatographed by semipreparative HPLC using MeOH:H₂O (9:11) as mobile phase (flow rate 2.0 mL/min) to yield compounds **11** (0.8 mg, R_t = 31.7 min) and **12** (0.5 mg, R_t = 31.8 min). Fractions 34-36 (20.2 mg) were chromatographed by semipreparative HPLC using MeOH:H₂O (2:3) as mobile phase (flow rate 2.0 mL/min) to yield compounds **1** (1.2 mg, R_t = 8.0 min), **2** (1.1 mg, R_t = 16.0 min) and **6** (0.9 mg, R_t = 26.0 min).

UHPLC-ESI/QTrap/MS/MS quantitative analysis

Quantitative analysis was carried out on instrument reported in general experimental procedures. LC separation was performed on a Phenomenex (Torrance, CA, USA) Luna Omega C18 column (100 x 2.1 mm, 1.6 μ m). The mobile phases were (A) water and (B) acetonitrile, both acidified at 0.1% formic acid. Elution gradient was: 0 min 5% B (held for 0.63 minutes), 9.16 min 23% B (held for 0.92 minutes), 18 min 26% B, 25.62 min 40% B, 27.14 min 100% B (held for 1.53 minutes), 28.82 min 5% B (held for 1.07 minutes). Source temperature was set at 349°C, column temperature was 40°C, flow rate was 0.44 mL/min and injection volume 10 μ L.

Total Phenolic Content

As reported in general experimental procedures.

DPPH• radical scavenging activity

As reported in general experimental procedures.

ABTS^{•+} radical scavenging activity

As reported in general experimental procedures.

NMR analysis

As reported in general experimental procedures.

1.5 References

¹Ammar, I.; Bardaab, S.; Mzidc, M.; Sahnounb, Z.; Rebaaic, T.; Attia, H.; Ennouri, M. Antioxidant, antibacterial and in vivo dermal wound healing effects of *Opuntia* flower extracts. *Int. J. Bio. Macr.* **2015**, 81, 483–490.

²Ammar, I.; Ennouri, M.; Bouaziz, M.; Amira, A. B.; Attia, H. Phenolic profiles, phytochemicals and mineral content of decoction and infusion of *Opuntia ficus-indica* flowers. *Plant Foods for Human Nutr.* **2015**, *70*, 388–394.

Amalesh, S.; Gouranga, D.; Sanjoy, K. Roles of flavonoids in plants. *Int J Pharm Sci Tech* **2011**, *6*.

Atmani, D.; Chaher, N.; Atmani, D.; Berboucha, M.; Debbache, N.; Boudaoud, H. Flavonoids in human health: from structure to biological activity. *Current Nutrition & Food Science*, **2009**, *5*, 225-237.

Benayada, Z.; Martinez-Villaluengaa, C.; Frias, J.; Gomez-Cordovesa, C.; Es-Safi, N. E. Phenolic composition, antioxidant and antiinflammatory activities of extracts from Moroccan *Opuntia ficus-indica* flowers obtained by different extraction methods. *Ind. Crops and Prod.* **2014**, *62*, 412–420.

Cushnie, T. P. T.; Lamb, A. J. Antimicrobial activity of flavonoids. *Int. J. Antimic. Agents.* **2005**, *26*, 343-356.

De Leo, M.; Bruzual De Abreu, M.; Pawlowska, A. M.; Cioni, P. L.; Braca, A. Profiling the chemical content of *Opuntia ficus-indica* flowers by HPLC–PDA-ESI-MS and GC/EIMS analyses. *Phyt. Lett.* **2010**, *3*, 48–52.

Di Lorenzo, F.; Silipo, A.; Molinaro, A.; Parrilli, M.; Schiraldi, C.; D'Agostino, A.; Izzo, E.; Rizza, L.; Bonina, A.; Bonina, F.; et al. The polysaccharide and low molecular weight components of *Opuntia ficus indica* cladodes: structure and skin repairing properties. *Carbohydrate Polymers.* **2017**, *157*, 128-136.

Hyun, S. K.; Jung, Y. J.; Chung, H. Y.; Jung, H. A.; Choi J. S. Isorhamnetin glycosides with free radical and ONOO- scavenging activities from the stamens of *Nelumbo nucifera*. *Arch. Pharm. Res.* **2006**, *29*, 287-292.

Jiang, J. Q.; Ye, W. C.; Chen, Z.; Lou, F. C.; Min, Z. D. Two new phenolic carboxylic acid esters from *Opuntia vulgaris*. *J Chin Pharm Sci*, **2002**, *11*, 1-3.

Kandaswami, C.; Lee, L. T.; Lee, P. P.; Hwang, J. J.; Ke, F. C.; Huang, Y. T.; Lee, M. T. The antitumor activities of flavonoids. *In Vivo.* **2005**, *19*, 895-909.

Kazuma, K.; Noda, N.; Suzuki, M. Malonylated flavonol glycosides from the petals of *Clitoria ternatea*. *Phytochemistry* **2003**, 62, 229–237.

Maier, C.; Conrad, J.; Carle, R.; Weiss, J.; Schweiggert, R. M. Phenolic constituents in commercial aqueous quillaja (*Quillaja saponaria* Molina) wood extracts. *J. Agr. Food Chem.* **2015**, 63, 1756-1762.

Mata, A.; Ferreira, J. P.; Semedo, C.; Serra, T.; Duarte, C. M. M.; Bronze, M. R. Contribution to the characterization of *Opuntia* spp. juices by LC–DAD–ESI/HRMS/MS. *Food Chemistry* **2016**, 210, 558–565.

Matias, A.; Nunes, S. L.; Poejo, J.; Mecha, E.; Serra, A. T.; Madeira, P. J. A.; Bronze, M. R.; Duarte, C. M. M. Antioxidant and antiinflammatory activity of a flavonoid-rich concentrate recovered from *Opuntia ficus-indica* juice. *Food & Function*. **2014**, 5, 3269-3280.

Pietta, P. Flavonoids as antioxidants. *J. Nat. Prod.* **2000**, 63, 1035-1042.

Pitrè, G. *Medicina Popolare Siciliana*. Firenze, Italy: Biblioteca delle Tradizioni Popolari Siciliane, seconda edizione. **1949**. G. Barbèra (Eds.).

Simmler, C.; Antheaume, C.; Andre, P.; Bonte, F.; Lobstein, A. Glucosyloxybenzyl eucomate derivatives from *Vanda teres* stimulate HaCaT Cytochrome c Oxidase, *J. Nat. Prod.* **2011**, 74, 949-955.

Xu, H. X.; Kadota, S.; Kurokawa, M.; Shiraki, K.; Matsumoto, T.; Namba, T. Isolation and structure of woodorien, a new glucoside having antiviral activity, from *Woodwardia orientalis*. *Chem. Pharm. Bull.* **1993**, 41, 1803-1806.

Chapter 2
Phytochemical investigation of PDO *Ficus carica* L.
cv. Dottato leaves

2.1 Introduction

Among the plant species growing in the Mediterranean basin, common fig (*Ficus carica* L.) certainly is one of the most widespread and characteristic, contributing to adorn the Italian landscapes, in particular the meridional coasts. It is a tree belonging to the Moraceae family and originating from Anatolia region, plenty cultivated for the production of its edible fruits. The part commonly considered to be the fruit is named syconium, a fleshy structure representing the inflorescence, with numerous little flowers not visible from the outside. They develop a large number of little achenes, representing the true fruits and forming an infructescence, with a sweet and juicy pulp considered the edible part. Only after ripening, with the tearing of the syconium, the flowers become visible. In most cases figs are eaten fresh, but often they are air-dried and employed for the manufacturing of traditional products. Campania region is famous for typical recipes, as the “fig skewers”, prepared by tucking the dried figs on wooden sticks, sometimes stuffed with almonds and covered with chocolate. For the preparation of such specialities a particular and very appreciated fig variety is employed, named Dottato, cultivated in the Cilento area (Salerno district) and characterized by reduced size, bright peel and pulp, intense and sweet taste. Due to its features and the cultivation site, this fig cultivar has been renamed “Fico bianco del Cilento”, and awarded with the Protected Designation of Origin (PDO) label.

The *Ficus* leaves found several applications in traditional medicine, in particular for treating diabetes, hypertension and to reduce triglycerides levels (Khadabadi et al., 2007; Gond et al., 2008; Perez et al., 1998). This evidence suggests the possible occurrence of phytochemicals with biological activity, prompting a potential use of *F. carica* leaves in secondary applications.

The aim of this work was to investigate the chemical composition of *F. carica* cv. Dottato leaves, in order to determine the bioactive constituents and to valorize such unexploited resource. In fact, to the best of our knowledge, there is only one

study carried out on the Italian cv. Dottato leaves, but originating from Calabria (Marrelli et al., 2014), with no information about the metabolite profile of the cv. Dottato leaves deriving from “Fico bianco del Cilento” PDO production.

Therefore, a comprehensive phytochemical investigation was carried out on *F. carica* cv. Dottato leaves “Fico bianco del Cilento” PDO, leading to the identification of several coumarins, peculiar constituents of the *Ficus* genus, minor phenolic derivatives and glycosylated flavonoids, both *O*- and *C*-glycosylated. In the present chapter, the following topics will be described:

- isolation and characterization by 1D and 2D NMR experiments of the main constituents detected in the LC-ESI/LTQOrbitrap/MS/MS experiments;
- comparison of different extracts by LC-ESI/LTQOrbitrap/MS experiments;
- evaluation of the total phenolic content and radical scavenging activity of the prepared extracts.

***Ficus carica* L. leaves**



The wide and thick leaves are deeply lobed with 3 or 5 lobes, with a dark green color and characterized by a peculiar fragrance.

2.2 Results and discussion

2.2.1 LC-ESI/LTQOrbitrap/MS/MS metabolite profiling of the MeOH extract of F. carica cv. Dottato leaves

The MeOH extract of *F. carica* cv. Dottato leaves was submitted to LC-ESI/LTQOrbitrap/MS/MS experiments in negative ion mode to achieve preliminary information about its chemical composition. The LC-HRMS profile (Fig. 2.1) exhibited several peaks whose accurate m/z values allowed the assignment of their molecular formula (Table 2.1). The analysis of the fragmentation pattern produced in LC-HRMS/MS experiments from each peak and the comparison of mass data with online databases and literature, permitted to putatively identify most of peaks as belonging to four main metabolite classes, i. e. C-glycosylated (**5, 8, 11, 12, 16**) and O-glycosylated flavonoids (**18, 21, 23, 24, 29**), phenolic derivatives (**1-3, 9, 27**) and coumarin derivatives (**6, 7, 10, 13-15, 17, 19, 20, 22, 25, 26, 28, 30-32**) (Table 2.1).

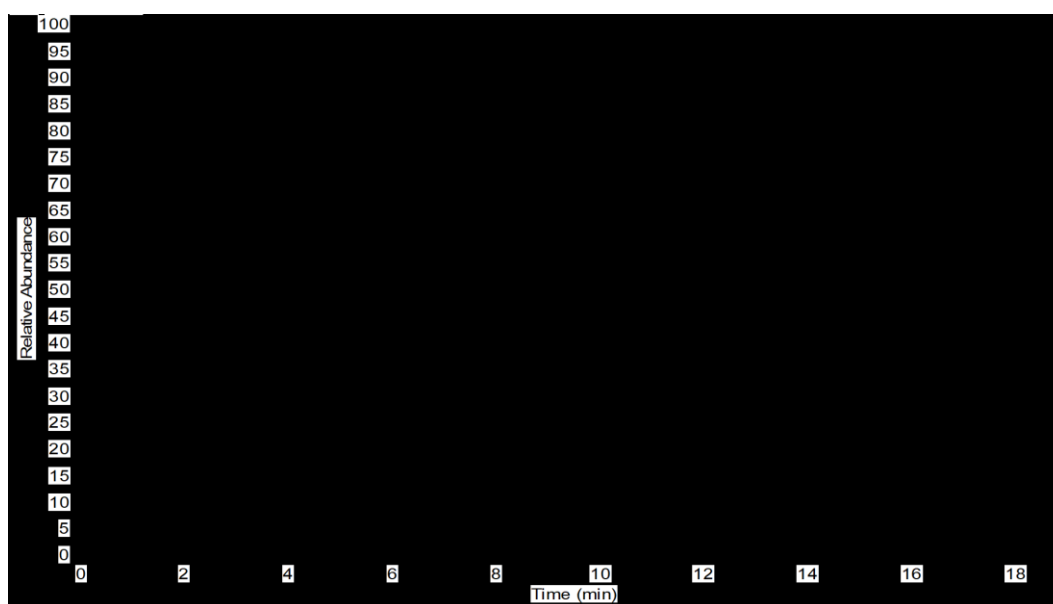


Figure 2.1 LC-HRMS profile in negative ion mode of the MeOH extract of *F. carica* cv. Dottato leaves

Table 2.1 Compounds identified and putatively identified in the MeOH extract of *F. carica* cv. Dottato leaves

N°	R _t	Calculated Mass	[M-H] ⁻	Δppm	MS ² (%)	Molecular Formula	Compound
1	3.81	286.0688	285.0622	0.54	153(100), 152(29), 109(12)	C ₁₂ H ₁₄ O ₈	dihydroxybenzoic acid pentoside
2	4.3	418.1111	417.1043	1.32	285(41), 241(100), 199(23), 153(40)	C ₁₇ H ₂₂ O ₁₂	dihydroxybenzoic acid dipentoside
3	4.58	354.0970	353.0890	1.62	191(100), 179(18), 173(23)	C ₁₆ H ₁₈ O ₉	3- <i>O</i> -caffeoylquinic acid
4	5.5		387.0690		387(100), 365(52), 225(39)		unknown
5	5.87	580.1428	579.1339	1.65	561(18), 519(17), 489(100), 459(97), 399(37), 369(32)	C ₂₆ H ₂₈ O ₁₅	luteolin C-hexoside C-pentoside
6	6.03	366.0950	365.0869	0.32	203(100), 159(32)	C ₁₇ H ₁₈ O ₉	psoralic acid ¹
7	6.21	396.1056	395.0971	0.90	233(61), 201(100), 189(19)	C ₁₈ H ₂₀ O ₁₀	3-[5-(β-D-glucopyranosyloxy)-7-methoxy-6-benzofuranyl]-(2 <i>Z</i>)-2-propenoic acid ¹
8	6.6	564.1479	563.1391	1.30	545(22), 503(36), 473(84), 443(100), 383(29), 353(43)	C ₂₆ H ₂₈ O ₁₄	apigenin C-hexoside C-pentoside
9	6.74	296.0532	295.0463	0.66	179(100), 133(68), 115(10)	C ₁₃ H ₁₂ O ₈	caffeoylmalic acid
10	6.78	364.0794	409.0766	1.47	363(8), 201(100)	C ₁₇ H ₁₆ O ₉	bergaprol hexoside
11	7.07	564.1479	563.1394	0.62	545(15), 503(21), 473(100), 443(81), 383(49), 353(58)	C ₂₆ H ₂₈ O ₁₄	apigenin C-hexoside C-pentoside
12	7.07	448.1005	447.0919	0.32	357(56), 327(100)	C ₂₁ H ₂₀ O ₁₁	luteolin C-hexoside
13	7.26	410.0849	409.0766	0.48	363(9), 201(100)	C ₁₈ H ₁₈ O ₁₁	bergaprol hexoside
14	7.39	368.11073	367.1026	0.55	205(100), 161(12)	C ₁₇ H ₂₀ O ₉	5-(β-D-glucopyranosyloxy)-6-benzofuranpropanoic acid ¹

15	7.73	162.0316	161.0249	1.63	117(100)	C ₉ H ₆ O ₃	umbrelliferone ¹
16	7.88	432.1056	431.0972	0.85	341(7), 311(100)	C ₂₁ H ₂₀ O ₁₀	apigenin C-hexoside
17	7.95	366.0950	365.0868	1.58	203(100), 159(12)	C ₁₇ H ₁₈ O ₉	isopsoralic acid ¹
18	8.05	610.1533	609.1445	1.21	301(100)	C ₂₇ H ₃₀ O ₁₆	quercetin 3- <i>O</i> - β -D-rutinoside ¹
19	8.06	204.0422	203.0354	1.56	159(100)	C ₁₁ H ₈ O ₄	3-(6-hydroxy-5-benzofuranyl)-(<i>E</i>)-2-propenoic acid ¹
20	8.5	396.1056	395.0974	0.22	233(100), 189(11)	C ₁₈ H ₂₀ O ₁₀	3-[5-(β -D-glucopyranosyloxy)-7-methoxy-6-benzofuranyl]-(<i>E</i>)-2-propenoic acid ¹
21	8.58	464.0954	463.0864	1.62	301(100), 300(26), 255(12)	C ₂₁ H ₂₀ O ₁₂	quercetin 3- <i>O</i> - β -D-glucopyranoside ¹
22	8.7	408.1420	407.1333	1.52	227(100)	C ₂₀ H ₂₄ O ₉	marmesinin
23	9.05	594.1584	593.1494	1.20	285(100)	C ₂₇ H ₃₀ O ₁₅	kaempferol <i>O</i> -rutinoside
24	9.55	448.1005	447.0917	1.04	285(100), 284(51)	C ₂₁ H ₂₀ O ₁₁	kaempferol <i>O</i> -hexoside
25	9.74	428.1318	427.1234	0.69	381(100), 219(92), 187(26)	C ₁₉ H ₂₄ O ₁₁	benzofuranpropanoic acid methyl ester hexoside
26	10.22	412.1369	411.1353	1.25	249(100)	C ₁₉ H ₂₄ O ₁₀	methylpicraquassioside A
27	10.46	360.0845	359.0783	1.34	197(38), 179(26), 161(100)	C ₁₈ H ₁₆ O ₈	rosmarinic acid
28	11.5	206.0579	205.0502	1.66	161(100)	C ₁₁ H ₁₀ O ₄	hydroxybenzofuranpropanoic acid
29	12.12	462.1162	461.1096	1.00	299(100)	C ₂₂ H ₂₂ O ₁₁	chrysoeriol <i>O</i> -hexoside
30	12.54	202.0266	201.0198	1.84	173(100)	C ₁₁ H ₆ O ₄	5-hydroxy psoralen ¹
31	14.02	186.0473	185.0384	0.48	141(100), 129(18), 113(24)	C ₁₁ H ₆ O ₃	psoralen ¹
32	16.44	218.0579	217.0487	0.43	202(100), 173(14)	C ₁₂ H ₁₀ O ₄	5-methoxy psoralen ¹

¹The identification of this compound was corroborated by isolation and NMR spectra analysis

In particular, for phenolic derivatives, both compound **1** (m/z 285.0622) and compound **2** (m/z 417.1043) showed in tandem mass spectrum a product ion at m/z 153 and 285, respectively, originated from the neutral loss of a pentosyl moiety (-132 Da), with only compound **2** yielding a further product ion at m/z 153 due to the neutral loss of a second pentosyl moiety (Table 2.1). By considering the assigned molecular formulae (C₁₂H₁₄O₈ for **1** and C₁₇H₂₂O₁₂ for **2**) and the occurrence in MS/MS spectra of a product ion at m/z 109 and 241, respectively, formed by neutral loss of a CO₂ molecule (-44 Da), compounds **1** and **2** could be tentatively assigned as dihydroxybenzoic acid pentoside (**1**) and dihydroxybenzoic acid dipentoside (**2**) in agreement with literature data (Tao et al., 2015) (Table 2.1).

The MS/MS spectrum of compound **3** (m/z 353.0890) showed the characteristic and diagnostic fragmentation pattern of a caffeoylquinic acid derivative, that, in

agreement with scientific literature data, could be putatively identified as 3-*O*-caffeoylquinic acid (Clifford et al., 2003) (Table 2.1).

Compound **9** (m/z 295.0463) yielded a fragmentation pattern characterized by two diagnostic product ions at m/z 179 and 133, originated by the neutral loss of a dehydrated malic acid and a caffeic acid moiety, respectively, so allowing to suggest for **9** the structure of caffeoylmalic acid (Ammar et al., 2015) (Table 2.1).

Furthermore, compound **27** (m/z 359.0783) exhibited in the tandem mass spectrum a base peak at m/z 161 likely corresponding to a dehydrated caffeic acid anion, along with two minor ions at m/z 197 and 179 likely corresponding to a hydroxyhydrocaffeic acid anion and to a caffeic acid anion, respectively, enabling a putative identification of compound **27** as rosmarinic acid (Boudiar et al., 2018) (Table 2.1).

Compounds **18**, **21**, **23**, **24**, and **29** exhibited a molecular formula and fragmentation patterns ascribable to *O*-glycosylated flavonoids, in particular all showing in MS/MS spectrum a base peak corresponding to the aglycone ion and originated by the neutral loss of a hexose moiety (-162 Da) or a hexose-dehydrohexose moiety (-308 Da). Thereby, considering the full HRMS spectrum, the accurate m/z value for each $[M-H]^-$ ion and data present in literature and in database (FoodB), compounds **18**, **21**, **23**, **24**, and **29** were putatively identified as quercetin 3-*O*- β -D-rutinoside, quercetin 3-*O*- β -D-glucopyranoside, kaempferol *O*-rutinoside, kaempferol *O*-hexoside and chrysoeriol *O*-hexoside, respectively (Table 2.1).

Differently, C-glycosylated flavonoids were easily recognized and identified by their highly diagnostic fragmentations, exhibiting peculiar neutral losses of 30, 60, 90 and 120 Da, related to the $^{2,3}A$, $^{0,4}A$, $^{0,3}A$ and $^{0,2}A$ cleavages occurring on the sugar rings, respectively. Jointly with the accurate m/z values determined in HRMS and the calculated molecular formulae, compounds **5**, **8**, **11**, **12**, and **16** were putatively identified as luteolin C-hexoside C-pentoside, apigenin C-hexoside C-

pentoside, apigenin C-hexoside C-pentoside (isomer), luteolin C-hexoside and apigenin C-hexoside, respectively, in agreement with database like FoodB (Table 2.1). On the contrary of their *O*-glycosylated homologous, this class of flavonoids has been underestimated over the years, although an increasing number of publications pointed out a wide range of biological activities, like antioxidant, anticancer, hepatoprotective, antidiabetic, antiinflammatory and antimicrobial, evidencing the beneficial effects for human health (Xiano et al., 2016).

Finally, compounds **6**, **7**, **10**, **13-15**, **17**, **19**, **20**, **22**, **25**, **26**, **28**, **30-32** showed in MS/MS experiments product ions originated by characteristic neutral losses of a carbon dioxide (-44 Da), of water molecules (-18 Da), and of dehydrated hexose moieties (-162 Da) (Table 2.1). On the basis of the structural information achieved from the fragmentation spectra, the accurate *m/z* values and the calculated formulae, compared with data reported in scientific literature and online databases, it was possible to putatively identify the compounds as coumarin derivatives (Table 2.1) (Ammar et al., 2015; Belguith-Hadrichea et al., 2017).

2.2.2 Isolation and characterization

With the aim to unambiguously determine the chemical structure of the main detected constituents, the MeOH extract of *F. carica* cv. Dottato leaves was first fractionated on a Sephadex LH-20 column, and then purified by RP-HPLC-RI and RP-HPLC-UV/Vis. The structure of the isolated molecules was elucidated by 1D and 2D heteronuclear (HSQC, HMBC) NMR experiments, and confirmed by ESI/HRMS/MS experiments.

Compounds **18** and **21** were identified as quercetin 3-*O*- β -D-rutinoside and quercetin 3-*O*- β -D-glucopyranoside, respectively (Fig. 2.2). Such quercetin derivatives have been extensively reported in scientific literature for their several biological activity, like antimicrobial, anticancer and antiviral, but mostly for their intense antioxidant and antiinflammatory properties (Shashank et al., 2013).

Moreover, various coumarin derivatives were identified as psoralic acid (**6**), 3-[5-(β -D-glucopyranosyloxy)-7-methoxy-6-benzofuranyl]-(2Z)-2-propenoic acid (**7**), 5-(β -D-glucopyranosyloxy)-6-benzofuranopropanoic acid (**14**), umbrelliferone (**15**), isopsoralic acid (**17**), 3-(6-hydroxy-5-benzofuranyl)-(E)-2-propenoic acid (**19**), 3-[5-(β -D-glucopyranosyloxy)-7-methoxy-6-benzofuranyl]-(2E)-2-propenoic acid (**20**), 5-hydroxypsoralen (**30**), psoralen (**31**) and 5-methoxypsoralen (**32**) (Fig. 2.2) by an extensive analysis of the 1D and 2D (HSQC, HMBC) NMR spectra and comparing the achieved spectral data with scientific literature (Wei et al., 2011; Luzl et al., 2015; Wei et al., 2014; Trinh et al., 2018; Takahashi et al., 2017; Cheng et al., 2017).

Furanocoumarins are a class of natural compounds characterized by a furan ring fused with a coumarin. They can be grouped into the linear type, where the (dihydro)furan ring is attached at C(6) and C(7), and the angular type, carrying the substitution at C(7) and C(8). Linear furocoumarins, also known as psoralens are principally distributed in four angiosperm families: Apiaceae, Moraceae, Rutaceae and Leguminosae, while the angular (dihydro)furanocoumarins are less widely distributed and primarily confined to the Apiaceae and Leguminosae (Bourgaud et al., 2006). Literature data on *Ficus* genus highlights the occurrence of linear furanocoumarins belonging both to psoralen and pseudopsoralen classes. In detail, psoralen and pseudopsoralen are the 7H-furo[3,2-g]chromen-7-one and the 6H-furo[2,3-g]chromen-6-one, respectively, derived by a different construction of a furan ring on the benzene moiety of coumarin. The chemical investigation of *F. carica* leaves afforded psoralen (**6**, **17**, **19**, **30-32**) and pseudopsoralen derivatives (**7**, **14** and **20**). Compounds **6**, **7**, **14**, **17**, **19** and **20** are coumarin derivatives. Therefore, their numbering is based referring to the coumarin skeleton.

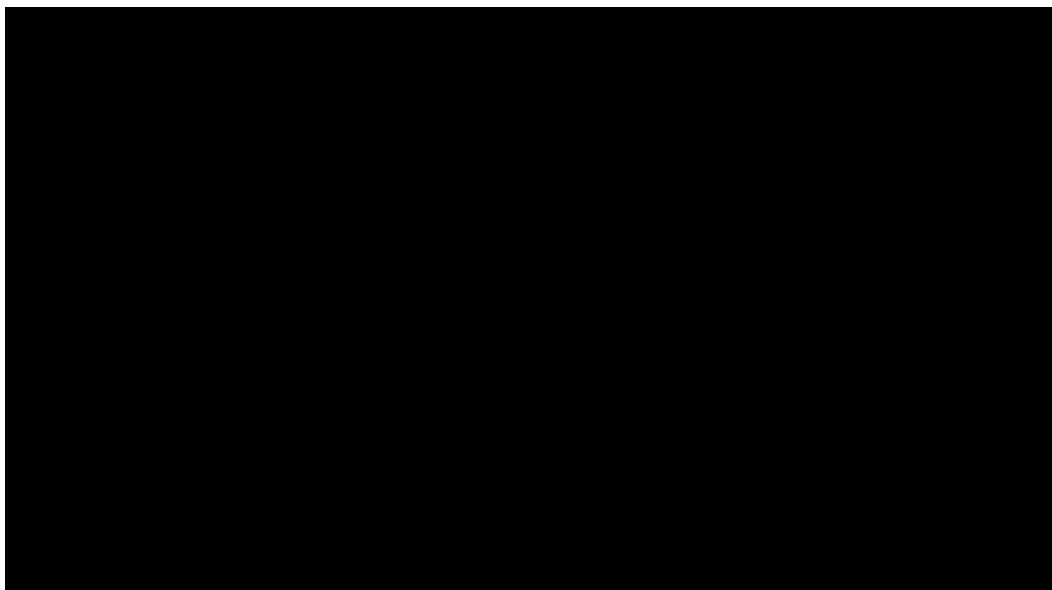


Figure 2.2 Compounds isolated from the MeOH extract of *F. carica* cv. Dottato leaves

The $^1\text{H-NMR}$ spectrum of compound **6** (Fig. 2.3) showed two singlets at δ 7.76 and 7.27, two doublets at δ 7.58 (d, $J = 2.5$ Hz) and at δ 6.66 (d, $J = 2.5$ Hz), typical of a benzofurane ring, confirmed by the correlations of each proton with the germinal carbon observed in the HSQC spectrum (Fig. 2.4). The signal ascribable to H-5 at δ 7.76 (s), exhibited in the HMBC spectrum (Fig. 2.5) correlations with C-4 at δ 131.7, C-7 at δ 154.4, C-9 at δ 152.2 and C-3' at δ 106.7. The $^1\text{H-NMR}$ signals at δ 5.89 and δ 7.15 (H-3 and H-4, respectively), with a J_{Hz} typical of a *cis* olefinic function, showed HMBC correlation with C-2 at δ 173.2, suggesting the occurrence of a *cis*-cinnamic acid derivative. Moreover, $^1\text{H-NMR}$ -spectrum showed an additional signal at δ 4.85 (d, $J = 8.0$ Hz, H-1 Glc), correlating in the HMBC spectrum with C-9 at δ 152.2. The achieved structural information, jointly with data of scientific reports, allowed to identify compound **6** as psoralic acid (Luzl et al., 2015).

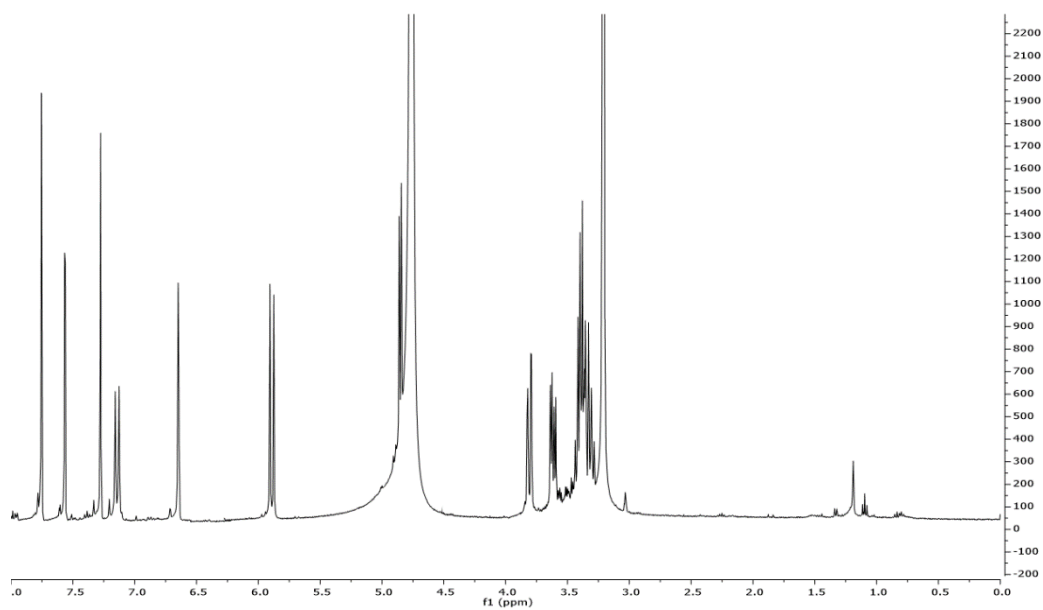
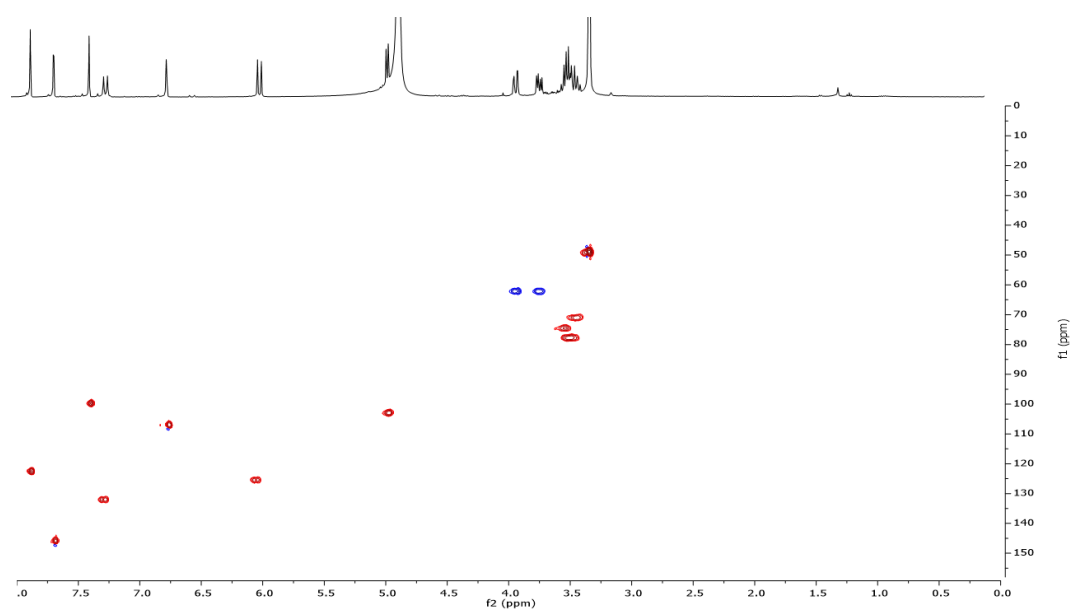
Figure 2.3 ^1H -NMR spectrum of compound 6

Figure 2.4 HSQC spectrum of compound

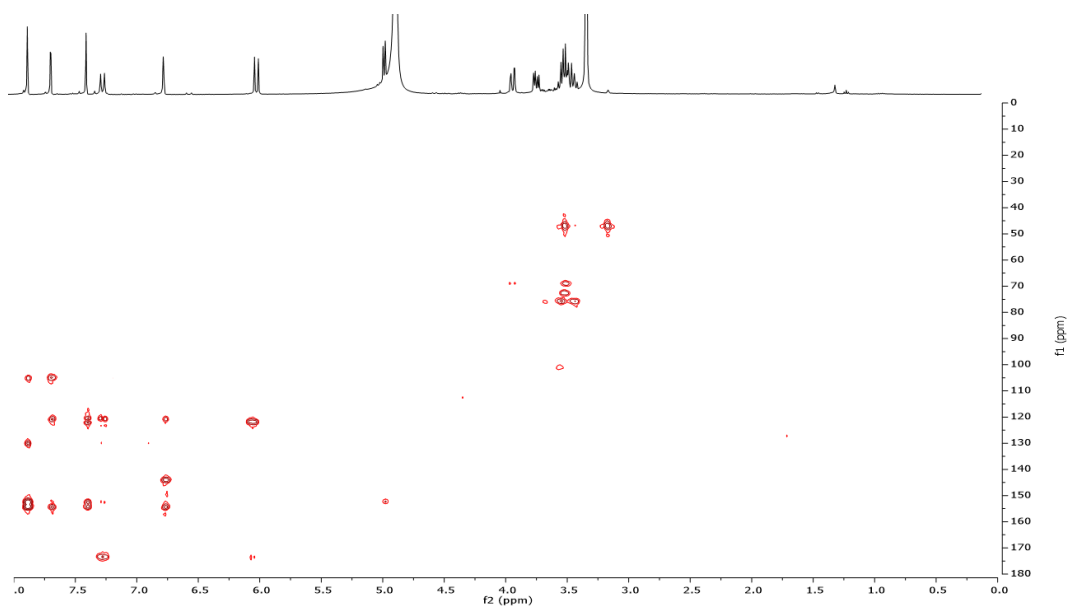


Figure 2.5 HMBC spectrum of compound 6

The ^1H -NMR spectrum of compound 17 (Fig. 2.6) was similar to that observed for compound 6. However, the J_{Hz} constants of the signals at δ 6.49 (d, $J = 16.2$ Hz, H-3) and 7.95 (d, $J = 16.2$ Hz, H-4), pointed out the occurrence of a *trans*-olefinic chain, suggesting compound 17 as isopsoralic acid (Cheng et al., 2017).

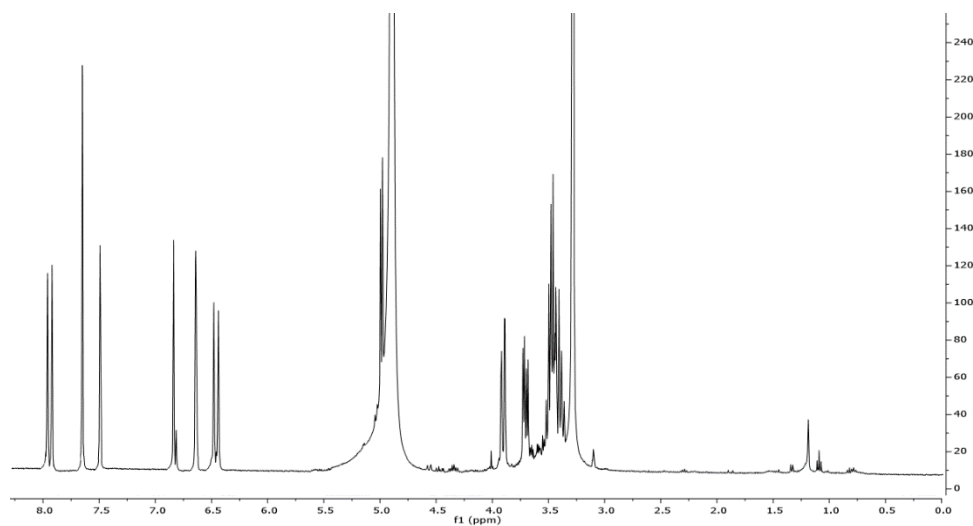


Figure 2.6 ^1H -NMR spectrum of compound 17

The $^1\text{H-NMR}$ spectrum of compound **7** (Fig. 2.7) showed signals at δ 7.11 (s), δ 7.64 (d, $J = 2.3$ Hz) and δ 7.03 (d, $J = 2.3$ Hz), typical of the benzofurane ring, and olefinic protons at δ 6.08 and δ 7.00 (each, d, $J = 12.7$ Hz). Moreover, a signal at δ 4.05 (s), ascribable to a methoxy function, was observed. The comparison of the NMR spectra of compounds **6** and **7** revealed the absence of the singlet proton H-5, replaced by a methoxyl function. The analysis of the HMBC correlations suggested a different construction of a furan ring on the benzene moiety respect to compound **6**. In detail, the HMBC spectrum (Fig. 2.9) showed correlations between the proton signal at δ 7.11 (H-8) with the carbon resonance at δ 157.1 (C-6), δ 154.1 (C-9), δ 114.3 (C-10) and at δ 105.5 (C-2'). The absence of further correlations with C-5 prompted us to establish for compound **7** pseudopsoralen-like structure. Finally, the $^1\text{H-NMR}$ spectrum showed an additional signal at δ 4.98 (d, $J = 7.8$ Hz, H-1 Glc), correlating in the HMBC spectrum with C-9 (δ 154.1). Thus, compound **7** was identified as 3-[5-(β -D-glucopyranosyloxy)-7-methoxy-6-benzofuranyl]-(2Z)-2-propenoic acid (Wei et al., 2014).

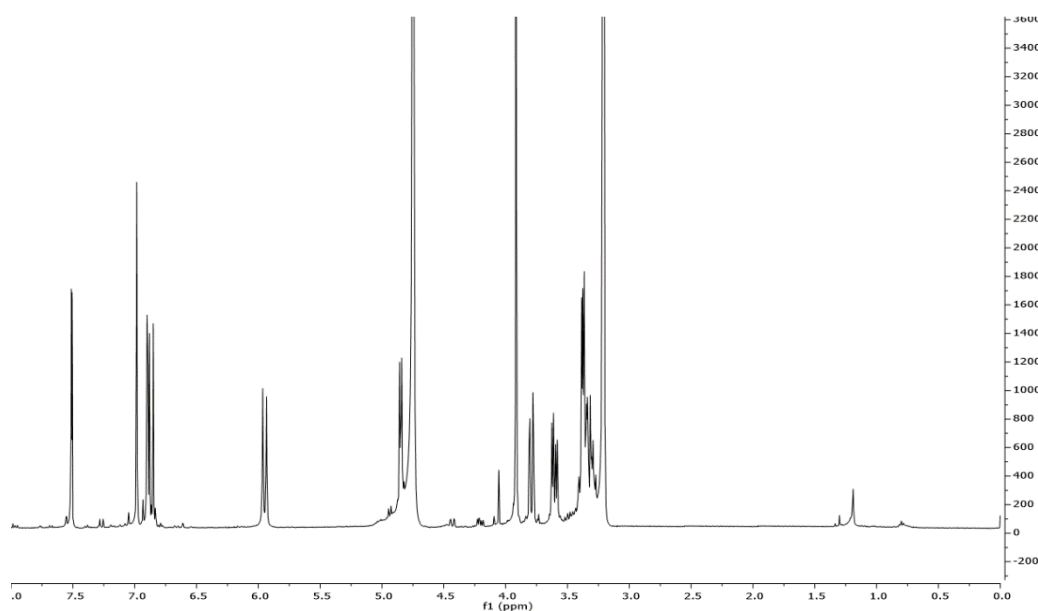


Figure 2.7 $^1\text{H-NMR}$ spectrum of compound **7**

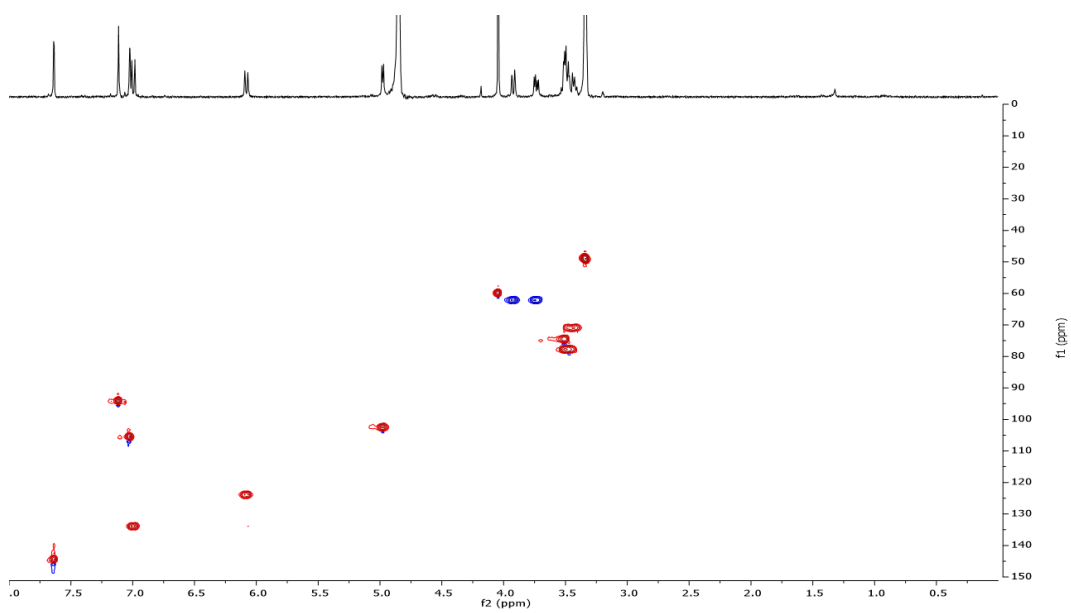


Figure 2.8 HSQC spectrum of compound 7

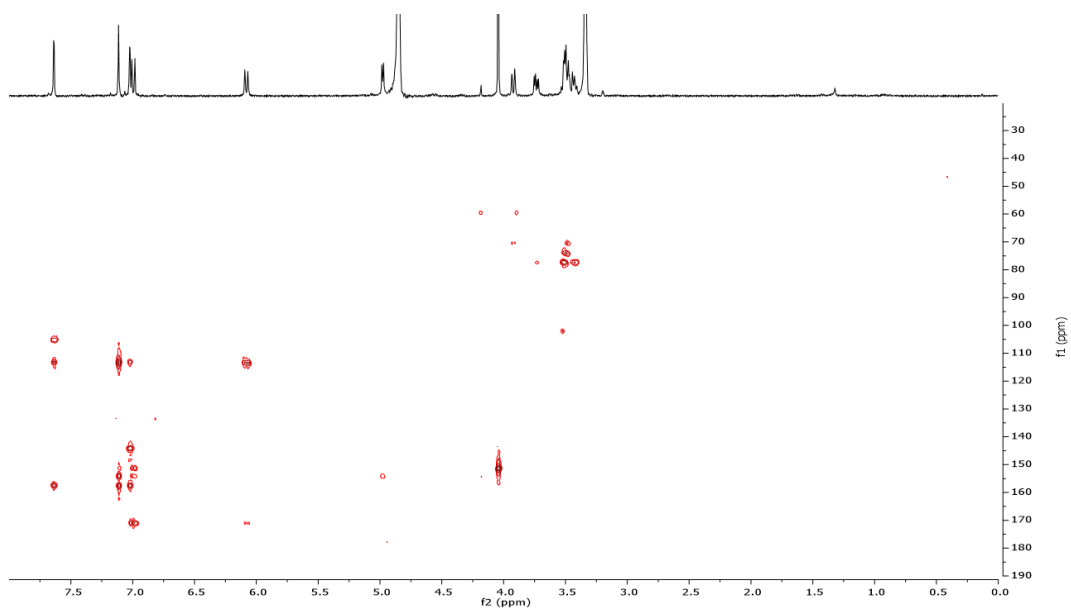


Figure 2.9 HMBC spectrum of compound 7

NMR data of compound **20** (Fig. 2.10) suggested that it differed from **7** only for the *trans* configuration of the olefinic function. Thus it was identified as 3-[5-(β -D-glucopyranosyloxy)-7-methoxy-6-benzofuranyl]-(2E)-2-propenoic acid (Trinh et al., 2018).

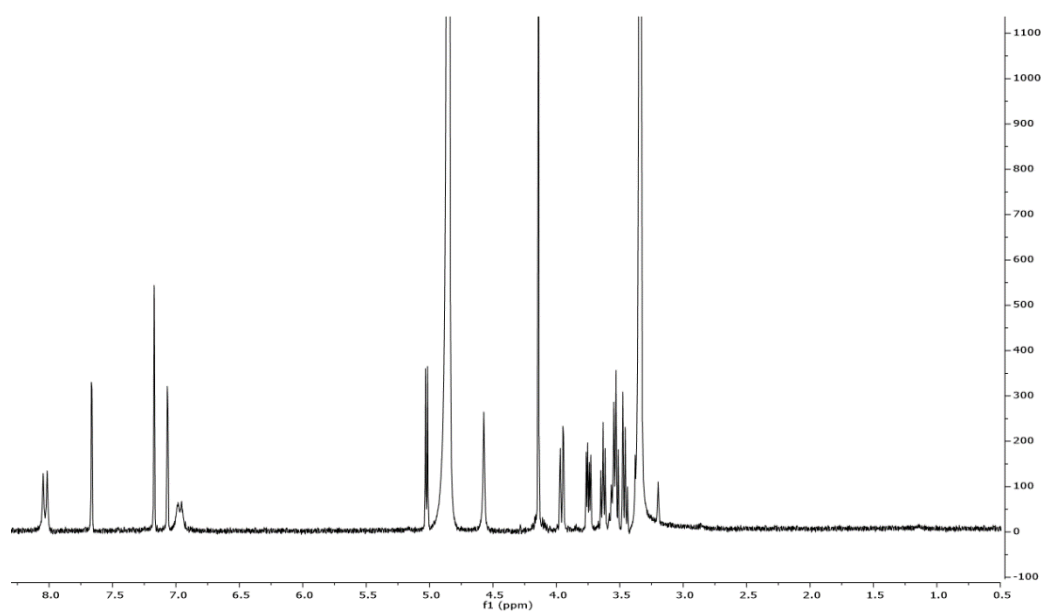


Figure 2.10 ¹H-NMR spectrum of compound **20**

Table 2.2 ^1H (600 MHz) and ^{13}C (150 MHz) NMR spectral data of compounds **6** and **7**

	6		7	
	δ_{C}	δ_{H} (J in Hz)	δ_{C}	δ_{H} (J in Hz)
1	-	-	-	-
2	173.2	-	170.8	-
3	125.5	5.89, d(12.4)	123.7	6.08, d(12.7)
4	131.7	7.15, d(12.4)	133.8	7.00, d(12.7)
5	122.2	7.76, s	151.4	-
6	123.2	-	157.1	-
7	154.4	-	113.0	-
8	99.6	7.27, s	94.1	7.11, s
9	152.2	-	154.1	-
10	129.6	-	114.3	-
2'	145.5	7.58, d(2.5)	105.5	7.03, d(2.3)
3'	106.7	6.66, d(2.5)	144.2	7.64, d(2.3)
Glc				
1	103.1	4.85, d(8.0)	102.1	4.98, d(7.8)
2	74.4	3.32, m	74.4	3.50, m
3	77.6	3.36, m	77.9	3.51, m
4	71.0	3.41, m	70.8	3.44, m
5	77.9	3.35, m	78.0	3.46, m
6	61.8	3.81, dd(2.1, 12.1) 3.62, dd(5.4, 12.1)	62.1	3.74, dd(5.5, 12.4) 3.92, dd(1.4, 12.4)
MeO			59.4	4.05, s

In MeOH- d_4

2.2.3 Coumarins

Coumarins are phenylpropanoid derivatives, originating from an *ortho*-hydroxylation followed by a cyclization occurring between the hydroxy and the carboxylic groups, with consequent loss of a water molecule. These biosynthetic steps generate the main backbone, which can be target of further substitutions and cyclizations, yielding different sub-classes like prenylated coumarins, linear furanocoumarins, methylenedioxy-coumarins, pyranocoumarins and angular furanocoumarins (Bourgaud et al., 2006) (Fig. 2.11).

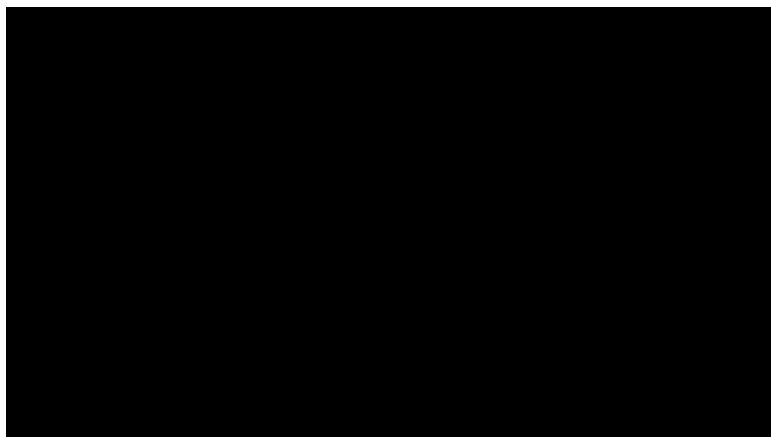


Figure 2.11 Most common coumarin classes

Their occurrence has been reported in several species belonging to *Ficus* genus (Wei et al., 2001; Trinh et al., 2018; Duan et al., 2018; Marrelli et al., 2014), and different biological activities were attributed to this class of compounds.

They showed to possess good antioxidant and radical scavenging properties (Al-Majedy et al., 2017), as well as potential anticancer activity (Thakur et al., 2015). However, coumarins are since long and mainly reported as powerful anticoagulants, due to their inhibitory effects on the vitamin K epoxide reductase, blocking the hepatic synthesis of several clotting factors (Lowenthal & Birnbaum, 1969). This interesting activity shown by coumarins led to their direct employment in anticoagulant therapy, aimed at controlling blood fluidity, and to a production of several synthetic analogues, finalized to enhance their efficacy and to reduce the main side effects, as hepatotoxicity (Kubrak et al., 2017). On the other hand, the anticoagulant properties made coumarins widely exploited for long time as rodenticides; notwithstanding, their massive use in disinfestations generated a concerning resistance of the survived animals and related offspring towards this class of compounds, resulting less effective and highlighting the need for new derivatives, mainly synthetically produced (Valchev et al., 2008).

Moreover, many coumarins showed to possess sunscreensing properties, while certain subclasses, as furanocoumarins, exhibited photosensitizing activity; however, it was taken advantage from this last one activity, leading to their successful employment in the treatment of vitiligo and psoriasis (Kasperkiewicz et al., 2016).

In addition, due to their noteworthy biological activities, many research groups showed great interest towards them, producing synthetic analogues which showed a noteworthy *in vitro* efficacy in inhibiting the TNF- α expression. Further derivatives proved to possess promising anticancer activity, along with the capacity to inhibit Monoamine Oxidase A and B (MAO-A/B) and acetylcholinesterase (AChE), suggesting a potential employment in the treatment of Alzheimer's disease (Li et al., 2012; Togna et al., 2014; Hirsh et al., 2001; Viña et al., 2012; Xie et al., 2013).

2.2.4 "Eco-friendly" extractions and comparison of their chemical composition by LC-ESI/LTQOrbitrap/MS experiments

F. carica leaves have been widely used in traditional medicine for the preparation of remedies as infusions to counteract adverse health conditions, in particular for treating diabetes and hypercholesterolemia. This kind of extraction method results compatible with human consumption, as well as for application in other fields. In order to propose extraction protocols suitable with the manufacturing of nutraceutical and cosmetic formulations, as well as human consumption, and moreover employing solvents relatively cheap, non-toxic and easily available, besides infusion, other typologies of extracts were prepared, and their chemical composition compared by LC-ESI/LTQOrbitrap/MS experiments.

For the preparation, ethanol (EtOH) 96% and water were employed. The dried leaves were extracted by maceration with EtOH 96% and an ethanol:water (EtOH:H₂O) (1:1, v/v) solution, while decoction and infusion were prepared by

using only water. The operative procedures were experimentally optimized, starting from protocols described in scientific reports.

The comparison of the LC-HRMS profiles (Fig. 2.12), acquired in negative ion mode, pointed out interesting differences among the employed methods, highlighting a discreet selectivity towards determined chemical classes.

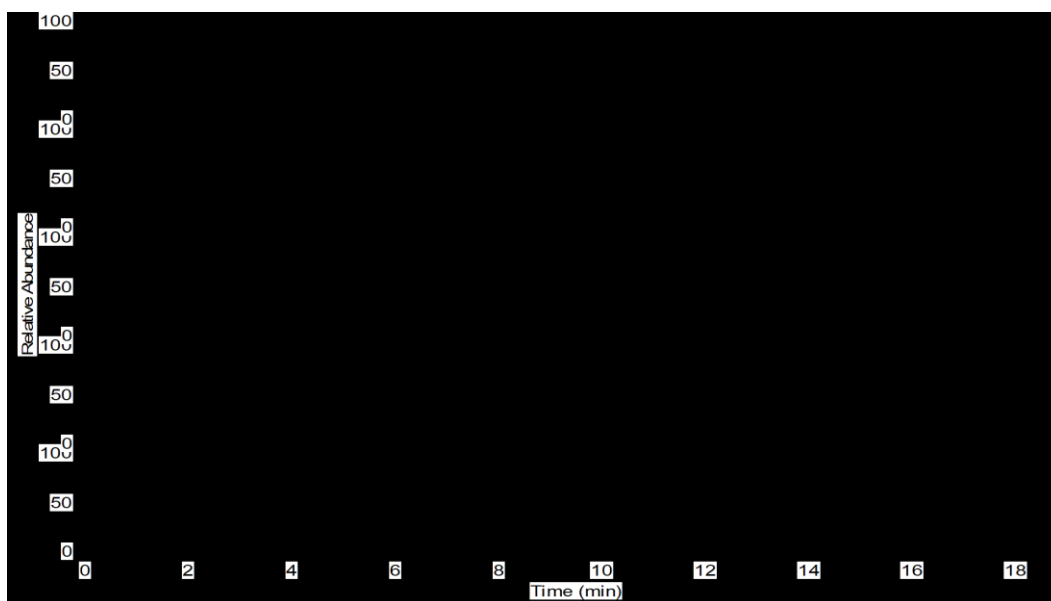


Figure 2.12 Comparison of LC-HRMS profiles, in negative ion mode, of the MeOH, EtOH, EtOH:H₂O extracts, infusion and decoction obtained from *F. carica* cv. Dottato leaves

In particular, EtOH and infusion resulted effective in extracting coumarins **6** and **7**, while the peak related to the C-glycosylated flavonoid **8** resulted more intense in decoction, even if, along with compound **9**, it was also evident in infusion and EtOH:H₂O extract. Similarly, coumarin **26** and compound **3** were detected in EtOH:H₂O extract, infusion and decoction; furthermore, in these last two, as well as in the EtOH extract, the peak ascribable to coumarin **14** was observed. Common feature to all the “eco-friendly” extracts was the occurrence of flavonoid **18** as major constituent.

These discussed results evidenced a good selectivity of the employed extraction methods towards phenolics, suggesting the employment of *F. carica* cv. Dottato

leaves for the manufacturing of herbal preparations with potential beneficial effects for human health.

2.2.5 Total phenolic content and radical scavenging activity of the different extracts of *F. carica* cv. Dottato leaves

The prepared extracts were tested to assess their total phenolic content (Table 2.3), and the results evidenced the EtOH:H₂O extract as the richest one in phenolics (76.42 ± 4.97 GAE mg/g dried extract), if compared to the others. The following evaluation of the radical scavenging activity, performed by DPPH• and ABTS^{•+} assays, confirmed it as the best one, since exerting the strongest activity (IC₅₀ = 55.20 ± 8.47 µg/mL and TEAC = 0.24 ± 0.02 mM) in comparison to the remaining extracts (Table 2.3). Thus, maceration by using the EtOH:H₂O (1:1, v/v) solution resulted the best method to prepare an extract with the highest phenolic content and antioxidant activity, among the proposed extraction methods.

Table 2.3 Total phenolic content, DPPH• and ABTS^{•+} radical scavenging activity of the different extracts of *F. carica* cv. Dottato leaves

Sample	Total phenolic content		DPPH•		ABTS ^{•+}	
	GAE ^a	SD ^d	IC ₅₀ ^b	SD ^d	TEAC ^c	SD ^d
MeOH	44.57	± 4.97	121.52	± 14.35	0.14	± 0.02
EtOH	31.79	± 1.15	213.28	± 35.40	0.06	± 0.01
EtOH:H ₂ O	76.42	± 4.97	55.20	± 8.47	0.24	± 0.02
Infusion	54.20	± 4.72	55.53	± 9.62	0.16	± 0.03
Decoction	26.61	± 3.89	66.61	± 6.57	0.09	± 0.01
Vit. C			5.16	± 0.11		
Quercetin					1.87	± 0.08

^a Values are expressed as gallic acid equivalents (GAE) mg/g of dried extract. ^b Values are expressed as µg/mL. ^c Values are expressed as concentration (mM) of a standard Trolox solution exerting the same antioxidant activity of a 1 mg/mL solution of the tested extract. ^d Standard Deviation of three independent experiments.

2.3 Conclusions

The accurate analysis of the LC-HRMS and LC-HRMS/MS spectra acquired for the MeOH extract of *F. carica* L. cv. Dottato leaves highlighted the occurrence of several coumarin derivatives, *O*-glycosylated and C-glycosylated flavonoids, and phenolic acids putatively identified on the basis of their spectral data compared with those reported in scientific literature.

The phytochemical investigation of the MeOH extract allowed the isolation and characterization of ten coumarins and two *O*-glycosylated flavonoids.

Moreover, EtOH:H₂O extract showed to possess a discreet phenolic content, as well as antioxidant activity.

The obtained results may support a potential employment of *F. carica* cv. Dottato leaves as a valuable source of bioactives for secondary scopes.

2.4 Experimental section

Plant material

The *F. carica* cv. Dottato leaves were collected in Prignano Cilento, Salerno, Italy, in September 2016, and air dried.

Chromatographic purification

Column chromatography was performed on Sephadex LH-20 (Pharmacia). HPLC-RI separations were performed on instrument described in general experimental procedures, using a Knauer Eurospher 100-10 C-18 column (300 x 8 mm, 10 μm). HPLC-UV/Vis separations were performed on instrument described in general experimental procedures, using a Phenomenex (Torrance, CA, USA) Synergi Hydro RP-80A column (250 x 10 mm, 10μ).

LC-ESI/LTQOrbitrap/MS/MS and LC-ESI/LTQOrbitrap/MS procedures

LC-HRMS experiments were carried out on instrument reported in general experimental procedures. LC separation was performed on a Phenomenex (Torrance, CA, USA) Kinetex EVO C-18 column (100 x 2.1 mm, 5 μ m), at a flow rate of 0.2 mL/min and a mobile phase consisting of water with 0.1% formic acid as eluent A and acetonitrile with 0.1% formic acid as eluent B. Elution gradient was from 10% B to 48% B in 19 min, returning to the starting conditions in 5 min. Injection volume was 2 μ L, keeping column at room temperature.

The ESI source parameters were set as following: source voltage at 5.0 kV, capillary voltage at -12 V, tube lens offset at -121.47 V, capillary temperature at 280 °C, sheath gas at 30 (arbitrary units) and auxiliary gas at 5 (arbitrary units).

Extraction and isolation

800.75 g of dried leaves were extracted by maceration using solvents with increasing polarity: petroleum ether (2.0 L, three times for three days), chloroform (1.7 L, three times for three days) and MeOH (1.8 L, three times for three days), affording 81.80 g of crude MeOH extract.

“Eco-friendly” extraction methods were prepared as following. 5.0 g of dried leaves were extracted with 150 mL of EtOH and EtOH:H₂O (1:1, v/v) solution by maceration, three times for three days, yielding 147.10 mg and 75.21 mg of crude extracts, respectively. Infusion was prepared by pouring 150 mL of boiling water to 5.0 g of dried leaves, and kept for 8 min followed by filtration, affording 681.26 mg of crude extract. Decoction was prepared by adding 5.0 g of dried leaves to 150 mL of cold water and heated till boiling point, held for 8 min, followed by filtration, yielding 634.17 mg of crude extracts.

For isolation procedures, 3.5 g of crude MeOH extract were dissolved in 8 mL of MeOH and fractionated on a Sephadex LH-20 column (100 x 5 cm), using MeOH as mobile phase, affording 65 fractions of 8 mL each, monitored by TLC.

Fractions 23-26 were chromatographed by RP-HPLC-RI using MeOH:H₂O (9:11) as mobile phase (flow rate 2.0 mL/min) to yield compounds **15** (2.6 mg, R_t = 8.2 min), **31** (2.9 mg, R_t = 16.4 min) and **32** (1.9 mg, R_t = 28.2 min). Fractions 27-32 were chromatographed by RP-HPLC-UV/Vis (elution gradient: 0 min 10% B, 30 min 100% B, 40 min 100% B; wavelength: 310 nm) to yield compounds **18** (1.7 mg, R_t = 14.6 min), compound **17** (2.0 mg, R_t = 15.7 min), compound **19** (1.8 mg, R_t = 20.4 min), compound **21** (1.7 mg, R_t = 20.6 min) and compound **30** (2.3 mg, R_t = 21.6 min). Fractions 19-22 were chromatographed by RP-HPLC-UV/Vis (elution gradient: 0 min 10% B, 15 min 20% B, held for 15 min, 60 min 100% B, 70 min 100% B; wavelength: 290 nm) yielding compounds **6** (2.1 mg, R_t = 29.1 min), **7** (1.8 mg, R_t = 30.2 min) and **14** (2.2 mg, R_t = 40.0 min). Fractions 10-13 were chromatographed by RP-HPLC-UV/Vis (elution gradient: 0 min 10% B, 13 min 49% B, 40 min 85% B, 45 min 100% B, 55 min 100% B; wavelength: 290 nm) yielding compound **20** (2.8 mg, R_t = 15.7 min).

Total Phenolic Content

As reported in general experimental procedures.

DPPH• radical scavenging activity

As reported in general experimental procedures.

ABTS^{•+} radical scavenging activity

As reported in general experimental procedures.

NMR analysis

As reported in general experimental procedures.

2.5 References

Al-Majedy, Y.; Al-Amiery, A.; Kadhum, A. A.; Mohamad, A. B. Antioxidant activity of coumarins. *Sys Rev Pharm.* **2017**, 8, 24-30.

Ammar, S. Contreras, M. M.; Belguith-Hadrich, O.; Bouaziz, M.; Segura-Carretero, A. New insights into the qualitative phenolic profile of *Ficus carica* L. fruits and leaves from Tunisia using ultra-high-performance liquid chromatography coupled to quadrupole-time-of-flight mass spectrometry and their antioxidant activity. *Royal Soc. Chem.* **2015**, 5, 20035-20050.

Belguith-Hadrichea, O.; Ammarb, S.; Contrerasc, M. M.; Fetouie, H.; Segura-Carreteroc, A.; El Fekia, A; Bouazizb, M. HPLC-DAD-QTOF-MS profiling of phenolics from leaf extracts of two Tunisian fig cultivars: Potential as a functional food. *Biomed. & Pharmacotherapy.* **2017**, 89, 185–193.

Boudiar, T.; Lozano-Sanchez, J.; Harfi, B.; del Mar Contreras-G'mez, M.; Segura-Carretero, A. Phytochemical characterization of bioactive compounds composition of *Rosmarinus eriocalyx* by RP-HPLC-ESI-QTOF-MS. *Nat. Prod. Res.* **2018**, Ahead of Print.

Bourgaud, F.; Hehn, A.; Larbat, R.; et al. Biosynthesis of coumarins in plants: a major pathway still to be unravelled for cytochrome P450 enzymes. *Phytochem Rev* **2006**, 5, 293-308.

Cheng, J.; Yi, X.; Wang, Y.; Huang, X.; He, X.. Phenolics from the roots of hairy fig (*Ficus hirta* Vahl.) exert prominent antiinflammatory activity. *J. Funct. Foods* **2017**, 31, 79-88.

Clifford, M N.; Johnston, K. L.; Kknight, S.; Kuhnert, N. Hierarchical scheme for lc-msn identification of chlorogenic acids. *J. Agric. Food Chem.* **2003**, 51, 2900-2911.

Duan, S.; Zhang, J.; Han, Q.; Zhang, Q.; Liang, H. A new coumarin and a new norlignan from *Ficus tsiangii*. *J. Asian Nat. Prod. Res.* **2018**.

Gond, N. Y.; Khadabadi, S. S., Hepatoprotective activity of *Ficus carica* leaf extract on rifampicin-induced hepatic damage in rats. *Indian J. Pharm. Sci.* **2008**, *70*, 364–366.

Hirsh, J.; Dalen, J. E.; Anderson, D. R.; Poller, L.; Bussey, H.; Ansell, J.; et al. Oral anticoagulants: mechanism of action, clinical effectiveness, and optimal therapeutic range. *Chest J.* **2001**, *119*, 8-21.

Kaspekiewicz, K.; Erkiert-Polguj, A.; Budzisz, E. Sunscreening and photosensitizing properties of coumarins and their derivatives. *Lett. Drug Design Disc.* **2016**, *13*, 465-474.

Khadabadi, S. S.; Gond, N. Y.; Ghiware, N. B.; Shendarkar, G. R. Hepatoprotective effect of *Ficus carica* leaf in chronic hepatitis. *Indian Drugs.* **2007**, *44*, 54–57.

Kubrak, T.; Podgorski, R.; Stompor, M. Natural and synthetic coumarins and their pharmacological activity. *Eur. J. Clin. Exp. Med.* **2017**, *15*, 169-175.

Li, Z.; Hu, J.; Sun, M.; Ji, H.; Chu, S.; Liu, G.; et al. Antiinflammatory effect of IMMLG5521, a coumarin derivative, on Sephadex-induced lung inflammation in rats. *Int.l Immunopharm.* **2012**, *14*, 145-149.

Lowenthal, J.; Birnbaum, H. Vitamin K and coumarin anticoagulants: dependence of anticoagulant effect on inhibition of vitamin K transport. *Science.* **1969**, *164*, 181-183.

Luz1, R. F.; Vieira1, I. J. C.; Braz-Filho, R.; Moreira, V. F. ¹³C-NMR data from coumarins from moraceae family. *Amer. J. Anal. Chem.* **2015**, *6*, 851-866.

Marrelli, M.; Statti, G. A.; Tundis, R.; Menichini, F.; Conforti, F. Fatty acids, coumarins and polyphenolic compounds of *Ficus carica* L. cv. Dottato: variation of bioactive compounds and biological activity of aerial parts. *Nat. Prod. Res.* **2014**, *28*, 271–274.

Perez, C.; Dom'inguez, E.; Ramiro, J. M.; Romero, A.; Campillo, J. E.; Torres, M. D. A study on the glycaemic balance in streptozotocin-diabetic rats treated with an aqueous extract of *Ficus carica* (fig tree) leaves. *Phytotherapy Research*. **1998**, 10, 82–83.

Shashank, K.; Abhay, P. K. Chemistry and biological activities of flavonoids: an overview. *The Scientific World Journal*. **2013**, 162750.

Takahashi, T.; Okiura, A.; Kohno, M. Phenylpropanoid composition in fig (*Ficus carica* L.) leaves. *J. Nat. Med.* **2017**, 71, 770-775.

Tao, Y.; Cai, H.; Li, W.; Cai, B. Ultrafiltration coupled with high-performance liquid chromatography and quadrupole-time-of-flight mass spectrometry for screening lipase binders from different extracts of *Dendrobium officinale*. *Anal. Bioanal. Chem.* **2015**, 407, 6081-6093.

Thakur, A.; Singla, R.; Jaitak, V. Coumarins as anticancer agents: A review on synthetic strategies, mechanism of action and SAR studies. *Eur. J. Med. Chem.* **2015**, 101, 476-495.

Togna, A. R.; Firuzi, O.; Latina, V.; Parmar, V. S.; Prasad, A. K.; Salemme, A. et al. 4-Methylcoumarin derivatives with antiinflammatory effects in activated microglial cells. *Bio. Pharm. Bull.* **2014**, 37, 60-66.

Trinh, P. H. N.; An, N. H.; An, P. N.; Tri, M. D.; Du, C. V.; Minh, P. N.; Thuy, N. T. L.; Tuan, N. T.; Thoa, V. T. K.; Tuan, N. N.; Dung, L. T. A new benzofuran derivative from the leaves of *Ficus pumila* L. *Nat. Prod. Res.*, **2018**, 32, 1648–1652.

Valchev, I.; Binev, R.; Yordanova, V.; Nikolov, Y. Anticoagulant rodenticide intoxication in animals – A Review. *Turk. J. Vet. Anim. Sci.* **2008**, 32, 237-243.

Viña, D.; Matos, M. J.; Yáñez, M.; Santana, L.; Uriarte, E. 3- Substituted coumarins as dual inhibitors of AChE and MAO for the treatment of Alzheimer's disease. *Med. Chem. Comm.* **2012**, 3, 213-218.

Wei, S.; Luan, J.; Lu, L.; Wu, W.; Ji, Z. A new benzofuran glucoside from *Ficus tikoua* Bur. *Int. J. Mol. Sci.* **2011**, 12, 4946-4952.

Wei, S.; Zhang, J.; Wu, W.; Ji, Z. Water-soluble constituents of *Ficus tikoua*. *Chem. Nat. Comp.* **2014**, 49.

Xiao, J.; Capanoglu, E.; Jassbi, A. R.; Miron, A. Advance on the flavonoid c-glycosides and health benefits. *Critical Rev. Food Sci. Nutr.* **2016**, 56, 29–45.

Xie, S.S.; Wang, X. B.; Li, J. Y.; Yang, L.; Kong, L. Y. Design, synthesis and evaluation of novel tacrine–coumarin hybrids as multifunctional cholinesterase inhibitors against Alzheimer's disease. *Eur. J. Med. Chem.* **2013**, 64, 540-553.

Yang, Y.; Ying, S.; Li, T.; Zhen, J.; Chen, D.; Wang, J. A sensitive LC–MS/MS-based bioanalytical method for quantification of salviaflaside and rosmarinic acid in rat plasma and its application in a pharmacokinetic study. *Biomed. Chrom.* **2018**, 32, 4259.

Chapter 3

Polar constituents, multi-class polar lipids and free fatty acids profiling of almonds (*Prunus dulcis* Mill. cvs. Toritto and Avola) by LC-ESI/HRMS/MS and GC-FID

3.1 Introduction

Almonds are among the most consumed nuts, not only fresh as they are, but mainly employed in cookery, pastry and confectionery. Besides the pleasant flavor which makes them highly appreciated, more and more scientific reports have pointed out their beneficial effects for human health. Such benefits resulted ascribable to the content of MonoUnsaturated Fatty Acids (MUFA) and PolyUnsaturated Fatty Acids (PUFA), reported for their capacity to reduce hematic Low Density Lypoproteins (LDL) and to enhance the High Density Lypoproteins (HDL) levels (Kamil et al., 2012; Ander et al., 2003).

Although much is known about the oily fraction, less information are available about polar lipids like phospholipids, which are not only part of biosynthetic pathways, but showed *in vivo* to ameliorate liver lipid metabolism and to counteract atherosclerosis onset (Wat et al., 2009).

Almonds find main applications in pastry and confectionery, for the manufacturing of typical recipes. For aesthetic and taste reasons, due to their use for decorations and confetti production, they are provided peeled and roasted.

Before roasting, almonds undergo peeling operations, consisting in exposing them to hot water steam in a rotating drum, allowing an easy skin removal by using a further rotating drum equipped with brushes; finally, peeled almonds are air dried and occasionally stirred. The described operations allow to easily obtain peeled almonds, although two collateral products originate from this workflow, represented by the removed integuments and the water used for blanching. Such by-products are usually discarded, even if almond skins are sometimes given to animals as fodder, and their disposal costs affect the finances of the producers, with repercussions on the final prize.

Moreover, it has been proved that the different growth conditions typical of a peculiar geographical area, such as soil, temperature, rainfalls, may affect the

metabolome of a plant species, and consequently foodstuff nutritive values (Wang et al., 2001; Brunsgaard et al., 1994).

Therefore, a comprehensive phytochemical investigation based on LC-HRMS analytical methods was carried out on *P. dulcis* (cvs. Toritto and Avola) seeds, aiming at defining the metabolite profile, focusing the attention on polar constituents. Moreover, lipidome of *P. dulcis* seeds (cvs. Toritto and Avola) was investigated to determine the main non-polar constituents, with particular interest addressed to polar lipids and free fatty acids. Finally, raw data of LC-HRMS experiments deriving from the non-polar fraction investigation were processed by multivariate statistical analysis techniques to achieve a rapid and simple data interpretation.

In this chapter the following topics will be discussed:

- LC-ESI/LTQOrbitrap/MS/MS metabolite profiling of *P. dulcis* cv. Toritto seeds, focusing on polar constituents;
- comparison of “eco-friendly” extracts by LC-ESI/LTQOrbitrap/MS experiments;
- chemical composition assessment of *P. dulcis* seeds main products and by-products of almond peeling process;
- comparison of the metabolite profiles of *P. dulcis* cv. Toritto seeds and cvs. Fascionello, Pizzuta and Romana;
- evaluation of radical scavenging activity and total phenolic content of the prepared extracts;
- lipidome profiling of *P. dulcis* cvs. Toritto and Avola seeds, achieved by LC-ESI/QToF/MS/MS experiments for polar lipids, and GC-FID analysis for free fatty acids;
- final raw data processing by multivariate data analysis approach for a quick and informative data interpretation.

3.2 LC-ESI/LTQOrbitrap/MS/MS based approach for a quick and exhaustive metabolite screening of the polar constituents of *P. dulcis* cv. Toritto seeds

Prunus dulcis Mill. seeds



The seeds are obovate, bright beige colored and enveloped in a brown wrinkled integument. The shape may differ according to the varieties.

3.2.1 Results and discussion

3.2.1.1 LC-ESI/HRMS/MS profiling of almond kernels

In order to achieve an overview on the main polar constituents of *P. dulcis* cv. Toritto seeds, the MeOH extract was submitted to LC-ESI/LTQOrbitrap/MS/MS experiments. The LC-HRMS profile (Fig. 3.1), acquired in negative ion mode, showed peaks with m/z values ascribable to phenolics belonging to different classes, as cyanogenic glycosides (**4** and **10**), caffeoylquinic acid derivative (**18**), alkyl and aromatic dihexosides (**1**, **3**, **8**), a terpene (**24**), and glycosylated flavonoids (**20-23**, **25-26**) (Table 3.1).

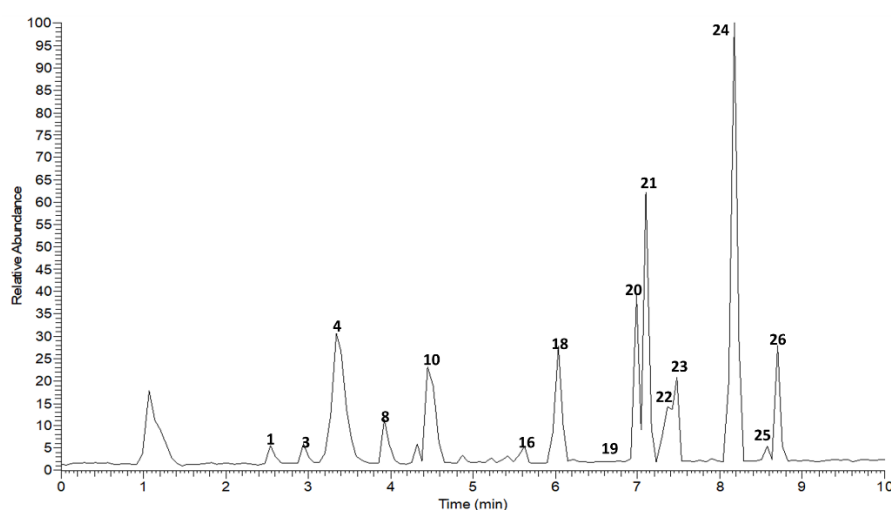


Figure 3.1 LC-HRMS profile in negative ion mode of the MeOH extract of *P. dulcis* cv. Toritto seeds

Detected compounds were putatively identified by determining their accurate m/z values, molecular formulae and characteristic fragmentation patterns, by comparing the obtained information with data reported in scientific literature, online databases (KnapSack, FoodB, PubChem, ChemSpider, KEGG) and by incorporating the fragmentation spectra in online database-assisted prediction tools (MetFrag). During the LC-ESI/LTQOrbitrap/MS/MS experiments, the “data dependent scan” mode was employed, enabling the MS software to select the precursor ion as the most intense peak in the LC-HRMS spectrum.

Table 3.1 Compounds putatively identified in the different parts and extracts obtained from *P. dulcis* cv. Toritto seeds

N°	R _t	Calculated Mass	[M-H] ⁻	Δppm	MS ² (%)	Molecular Formula	Compound
1	2.54	432.1631	477.1598 ¹	1.94	431(100), 269(47)	C ₁₉ H ₂₈ O ₁₁	benzyl dihexoside
2	2.70	578.1424	577.1337	0.57	559(15), 451(35), 425(100), 407(62), 289(26), 287(21)	C ₃₀ H ₂₆ O ₁₂	EC-EC
3	2.95	412.1944	457.1911 ¹	1.35	411(100), 249(42)	C ₁₇ H ₃₂ O ₁₁	(iso)pentyl dihexoside
4	3.34	457.1584	456.1498	0.84	323(100), 263(22), 221(41), 179(56)	C ₂₀ H ₂₇ NO ₁₁	amygdalin
5	3.50	290.0790	289.0709	1.02	245(100), 205(40), 179(19)	C ₁₅ H ₁₄ O ₆	(+)-catechin ²
6	3.50	866.2058	865.1960	0.95	739(30), 713(35), 695(100), 577(57), 575(48), 449(18), 407(24)	C ₄₅ H ₃₈ O ₁₈	EC-EC-EC
7	3.83	562.1475	561.1389	0.76	543(41), 435(56), 425(18), 407(19), 289(100), 271(26)	C ₃₀ H ₂₆ O ₁₁	EA-EC
8	3.93	446.1788	491.1753 ¹	1.14	445(100), 283(21)	C ₂₀ H ₃₀ O ₁₁	phenethanol-dihexoside
9	4.10	578.1424	577.1339	0.63	559(12), 451(29), 425(100), 407(51), 289(24)	C ₃₀ H ₂₆ O ₁₂	EC-EC

10	4.45	295.1055	340.1032 ¹	1.05	294(100), 161(59)	C ₁₄ H ₁₇ NO ₆	prunasin
11	4.50	290.0790	289.0718	1.58	245(100), 205(44), 179(12)	C ₁₅ H ₁₄ O ₆	(-)-epicatechin ²
12	4.95	864.1901	863.1806	1.19	711(100), 693(31), 575(72), 573(24)	C ₄₅ H ₃₆ O ₁₈	EC-EC-A ₁ -EC
13	5.04	866.2058	865.1954	1.61	847(11), 739(52), 713(40), 695(100), 587(22), 577(62), 575(38), 543(14), 451(21), 449(20), 407(29), 405(8), 289(8), 287(15)	C ₄₅ H ₃₈ O ₁₈	EC-EC-EC
14	5.23	562.1475	561.1385	0.41	543(51), 435(62), 425(18), 407(24), 289(100), 271(19)	C ₃₀ H ₂₆ O ₁₁	EA-EC
15	5.32	1154.2692	1153.2595	1.86	1135(67), 1001(59), 865(83), 575(100), 423(25)	C ₆₀ H ₅₀ O ₂₄	EC-EC-EC-EC
16	5.86	850.2109	849.2012	0.44	831(24), 723(71), 679(69), 577(86), 561(63), 559(100), 407(22)	C ₄₅ H ₃₈ O ₁₇	EA-EC-EC
17	5.92	576.1267	575.1182	1.14	539(24), 529(21), 449(100), 423(36), 407(15), 289(24), 285(20)	C ₃₀ H ₂₄ O ₁₂	EC-A ₁ -EC
18	6.03	530.1424	529.1313	1.94	367(100), 353(63), 179(144), 193(12)	C ₂₆ H ₂₆ O ₁₂	feruloyl caffeoylquinic acid
19	6.62	464.0954	463.0869	0.43	301(100)	C ₂₁ H ₂₀ O ₁₂	quercetin 3- <i>O</i> - β -D- glucopyranoside ²
20	7.00	594.1584	593.1490	0.54	285(100)	C ₂₇ H ₃₀ O ₁₅	kaempferol 3- <i>O</i> - β - D-rutinoside ²
21	7.21	624.1690	623.1607	0.64	315(100), 300(24)	C ₂₈ H ₃₂ O ₁₆	isorhamnetin 3- <i>O</i> - β -D-rutinoside ²
22	7.37	478.1111	477.1020	1.68	357(21), 315(100)	C ₂₂ H ₂₂ O ₁₂	isorhamnetin 3- <i>O</i> - β -D- galactopyranoside ²
23	7.48	478.1111	477.1023	1.14	357(21), 315(100)	C ₂₂ H ₂₂ O ₁₂	isorhamnetin 3- <i>O</i> - β -D- glucopyranoside ²
24	8.18	512.2621	557.2589 ¹	1.95	511(100), 349(26)	C ₂₆ H ₄₀ O ₁₀	amygdaloside
25	8.54	636.1690	635.1601	0.15	575(100), 285(76)	C ₂₉ H ₃₂ O ₁₆	multiflorin A
26	8.77	666.1796	665.1707	0.48	605(48), 315(100), 300(22)	C ₃₀ H ₃₄ O ₁₇	isorhamnetin acetylrutinoside

¹Observed as formate adduct. EC=(epi)catechin, EA=(epi)afzelechin, A₁=A-type linkage. Where not specified B-type linkage is intended. ² The identification of this compound was corroborated by comparison with standard solution

Compounds **1**, **3** and **8**, detected as formate adducts [M-H+HCOOH]⁻, showed in their MS/MS spectra product ions deriving from the neutral loss of a dehydrated hexose moiety (-162 Da). The accurate *m/z* values and the calculated molecular formulae allowed to tentatively determine their aglycone moieties, by comparison with data reported in databases and literature, allowing their putative identification as benzyl dihexoside (**1**), (iso)pentyl dihexoside (**3**) and phenethanol dihexoside (**8**) (Pimanovà et al., 2015; De Rosa et al., 1996; Karioti et al., 2014) (Table 3.1).

Compounds **4** and **10** showed in HRMS precursor ions [M-H]⁻ at *m/z* 456.1498 and 340.1032 (the latter detected as formate adduct [M-H+HCOOH]⁻), respectively, suggesting the presence of an odd number of nitrogen atoms.

Compound **4** exhibited in the tandem mass spectrum (Fig. 3.2) a base peak at m/z 323 originated from the neutral loss of a mandelonitrile moiety, along with product ions at m/z 263 and 221, generated by the cleavage of cross-ring bonds of hexose 2; additionally, a fragment ion at m/z 179, ascribable to a deprotonated hexose, was observed.

Otherwise, the MS/MS spectrum of compound **10** was characterized by the only base peak at m/z 161, generated by the neutral loss of the mandelonitrile moiety. The observed fragmentation patterns were in agreement with data reported in literature, allowing to putatively identify compound **4** as amygdalin and compound **10** as prunasin (Lee et al., 2013; Bottone et al., 2018) (Table 3.1). Cyanogenic glycosides have been widely reported in Rosaceae, especially in the seeds of *Prunus* genus, and are known for their toxic effects due to the release of hydrogen cyanide, produced by enzymatic hydrolysis, able to complex iron and copper ions of the cytochrome C oxidase active site. However, besides the proved toxicity, this class of compounds has shown a potential anticancer activity (Lee et al., 2013; Song et al., 2014) (Table 3.1).

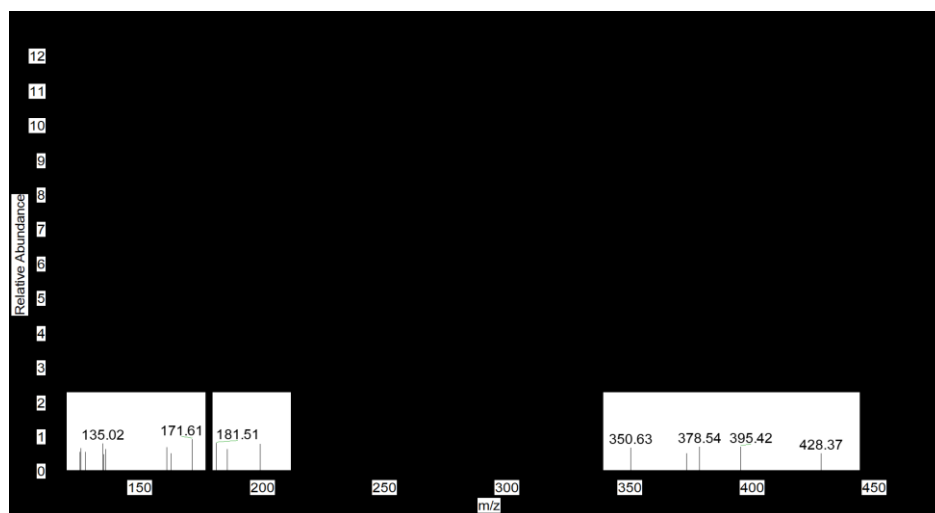


Figure 3.2 ESI/MS/MS spectrum of compound **4** in negative ion mode

Compound **18** (m/z 529.1313), whose molecular formula was established as $C_{26}H_{26}O_{12}$, exhibited in the MS/MS spectrum a base peak at m/z 367, due to the loss

of a caffeic acid moiety, with a product ion at m/z 353 ascribable to the loss of a ferulic acid moiety, whose presence was confirmed by the product ion at m/z 193. Hence, according to data found in scientific literature, it was possible to tentatively identify compound **18** as feruloyl caffeoylquinic acid (Xue et al., 2016) (Table 3.1).

Compound **24** was detected in HRMS as formate adduct $[M-H+HCOOH]^-$ at m/z 557.2589, showing in the MS/MS spectrum a fragment ion at m/z 511, due to the loss of formic acid, and an additional product ion at m/z 349 originated from the loss of a dehydrated hexose moiety (-162 Da). Molecular formula was established as $C_{26}H_{40}O_{10}$. By comparing the achieved information with scientific literature, compound **24** was tentatively identified as amygdalosyde, a diterpene glycoside showing an unusual B ring-cleaved kauranoid skeleton, previously identified in almond kernels (Sang et al., 2003). The occurrence of kaurane diterpenes has been also widely reported in Labiatae, Euphorbiaceae and Compositae, and they showed to possess several biological activities, such as anti-HIV, antibacterial, antitumoral and antiinflammatory (Sang et al., 2003) (Table 3.1).

Furthermore, the analysis of the LC-HRMS/MS spectrum pointed out the occurrence of several *O*-glycosylated flavonoids (**19**, **20**, **21**, **22**, **25** and **26**), which showed in their fragmentation patterns peculiar product ions ascribable to the neutral loss of the sugar moieties (-162 Da for hexoses, -308 Da for rutoses), while for compounds **25** and **26** an additional loss of 60 Da suggested the presence of an acetyl group in their structure. For an unambiguous identity attribution, the retention times of the detected compounds and standard solutions, analyzed in the same LC-HRMS conditions, were compared. This allowed to identify the glycosylated flavonoids as quercetin 3-*O*- β -D-glucopyranoside (**19**), kaempferol 3-*O*- β -D-rutinoside (**20**), isorhamnetin 3-*O*- β -D-rutinoside (**21**), isorhamnetin 3-*O*- β -D-galactopyranoside (**22**) and isorhamnetin 3-*O*- β -D-glucopyranoside (**23**), while compounds **25** and **26** were putatively identified as multiflorin A and isorhamnetin acetylrutinoside (Shirosaki et al., 2012; Yoshikawa et al., 2002) (Table 3.1).

3.2.1.2 “Eco-friendly” extractions of *P. dulcis* cv. Toritto seeds

With the aim to propose “green” extraction methods, employing relatively non-toxic solvents, different extracts were prepared by maceration using EtOH 96% and an EtOH:H₂O (1:1, v/v) solution. The obtained extracts were successively submitted to LC-ESI/LTQOrbitrap/MS experiments, and the profiles compared (Fig. 3.3).

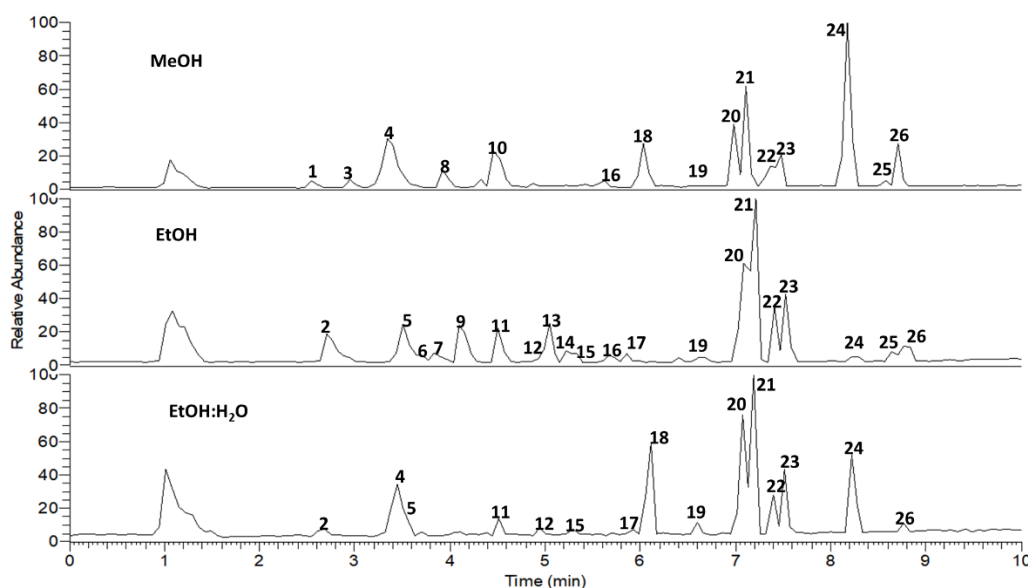


Figure 3.3 LC-HRMS profiles in negative ion mode of the MeOH, EtOH, EtOH:H₂O extracts of *P. dulcis* cv. Toritto seeds

In the LC-HRMS profile of the EtOH extract peaks related to amygdalin (**4**), prunasin (**10**) and feruloyl caffeoylquinic acid (**18**) were not observed, while amygdaloside (**24**) represented a minor constituent. On the other hand, in the EtOH:H₂O extract profile, compounds **4**, **18** and **24** were among the major constituents. Moreover, the LC-HRMS profiles of the “eco-friendly” extracts showed compounds **20** and **21** as main constituents, and additional peaks with *m/z* values ascribable to catechins and proanthocyanidins, not observed in the MeOH extract, suggesting a good selectivity of the employed solvents towards this class of compounds.

3.2.1.3 Catechins and proanthocyanidins

Catechins are flavan-3-ol derivatives, characterized by the absence of the 2,3 double bond and the ketone group in position 4. Proanthocyanidins are catechin polymers, differing in the subunits and for the linkage typology: B-type proanthocyanidins are characterized by C₄-C₈ or C₄-C₆ bonds, while A-type proanthocyanidins possess an additional C₂-O-C₇ or C₂-O-C₅ bond. This class of phenolics has been reported for the antioxidant and anti-inflammatory activities, as well as for their antimicrobial properties (Lin et al., 2014).

The structural information achieved from tandem mass experiments, along with researches in scientific literature and databases (FoodB), allowed to putatively determine for polymers the sequence and identity of each subunit, as well as the linkage typology.

Compounds **5** and **11** showed similar fragmentation spectra, with a base peak at m/z 245 originated by the neutral loss of acetaldehyde (-44 Da) produced by a retro Diels-Alder reaction occurred at the C-ring; for both compounds the molecular formula was established as C₁₅H₁₄O₆, suggesting two stereoisomers. Thus, for an unambiguous identification, the retention times of the detected compounds were compared with standard solutions analyzed in the same experimental conditions, allowing to assess compound **5** as (+)-catechin and compound **11** as (-)-epicatechin (Table 3.1).

Compounds **7** and **14** also showed similar MS/MS spectra. Both exhibited a product ion at m/z 435 generated by a heteronuclear ring fission (-126 Da), while the diagnostic signals at m/z 289 and 271 allowed to determine the subunits as (epi)catechin and (epi)afzelechin, respectively, representing the terminal and the extension units, respectively, linked by a B-type linkage; molecular formula was established as C₃₀H₂₆O₁₁. In agreement with scientific literature, compounds **7** and

14 were putatively identified as B-type (epi)epiafzelechin-(epi)catechin (Lin et al., 2014) (Table 3.1).

Compound **17** (m/z 575.1182) showed a fragmentation pattern (Fig. 3.4) characterized by a base peak at m/z 449, due to the heteronuclear ring fission (-126 Da), and a product ion at m/z 423 originated by a retro Diels-Alder reaction; in addition, two diagnostic ions at m/z 289 and 285, originated from the quinone methide fission, suggested two (epi)catechin units bonded by an A-type linkage. Molecular formula was established as $C_{30}H_{24}O_{12}$. The achieved information, in accordance with literature, allowed to identify compound **17** as A-type (epi)catechin dimer (Lin et al., 2014) (Table 3.1).

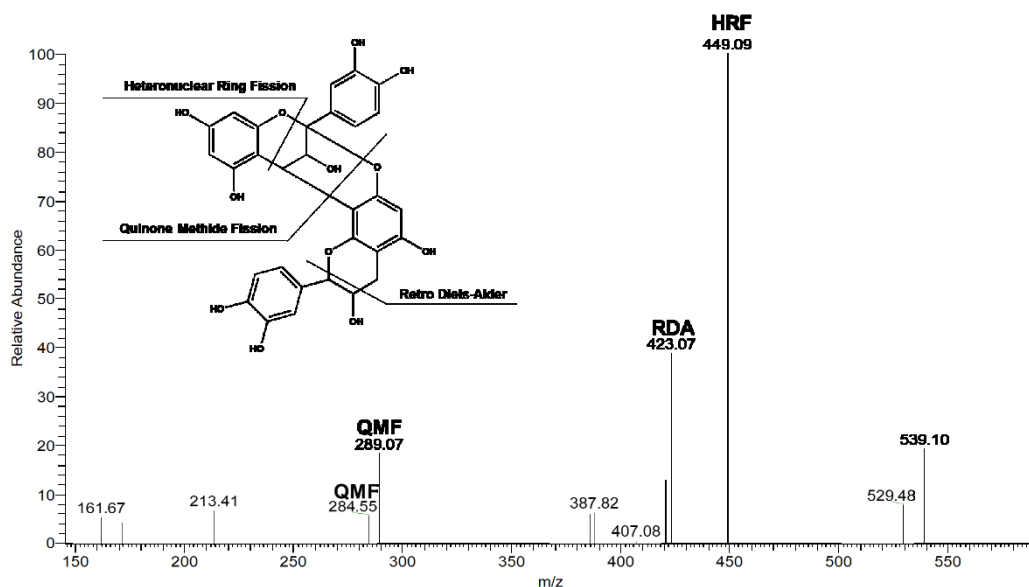


Figure 3.4 ESI/MS/MS spectrum of compound **17** in negative ion mode

Compound **2** and **9** showed in the MS/MS spectra (Fig. 3.5) a base peak at m/z 425 generated by the neutral loss of the B-ring due to a retro Diels-Alder reaction (-152 Da); in addition, a product ion at m/z 451 derived from the heteronuclear ring fission was observed, along with two product ions at m/z 289 and 287, which suggested two (epi)catechin units linked through a B-type linkage. Molecular formula was established as $C_{30}H_{26}O_{12}$. In agreement with scientific literature and

databases (FoodB), compounds **2** and **9** were putatively identified as B-type (epi)catechin dimers (Lin et al., 2014) (Table 3.1).

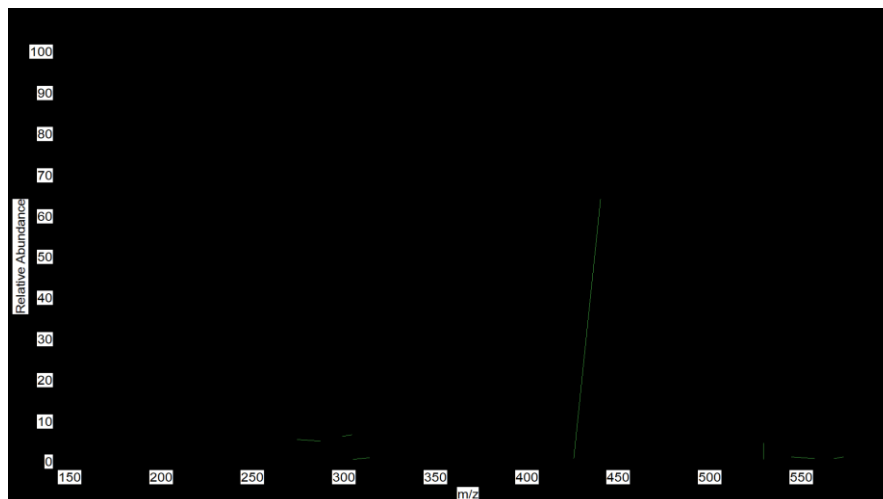


Figure 3.5 ESI/MS/MS spectrum of compound **2** in negative ion mode

Compounds **6** and **13** showed a fragmentation pattern (Fig. 3.6) characterized by a base peak at m/z 695 originated from the loss of a water molecule and a contemporary retro Diels-Alder reaction (-152 Da); moreover, the product ions observed at m/z 577 and 575 suggested the loss of a (epi)catechin unit from both the extension and terminal units, respectively, bonded to the central unit by B-type linkages. Molecular formula was established as $C_{45}H_{38}O_{18}$, suitable with the identity putatively attributed to compounds **6** and **13** as B-type (epi)catechin trimers (Lin et al., 2014) (Table 3.1).

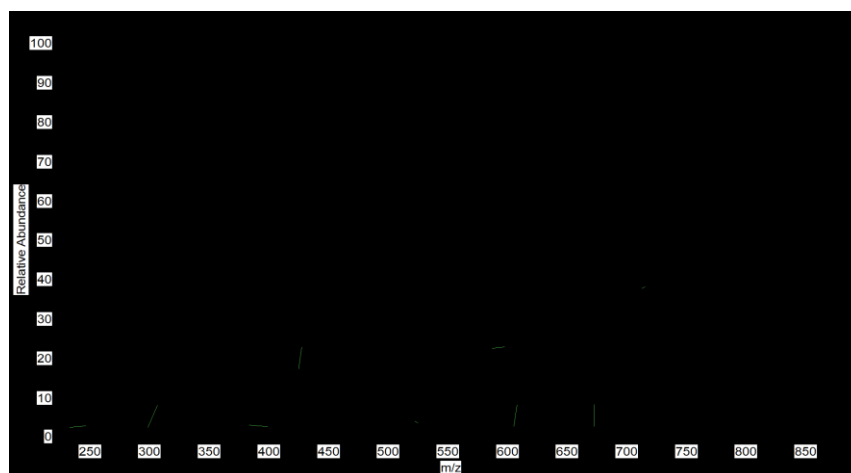


Figure 3.6 ESI/MS/MS spectrum of compound **13** in negative ion mode

Compound **12** (m/z 863.1806) showed in the MS/MS spectrum two fragment ions at m/z 575 and 573 originated from the quinone methide fissions, with the loss of a (epi)catechin extension unit and a (epi)catechin terminal unit, respectively, linked to the central unit by a B-type and an A-type linkage, respectively. Molecular formula was established as $C_{45}H_{36}O_{18}$. In agreement with scientific literature, compound **12** was putatively identified as (epi)catechin trimer (Lin et al., 2014) (Table 3.1).

Furthermore, compound **16** (m/z 849.2012) exhibited a fragmentation pattern characterized by the base peak at m/z 559 due to the loss of a (epi)catechin terminal unit, and a product ion at m/z 577 originated from the loss of an (epi)afzelechin extension unit, both bonded to the central (epi)catechin by a B-type linkage. Considering the molecular formula established as $C_{45}H_{38}O_{17}$, and data reported in literature, compound **16** was putatively identified as (epi)afzelechin-(epi)catechin-(epi)catechin (Lin et al., 2014) (Table 3.1).

Finally, compound **15** (m/z 1153.2595) showed in MS/MS experiments a product ion at m/z 865 produced by the loss of a terminal (epi)catechin unit, and a base peak at m/z 575 generated by the successive loss of a (epi)catechin extension unit.

Molecular formula was established as $C_{60}H_{50}O_{24}$. In agreement with data reported in scientific literature and online databases (FoodB), compound **15** was putatively identified as B-type (epi)catechin tetramer (Lin et al., 2014) (Table 3.1).

3.2.1.4 Almond peeling main product and by-products metabolite profiling

Aiming at valorizing the main by-products deriving from the almond peeling processes, represented by removed skins and blanching waters, as well as establishing the originating matrix of the identified constituents, whole almonds were peeled in laboratory; however, contrary to industrial processes, mild conditions were adopted in order to avoid compounds degradation. Successively, the MeOH extracts of *P. dulcis* cv. Toritto peeled seeds, integuments and blanching water were submitted to LC-ESI/LTQOrbitrap/MS experiments, and the profiles compared (Fig. 3.7).

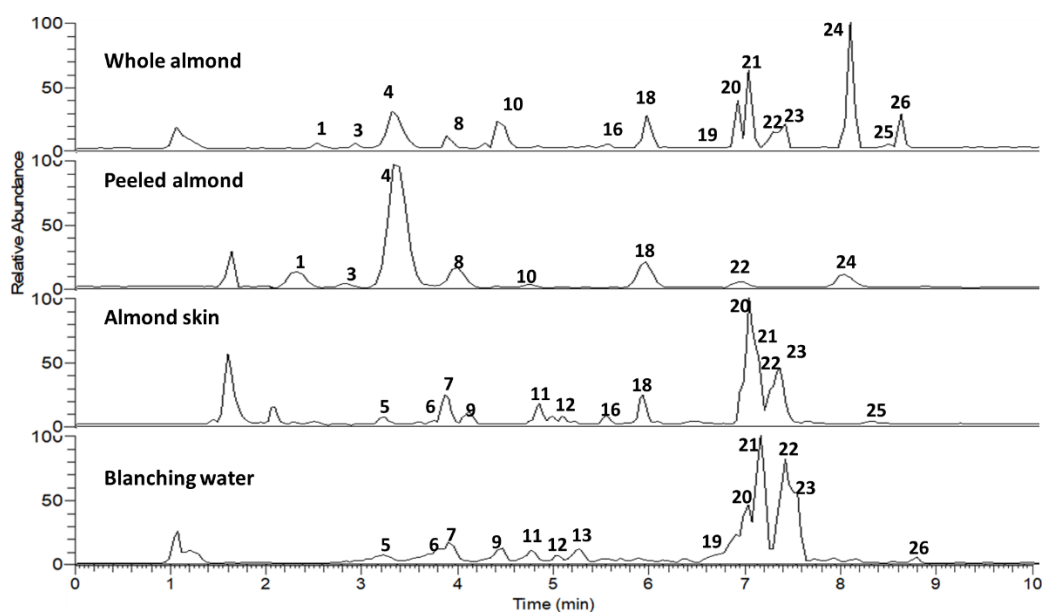


Figure 3.7 LC-HRMS profiles in negative ion mode of the blanching water and the MeOH extracts of *P. dulcis* cv. Toritto whole seeds, peeled seeds and skins

Amygdalin (**4**) represented the major constituent in the profile of the peeled almonds, while amygdaloside (**24**) was one of the less abundant; in addition, both compounds were not detected in almond skins and blanching water.

On the other hand, several peaks related to proanthocyanidins were detected in the LC-HRMS profiles of these last two matrices, along with glycosylated flavonoids **20-23**, which represented the main constituents.

The achieved results highlighted the occurrence of cyanogenic glycosides only in the seeds, while proanthocyanidins and glycosylated flavonoids were mainly detected in integuments, and effectively extracted by water during the almonds peeling process.

Almond skins have been reported for their high phenolic content, as a rich source of dietary fibers and as prebiotics, suggesting their potential employment in the production of dietary supplements for the regularization of the intestinal transit (¹Mandalari et al., 2010; ²Mandalari et al., 2010).

However, further investigations must be carried out since the analyzed almond parts, as well as the blanching water, were obtained from a laboratory process performed in mild conditions to avoid compounds degradation, while the operating conditions in industrial processes occur at higher temperatures and hence the possibility that secondary metabolites, mainly glycosylated flavonols and proanthocyanidins, may degrade due to the excessive heat, resulting in a loss of bioactivity (Hughey et al., 2012).

3.2.1.5 Comparison of the MeOH extracts chemical composition of P. dulcis seeds cvs. Toritto and Avola

The almonds of cv. Toritto originate from Apulia, a region located in the South-eastern part of Italy, representing the heel of the boot. This area is characterized by fresh summers and rainy winters, and snowing is not a rare event. On the other hand, the almonds of the three cvs. Fascionello, Pizzuta and Romana originate from

Avola, located in the most Southern part of Sicily, whose climate is typically Mediterranean, with mild and rainy winters, while summers are often really warm and dry, with occasional drought events.

To establish if the above mentioned and other growing conditions may affect the metabolome of a plant species originating from different regions, the LC-ESI/HRMS/MS profiles of the Apulian almonds extracts were compared with those of the three Sicilian cvs. (Figure 3.8).

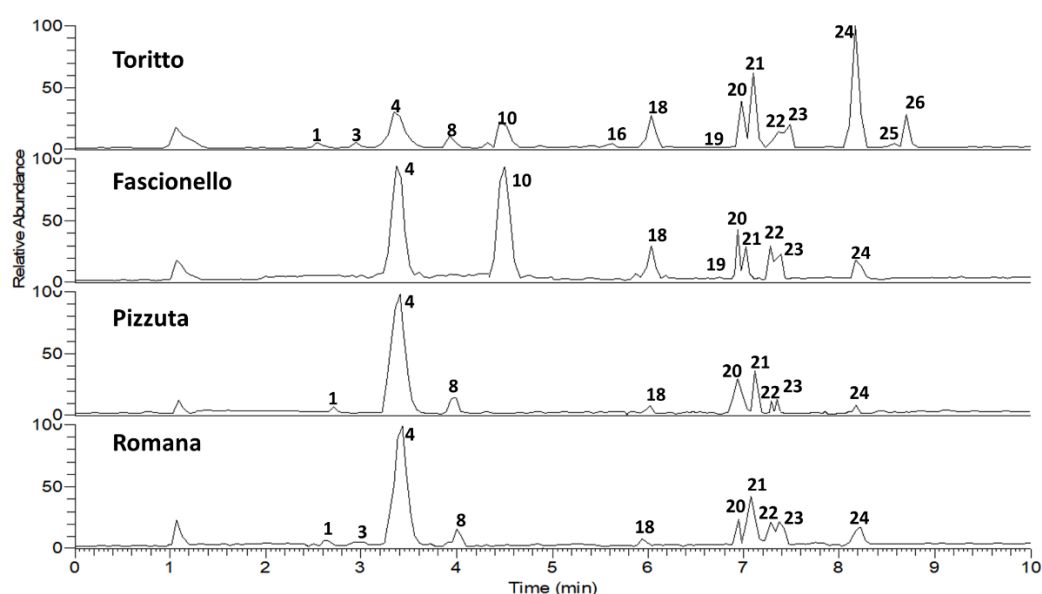


Figure 3.8 LC-HRMS profiles in negative ion mode of the MeOH extracts of *P. dulcis* cvs. Toritto, Fascionello, Pizzuta and Romana whole seeds

A first overview of the LC-HRMS profiles evidenced clear differences among the chemical composition of the analyzed whole seeds MeOH extracts, highlighting the constant presence of glycosylated flavonols (**20-23**), feruloyl caffeoylquinic acid (**18**) and amygdaloside (**24**), even if this last one resulted as minor constituent in the Sicilian almonds unlike the Apulian ones. However, it was interesting to notice that amygdalin (**4**) resulted the major constituent in the three Sicilian cvs., while prunasin (**10**) was detected at high level only in the cv. Fascionello.

Cyanogenic glycosides have been widely reported in the seeds of the *Prunus* genus, and are well known for their poisonous effects due to the release of cyanide hydrogen, also responsible of the bitterness of certain almond varieties. According to cyanogenic glycosides concentration, almonds are classified in sweet, semi-bitter and bitter (Chaouali et al., 2013). Hence, the occurrence of such constituents in the Apulian and Sicilian *P. dulcis* seeds may affect their taste (Sánchez-Pérez et al., 2008). However, since produced almonds are usually provided peeled and roasted, the exposure to high temperature during the refinement processes has proved to down the cyanogenic glycosides content, with amelioration of the flavor (Imran et al., 2013).

3.2.1.6 Peeling process by-products showed good phenolic content and radical scavenging activity

All the extracts produced from the different almond parts, both Sicilian and Apulian, as well as the blanching waters, were submitted to Folin-Ciocalteu assay to determine the phenolic content, and to DPPH• and ABTS^{•+} assays to evaluate the radical scavenging activity (Table 3.2).

Whole seeds of all the investigated cultivars showed a discreet phenolic content and radical scavenging activity. However, remarkable differences were pointed out by comparing the different almond parts and the blanching waters: peeled almonds showed a substantial lower phenolic content and a weak radical scavenging activity. On the contrary, for almond integuments, specially the EtOH:H₂O extracts, a high content of phenolics was observed, exerting in DPPH• and ABTS^{•+} assays a remarkable antioxidant activity. Nevertheless, an even higher phenolic content was observed for blanching water, showing as well good radical scavenging properties.

The achieved results highlighted how consuming unpeeled almonds may provide a higher amount of antioxidant phenolics, with additional beneficial effects for human health (Mandalari G., 2012).

Table 3.2 Total phenolic content, DPPH• and ABTS^{•+} radical scavenging activity of the extracts and blanching waters of *P. dulcis* cvs. Toritto and Avola (Fascionello, Pizzuta and Romana) seeds

Sample	Total Phenolic Content		DPPH•		ABTS ^{•+}	
	GAE ^a	SD ^d	IC ₅₀ ^b	SD ^d	TEAC ^c	SD ^d
Toritto whole seed MeOH	64.57 ± 2.56		49.58 ± 6.24		0.31 ± 0.05	
Toritto whole seed EtOH	84.38 ± 3.64		34.61 ± 4.89		0.52 ± 0.05	
Toritto whole seed EtOH/H ₂ O	18.64 ± 1.78		138.28 ± 12.45		0.19 ± 0.05	
Fascionello whole seed MeOH	68.27 ± 4.17		57.94 ± 3.68		0.02 ± 0.01	
Fascionello whole seed EtOH	90.52 ± 5.89		34.89 ± 2.48		0.39 ± 0.04	
Fascionello whole seed EtOH/H ₂ O	15.12 ± 1.78		77.67 ± 5.61		0.12 ± 0.01	
Pizzuta whole seed MeOH	40.31 ± 4.16		59.71 ± 7.38		0.26 ± 0.09	
Pizzuta whole seed EtOH	51.79 ± 2.10		50.3 ± 4.42		0.64 ± 0.11	
Pizzuta whole seed EtOH/H ₂ O	19.38 ± 1.11		83.09 ± 9.41		0.43 ± 0.04	
Romana whole seed MeOH	35.68 ± 2.46		79.51 ± 8.65		0.46 ± 0.10	
Romana whole seed EtOH	46.61 ± 2.00		78.47 ± 6.65		0.55 ± 0.06	
Romana whole seed EtOH/H ₂ O	29.01 ± 2.79		130.43 ± 14.85		0.40 ± 0.06	
Toritto peeled seed MeOH	14.38 ± 1.46		109.70 ± 9.62		N/A	
Toritto peeled seed EtOH	9.75 ± 1.32		154.11 ± 14.33		N/A	
Toritto peeled seed EtOH/H ₂ O	10.68 ± 1.54		148.73 ± 14.28		0.03 ± 0.01	
Fascionello peeled seed MeOH	5.87 ± 1.32		252.01 ± 14.47		0.02 ± 0.01	
Fascionello peeled seed EtOH	11.98 ± 1.15		305.55 ± 28.93		N/A	
Fascionello peeled seed EtOH/H ₂ O	17.72 ± 1.89		100.46 ± 9.95		0.02 ± 0.01	
Pizzuta peeled seed MeOH	9.57 ± 2.62		401.00 ± 38.31		0.04 ± 0.01	
Pizzuta peeled seed EtOH	9.38 ± 2.05		223.53 ± 22.21		N/A	
Pizzuta peeled seed EtOH/H ₂ O	14.01 ± 1.24		462.54 ± 65.57		0.06 ± 0.02	
Romana peeled seed MeOH	8.83 ± 1.92		651.33 ± 55.98		N/A	
Romana peeled seed EtOH	10.87 ± 1.65		1240.88 ± 94.52		N/A	
Romana peeled seed EtOH/H ₂ O	14.94 ± 2.23		457.12 ± 49.64		N/A	
Toritto tegument MeOH	44.01 ± 2.56		176.41 ± 14.84		0.09 ± 0.01	
Toritto tegument EtOH	105.50 ± 7.47		31.94 ± 6.97		0.36 ± 0.05	
Toritto tegument EtOH/H ₂ O	254.20 ± 17.51		17.78 ± 4.35		1.34 ± 0.18	
Fascionello tegument MeOH	31.79 ± 2.23		171.35 ± 11.93		0.14 ± 0.03	
Fascionello tegument EtOH	170.50 ± 21.68		81.25 ± 7.61		0.30 ± 0.04	
Fascionello tegument EtOH/H ₂ O	236.24 ± 15.21		26.23 ± 3.48		0.51 ± 0.07	
Pizzuta tegument MeOH	100.68 ± 5.67		59.13 ± 3.38		0.39 ± 0.06	
Pizzuta tegument EtOH	123.09 ± 6.24		26.58 ± 2.22		0.44 ± 0.06	
Pizzuta tegument EtOH/H ₂ O	239.57 ± 6.62		14.76 ± 2.47		0.85 ± 0.04	
Romana tegument MeOH	180.68 ± 19.41		93.64 ± 6.35		0.33 ± 0.02	
Romana tegument EtOH	201.61 ± 26.19		24.70 ± 3.36		0.42 ± 0.06	
Romana tegument EtOH/H ₂ O	320.31 ± 22.45		19.55 ± 1.94		1.44 ± 0.09	

Toritto blanching water	334.20 ± 67.10	14.43 ± 1.14	0.32 ± 0.03
Fascionello blanching water	496.79 ± 51.27	6.88 ± 0.57	0.68 ± 0.06
Pizzuta blanching water	463.83 ± 56.04	8.23 ± 0.99	1.59 ± 0.14
Romana blanching water	410.31 ± 40.46	8.11 ± 0.89	1.17 ± 0.13
Vit. C		5.16 ± 0.11	
Quercetin			1.87 ± 0.08

^a Values are expressed as gallic acid equivalents (GAE) mg/g of dried extract. ^b Values are expressed as µg/mL. ^c Values are expressed as concentration (mM) of a standard Trolox solution exerting the same antioxidant activity of a 1 mg/mL solution of the tested extract. ^d Standard Deviation of three independent experiments.

3.3 LC-ESI/QToF/MS/MS multi-class polar lipids profiling of *P. dulcis* seeds (cvs. Toritto and Avola)

3.3.1 Results and discussion

3.3.1.1 Polar lipids: a brief overview

Polar lipids represent a wide class of biomolecules, found in animal and plant tissues mainly as structural units. They are constituted by a polar moiety (head group), characterizing the class, and aliphatic side chains, usually connected to the head group as ethers or acyl derivatives, featured by variable length and unsaturation degrees (Fig. 3.9).

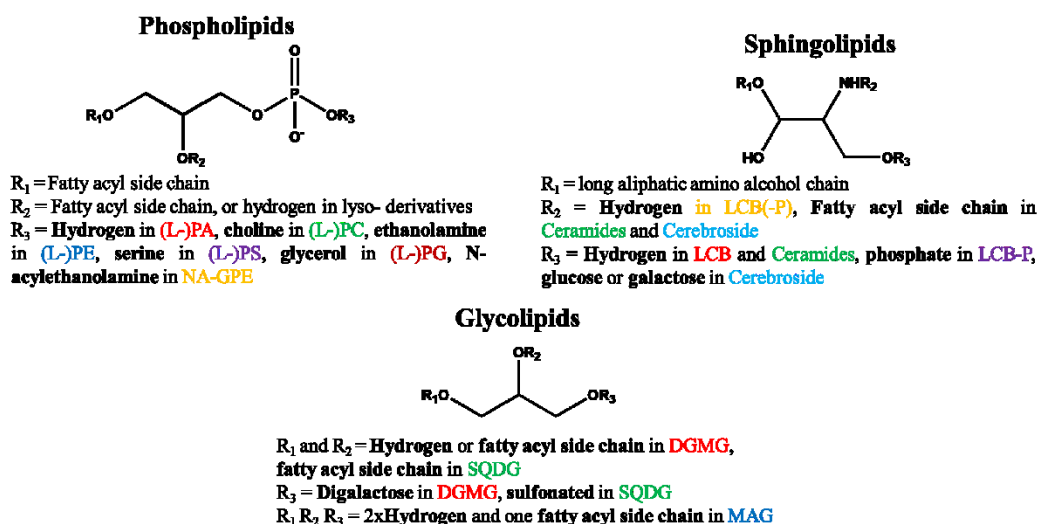


Figure 3.9 Different classes of polar lipids

3.3.1.2 LC-HRMS/MS in lipidomics

Mass spectrometry proved to be an elective analytical method in lipidomics, allowing to return a high number of information in a single analysis. Several advantages may be provided by using mass spectrometry in lipid profiling, as the employment of low amounts of samples, and no additional separations of constituents into classes. Moreover, acquiring spectra in positive and negative ionization mode on instruments equipped with high resolution analyzers can afford sufficient information for an unambiguous identification of the class and fatty acyl composition as well, providing details about chain length and unsaturation degree. However, in case of uncertain identity assignment due to ambiguous definition of fatty acid side chains or presence of isobaric species showing same m/z value, coupling tandem mass spectrometry to liquid chromatography may represent a resolute approach. In particular, in MS/MS experiments polar lipids may generate ion products deriving from the neutral loss of their head group, allowing an univocal classification of the analyzed ion. Furthermore, tandem mass spectra can provide elucidations about fatty acyl chains length, unsaturation degree, bond site in case of glycerol derivatives, while MS/MSⁿ experiments can allow to establish the position of eventual unsaturations on alkyl/acyl side chains (Knittelfelder et al., 2014; Cajka et al., 2017).

Therefore, with the aim to investigate the lipid profile of *P. dulcis* seeds (cvs. Toritto and Avola), with particular interest for polar lipids, LC-ESI/QToF/MS/MS based analyses were carried out. In addition, in order to evaluate if growing conditions and geographical origin, as well as cultivar differences, may affect the metabolome of edible parts of plant species, the lipid profiles of the Apulian “Mandorla di Toritto” and the Sicilian “Mandorla d’Avola”, represented by the three cvs. Fascionello, Pizzuta and Romana, were compared.

3.3.1.3 LC-ESI/QToF/MS/MS analysis of the polar lipids of “Mandorla di Toritto” and “Mandorla d’Avola”

Since interest was mainly focused on polar lipids, a targeted protocol was applied for a selective extraction of the compounds of interest. In particular, extraction method described by Bligh & Dyer was carried out (Bligh & Dyer, 1959), with slight modifications in order to maximize extraction yields. In brief, almonds were milled, frozen and successively freeze-dried; samples were extracted with MeOH:CHCl₃ mixtures, and for an optimal extraction an additional homogenization process was incorporated. Finally, in order to allow the easy separation of solvent phases, water addition and centrifugation were performed. Once phases separation occurred, the bottom lipid-containing phase was taken, and by a “dilute and shot” approach analyzed by LC-ESI/QToF/MS/MS experiments.

To achieve a preliminary class separation of the non-polar constituents, depending on their polarity and size, the LC separation was carried out by using a RP C-18 column, employing a strong organic mobile phase (acetonitrile:isopropanol, 1:3, v/v).

Due to the occurrence of several classes of polar lipids, differing in their capacity to produce different molecular ions depending on the selected polarity, experiments were performed both in negative and in positive electrospray ionization mode.

By following this analytical approach, the detection of various classes of phospholipids, differing for their head group and fatty acyl side chains number, length and unsaturation degree, was obtained. Furthermore, besides phospholipids, diacylglycerols and triacylglycerols were detected as well. The information achieved by tandem mass spectrometry experiments enabled to determine length and unsaturation level of the constituting fatty acyl chains.

Identification of the detected phospholipids and glycerides was carried out by accurate *m/z* values determination, chromatographic behaviour evaluation, and analysis of their characteristic fragmentation patterns. The achieved information

were compared with data reported in scientific literature, as well as online databases (FoodB, Lipid Maps), and additionally by incorporating the MS/MS spectra in online database-assisted prediction tools (MetFrag) (Shen et al., 2013; Song et al., 2018).

3.3.1.4 Phospholipids identification

Phospholipids play an important role in plant and animal organisms, with structural and functional properties. They represent the main constituents of cell membranes, and showed to exert a wide range of beneficial effects on human health. As example, phospholipid-containing foods consumption showed liver weight and its lipid content decreasing properties, as well as gastroprotection functions, in particular phosphatidylcholines showed to reduce inflammation affecting the gastrointestinal tract. In addition, a phospholipid rich diet may reduce the incidence of several effects related to chronic arthritis. Moreover, *in vivo* hematic cholesterol reduction was observed, jointly with neuroprotective effects and amelioration of the main symptoms related to Alzheimer and Parkinson diseases (Abdelmoneim et al., 2017).

On a chemical point of view, phospholipids (PL) are made up of different polar head groups linked to a glycerol moiety possessing fatty acyl side chains on *sn*-1 and *sn*-2 positions, except for lysophospholipids (l-PLs), possessing only one fatty acyl chain. These last ones represent minor constituents in foods and are less often described.

LC-ESI/QToF/MS/MS analysis of *P. dulcis* cvs. Toritto and Avola seeds highlighted the occurrence of 26 phospholipids: 3 lysophosphatidylcholines (l-PCs), 10 phosphatidylcholines (PCs), 6 phosphatidylethanolamines (PEs), 5 phosphatidylinositols (PIs), 2 phosphatidylglycerols (PGs) (Table 3.3). Each class was assigned by analyzing the informative and diagnostic fragmentation spectra,

exhibiting characteristic neutral losses in accordance with data reported in literature (Pulfer & Murphy, 2003).

1-PCs and PCs exhibited in MS/MS spectra acquired in positive ion mode a diagnostic base peak at m/z 184, ascribable to the phosphocoline ion, allowing an unambiguous identification of the class (Fig. 3.10). Similarly, PEs showed in their fragmentation spectra in positive ion mode product ions deriving from the loss of the phosphoethanolamine head group (-141 Da) (Fig. 3.10). Otherwise, PIs were detected in negative ion mode, and were unambiguously identified by the occurrence of two highly diagnostic product ions: the first one was observed at m/z 241, and was ascribable to the inositol phosphate ion generated by an initial loss of the *sn*-2 fatty acyl as ketene; the second one was the product ion at m/z 153 originated by an intramolecular cyclization of the glycerol moiety with phosphate, generating a dioxaphosphorinanol oxide moiety (Fig. 3.10). In negative ion mode also PGs were observed. This phospholipid class was featured by the occurrence of the typical product ion at m/z 171 ascribable to the phosphoglycerol ion, and by the presence in the tandem mass spectrum of product ions formed by the neutral loss from the $[M-H]^-$ ion of 74 Da, corresponding to the dehydrated glycerol moiety (Fig. 3.10). Once that the phospholipid classes were assigned, the identification of the fatty acyl side chains was carried out. PCs, PEs and PGs showed in the MS/MS spectra product ions related to the diacylglycerol moiety, generated by the neutral loss of the head group, preliminarily suggesting a set of possible combinations of acyl side chains. For 1-PCs, PCs and PEs the identity of the side chains was unequivocally assessed by the occurrence of the monoacylglycerol moieties, which allowed to determine their length and unsaturation degree (Fig. 3.10). Differently, both PGs and PIs showed MS/MS spectra in which product ions related to monoacylglycerols were not detectable, while acyl side chains were detected as $[fatty\ acid-H]^-$ ions (Fig. 3.10). Unfortunately, even if the achieved information allowed to certainly identify the phospholipid classes and the fatty acyl side chains,

it was not possible to determine the *sn*-1 and *sn*-2 position on glycerol backbone, as well as the unsaturation positions.

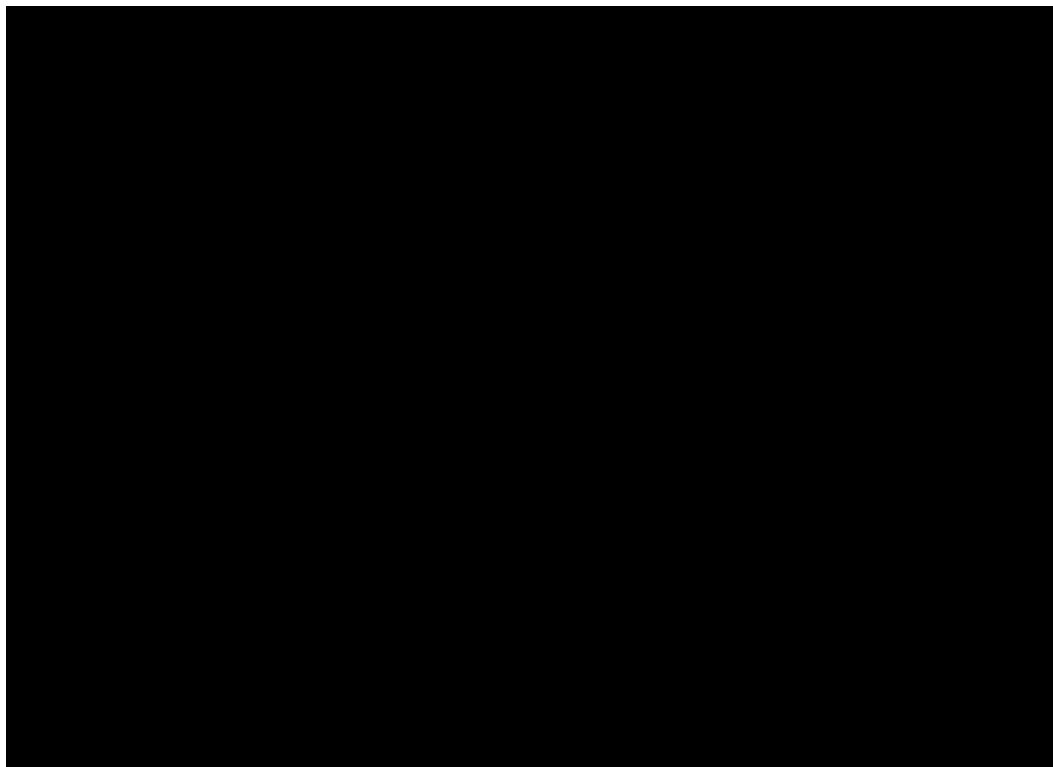


Figure 3.10 Fragmentations observed for phospholipids. R = polar head group. R₁/R₂ = fatty acids side chains, for phospholipids. R₁/R₂ = H/fatty acid side chain or fatty acid side chain/H for lysophospholipids.

It is worthy to notice how detected phospholipids were not homogeneously distributed in the investigated almond cultivars. Although all detected l-PCs and PIs occurred in Apulian and Sicilian almonds, the remaining phospholipid classes showed heterogeneous distribution, occasionally found in only one cultivar, as observed for compounds **31** and **34**, detected only in cv. Pizzuta, and compound **42**, occurring only in cv. Romana.

Table 3.3 Phospholipids putatively identified in *P. dulcis* seeds cvs. Toritto and Avola

N°	Compound	Toritto	Fascionello	Pizzuta	Romana	R _t	m/z	Ion	Ion Mode	Molecular Formula	MS/MS
27	l-PC(18:2)	X	X	X	X	4.1	520.3357	[M+H] ⁺	+	C ₂₆ H ₅₀ NO ₂ P	337, 184
28	l-PC(16:0)	X	X	X	X	5.0	520.3357	[M+H] ⁺	+	C ₂₆ H ₅₀ NO ₂ P	313, 184
29	l-PC(18:1)	X	X	X	X	5.2	522.3554	[M+H] ⁺	+	C ₂₆ H ₅₂ NO ₂ P	339, 184
30	PC(16:0/16:0)		X		X	10.2	730.5351	[M+H] ⁺	+	C ₄₀ H ₈₀ NO ₈ P	551, 313, 184
31	PC(16:1/16:1)			X		10.3	728.5363	[M+H] ⁺	+	C ₄₀ H ₇₆ NO ₈ P	547, 311, 184
32	PC(16:0/18:1)	X	X	X	X	12.6	760.5864	[M+H] ⁺	+	C ₄₄ H ₈₂ NO ₈ P	577, 339, 313, 184
33	PC(16:0/18:2)	X	X	X	X	11.6	758.5686	[M+H] ⁺	+	C ₄₂ H ₈₀ NO ₈ P	575, 337, 313, 184
34	PC(16:1/18:2)			X		10.2	756.5535	[M+H] ⁺	+	C ₄₂ H ₇₈ NO ₈ P	573, 337, 311, 184
35	PC(18:0/18:1)	X	X	X	X	14.2	788.6166	[M+H] ⁺	+	C ₄₄ H ₈₆ NO ₈ P	605, 341, 339, 184
36	PC(18:0/18:2)	X		X	X	13.8	786.5995	[M+H] ⁺	+	C ₄₄ H ₈₄ NO ₈ P	603, 341, 337, 184
37	PC(18:1/18:1)	X	X	X	X	12.6	786.6025	[M+H] ⁺	+	C ₄₄ H ₈₄ NO ₈ P	603, 339, 184
38	PC(18:1/18:2)	X	X	X	X	11.6	784.5848	[M+H] ⁺	+	C ₄₄ H ₈₂ NO ₈ P	601, 339, 337, 184
39	PC(18:2/18:2)	X	X	X	X	10.7	782.5693	[M+H] ⁺	+	C ₄₄ H ₈₀ NO ₈ P	599, 337, 184
40	PE(16:0/18:1)	X	X	X	X	11.2	718.5346	[M+H] ⁺	+	C ₃₉ H ₇₆ NO ₈ P	577, 339, 313
41	PE(16:0/18:2)		X	X		10.4	716.5205	[M+H] ⁺	+	C ₃₉ H ₇₄ NO ₈ P	575, 337, 313
42	PE(18:1/18:1)				X	9.9	744.5504	[M+H] ⁺	+	C ₄₁ H ₇₈ NO ₈ P	603, 339, 265
43	PE(18:0/18:2)	X	X	X	X	11.3	744.5504	[M+H] ⁺	+	C ₄₁ H ₇₈ NO ₈ P	603, 341, 337
44	PE(18:1/18:2)	X	X	X	X	10.7	742.5342	[M+H] ⁺	+	C ₄₁ H ₇₆ NO ₈ P	601, 339, 337
45	PE(18:2/18:2)		X	X		11.2	740.5169	[M+H] ⁺	+	C ₄₁ H ₇₄ NO ₈ P	599, 337
46	PI(16:0/18:1)	X	X	X	X	5.8	835.5363	[M-H] ⁻	-	C ₄₃ H ₈₁ O ₁₃ P	281, 255, 241, 153
47	PI(16:0/18:2)	X	X	X	X	5.3	833.5218	[M-H] ⁻	-	C ₄₃ H ₇₉ O ₁₃ P	279, 255, 241, 153
48	PI(18:0/18:1)	X	X	X	X	6.0	863.5653	[M-H] ⁻	-	C ₄₅ H ₈₅ O ₁₃ P	283, 281, 241, 153
49	PI(18:0/18:2)	X	X	X	X	5.6	861.5498	[M-H] ⁻	-	C ₄₅ H ₈₃ O ₁₃ P	283, 279, 241, 153
50	PI(18:0/18:3)	X	X	X	X	5.3	859.5359	[M-H] ⁻	-	C ₄₅ H ₈₁ O ₁₃ P	283, 277, 241, 153
51	PG(16:0/18:1)	X	X	X	X	6.0	747.5194	[M-H] ⁻	-	C ₄₀ H ₇₇ O ₁₀ P	673, 281, 255, 171
52	PG(16:0/18:2)			X	X	5.8	745.5038	[M-H] ⁻	-	C ₄₀ H ₇₅ O ₁₀ P	671, 279, 255, 171

l-PC = lysophosphatidylcholine, PC = phosphatidylcholine, PE = phosphatidylethanolamine, PI = phosphatidylinositol, PG = phosphatidylglycerol,

3.3.1.5 Diacylglycerols and triacylglycerols identification

Triacylglycerols play an important role in plant metabolism since they represent one of the main energy storages, mostly located in the seeds, available in case of protract drought. They also provide energy to sprouting seeds in their first growth steps. However, besides energy supplement, recent scientific findings pointed out their essential role in cell division and expansion, as well as in membrane lipid modeling, reproductive organs formation and impollination (Yang et al., 2018).

In humans, after dietary intake, triacylglycerols are hydrolyzed by pancreatic lipases, leading to free fatty acids release, jointly with diacylglycerols and glycerol. Such lysis is needed for the impossibility of lipids to be absorbed as triacylglycerols in duodenum, contrarily to fatty acids, monoacylglycerols, and some diacylglycerols. Once absorbed, triacylglycerols are reassembled in enterocytes and incorporated into chylomicrons, to be delivered to different tissues. When a lack of energy occurs, triacylglycerols undergo a breakdown to release fatty acids, used as energy source, and glycerol, used to synthesize glucose, used by brain cells due to their incapacity to use fatty acid as energy source (unless converted in ketones) (White & Venkatesh, 2011; Lambert & Parks, 2012).

As advanced, triacylglycerols are mainly found in seeds, and nuts showed to be a rich source, proved by the high calories content, in a range of 550-650 kcal for 100 g of dried nuts.

The investigation of the non-polar fraction of *P. dulcis* seeds further highlighted the occurrence of diacylglycerols and triacylglycerols, constituted by fatty acids with variable number of carbons and saturations (Table 3.4).

The identification of the detected glycerides was carried out by comparing the data obtained from the analysis of their fragmentation spectra and their accurate m/z values with the scientific literature, already reporting their occurrence in sweet almonds, and online databases and by incorporating the MS/MS spectra in online database-assisted prediction tools (Shen et al., 2013; Holčapek et al., 2003; McAnoy et al., 2005; Martín-Carratala et al., 1999).

All glycerides were detected in positive ion mode as ammonium adducts. The accurate m/z values determined in LC-HRMS analysis allowed to preliminarily establish the total number of carbons of the fatty acyl chains constituting the glycerides, and the total unsaturation degree as well. However, a comprehensive analysis of the fragmentation spectra led to the identification of the acyl side chains bonded to the glycerol backbone. In depth, submitted to multicollisional

fragmentation events, triacylglycerols yielded product ions originated by the loss of a fatty acyl side chain, and producing different diacylglycerol combinations which led to the identification of the lost acyl side chain. However, only for compound **60-62** it was not possible to unambiguously assess the fatty acyl identity. On the other hand, diacylglycerols showed in their MS/MS spectra product ions deriving from the loss of a water molecule, as well as signals ascribable to monoacylglycerol moieties deriving from the loss of one of the constituting acyl chains; occasionally, the identity of the fatty acyl chains was further confirmed by the presence of their related [acyl]⁺ ions.

Curiously, two triacylglycerols with a short C 2:0 acyl side chain were detected (**58-59**). Starting perplexities were clarified by their occurrence reported in hazelnut (*Corylus avellana* L.) by Klockmann et al. (Klockmann et al., 2016).

Noteworthy, compounds **63-70** showed a fatty acyl chain with an odd number of carbons. It was for long time assessed that in plant kingdom only even-numbered fatty acids could be deriving from biosynthetic processes; however, recent findings pointed out their occurrence in plant species as minor constituents (Holčápek et al., 2003; Rezanka & Sigler, 2009).

Table 3.4 Glycerides putatively identified in *P. dulcis* seeds cvs. Toritto and Avola

N°	Compound	Toritto	Fascionello	Pizzuta	Romana	R _t	m/z	Ion	Ion Mode	Molecular Formula	MS/MS
53	DG(16:0/18:1)		X		X	13.3	612.5576	[M+NH ₄] ⁺	+	C ₃₇ H ₇₀ O ₅	577, 339, 313
54	DG(18:1/18:1)	X	X	X	X	13.4	638.5732	[M+NH ₄] ⁺	+	C ₃₉ H ₇₂ O ₅	603, 339, 265
55	DG(18:1/18:2)	X	X	X	X	12.6	636.5573	[M+NH ₄] ⁺	+	C ₃₉ H ₇₀ O ₅	601, 339, 337, 265, 263
56	DG(18:2/18:2)		X	X	X	11.9	634.5413	[M+NH ₄] ⁺	+	C ₃₉ H ₆₈ O ₅	599, 337, 263
57	DG(20:1/22:4)	X	X	X	X	15.6	716.5949	[M+NH ₄] ⁺	+	C ₄₃ H ₇₈ O ₅	429, 413, 375, 357
58	TG(2:0/16:0/18:1)		X	X	X	14.1	654.5635	[M+NH ₄] ⁺	+	C ₃₉ H ₇₂ O ₆	577, 381, 355
59	TG(2:0/18:1/18:1)	X	X	X	X	14.2	680.5835	[M+NH ₄] ⁺	+	C ₄₁ H ₇₄ O ₆	603, 381, 265
60	TG(56:2)	X	X			14.9	932.7906	[M+NH ₄] ⁺	+	C ₅₉ H ₁₁₀ O ₆	773, 615, 603, 491, 277
61	TG(56:3)	X	X	X		14.4	930.7759	[M+NH ₄] ⁺	+	C ₅₉ H ₁₀₈ O ₆	771, 613, 615, 601
62	TG(56:4)		X			13.8	928.7558	[M+NH ₄] ⁺	+	C ₅₉ H ₁₀₆ O ₆	769, 613, 599, 489, 261
63	TG(16:0/18:1/19:1)	X	X	X	X	17.0	890.7790	[M+NH ₄] ⁺	+	C ₅₆ H ₁₀₄ O ₆	617, 591, 577
64	TG(16:0/18:2/19:1)	X	X	X		16.3	888.7613	[M+NH ₄] ⁺	+	C ₅₆ H ₁₀₂ O ₆	615, 591, 575
65	TG(17:1/17:1/19:1)		X			16.5	888.7666	[M+NH ₄] ⁺	+	C ₅₆ H ₁₀₂ O ₆	603, 575

66	TG(18:1/18:1/19:0)		X			17.1	918.8088	[M+NH ₄] ⁺	+	C ₅₈ H ₁₀₈ O ₆	619, 603
67	TG(18:1/18:2/19:0)				X	16.0	916.7936	[M+NH ₄] ⁺	+	C ₅₈ H ₁₀₆ O ₆	615, 601, 599
68	TG(18:1/18:1/19:1)	X	X	X	X	17.0	916.7954	[M+NH ₄] ⁺	+	C ₅₈ H ₁₀₆ O ₆	617, 603
69	TG(18:1/18:2/19:1)	X	X	X	X	16.5	914.7836	[M+NH ₄] ⁺	+	C ₅₈ H ₁₀₄ O ₆	617, 615, 601
70	TG(18:2/18:2/19:1)	X	X	X		15.9	912.7669	[M+NH ₄] ⁺	+	C ₅₈ H ₁₀₂ O ₆	615, 599

DG = diacylglycerol, TG = triacylglycerol

3.3.1.6 Free fatty acids identification

Fatty acids are widespread in animal and plant species, representing the main energy source for metabolic pathways. Besides their conclamate role in energy supplementation, fatty acids, specially mono- and polyunsaturated derivatives, showed beneficial effects for human health due to their capacity to reduce hematic LDL levels and enhance HDL, reducing the onset incidence of cardiovascular diseases ascribable to atherosclerotic plaques genesis (Woollett & Dietschy, 1994).

Nuts have been widely described for their high content of MUFA and PUFA and the resulting benefits exerted on health. In addition, a steady almond consumption showed to produce positive effects, with long-term benefits (Berryman et al., 2011). Therefore, it resulted worthy to extend our lipidome profiling to this class of constituents.

Free fatty acids were detected in negative ion mode as [M-H]⁻ pseudomolecular ions, and the accurate *m/z* values allowed to determine the chain length and the unsaturation degree. In MS/MS experiments they exhibited the same behaviour, originating [M-H-18]⁻ and [M-H-44]⁻ product ions formed by neutral loss of a water molecule and of the carboxylic group as carbon dioxide, respectively (Table 3.5). Unfortunately, no further structural information were provided, unabling to determine the position of the unsaturations.

Table 3.5 Free fatty acids putatively identified in *P. dulcis* seeds cvs. Toritto and Avola

N°	Compound	Toritto	Fascionello	Pizzuta	Romana	R _t	<i>m/z</i>	Ion	Ion Mode	Molecular Formula	MS/MS
71	Palmitic acid	X	X	X	X	6.2	255.2339	[M-H] ⁻	-	C ₁₆ H ₃₂ O ₂	237, 211
72	Stearic acid	X	X	X	X	6.9	283.2653	[M-H] ⁻	-	C ₁₈ H ₃₆ O ₂	265, 239
73	Oleic acid	X	X	X	X	6.4	281.2511	[M-H] ⁻	-	C ₁₈ H ₃₄ O ₂	263, 237
74	Linoleic acid	X	X	X	X	5.9	279.2339	[M-H] ⁻	-	C ₁₈ H ₃₂ O ₂	261, 235

3.3.1.7 Multivariate data analysis

Several studies carried out on different nut cultivars highlighted a putative influence of different growing conditions, like soil composition, temperatures, rainfalls, altitude, affecting the metabolite profile of a plant species (Shen et al., 2013; Klockmann et al., 2016; Hüseyin et al., 2014). In case of edible parts, such variations in the chemical composition may have an important role in determining their taste and nutritional values.

A quick overview on data obtained from the previous LC-HRMS/MS analysis of *P. dulcis* seeds (cvs. Toritto and Avola) non-polar constituents pointed out clear differences in their metabolome, further validating the geographical area/composition relationship. However, the only analysis of LC-HRMS profiles and related tables may not allow a simple and immediate data interpretation. Therefore, raw data obtained from LC-HRMS experiments were processed by a multivariate data analysis approach, with the aim to achieve a quicker and simpler data interpretation.

Multivariate data analysis has proved to be a powerful tool in metabolomics to rapidly spot differences and similarities when a high number of information is provided, becoming an elective data processing method when a high number of observations (in this case, almond cultivars) and variables (in this case, peak areas of detected metabolites) are correlated, necessitating of a graphical data interpretation.

LC-HRMS raw data were used to generate a data matrix in which different almond cultivars (observations) and peak areas of the detected compounds (variables) were reported. Principal Component Analysis (PCA) was first performed to achieve an overview of the dataset, paying attention to detect eventual correlations among observations. In PCA score plot (Fig. 3.11) a remarkable clustering was observed, since cv. Toritto (T1-8) was located in the lower left area

of the plot while the cvs. Avola were diagonally opposed, evidencing a difference among Apulian and Sicilian cultivars. In addition, a further clustering among the three Sicilian cultivars was observed, with Fascionello (F1-8), Pizzuta (P1-8) and Romana (R1-8) located in three different regions of the plot. Such evidence suggested a metabolome variation occurring in *P. dulcis* seeds due to inequalities in the metabolic pathways of the investigated cultivars. PC1 contributed to 41.8% of the variance, while PC2 to 29.7%, with a total variance of 71.5%, suggesting a satisfying discrimination among the observed clusters.

On the other hand, the PCA loading plot showed the influence of the detected constituents in determining the differences observed in the score plot (Fig. 3.11).

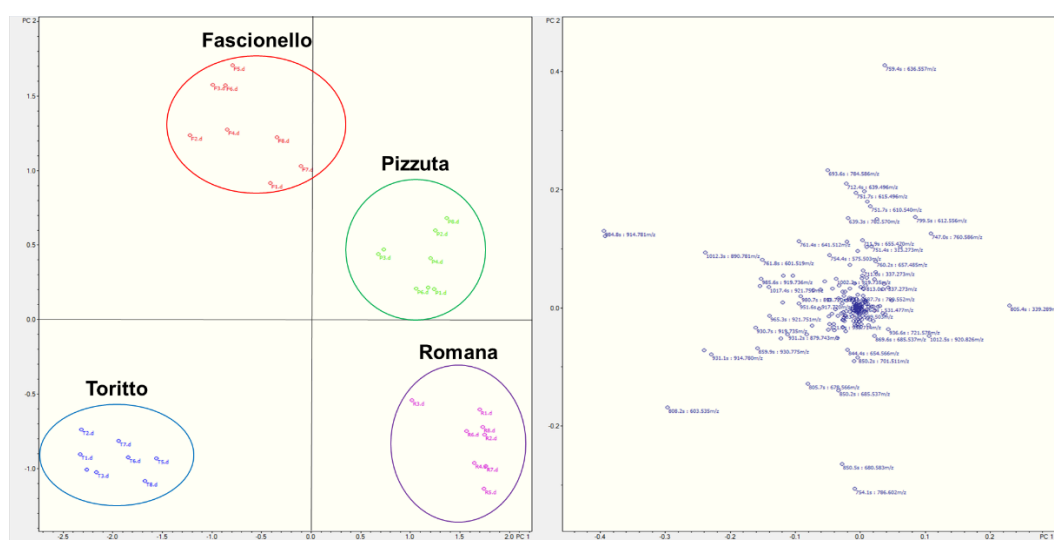


Figure 3.11 PCA score plot and loading plot of *P. dulcis* seeds (cvs. Toritto and Avola)

In addition, by performing a Bucket evaluation, it was possible to observe how the most differentiating metabolites affected dissimilarities shown in the score plot; in particular, their distribution in the investigated cultivars was assessed.

TG (18:1/18:1/19:1) (**68**) resulted abundant in Toritto and Fascionello cvs., as well as TG (18:1/18:2/19:1) (**69**) and TG (16:0/18:1/19:1) (**63**), while TG

(2:0/18:1/18:1) (**59**) and PC (18:1/18:2) (**38**) showed higher occurrence in Toritto and Romana cvs. DG (18:1/18:2) (**55**) resulted abundant in Fascionello and also in Pizzuta cultivars. Even if the loading plot of PCA suggested their possible role in cultivars differentiation, metabolites with m/z 603.535 and 339.289 were not considered in Bucket evaluation, since after an accurate analysis of the LC-HRMS/MS spectra, together with the consideration of their retention time and their signal level distribution, they resulted to be product ions corresponding to DG (18:1/18:1) or DG (18:0/18:2) and to MG (18:1), respectively, detected as $[\text{acyl}+74]^+$ ions, originating from in-source fragmentation events.

Furtherly, Partial Least Square (PLS) score plot (Fig. 3.12) highlighted differences among the metabolite profiles of the investigated cultivars as well. The component one accounted 23% of the variation, while, component two 39%. Furtherly, good values of predictability ($Q^2 = 0.89$) and separation ($R^2Y = 0.94$) were observed; in order to assess the model robustness and reliability, validating permutation tests were carried out. Cv. Toritto (T1-8) resulted located in the lower right section of the plot, while Sicilian cvs. were located on the opposite side, suggesting once again a potential influence of different growing conditions on the metabolite pathways of a plant species. Nevertheless, as observed in PCA, Fascionello (F1-8), Pizzuta (P1-8) and Romana (R1-8) cultivars were placed in three different sections of the plot, hinting the occurrence of inter-cultivars metabolome dissimilarities.

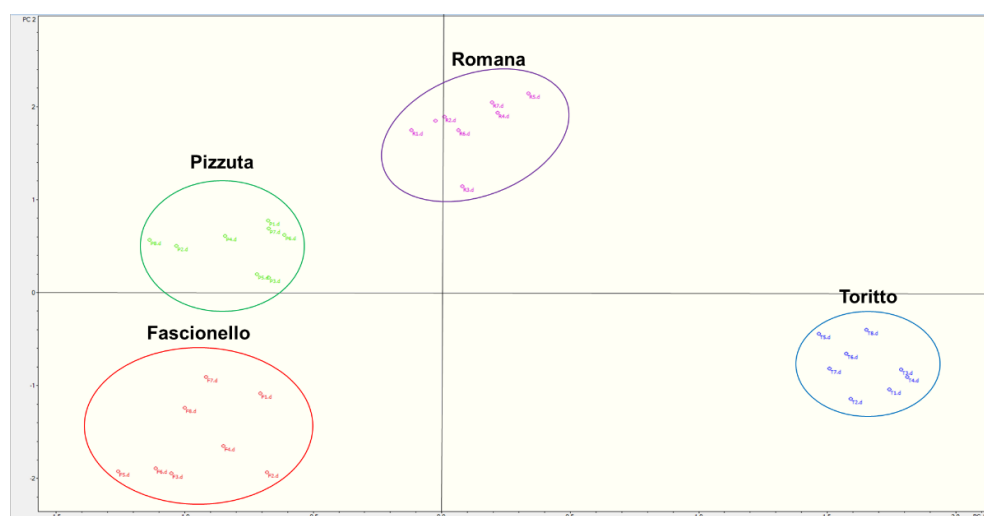


Figure 3.12 PLS analysis score plot of *P. dulcis* seeds (cvs. Toritto and Avola)

3.4 Free fatty acids GC-FID quali-quantitative analysis of *P. dulcis* seeds (cvs. Toritto and Avola)

3.4.1 Results and discussion

3.4.1.1 GC-FID analysis

Gas chromatography proved over the years to be a robust and elective analytical method for the analysis of several classes of compounds, finding applications in many fields, as environmental analysis, food and drug quality controls, forensic sciences, cosmetics. The main advantages showed by GC are due to the capacity to rapidly and satisfyingly separate compounds otherwise not analyzable by liquid chromatography because of their chemical properties.

In food analysis, GC is mostly employed for separating volatile and non-polar constituents, successively detected by specific (ECD, FPB) or universal (FID) detectors, even if it has achieved its maximum potential by the coupling with mass spectrometers.

Pursuing the investigation on the non-polar fraction of *P. dulcis* seeds, the oily fraction was submitted to GC-FID analyses in order to identify the main occurring free fatty acids, previous derivatization to make sample suitable with GC experiments.

The main free fatty acids (palmitic, palmitoleic, stearic, oleic and linoleic acids) were detected and quantified.

3.4.1.2 Fatty acids extraction and fatty acid methyl esters (FAMEs) synthesis

Fatty acids were extracted by using non-polar solvent (*n*-hexane) by stirring, and the obtained extract dried till constant weight by rotary evaporator and by nitrogen gurgling. Prior to GC analysis, samples were converted to their respective methyl esters following the method described by Ichihara & Fukubayashi, with slight modifications: a small amount of sample was dissolved in *n*-hexane and MeOH, and HCl 2 M was successively added (Ichihara & Fukubayashi, 2010).

Successively, the obtained FAMEs were analyzed by GC-FID.

3.4.1.3 Identification and quantification of the major free fatty acids

The identification of the detected free fatty acids was carried out by comparing the retention times (R_t) showed in their GC-FID chromatograms (Fig. 3.13) with a FAMEs standard solution analyzed in the same experimental conditions (Fig. 3.14).

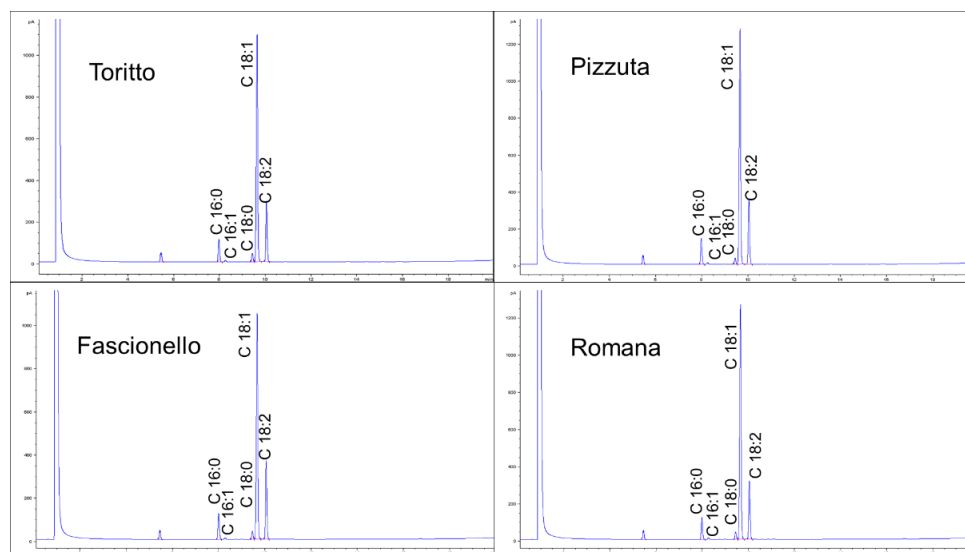


Figure 3.13 GC-FID chromatograms of FAMES identified in *P. dulcis* seeds (cvs. Toritto, Fascionello, Pizzuta and Romana)

To achieve an accurate comparison of the R_t , a signal alignment of the detected peaks was performed, by using as reference peak the one related to butylhydroxytoluene (BHT). This led to the identification of two saturated fatty acids (palmitic and stearic acids), two monounsaturated fatty acids (palmitoleic and oleic acids) and one polyunsaturated fatty acid (linoleic acid), previously detected in LC-HRMS experiments. Successively, calibration curves (Table 3.6) were assessed by analyzing increasing concentrations of the FAMES standard solution, and main fatty acids quantified by performing peak areas integration. Fatty acids concentration was expressed as amount percentage of total content (Table 3.7).

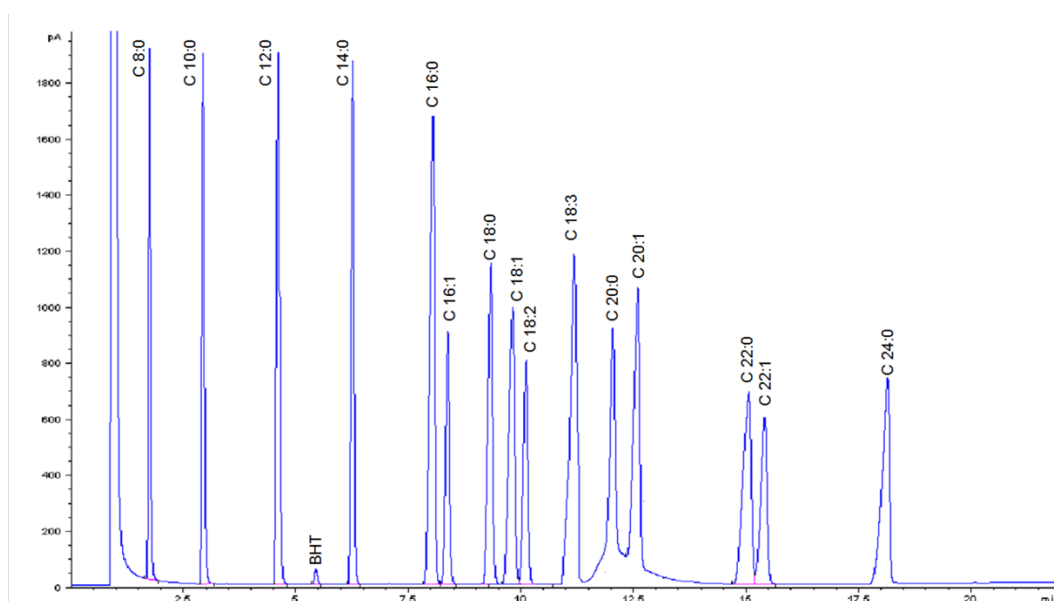
Table 3.6 Quantitative data of *P. dulcis* (cvs. Toritto and Avola) seeds oily fraction. Five-point calibration, with a multi-component standard. LOQ (Limit of quantification) and LOD (Limit of detection) expressed in $\mu\text{g/mL}$

Compound	R_t	R^2	Regression line	LOQ ($\mu\text{g/mL}$)	LOD ($\mu\text{g/mL}$)
palmitic acid (C 16:0) (71)	8.01	0.9981	$y=2580x-71$	0.18	0.06
palmitoleic acid (C 16:1) (75)	8.46	0.9996	$y=1524x-17$	0.12	0.05
stearic acid (C 18:0) (72)	9.39	0.9972	$y=640x-35$	0.20	0.09
oleic acid (C 18:1) (73)	9.87	0.9971	$y=8123x-214$	0.14	0.05
linoleic acid (C 18:2) (74)	10.17	0.9978	$y=349x+19$	0.16	0.07

Table 3.7 Amount (%) \pm SD of the main fatty acids quantified in the oily fraction of the Italian almond cvs. Toritto and Avola

N°	Compound	Toritto	Fascionello	Pizzuta	Romana
71	Palmitic acid (C 16:0)	4.42 \pm 0.31	4.71 \pm 0.24	4.98 \pm 0.26	4.19 \pm 0.14
75	Palmitoleic acid (C 16:1)	0.46 \pm 0.07	0.47 \pm 0.06	0.34 \pm 0.02	0.43 \pm 0.07
72	Stearic acid (C 18:0)	2.83 \pm 0.07	2.26 \pm 0.03	1.79 \pm 0.11	2.29 \pm 0.14
73	Oleic acid (C 18:1)	65.74 \pm 162	60.85 \pm 1.47	66.16 \pm 2.09	68.05 \pm 1.55
74	Linoleic acid (C 18:2)	26.55 \pm 0.57	31.71 \pm 1.02	26.73 \pm 0.85	25.04 \pm 0.77

Results expressed as percentage of the total amount of the detected free fatty acids.
Standard Deviation of three independent experiments.

**Figure 3.14** GC-FID chromatogram of FAMES standard mixture

Quali-quantitative analysis results were in accordance with previous investigations carried out on other almond cultivars (Hüseyin et al., 2014; Popa et al., 2013). Oleic acid (**73**) resulted the major constituent, followed by linoleic (**74**) and palmitic acid (**71**). Nevertheless, compared to data reported in literature, linoleic acid (**74**) exhibited a higher concentration (Hüseyin et al., 2014; Popa et al., 2013). However, linolenic acid signal was slightly detected, and its quantification was impossible to perform.

Free fatty acids identified in the oily fraction of almonds have been exhaustively reported in scientific literature for the beneficial effects exerted on human health, mainly due to the reduction of hematic LDL levels, and promoting the enhancement of HDL levels, leading to a lower incidence of cardiovascular adverse events onset (Heyden S., 2014). Moreover, almond oil showed to possess anticancer activity in colon carcinoma, while *in vivo* hepatoprotective effects against liver injuries induced by carbon tetrachloride were observed (Mericlia et al., 2017; Xiao-Yan et al., 2011).

3.5 Conclusions

Phytochemical investigations carried out on the polar fraction of *P. dulcis* whole seeds pointed out the occurrence of several phenolic constituents reported for their antioxidant activity, effectively extracted by the “eco-friendly” extraction methods. Following studies carried out on the main product and by-products deriving from peeling processes allowed to determine the originating matrices of the identified compounds, highlighting discarded almond skins and blanching waters as a rich source of phenolics, as supported by the results achieved from Folin-Ciocalteu assay, suggesting a potential employment in industrial applications for the manufacture of phenolics-/fibers-rich dietary supplements.

Comparison of the polar fractions LC-HRMS profiles evidenced visible differences among the Apulian and the Sicilian cultivars, suggesting a possible influence of different growing conditions on the metabolome of a plant species. Such differences were also highlighted by comparing the data obtained from the LC-HRMS profiles acquired in the investigation of the non-polar fraction of *P. dulcis* seeds, processed by a multivariate data analysis approach, which allowed to identify different classes of phospholipids, jointly with di-/triacylglycerols. In addition, GC-FID experiments carried out on almonds oily fraction pointed out the occurrence of mono-/polyunsaturated fatty acids.

The obtained results can provide an added value to the Italian “Mandorla di Toritto” and “Mandorla d’Avola”, highlighting the potential beneficial effects deriving from a moderate daily consumption.

3.6 Experimental procedures

Plant material

Apulian “Mandorla di Toritto” (cv. Filippo Cea) samples were provided by “La Fattoria della mandorla” (Toritto, Italy), while samples of the “Mandorla d’Avola” (cvs. Fascionello, Pizzuta and Romana) were provided by the “Consortium of the Mandorla d’Avola” (Avola, Italy).

Extraction of polar constituents

In order to ease the analysis of the polar constituents, almond samples were submitted to defatting extraction processes. 1.6 kg of almonds of the cv. Toritto were extracted by maceration employing petroleum ether (1.5 L, three times for three days), chloroform (1.5 L, three times for three days) and MeOH (1.5 L, three times for three days), yielding 61.1 g of crude MeOH extract. A small amount (5.0 g) of the crude MeOH extract was then submitted to a liquid-liquid extraction process, by using *n*-hexane and MeOH (three times), in order to remove fats eventually still present, and to a successive liquid-liquid extraction by using BuOH and H₂O (three times), in order to remove the high content of sugars, detected by TLC analysis, yielding 1.4 g of BuOH extract.

The whole seeds were also extracted by using EtOH 96% and a mixture of EtOH and H₂O (1:1, v/v): 10 g of almond samples were extracted by maceration with 100 mL of solvent, three times for three days, yielding 521.36 mg and 642.3 mg of extract, respectively. Moreover, almonds were peeled in order to separately analyze the metabolite profile of the integuments and peeled kernels. In brief, 100 g of almonds were submerged in 500 mL of warm water at a constant temperature of 40°C for 30 min, and then carefully hand peeled. The obtained peeled almonds (80 g) and skins (15 g) were extracted by following the same protocols employed for

the whole seeds, but using a lower amount of solvents (0.5 L for peeled almonds, 0.2 L for integuments), yielding 1.7 g and 1.1 g of crude MeOH extracts, respectively. In addition, H₂O used for separating the kernels from the integuments (blanching water) was frozen and freeze-dried, returning 2.6 g of lyophilized extract.

Almonds of Avola cvs. (Fascionello, Pizzuta and Romana) were extracted at the same way of the Toritto cv.

LC-ESI/LTQOrbitrap/MS/MS and LC-ESI/LTQOrbitrap/MS analysis of polar constituents

LC-HRMS experiments were carried out on instrument reported in general experimental procedures. LC separation was performed on a Phenomenex (Torrance, CA, USA) Kinetex C-18 column (100 x 2.10 mm, 2.6 μm), at a flow rate of 0.2 mL/min. Employed mobile phases were (A) water and (B) acetonitrile, both acidified at 0.1% formic acid. Elution gradient was: 0 min 10% B, 10 min 40% B, returning to starting conditions in 7 min. Injection volume was 10 μL, keeping the column at room temperature. The ESI source parameters were set as following: source voltage at 5 kV, capillary voltage at -12 V, tube lens offset at -121.47 V, capillary temperature at 280°C; sheath gas at 30 (arbitrary unit) and auxiliary gas flow at 5 (arbitrary unit).

Polar lipids extraction

As reported in general experimental procedures.

LC-ESI/QToF/MS/MS and LC-ESI/QToF/MS analysis of polar lipids

As reported in general experimental procedures.

Free fatty acids extraction

As reported in general experimental procedures. Extraction operations yielded for Toritto, Fascionello, Pizzuta and Romana, 17.1 g, 17.5 g, 18.0 g and 18.1 g of oily extract, respectively.

Fatty acids methyl esters (FAME) synthesis

As reported in general experimental procedures.

GC-FID quali-quantitative analysis of free fatty acids

As reported in general experimental procedures.

*Chemometrics**Data analysis*

Raw data obtained from the LC-ESI/QToF/MS experiments were first filtered by using Data Analysis 4.1 software (Bruker Daltonics). In particular, data reduction, gap filling, baseline correction, peak detection, noise elimination were carried out, as well as discard of m/z values originated from in-source fragmentation events, always aiming at preserving the variance of the detected compounds. Successively, filtered data were processed and a data matrix, employed for multivariate data analysis, was obtained. In addition, metabolites identification was performed by comparing m/z values and R_t reported in data matrix with those obtained from previous characterization. Samples were analyzed eight times.

Multivariate data analysis

Aiming at identifying possible differences among the analyzed *P. dulcis* almonds cultivars, the data obtained from the LC-HRMS experiments were submitted to chemometric analyses, in particular PCA and PLS. PCA is an unsupervised method,

widely employed in metabolomics to detect significant patterns related to genetic and environmental factors that, synergistically with PLS, a supervised statistic model, may support the discrimination of varieties originating from different regions.

Evaluation of the raw data obtained from the LC-HRMS analyses, as well as the elaboration of the processed data, were performed with Data Analysis 4.1 software (Bruker Daltonics), applying Pareto scaling on all the data of the obtained matrix. This last one (32 samples x 228 signals) was first analyzed by PCA, in order to define homogeneous samples clusters. Successively, to achieve a satisfactory clustering overview of the analyzed almond cultivars, score and loading plots of PCA were generated for the whole datasets. The known clusters confirmed by PCA were used as Y classes in PLS. Data were modeled by PLS as a supervised approach too, to visualize clustering relationships.

Method validation

Analyses were performed on 8 samples for each cultivar, and all the models were validated by cross-validation techniques and permutation tests, in accordance with standardized good practices, to minimize false discoveries and achieve robust statistical models. $R^2(x)$ values were used to evidence the robustness of the statistical method. In addition, Bucket evaluation of the main discriminant m/z values observed in the PCA loading plot was carried out, in order to further reduce the risk of false positives due to the presence of artifacts, like product ions due to in-source fragmentation events.

Total phenolic content

As reported in general experimental procedures

DPPH• radical scavenging activity

As reported in general experimental procedures

ABTS^{•+} radical scavenging activity

As reported in general experimental procedures

3.7 References

Abdelmoneim, H. A.; Xiaoqiang, Z.; Sherif, M. A.; Sameh, A. K.; Qingzhe, J.; Xingguo, W. Natural phospholipids: occurrence, biosynthesis, separation, identification, and beneficial health aspects. *Critical Rev. Food Sci. Nutr.* **2017**, *18*, 1-23.

Ander, B. P.; Dupasquier, C. M. C.; Prociuk, M. A.; Pierce, G. N. Polyunsaturated fatty acids and their effects on cardiovascular disease. *Exp. Clin. Cardiol.* **2003**, *8*, 164–172.

Berryman, C. E.; Preston, A. G.; Karmally, W.; Deckelbaum, R. J.; Kris-Etherton, P. M. Effects of almond consumption on the reduction of LDL-cholesterol: a discussion of potential mechanisms and future research directions. *Nutr. Rev.* **2011**, *69*, 171-185.

Bligh, E. G.; Dyer, W. J. A rapid method of total lipid extraction and purification. *Canad. J. Biochem. Phys.* **1959**, *37*, 911-917.

Bottone, A.; Montoro, P.; Masullo, M.; Pizza, C.; Piacente, S. Metabolomics and antioxidant activity of the leaves of *Prunus dulcis* Mill. (Italian cvs. Toritto and Avola). *J. Pharm. Biomed. Anal.* **2018**, *158*, 54-65.

Brunsgaard, G.; Kidmose, U.; Sørensen, L.; Kaack, K.; Eggum, B. O. The influence of variety and growth conditions on the nutritive value of carrots. *J. Sci. Food Agr.* **1994**, *65*, 163-170.

Cajka, T.; Fiehn, O. LC-HRMS-Based lipidomics and automated identification of lipids using the lipidblast in-silico MS/MS library. *Methods Mol Biol.* **2017**, 1609, 149-170.

Chaouali, N.; Gana, I.; Dorra, A. et al., Potential toxic levels of cyanide in almonds (*prunus amygdalus*), apricot kernels (*prunus armeniaca*), and almond syrup. *ISRN Toxicology*, **2013**, 6.

De Rosa, S.; De Giulio, A.; Tommonaro, G. Aliphatic and aromatic glycosides from the cell cultures of *Lycopersicon esculentum*. *Phytochemistry*. **1996**, 42, 1031-1034.

Emwas, A. H. The strengths and weaknesses of NMR spectroscopy and mass spectrometry with particular focus on metabolomics research. *Methods Mol Biol.* **2015**, 1277, 161-93.

Heyden, S. Polyunsaturated and monounsaturated fatty acids in the diet to prevent coronary heart disease via cholesterol reduction. *Ann Nutr Metab.* **1994**, 38, 117–122.

Holčapek, M.; Jandera, P.; Zderadička, P.; Hrubà, L. Characterization of triacylglycerol and diacylglycerol composition of plant oils using high-performance liquid chromatography–atmospheric pressure chemical ionization mass spectrometry. *J. Chrom. A.* **2003**, 1010, 195–215.

Hughey, C. A.; Januszewicz, R., Minardi, C. S.; Phung, J.; Huffman, B. A.; Reyes, L.; Wilcox, B. E.; Prakash, A. Distribution of almond polyphenols in blanch water and skins as a function of blanching time and temperature. *Food Chem.* **2012**, 131, 1165–1173.

Hüseyin, K.; Ahmet, Ş.; Ökkeş, Y.; Abdullah, A. Major fatty acids composition of 32 almond (*Prunus dulcis* [Mill.] D.A. Webb) genotypes distributed in East and Southeast of Anatolia. *Turk J Biochem.* **2014**, 39, 307–316.

Ichihara, K.; Fukubayashi, Y. Preparation of fatty acid methyl esters for gas-liquid chromatography. *J. Lipid Res.* **2010**, 51, 635–640.

Imran, M.; Anjum, F. M.; Butt, M. S.; Siddiq, M.; Munir, A, M. Reduction of cyanogenic compounds in flaxseed (*linum usitatissimum* l.) meal using thermal treatment. *Int. J. Food Prop.* **2013**, 16, 1809-1818.

Kamil, A.; Chen, C. Y. Health benefits of almonds beyond cholesterol reduction. *J. Agric. Food Chem.* **2012**, 60, 6694 – 6702.

Karioti, A.; Chiarabini, L.; Alachkar, A.; Fawaz Chehna, M.; Vincieri, F. F.; Bilia, A. R. HPLC–DAD and HPLC–ESI-MS analyses of *Tiliae flos* and its preparations. *J. Pharm. Biomed. Anal.* **2014**, 100, 205-214.

Klockmann, S.; Reiner, E.; Bachmann, R.; Hackl, T.; Fischer, M. Food fingerprinting: metabolomic approaches for geographical origin discrimination of hazelnuts (*Corylus avellana*) by UPLC-QTOF-MS. *J. Agric. Food Chem.* **2016**, 64, 9253–9262.

Knittelfelder, O. L.; Weberhofer, B. P.; Eichmann, T. O.; Kohlwein, S. D.; Rechberger, G. N. A versatile ultra-high performance LC-HRMS method for lipid profiling. *J Chromatogr B Analyt Technol Biomed Life Sci.* **2014**, 100, 119-128.

Lambert, J. E.; Parks, E. J. Postprandial metabolism of meal triglyceride in humans. *Biochim Biophys Acta.* **2012**, 1821, 721–726.

Lee, J.; Zhang, G.; Wood, E.; Castillo, C. R.; Mitchell, A. E. Quantification of amygdalin in nonbitter, semibitter, and bitter almonds (*Prunus dulcis*) by UHPLC-(ESI)QqQ MS/MS. *J. Agric. Food Chem.* **2013**, 61, 7754–7759.

Lin, L.; Sun, J.; Chen, P.; Monagas, M. J.; Harnly, J. M. UHPLC-PDA-ESI/HRMSn profiling method to identify and quantify oligomeric proanthocyanidins in plant products. *J. Agric. Food Chem.* **2014**, 62, 9387–9400.

Mandalari, G. Potential health benefits of almond skin. *J Bioprocess Biotech* **2012**, 2, 5.

¹Mandalari, G.; Faulks, R. M.; Bisignano, C.; Waldron, K. W.; Narbad, A.; et al. *In vitro* evaluation of the prebiotic properties of almond skins (*Amygdalus communis* L.). *Microbiol. Lett.* **2010**, 304, 116-122.

²Mandalari, G.; Tomaino, A.; Rich, G. T.; Lo Curto, R.; Arcoraci, T.; et al. Polyphenol and nutrient release from skin of almonds during simulated human digestion. *Food Chem.* **2010**, 122, 1083-1088.

Martin-Carratala, M. L.; Llorens-Jorda, C.; Berenguer-Navarro, V.; Grane'-Teruel, N. Comparative study on the triglyceride composition of almond kernel oil. a new basis for cultivar chemometric characterization. *J. Agric. Food Chem.* **1999**, 47, 3688-3692.

McAnoy, A. M.; Wu, C. C., Murphy, R. C. Direct qualitative analysis of triacylglycerols by electrospray mass spectrometry using a linear ion trap. *J Am Soc Mass Spectrom* **2005**, 16, 1498–1509.

Mericlia, F.; Becerb, E.; Kabadayic, H.; Hanoglu, A.; Yigit, D.; Hanoglu, D.; Ozkum, Y.; Temel, O.; Vatansever, S. Fatty acid composition and anticancer activity in colon carcinoma cell lines of *Prunus dulcis* seed oil. *Pharm. Biol.* **2017**, 55, 1239–1248.

Pimanová, M.; Neilson, E. H.; Motawia, M. S.; Olsen, C. E.; Agerbirk, N.; J. Gray, C.; Flitsch, S.; Meier, S.; Silvestro, D.; Jørgensen, K.; Sánchez-Pérez, R.; Møller, B. L.; Bjarnholt, N. A recycling pathway for cyanogenic glycosides evidenced by the comparative metabolic profiling in three cyanogenic plant species. *Biochem. J.* **2015**, 469, 375-389.

Popa, V.; Raba, D. N.; Moldovan, C.; Dumbravă, D. G.; Mateescu, C.; Gruia, A. The possibilities of obtaining, characterizing and valorification of almond oil (*Prunus Amygdalus*). *J. Agroalim. Proc. Tech.* **2013**, 19, 455-458.

Pulfer, M.; Murphy, R. C. Electrospray mass spectrometry of phospholipids. *Mass Spectrometry Reviews.* **2003**, 22, 332– 364

Rezanka, T.; Sigler, K. Odd-numbered very-long-chain fatty acids from the microbial, animal and plant kingdoms. *Prog. Lipid Res.* **2009**, 48, 206–238.

Sánchez-Pérez, R.; Jørgensen, K.; Olsen, C. E.; Dicenta, F.; Møller, B. L. Bitterness in Almonds. *Plant Physiol.* **2008**, 146, 1040–1052.

Sang, S.; Li, G.; Tian, S.; Lapsley, K.; Stark, R. E.; Pandey, R. K.; Rosena, R. T.; Hoa, C. An unusual diterpene glycoside from the nuts of almond (*Prunus amygdalus* Batsch). *Tetrahedron Letters*. **2003**, 44, 1199–1202.

Shen, Q.; Dong, W.; Yang, M.; Li, L.; Cheung, H.; Zhang, Z. Lipidomic fingerprint of almonds (*Prunus dulcis* L. cv Nonpareil) using TiO₂ nanoparticle based matrix solid-phase dispersion and MALDI-TOF/MS and its potential in geographical origin verification. *J. Agric. Food Chem.* **2013**, 61, 7739–7748.

Shirosaki, M.; Goto, Y.; Hirooka, S.; Masuda, H.; Koyama, T.; Yazawaa, K. Peach leaf contains multiflorin A as a potent inhibitor of glucose absorption in the small intestine in mice. *Biol. Pharm. Bull.* **2012**, 35, 1264–1268.

Song, S.; Cheong, L.; Wang, H.; Man, Q.; Pang, S.; Li, Y.; Ren, B.; Wang, Z.; Zhang, J. Characterization of phospholipid profiles in six kinds of nut using HILIC-ESIIT-TOF-MS system. *Food Chem.* **2018**, 240, 1171–1178.

Song, Z.; Xu, X. Advanced research on antitumor effects of amygdalin. *J. Can. Res. Ther.* **2014**, 10, 3-7.

Wang, S. Y.; Zheng, W. Effect of plant growth temperature on antioxidant capacity in strawberry. *J. Agric. Food Chem.* **2001**, 49, 4977–4982.

Wat, E.; Tandy, S.; Kapera, E.; Kamili, A.; Chung, R. W. S.; Brown, A.; et al. Dietary phospholipid-rich dairy milk extract reduces hepatomegaly, hepatic steatosis and hyperlipidemia in mice fed a high-fat diet. *Atherosclerosis*. **2009**, 205, 144–150.

White, H.; Venkatesh, B. Clinical review: ketones and brain injury. *Critical Care*. **2011**, 15, 219-229.

Woollett, L. A.; Dietschy, J. M. Effect of long-chain fatty acids on low-density-lipoprotein-cholesterol metabolism. *Am. J. Clin. Nutr.* **1994**, 60, 991–996.

Xiao-Yan, J.; Qing-An, Z.; Zhi-Qi, Z.; Yan, W.; Jiang-Feng, Y.; Hong-Yuan, W.; Di, Z. Hepatoprotective effects of almond oil against carbon tetrachloride induced liver injury in rats. *Food Chem.* **2011**, 125, 673–678.

Xue, M.; Shi, H.; Zhang, J.; Liu, Q.; Guan, J.; Zhang, J.; Ma, Q. Stability and degradation of caffeoylquinic acids under different storage conditions studied by high-performance liquid chromatography with photo diode array detection and high-performance liquid chromatography with electrospray ionization collision-induced dissociation tandem mass spectrometry. *Molecules*, **2016**, 21, 948-960.

Yang, Y.; Benning, C. Functions of triacylglycerols during plant development and stress. *Current Opinion Biotech.* **2018**, 49, 191-198.

Yoshikawa, M.; Murakami, T.; Ishiwada, T.; Morikawa, T.; Kagawa, M.; Higashi, Y.; Matsuda, H. New flavonol oligoglycosides and polyacylated sucroses with inhibitory effects on aldose reductase and platelet aggregation from the flowers of *Prunus mume*. *J. Nat. Prod.* **2002**, 65, 1151-1155.

Chapter 4
***Prunus dulcis* Mill. (cvs. Toritto and Avola)**
biomasses (leaves, husks and shells) as potential
source of bioactives

4.1 Introduction

Prunus dulcis Mill. is a tree belonging to the Rosaceae family, with pink-white flowers appearing before the leaves, dark green colored and spear shaped. The fruit is a drupe, showing peculiar features: it is constituted by a leathery husk, enveloping a wooden and porous shell containing an edible seed rich of oil, commonly known as sweet almond.

Although widely consumed fresh or roasted as they are, almonds are mostly employed in cookery, pastry and above all confectionery on industrial level, causing therefore remarkable amounts of biomasses deriving from the production processes, mainly represented by leaves, shells and husks, considered as waste materials whose disposal costs burden on the farmers. In order to overcome the removal expenses, alternative uses were proposed, like animal fodder, mulching or as cheap fuel for stoves. However, in recent times an increasing number of scientific reports proved agricultural by-products to be a valuable source of bioactives (Tang et al., 2018; Kumar et al., 2017), suggesting their potential employment in other fields, denoting such biomasses no more as wastes of production workflows but rather as a potential economical resource, from which farmers and minor business owners may take advantage. In this study attention was payed on the main by-products deriving from the manufacturing processes of two of the most appreciated Italian almond varieties, that are the “Mandorla di Toritto” and “Mandorla d’Avola”. The first one originates from the territory surrounding Toritto, a small town located in Northern Apulia, and is represented by the cv. Filippo Cea; the second one is represented by the three cvs. Fascionello, Pizzuta and Romana, cultivated in the territory of Avola, an expanding town in the most Southern area of Sicily.

Thus, aiming at proposing *P. dulcis* leaves, husks and shells as perspective sources of biologically active compounds, an exhaustive phytochemical investigation was carried out in order to assess the chemical composition of the non-edible plant parts, focusing the attention on the polar fraction. Moreover, due to the

different provenances of the investigated cultivars, possible dissimilarities in the metabolite profiles were evaluated, looking at establishing if different growing conditions may affect the metabolome of a plant species. In addition, different extracts were prepared by employing “green” solvents, also adapt to human consumption.

Thus, different classes of secondary metabolites were identified, as flavonoids, terpenes, cyanogenic glycosides, lignans and neolignans. In addition, “eco-friendly” extraction methods showed chemical class selectivity, as well as good phenolic content and antioxidant activity. Furthermore, LC-HRMS profiles comparison, and multivariate statistical analysis as well, highlighted differences in the metabolome of the different cultivars.

In this chapter the following topics will be discussed:

- LC-ESI/LTQOrbitrap/MS/MS metabolite profiling of the MeOH extract of *P. dulcis* cvs. Toritto and Avola leaves, husks and shells;
- characterization by NMR experiments of the main polar constituents isolated from the MeOH extracts of *P. dulcis* cvs. Toritto and leaves, husks and shells, previously detected in the LC-ESI/LTQOrbitrap/MS/MS profiles;
- preparation of extracts by employing “eco-friendly” protocols, and comparison of their chemical composition by LC-ESI/LTQOrbitrap/MS analyses;
- determination of the total phenolic content by Folin-Ciocalteu assay of all the prepared extracts, as well as evaluation of the radical scavenging activity by DPPH• and ABTS^{•+} assays;
- comparison of the LC-ESI/LTQOrbitrap/MS profiles of the extracts of the cvs. Toritto and Avola leaves, husks and shells, with the aim to detect similarities and possible differences in the chemical composition, eventually supported by a multivariate data analysis approach.

4.2 Metabolite profiling of the polar fraction of *Prunus dulcis* Mill. leaves, cvs. Toritto and Avola

Prunus dulcis Mill. leaves



P. dulcis is a hysterantous tree, meaning that the leaves appear successively to the blooming. The leaves are 7-12 cm long and 2-3 cm wide, dark green, lance-shaped and with a serrated margin.

4.2.1 Results and discussion

4.2.1.1 Qualitative analysis of the MeOH extract of *P. dulcis*, cv Toritto leaves

To achieve a preliminary overview of the MeOH extract chemical composition of *P. dulcis* leaves, LC-ESI/LTQOrbitrap/MS/MS experiments were carried out both in positive and in negative ion mode. An accurate analysis of the obtained LC-HRMS/MS spectra (Fig. 4.1) suggested the occurrence of multiple classes of secondary metabolites, evidencing the metabolite complexity of the analyzed plant matrix. In particular, glycosylated flavonoids (**14-19**, **21**, **23-24**) resulted the main constituents, together with different typologies of terpenes (**5**, **10-11**, **13**, **20**, **25-27**), phenolic derivatives (**1**, **3**, **6-7**, **22**) and a cyanogenic glycoside (**9**) (Table 4.1).

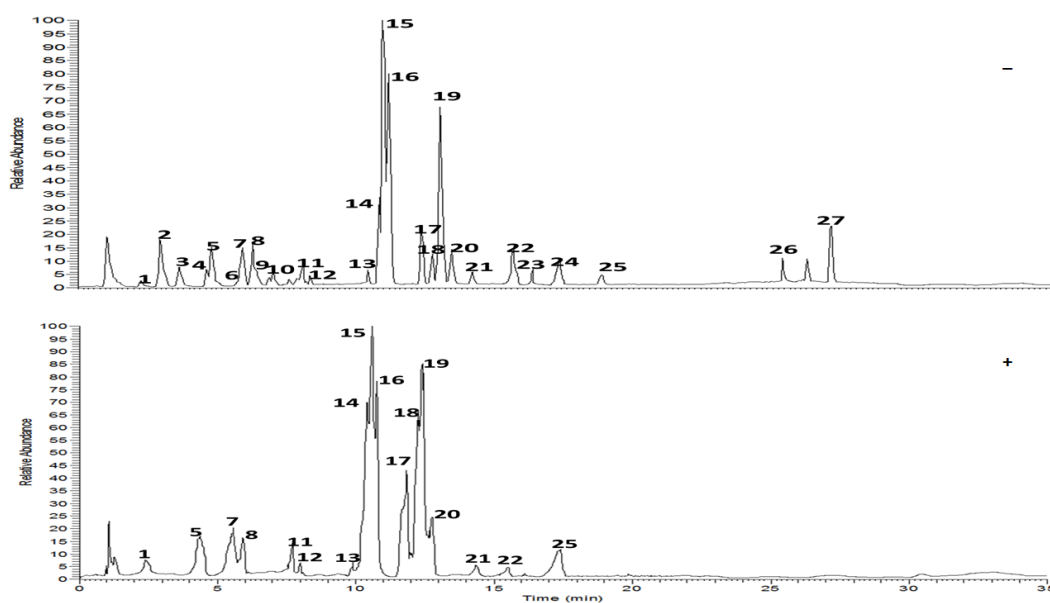


Figure 4.1 LC-HRMS profile in negative and positive ion mode of the MeOH extract of *P. dulcis* cv. Toritto leaves

Table 4.1 Compounds identified and tentatively identified in the MeOH extract of *P. dulcis* cv. Toritto leaves

N°	R _t	Calculated Mass	Appm	[M-H] ⁻	MS ² (%)	[M+H] ⁺	MS ² (%)	Molecular formula	Compound
1	2.24	313.1162	0.86	312.1156 ¹	161(100), 150 (92)	314.1233	152(100)	C ₁₄ H ₁₉ NO ₇	prunasin amide
2	2.94	452.2251	0.48	451.2171	179(100), 243 (24)			C ₂₀ H ₃₆ O ₁₁	unidentified
3	3.63	314.1002	0.96	313.0923	151(100), 269(71)			C ₁₄ H ₁₈ O ₈	prunasinic acid
4	4.21	296.1631	1.54	295.0831	121(100), 173(41)			C ₁₄ H ₁₆ O ₇	unidentified
5	4.83	406.1038	1.03	405.0924	243(100)	407.0864	277(100)	C ₁₉ H ₃₄ O ₉	kiwiionoside ²
6	5.78	326.2192	0.99	325.2112	163(100)			C ₁₅ H ₁₈ O ₈	<i>p</i> -coumaric acid β-glucopyranoside ²
7	5.90	354.0970	1.55	353.0890	191(100), 179(42), 135(23)	355.0994	193(100)	C ₁₆ H ₁₈ O ₉	3- <i>O</i> - caffeoylquinic acid
8	6.29	448.1577	1.03	447.1504	285(100)	449.1647	431(100)	C ₁₉ H ₂₈ O ₁₂	barlerin
9	6.39	295.2173	1.54	294.0973 ¹	161(100)			C ₁₄ H ₁₇ NO ₆	prunasin
10	7.03	386.0926	0.85	385.0845	223(100), 161(42)			C ₁₉ H ₃₀ O ₈	roseoside
11	8.08	386.1043	0.42	385.0037	223(100)	387.1127	341(100)	C ₁₉ H ₃₀ O ₈	asicariside B1 ²
12	8.34	416.0149	0.88	415.0069	299(100)	417.1647	371(100)	C ₁₈ H ₂₄ O ₁₁	unidentified
13	10.44	402.2436	1.74	401.0341	383(100)	403.2146	279(100)	C ₁₉ H ₃₀ O ₉	glochidioniosid e E ²

14	10.84	610.1527	1.33	609.1447	301(100), 300(45)	611.1657	303(100)	C ₂₇ H ₃₀ O ₁₆	rutin ²
15	10.95	464.0951	0.86	463.0871	300(100), 301(64)	465.1982	303(100)	C ₂₁ H ₂₀ O ₁₂	quercetin 3- <i>O</i> -β-D-galactopyranoside ²
16	11.18	464.0951	1.53	463.0871	300(100), 301(57)	465.1982	303(100)	C ₂₁ H ₂₀ O ₁₂	quercetin 3- <i>O</i> -β-D-glucopyranoside ²
17	12.36	448.0998	1.64	447.0918	300(100), 301(61)	449.1634	303(100)	C ₂₁ H ₂₀ O ₁₁	quercetin 3- <i>O</i> -α-L-rhamnopyranoside ²
18	12.74	594.1572	0.63	593.1492	285(100)	595.1843	287(100)	C ₂₇ H ₃₀ O ₁₅	multiflorin B ²
19	13.04	478.1107	1.59	477.1027	314(100), 315(52)	479.3416	317(100)	C ₂₂ H ₂₂ O ₁₂	isorhamentin 3- <i>O</i> -β-D-glucopyranoside ²
20	13.44	418.1603	1.32	417.0069	399(100), 255(47)	419.2493	267(100)	C ₂₁ H ₃₈ O ₈	icariside C3 ²
21	14.08	448.1577	0.50	447.1497	285(100)	449.1384	287(100)	C ₂₁ H ₂₀ O ₁₁	kaempferol 3- <i>O</i> -β-D-glucopyranoside ²
22	15.79	420.1072	1.03	419.0992	153(100), 297(26), 375(14)			C ₂₀ H ₂₀ O ₁₀	shomaside F ²
23	16.34	432.2016	0.10	431.1936	285(100)			C ₂₁ H ₂₀ O ₁₀	kaempferol 3- <i>O</i> -α-L-rhamnopyranoside ²
24	17.26	462.1731	1.89	461.1651	299(100)			C ₂₂ H ₂₂ O ₁₁	kaempferide 3- <i>O</i> -β-D-glucopyranoside ²
25	18.82	650.2404	0.44	649.2324 ¹	487(100)	651.3461	615(100)	C ₃₆ H ₅₈ O ₁₀	lucyoside I
26	25.29	488.3334	1.00	487.3254	249(100)			C ₃₀ H ₄₈ O ₅	arjunolic acid ²
27	27.06	444.3575	0.63	443.3495	399(100), 383(51), 313(52)			C ₂₉ H ₄₈ O ₃	rubrajaleol ²

¹Observed as formate adduct. ²The identification of this compound was corroborated by isolation and NMR spectra analysis

In order to unambiguously determine their chemical structure by NMR experiments, the MeOH extract was submitted to size-exclusion chromatography and the obtained fractions were further purified by RP-HPLC. The isolated compounds were then analyzed by 1D and 2D NMR experiments, and the assigned identity was additionally confirmed by ESI/HRMS/MS analyses.

These operations led to the identification of a relevant number of glycosylated flavonoids (Fig. 4.2), namely quercetin 3-*O*-β-D-rutinoside (**14**), quercetin 3-*O*-β-D-galactopyranoside (**15**), quercetin 3-*O*-β-D-glucopyranoside (**16**), quercetin 3-*O*-α-L-rhamnopyranoside (**17**), kaempferol 3-*O*-β-D-glucopyranosyl-(1→4)-*O*-α-L-rhamnopyranoside (**18**), isorhamentin 3-*O*-β-D-glucopyranoside (**19**), kaempferol

3-*O*- β -D-glucopyranoside (**21**), kaempferol 3-*O*- α -L-rhamnopyranoside (**23**) and kaempferide 3-*O*- β -D-glucopyranoside (**24**) (Nascimento et al., 2017; Ieri et al., 2015; Deep et al., 2012; Mari et al., 2014; Nguyen Ngoc et al., 2018; Kazuma et al., 2003).



Figure 4.2 Compounds isolated from the MeOH extract of *P. dulcis* cv. Toritto leaves

To the best of our knowledge there is only one report about the chemical composition of *P. dulcis* leaves, describing the isolation and characterization of compound **15**, highlighting a lack of information about the metabolome of the aerial parts of almond tree (Tomas F., 1977). However, the identified flavonoids have been reported in different parts of other species belonging to *Prunus* genus, in particular compound **18**, also known as multiflorin B, occurring in different species of the Rosaceae family (Kim et al., 2008). The listed phenolics, in particular compounds **15** and **16**, have been exhaustively reported for the considerable number of beneficial effects exerted on human health, able to prevent the onset or to counteract already existing diseases, mainly thanks to their antioxidant and antiinflammatory properties (Kim et al., 2002; D'Andrea G., 2015). Besides

flavonoids, a further phenolic compound was isolated and identified as shomaside F (**22**); this compound was firstly identified in *Cimicifuga simplex* and *Cimicifuga japonica*, and successively in *Meehania urticifolia* (Iwanaga et al., 2010; Murata et al., 2011). However, to the best of our knowledge, shomaside F (**22**) has never been reported before in the Rosaceae family. In addition to phenolics, six terpenes were isolated and identified. In particular, a linear sesquiterpene named icariside C₃ (**20**), which showed to possess a slow vasorelaxant activity against noradrenaline-induced contraction of isolated rat aorta (Oshimi et al., 2008), three glycosylated megastigmanes known as kiwiionoside (**5**), glochidionoside E (**13**) and asicariside B₁ (**11**), together with two triterpenes, arjunolic acid (**26**) and rubrajallelol (**27**), the former reported for its promising antimicrobial activity against *Mycobacterium bovis* and the latter for its moderate antioxidant and antiurease activities (Mann et al., 2012; Miyase et al., 1987; Wang et al., 2014; Otsuka et al., 2003; Akhtar et al., 2013; Hisamoto et al., 2004).

For an unambiguous identification of terpenes, NMR spectroscopy resulted indispensable, allowing to discriminate among the possible structural isomers and stereoisomers. As example, hereafter the structural elucidation of compounds **26** and **27** will be described.

The ¹H-NMR spectrum of compound **26** (Fig. 4.3) showed six signals between δ 0.71 and 1.21, suggesting the occurrence of methyl groups bonded to quaternary carbons. Two signals at δ 3.71 (m) and 3.38 (d, J = 9.8 Hz), indicative of secondary alcoholic functions, along with signals at δ 3.30 (d, J = 10.8 Hz) and 3.54 (d, J = 10.8 Hz), corresponding to a primary alcoholic function, were evident. A typical signal at δ 5.29 (t, J = 3.4 Hz), ascribable to H-12 of a triterpene skeleton, could be observed. The COSY spectrum (Fig. 4.6) showed the correlation between the signals at δ 3.71 and 3.38, which in turn correlated in the HMBC spectrum (Fig. 4.5) with the carbon resonances at δ 43.7 (C-4), 69.4 (C-2), 66.2 (C-23) and 13.2 (C24). Thus, the two secondary alcoholic functions were attributed to C-2 and C-3.

The ^{13}C -NMR spectrum showed 30 carbon resonances, typical of an oleanane-triterpene. On the basis of the achieved information and comparison with literature, compound **26** was identified as arjunolic acid (Mann et al., 2012)

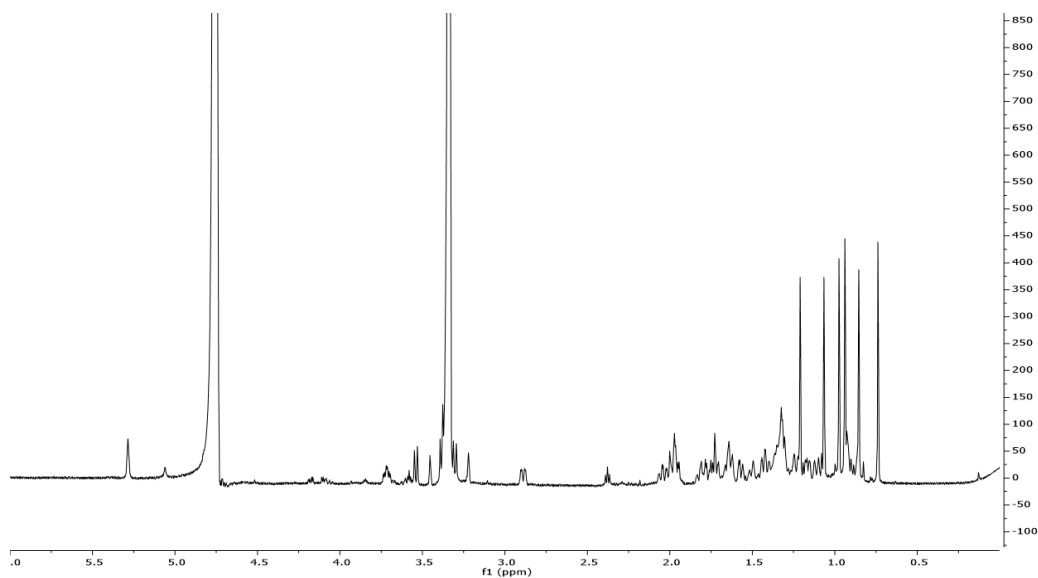


Figure 4.3 ^1H -NMR spectrum of compound **26**

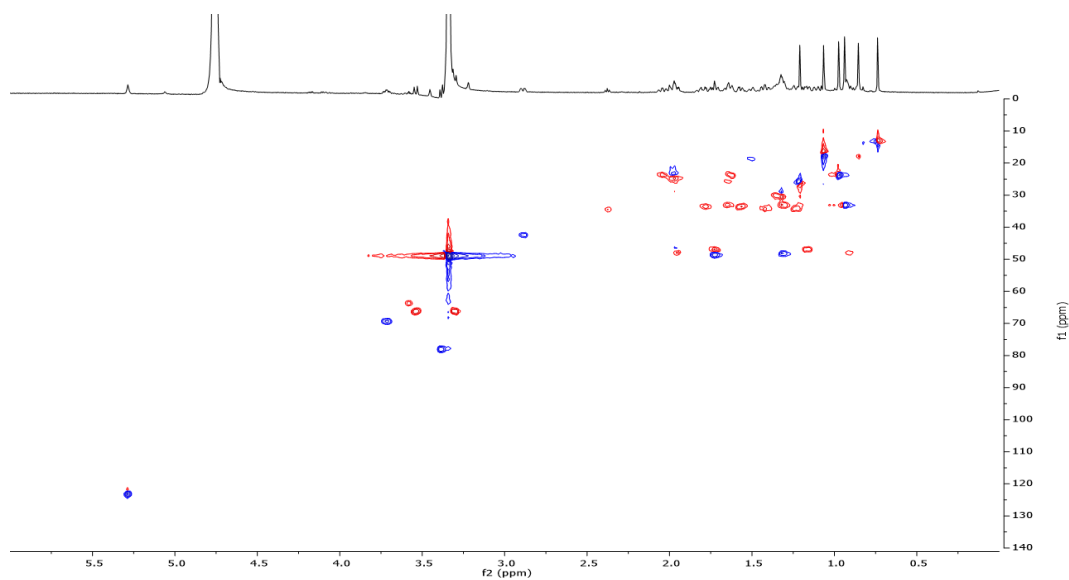


Figure 4.4 HSQC spectrum of compound **26**

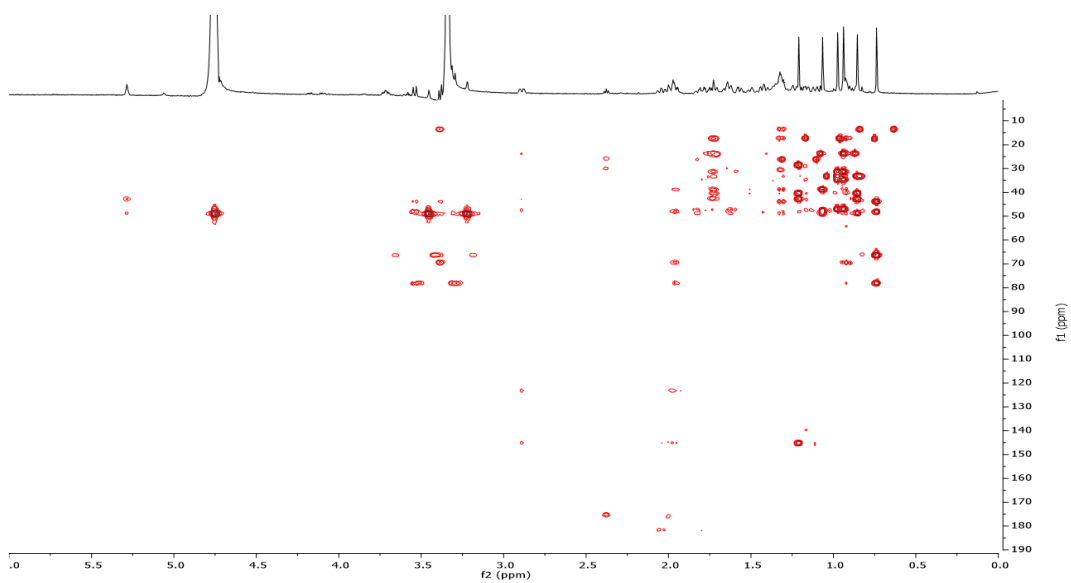


Figure 4.5 HMBC spectrum of compound 26

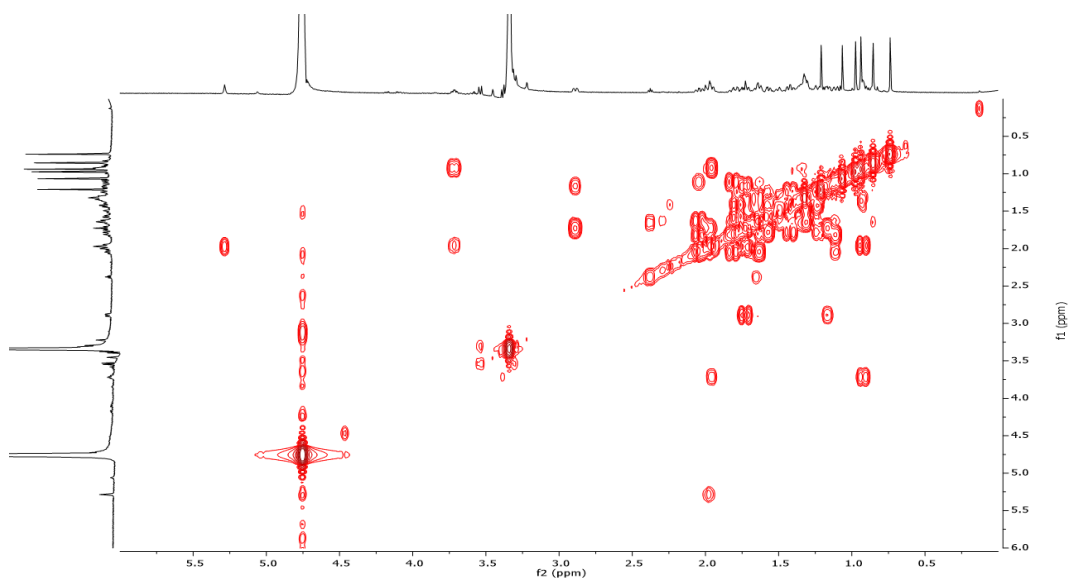


Figure 4.6 COSY spectrum of compound 26

The NMR data of **27**, in comparison with **26**, showed differences related to ring E. The $^1\text{H-NMR}$ spectrum of compound **27** (Fig. 4.7) showed a signal ascribable to H-29 at δ 0.92 (d, $J = 6.7$ Hz), correlating in the HMBC spectrum (Fig. 4.9) with C-19 at δ 40.2, suggesting a methyl group bonded to a tertiary carbon; moreover, H-28 at δ 1.00 (s) showed HMBC correlation with C-18 at δ 54.1. In addition, the COSY spectrum (Fig. 4.10) showed sequential correlations from H-18 at δ 2.25 (d, $J = 11.1$ Hz) to H-22 at δ 1.04/1.47 (m). Thus, compound **27** could be identified as rubrajalelol, a nor-ursene derivative (Akhtar et al., 2013).

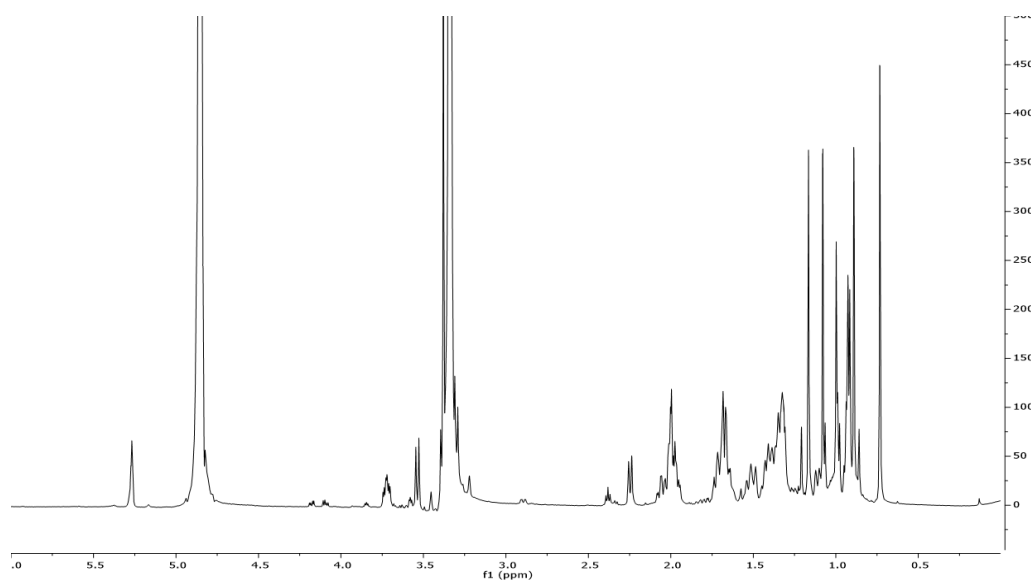


Figure 4.7 $^1\text{H-NMR}$ spectrum of compound **27**

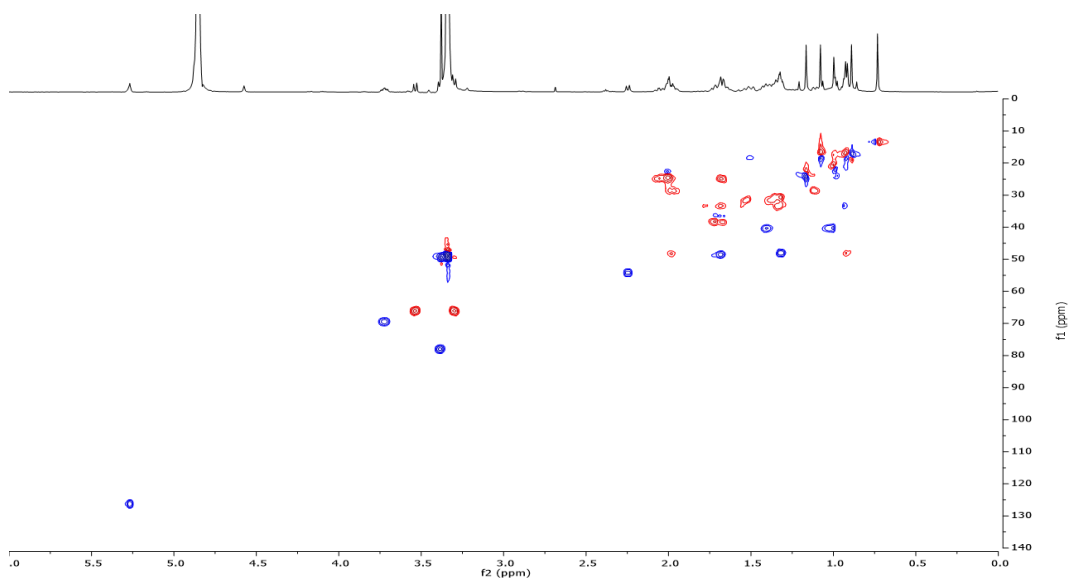


Figure 4.8 HSQC spectrum of compound 27

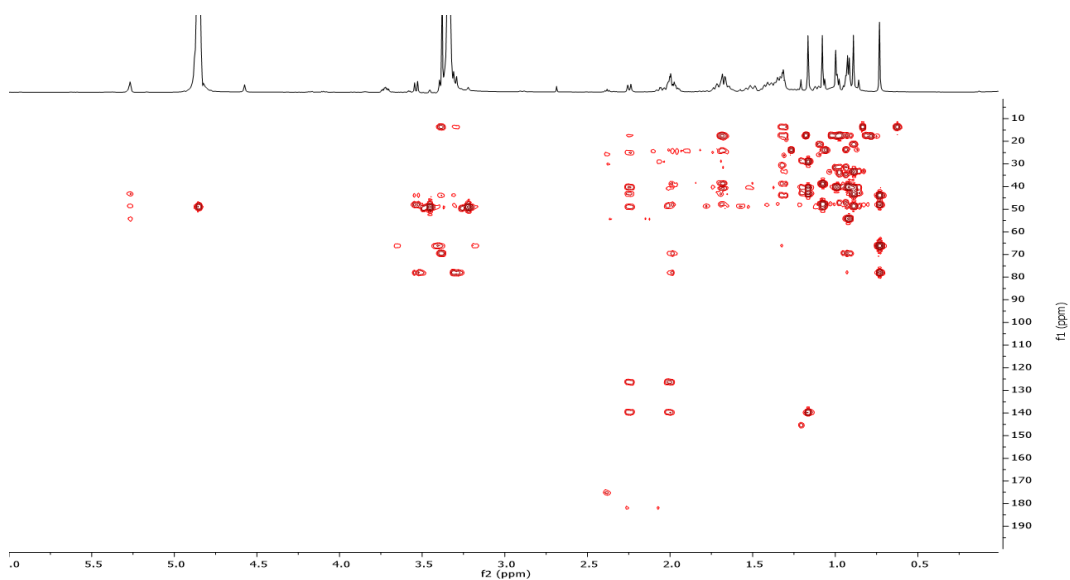


Figure 4.9 HMBC spectrum of compound 27

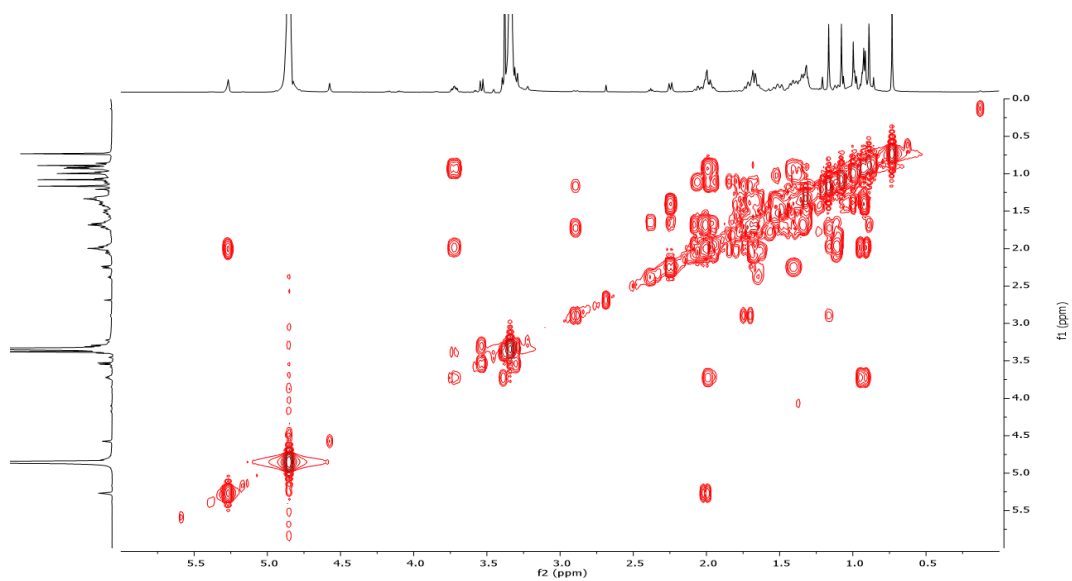


Figure 4.10 COSY spectrum of compound 27

Table 4.2 ^1H (600 MHz) and ^{13}C (150 MHz) NMR spectral data of compounds **26** and **27**

	26		27	
	δ_{C}	δ_{H} (J in Hz)	δ_{C}	δ_{H} (J in Hz)
1	47.9	0.92, 1.95, m	48.1	0.92, 1.99, m
2	69.4	3.71, m	69.4	3.72, ddd (4.6, 9.8, 11.3)
3	77.9	3.38, d(9.8)	78.0	3.39, d(9.6)
4	43.7	-	43.6	-
5	48.1	1.32, m	47.9	1.32, m
6	19.5	1.62, 1.44, m	19.8	1.42, 1.61, m
7	33.0	1.32, 1.65, m	33.2	1.37, 1.53, m
8	40.3	-	40.4	-
9	48.6	1.73, m	48.5	1.68, m
10	38.7	-	38.7	-
11	24.7	1.97, 1.68, m	24.5	2.00, m
12	123.2	5.29, t(3.4)	126.2	5.27, t(3.6)
13	145.2	-	139.4	-
14	42.8	-	42.7	-
15	28.6	1.15, m	28.9	1.12, d(11.2)
16	23.7	1.62, 2.04, m	34.1	1.53, 1.89, m
17	47.5	-	40.4	-
18	42.4	2.89, m	54.1	2.25, d(11.1)
19	47.0	1.17, 1.73, m	40.2	1.14, 1.69, m
20	31.1	-	19.1	1.01, 1.42, m
21	34.6	1.22, 1.42, m	31.4	1.32, 1.56, m
22	33.5	1.56, 1.78, m	34.9	1.04, 1.47, m
23	66.2	3.30, d(10.8) 3.54, d(10.8)	66.0	3.30, d(11.4) 3.54, d(11.4)
24	13.2	0.71, s	13.3	0.73, s
25	17.0	1.07, s	17.2	1.07, s
26	17.9	0.85, s	17.7	0.89, s
27	25.8	1.21, s	23.3	1.16, s
28	181.0	-	21.0	1.00, s
29	33.2	0.93, s	17.6	0.92, d(6.7)
30	23.7	0.97, s		

In MeOH- d_4

Furthermore, the LC-ESI/LTQOrbitrap/MS/MS spectra of the MeOH extract of *P. dulcis* cv. Toritto leaves showed peaks with m/z values related to compounds not isolated, putatively identified by exploiting the potentialities of a high resolution mass spectrometer as the Orbitrap is, by measuring the accurate m/z values and determining the molecular formulae, as well as evaluating the fragmentation

patterns showed in the MS/MS spectra, and comparing the obtained information with online databases and data reported in literature (Table 4.1). In some cases it was possible to detect certain compounds both in positive and in negative ion mode, rendering a high number of information useful to their characterization.

Compound **7** (m/z 353.0890) exhibited in the MS/MS spectrum a product ion at m/z 191, due to the loss of the caffeic acid moiety, a fragment ion at m/z 179 ascribable to the loss of the quinic acid moiety and a further product ion at m/z 135, related to the decarboxylated caffeic acid; in this case, the evaluation of the fragment ions intensities observed in the MS/MS spectrum allowed to determine with a higher certainty level the structure of the analyzed compound, in particular the binding position of caffeic acid with quinic acid; the molecular formula was established as $C_{16}H_{18}O_9$, corresponding to 3-*O*-caffeoylquinic acid (Clifford et al., 2003) (Table 4.1).

Compound **10** (m/z 385.0845) showed in the fragmentation spectrum a base peak at m/z 223 originated by the neutral loss of a dehydrated hexose, confirmed by the signal at m/z 161; the molecular formula was established as $C_{19}H_{30}O_8$; the tentative identification of compound **10** as roseoside was supported by the isolation of three megastigmanes from the MeOH extract of cv. Toritto leaves (Jiménez-López et al., 2017) (Table 4.1).

Compound **25** (m/z 649.2324) showed in the MS/MS spectrum in negative ion mode a fragment ion at m/z 487 originated from the loss of a dehydrated hexose unit; the molecular formula was established as $C_{36}H_{58}O_{10}$ and compound **25** was tentatively identified as arjunolic acid 3-*O*-glucoside, also known as lucyoside I, in agreement with the isolation of the corresponding aglycone arjunolic acid (**26**) (Lima et al., 2002) (Table 4.1).

The HRMS spectrum of compound **1** showed a pseudomolecular ion $[M-H]^-$ at m/z 312.1156, hence with an odd number of nitrogen atoms, and a daughter ion at m/z 150 generated from the loss of a hexose moiety, and a fragment ion at m/z 161

due to the loss of the mandelamide moiety. Thus the molecular formula was established as $C_{14}H_{19}NO_7$ and compound **1** was tentatively identified as prunasin amide (Sendker et al., 2016) (Table 4.1).

Compound **3** (m/z 313.0923) exhibited in the tandem mass spectrum a base peak at m/z 151 due to the loss of a hexose unit; the molecular formula was established as $C_{14}H_{18}O_8$, and compound **3** was tentatively identified as prunasinic acid (Sendker et al., 2016) (Table 4.1).

Compound **9** (m/z 294.0973) showed in the MS/MS spectrum a base peak at m/z 161, attributed to the loss of a mandelonitrile moiety; thus the molecular formula was established as $C_{14}H_{17}NO_6$, suitable with the cyanogenic glucoside prunasin (Sendker et al., 2016) (Table 4.1).

Compounds **1**, **3** and **9** have been reported in *Prunus laurocerasus* as part of a decomposition pathway occurring in the leaves during the pseudosenescence and senescence phases. Prunasin (**9**) represents the precursor of the decomposition pathway in which it is oxidized to prunasin amide (**1**) during the pseudosenescence stage, followed by a deamination reaction, occurring during the senescence period, returning prunasinic acid (**3**). The described reactions explain the contemporaneous presence of compounds **1**, **3** and **9** as deriving from a common catabolic pathway (Sendker et al., 2016).

Cyanogenic glycosides, like prunasin (**9**), have been widely reported for their occurrence in plant species belonging to the Rosaceae family, in particular those of the *Prunus* genus. Most commonly identified in the seeds, like in sweet or bitter almonds (*Prunus dulcis* var. *dulcis* and *amara*, respectively), wild peach (*Prunus davidiana*) and black cherry (*Prunus serotina*), their presence has been assessed in the leaves as well, like in cherry laurel (*Prunus laurocerasus*) (Sendker et al., 2016; Santos Pimenta et al., 2014; Chen et al., 2013).

4.2.1.2 LC-ESI/LTQOrbitrap/MS analysis and comparison of eco-friendly extracts

With the aim to propose simple and cheap extraction protocols for the isolation of secondary metabolites from plant material, suitable with the production of nutraceutical and cosmetic formulations, as well as to evaluate the extraction selectivity of different solvents and extraction methods, sundry typologies of extracts were prepared by employing simple and quick extraction protocols, and using relatively cheap and non-toxic solvents. Therefore, the cv. Toritto leaves were extracted by maceration using EtOH 96% and a EtOH:H₂O solution (1:1, v/v), as well as by decoction and infusion using water as solvent.

The analysis of the obtained extracts by LC-ESI/HRMS/MS experiments in negative ion mode and the comparison with the MeOH extract profile (Fig. 4.11) highlighted the selectivity of the “eco-friendly” methods in extracting only certain classes of compounds. It is interesting to note that in all the profiles the occurrence of the major constituents quercetin 3-*O*-β-D-galactopyranoside (**15**), quercetin 3-*O*-β-D-glucopyranoside (**16**) and isorhamnetin 3-*O*-β-D-glucopyranoside (**19**) is constant, while there are differences for the other compounds; in particular, kaempferol derivatives (**21**, **23**, **24**), shomaside F (**22**) and triterpenes (**25-27**) are not evident in the LC-MS profile of the EtOH extract, while in the EtOH:H₂O, decoction and infusion extracts, even if they are present, they still represent minor constituents. On the other hand, decoction and infusion resulted much more effective in extracting glycosylated phenolics and the cyanogenic glycoside prunasin (**9**), if compared to the macerations with EtOH and EtOH: H₂O. Moreover, the EtOH extract showed a lower peak related to prunasin (**9**), suggesting that the employment of EtOH as extraction solvent may selectively reduce the amount of the cyanogenic glycoside **9** in the extract without influencing the major constituents, despite the other “eco-friendly” methods, where the peak related to prunasin (**9**) resulted more intense if compared to the MeOH extract.

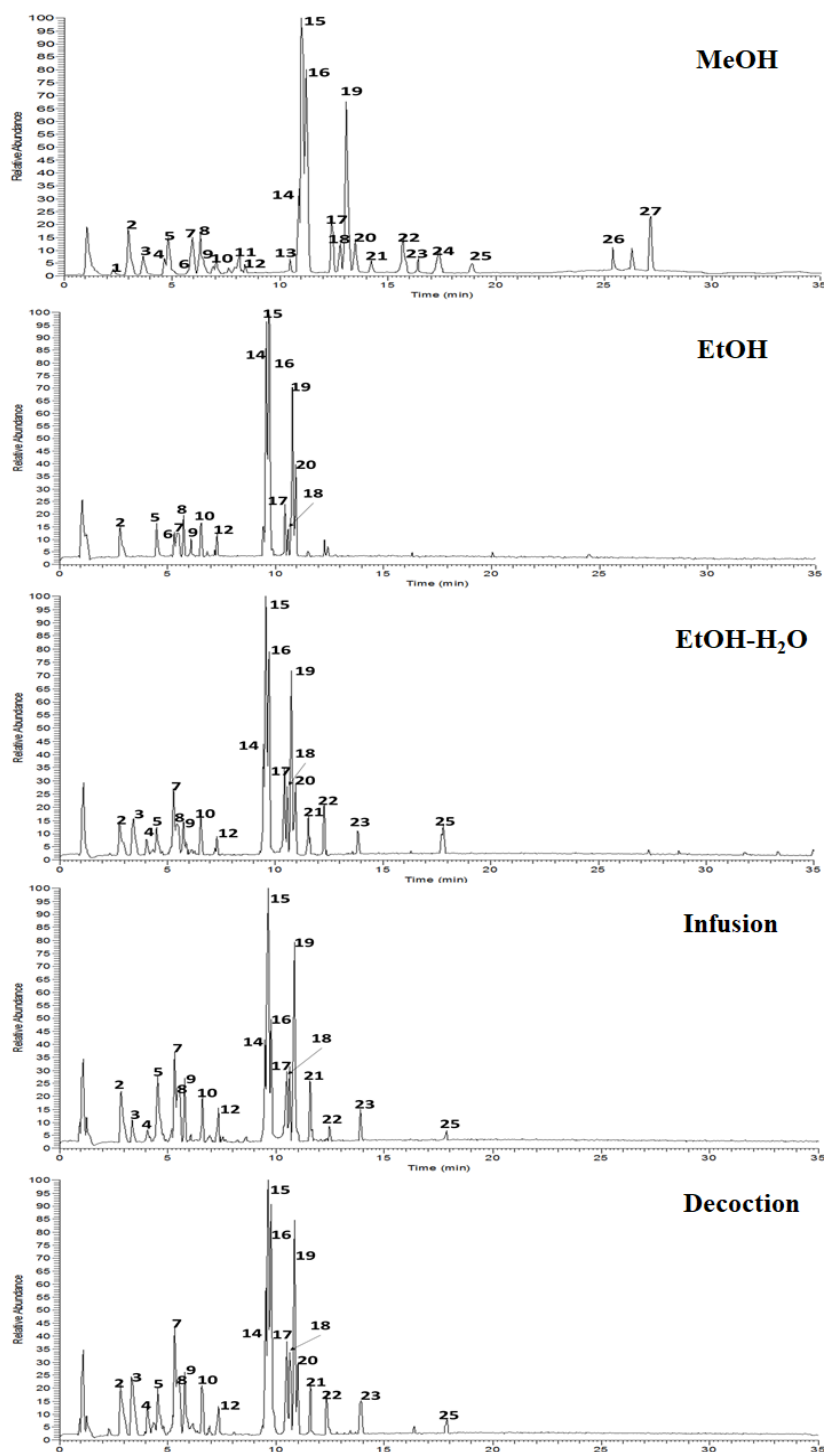


Figure 4.11 LC-MS profiles comparison of the extracts of *P. dulcis* cv. Toritto leaves, in negative ion mode

4.2.1.3 Comparison among the Apulian (cv. Toritto) and the Sicilian (cvs. Fascionello, Pizzuta and Romana) P. dulcis leaves by LC-ESI/LTQOrbitrap/MS experiments

To establish if different growing conditions, like soil composition, temperature and rainfall, may somehow affect the metabolome of a plant species originating from different regions, and also to evaluate if different varieties cultivated in the same area may possess different metabolite profiles, the MeOH extract LC-HRMS profile of the Apulian cv. Toritto leaves was compared with those of the Sicilian cvs. Fascionello, Pizzuta and Romana. These last ones were submitted to the same extraction protocols employed for the Apulian cv., with the only difference that lower amounts of dried plant material and solvents were used; the obtained extracts were then analyzed by LC-ESI/LTQOrbitrap/MS experiments and the profiles finally compared (Fig. 4.12).

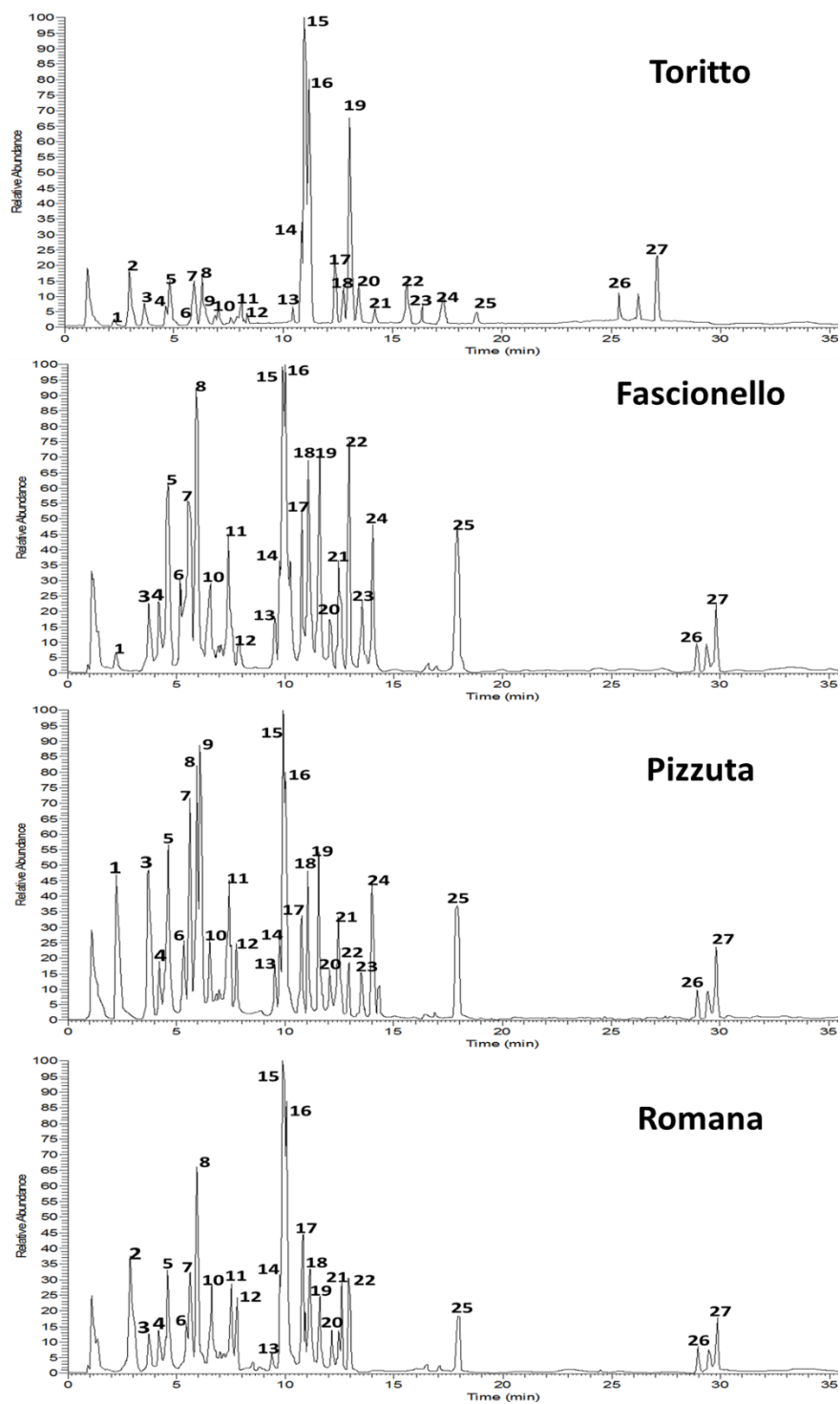


Figure 4.12 LC-HRMS profiles in negative ion mode of the leaves MeOH extracts of *P. dulcis* cvs. Toritto, Fascionello, Pizzuta and Romana

The comparison of the LC-HRMS profiles (Figure 4.12) in negative ion mode highlighted clear differences among the different cvs. leaves. As in the cv. Toritto, also in the MeOH extracts of the three cvs. Avola leaves, quercetin 3-*O*- β -D-galactopyranoside (**15**) and quercetin 3-*O*- β -D-glucopyranoside (**16**) resulted the major constituents. In the cv. Pizzuta intense peaks related to prunasin amide (**1**) and prunasinic acid (**3**) could be observed, while these compounds resulted minor constituents in the other two cvs. Avola. In the cv. Romana the peaks related to kiwiflavin (**5**) and 3-*O*-caffeoylquinic acid (**7**) were less intense if compared to the cvs. Fascionello and Pizzuta. Moreover, the peaks related to multiflorin B (**18**), isorhamnetin 3-*O*- β -D-glucopyranoside (**19**) and shomaside F (**22**) resulted to be more intense in the profile of the cv. Fascionello than in the cvs. Pizzuta and Romana. Finally, arjunolic acid glycoside (**25**) resulted one of the major constituents in the cvs. Fascionello and Pizzuta than in the cv. Romana.

It is interesting to note that only in the Pizzuta variety prunasin (**9**) represented one of the major constituents; the occurrence of a cyanogenic glycoside in the metabolite profile of a plant species may be considered as a consequence of a defense mechanism against recurrent attacks of certain typologies of herbivores or insects (Gleadow et al., 2002).

4.2.1.4 Multivariate data analysis

Multivariate data analysis has proved over time to be a powerful statistical technique, especially useful in processing large data sets when more than one observation are involved. Due to its effectiveness in making data quick and plain, it is nowadays widely employed for several applications in industrial and scientific fields, like processes control and optimization, quality controls, research and development (D'Urso et al., 2016).

In the present study, the metabolite profiles of the leaves of the cv. Toritto and the three cvs. Avola were compared, as well as the extracts obtained by employing

different extraction protocols. The obtained extracts were submitted to LC-HRMS experiments and the raw data were first filtered by using MZmine 2.0 software, and then processed by using SIMCA-P+ software.

For PCA, a data matrix was generated by reporting the different varieties and the employed extraction protocols (observations), and the peak areas of the identified metabolites (variables), obtained from the raw data deriving from the by LC-ESI/LTQOrbitrap/MS experiments. PCA was employed to achieve a preliminary overview of the dataset, focusing on detecting eventual relations among the observations. The PCA score plot allows to visualize separation of the analyzed samples into clusters, while the loading plot allows to identify the metabolites most influencing the separation.

The Principal Component Analysis (PCA) score plot (Figure 4.13) highlighted significant differences among the extraction methods, showing how different the chemical compositions of the MeOH extracts (M1-2) and the “eco-friendly” extracts (E1-2, EH1-2, I1-2, D1-2) are, since they are located on the opposite sides of the plot, confirming the different selectivity of the employed methods. Moreover, it is possible to note a further discrimination among the “eco-friendly” extraction methods: EtOH extracts (E1-2) are located in the lower right region of the plot, while EtOH:H₂O (EH1-2), decoction (D1-2) and infusion (I1-2) extracts are located in the upper right region of the plot. This difference is most attributable to the presence of water, highly affecting the polarity and hence the selectivity of the extraction methods. PC1 contributed to 44.7% of the variance, while PC2 24.1%, with a total variance of 68.8%, suggesting a satisfying discrimination between the two clusters. On the other hand, the loading plot showed the *m/z* values of the metabolites affecting the separation, although no significant discrimination was observed.

($Q^2 = 0.81$) were observed, and the model validated by permutation tests, assessing its reliability and robustness.

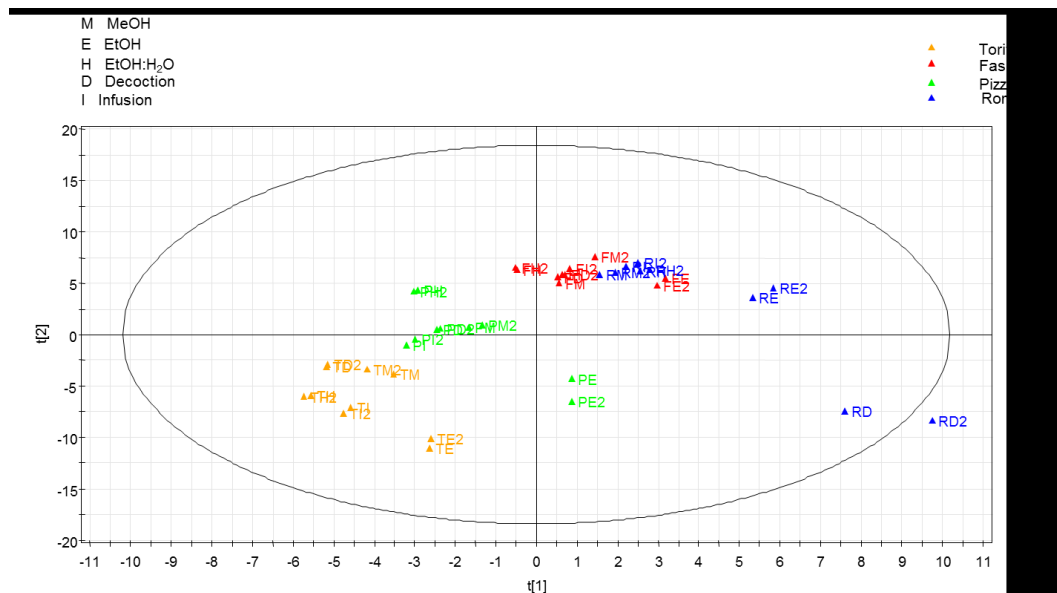


Figure 4.14 Partial Least Square Discriminant Analysis (PLS-DA) score plot of *P. dulcis* cvs. Toritto and Avola (Fascionello, Pizzuta and Romana) leaves extracts.

Furthermore, the PLS-DA loading plot (Fig. 4.15) showed the metabolites potentially contributing to the separation: the higher the distance from the plot center, the higher such compounds affect the distribution in the score plot, and might be considered as chemical markers both of the extraction procedures and the investigated cultivars. According to these considerations, prunasinic acid (**3**) resulted the most influencing compound, significantly affecting the discrimination among the analyzed *P. dulcis* cultivars.

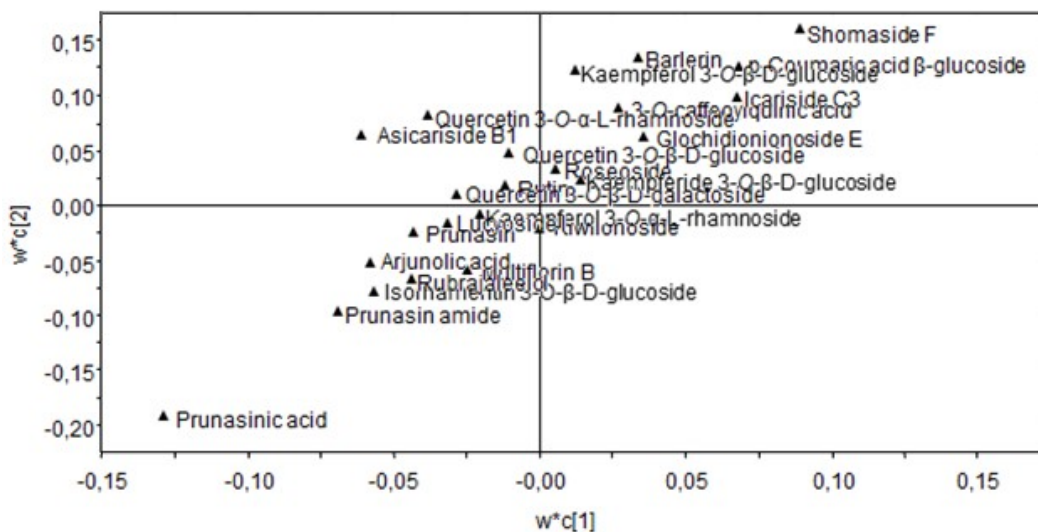


Figure 4.15 Partial Least Square Discriminant Analysis (PLS-DA) loading plot of *P. dulcis* cvs. Toritto and Avola (Fascionello, Pizzuta and Romana) leaves extracts.

4.2.1.5 Total phenolic content and antioxidant activity evaluation

Finally, for all the prepared extracts the total phenolic content was assessed by Folin-Ciocalteu assay, along with radical scavenging activity evaluated by DPPH• and ABTS^{•+} assays.

The results (Table 4.3) highlighted the MeOH extract of the cv. Toritto leaves possessing the highest phenolic content (174.69 ± 11.03 GAE mg/g dried extract) if compared to the “eco-friendly” extracts, and also higher than the MeOH extracts of the Sicilian cvs. Fascionello (100.51 ± 2.62 GAE mg/g dried extract), Pizzuta (114.72 ± 13.83 GAE mg/g dried extract) and Romana (79.94 ± 3.88 GAE mg/g dried extract).

Moreover, the MeOH extracts, and so the EtOH and EtOH:H₂O extracts, exerted the strongest antioxidant activity if compared to infusions and decoctions (Table 4.3), while the MeOH extract of the cv. Toritto leaves exerted the strongest antioxidant activity ($IC_{50} = 30.95 \pm 0.55$ μg/mL) in comparison to the other cvs.

ABTS^{•+} assay further confirmed the results obtained in the previous experiments (Table 4.3). MeOH extracts exerted the most intense radical scavenging activity, in

particular that one of the Apulian cv. (1.03 ± 0.09 mM), followed by the Sicilian Fascionello (0.73 ± 0.08 mM), Pizzuta (0.62 ± 0.04 mM) and Romana (0.55 ± 0.05 mM).

Table 4.3 Total phenolic content, DPPH• and ABTS^{•+} radical scavenging activity of the extracts of *P. dulcis* cvs. Toritto and Avola (Fascionello, Pizzuta and Romana) leaves

Sample	Total phenolic content		DPPH•		ABTS ^{•+}	
	GAE ^a	SD ^d	IC ₅₀ ^b	SD ^d	TEAC ^c	SD ^d
TORITTO MeOH (TM)	174.69	± 11.03	30.95	± 0.55	1.03	± 0.09
TORITTO EtOH (TE)	50.90	± 3.34	73.41	± 1.12	0.31	± 0.02
TORITTO EtOH/H ₂ O (TH)	28.39	± 3.61	54.31	± 0.97	0.21	± 0.02
TORITTO DECOCTION (TD)	52.91	± 2.24	110.42	± 2.39	0.41	± 0.03
TORITTO INFUSION (TI)	43.43	± 2.93	144.60	± 3.65	0.48	± 0.06
FASCIONELLO MeOH (FM)	100.51	± 2.62	65.83	± 2.18	0.73	± 0.08
FASCIONELLO EtOH (FE)	19.94	± 3.88	31.54	± 0.53	0.12	± 0.01
FASCIONELLO EtOH/H ₂ O (FH)	23.14	± 1.69	55.63	± 0.91	0.18	± 0.01
FASCIONELLO DECOCTION (FD)	34.58	± 2.42	137.21	± 3.37	0.39	± 0.03
FASCIONELLO INFUSION (FI)	47.05	± 3.94	136.54	± 4.56	0.32	± 0.03
PIZZUTA MeOH (PM)	114.72	± 13.83	58.61	± 1.58	0.62	± 0.04
PIZZUTA EtOH (PE)	31.33	± 3.78	82.62	± 2.36	0.16	± 0.01
PIZZUTA EtOH/H ₂ O (PH)	48.04	± 2.54	39.79	± 0.37	0.36	± 0.02
PIZZUTA DECOCTION (PD)	11.28	± 3.39	105.81	± 2.11	0.32	± 0.02
PIZZUTA INFUSION (PI)	39.38	± 3.33	132.70	± 3.78	0.18	± 0.01
ROMANA MeOH (RM)	79.94	± 3.88	65.81	± 1.43	0.55	± 0.05
ROMANA EtOH (RE)	37.16	± 2.57	63.92	± 1.66	0.19	± 0.01
ROMANA EtOH/H ₂ O (RH)	22.72	± 1.66	53.61	± 2.13	0.35	± 0.04
ROMANA DECOCTION (RD)	31.61	± 3.88	113.65	± 3.19	0.24	± 0.01
ROMANA INFUSION (RI)	36.46	± 2.24	160.25	± 4.72	0.11	± 0.01
Vit. C			5.16	± 0.11		
Quercetin					1.87	± 0.08

^a Values are expressed as gallic acid equivalents (GAE) mg/g of dried extract. ^b Values are expressed as µg/mL. ^c Values are expressed as concentration (mM) of a standard Trolox solution exerting the same antioxidant activity of a 1 mg/mL solution of the tested extract. ^d Standard Deviation of three independent experiments

4.3 LC-ESI/LTQOrbitrap/MS based metabolite profiling of *Prunus dulcis* Mill. (Italian cvs. Toritto and Avola) husks and evaluation of antioxidant activity

Prunus dulcis Mill. husks



The husk, also known as hull, represents the thick and leathery exocarp of *P. dulcis* fruits, namely drupe. Ordinary green, and totally enveloping the wooden endocarp containing the edible seed, it turns brown-grey during ripening.

4.3.1 Results and discussion

4.3.1.1 Qualitative analysis of the MeOH extract of *P. dulcis* cv. Toritto husks

A preliminary metabolite fingerprint of the MeOH extract of *P. dulcis* cv. Toritto husks was obtained by LC-ESI/LTQOrbitrap/MS analysis in negative ion mode. The obtained LC-HRMS profile (Fig. 4.16) suggested the occurrence of alkylated saccharides (28, 29) phenolic derivatives (30, 31, 33, 34, 35, 39, 41, 43), flavonoids (19, 38, 42, 44, 45) and terpenes (11, 26, 27, 46-48) (Table 4.4).

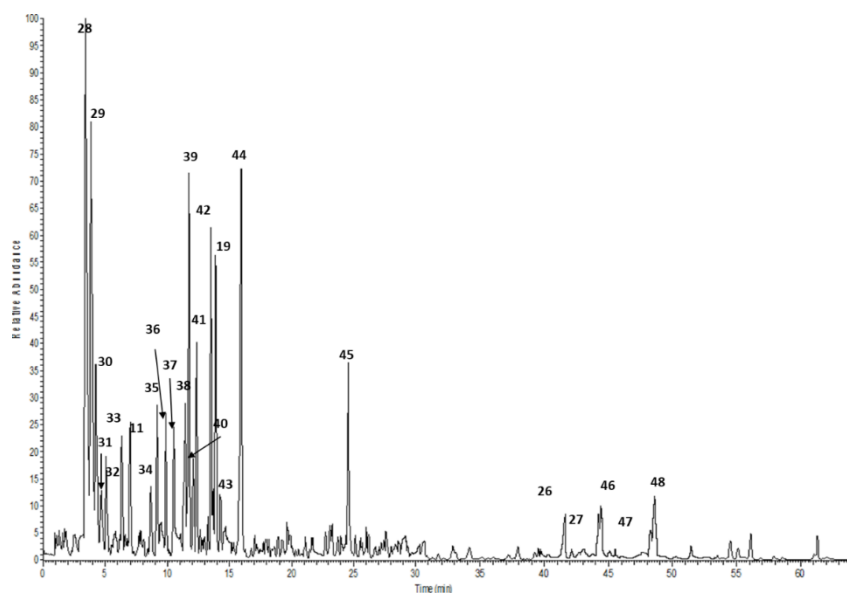


Figure 4.16 LC-HRMS profile in negative ion mode of the MeOH extract of *P. dulcis* cv. Toritto husks.

LC-ESI/LTQOrbitrap/MS/MS experiments using the “data dependent scan” mode, in which the MS software selects precursor ions corresponding to the most intense peaks in LC-MS spectrum, were carried out. Some of the main peaks were tentatively attributed according to the accurate m/z values, characteristic fragmentation patterns, retention times and by comparison with literature data on *P. dulcis*. With the purpose to achieve an in depth knowledge of the polar constituents of the husks, and to unambiguously attribute the main peaks observed in the LC-ESI/LTQOrbitrap/MS profile, a phytochemical investigation of the MeOH extract was performed. The MeOH extract of the husks of *P. dulcis* cv. Toritto was fractionated on a Sephadex LH-20 column and the obtained fractions were further purified by RP-HPLC to afford pure compounds, of which the structures were elucidated by 1D and 2DNMR experiments (Figure 4.17).

Table 4.4 Compounds identified and tentatively identified in the MeOH extract of *P. dulcis* cv. Toritto husks.

N°	R _t	Accurate Mass	[M-H] ⁻	Δppm	MS ² (%)	Molecular formula	Compound
28	3.38	396.1631	395.0062	0.438	293(100), 149(22)	C ₁₆ H ₂₈ O ₁₁	(iso)pentyl pentoside hexoside
29	3.83	396.1643	394.8654	1.578	293(100), 339(30), 275(15), 149(22)	C ₁₆ H ₂₈ O ₁₁	(iso)pentyl pentoside hexoside
30	4.22	330.0950	329.0885	0.958	167(100)	C ₁₄ H ₁₈ O ₉	4-β-glucosidyl-2-O-methyl-phloroglucinaldehyde ²
31	4.61	330.0950	329.0882	1.652	167(100), 123(60), 239(44), 209(42), 191(26)	C ₁₄ H ₁₈ O ₉	myrciaphenone A ²
32	5.05		351.1303				unidentified
33	6.33	296.1259	295.1192	0.998	133(100), 161(42)	C ₁₅ H ₂₀ O ₆	chavicol hexoside
11	7.00	386.1940	385.2942	1.117	223(100), 179(55)	C ₁₉ H ₃₀ O ₈	asicaric acid B1
34	8.67	524.2257	523.2194	1.038	361(100), 343(26), 163(18)	C ₂₆ H ₃₆ O ₁₁	secoisolaricresinol hexoside
35	9.17	390.1314	389.1251	1.333	227(100)	C ₂₀ H ₂₂ O ₈	piceid ²
36	9.89		521.0670		341(100), 329(92), 359(100)		unidentified
37	10.47		368.8834				unidentified
38	11.45	464.0954	463.0889	0.589	300(100), 301(26)	C ₂₁ H ₂₀ O ₁₂	quercetin 5-O-β-D-glucopyranoside ²
39	11.72	368.1471	367.0734	0.675	205(100)	C ₁₈ H ₂₄ O ₈	malaxinic acid ²
40	12.10		551.2146				unidentified
41	12.34	522.2101	521.0670	1.348	341(100), 179(80), 359(44)	C ₂₆ H ₃₄ O ₁₁	isolaricresinol hexoside
42	13.51	478.1111	477.1044	0.654	314(100), 315(52), 300(40)	C ₂₂ H ₂₂ O ₁₂	isorhamnetin 3-O-β-D-galactopyranoside ²
19	13.90	478.1111	477.1046	0.661	314(100), 315(50), 300(36)	C ₂₂ H ₂₂ O ₁₂	isorhamnetin 3-O-β-D-glucopyranoside ²
43	14.29	318.1391	417.1406 ¹	1.965	371(100), 399(67), 373(20), 209(41), 191(56),	C ₁₇ H ₂₄ O ₉	syringin
44	15.95	320.0532	319.0465	0.333	193(100)	C ₁₅ H ₁₂ O ₈	ampelopsin
45	24.46	316.0583	315.0514	1.845	300(100), 301(10)	C ₁₆ H ₁₂ O ₇	isorhamnetin ²
26	41.84	488.3501	487.3254	1.569	249(100)	C ₃₀ H ₄₈ O ₅	arjunolic acid ²
27	44.37	444.3603	443.3495	1.548	399(100), 383(51), 313(52)	C ₂₉ H ₄₈ O ₃	rubrajaleol ²
46	44.42	472.3552	471.3483	1.224	307(100)	C ₃₀ H ₄₈ O ₄	alphaltolic acid ²
47	48.34	456.3603	455.3530	1.935	189(100), 207(59)	C ₃₀ H ₄₈ O ₃	betulinic acid ²
48	48.62	456.3603	455.3499	1.608	407(100)	C ₃₀ H ₄₈ O ₃	oleanolic acid ²

¹Observed as formate adduct. ² The identification of this compound was corroborated by isolation and NMR spectra analysis

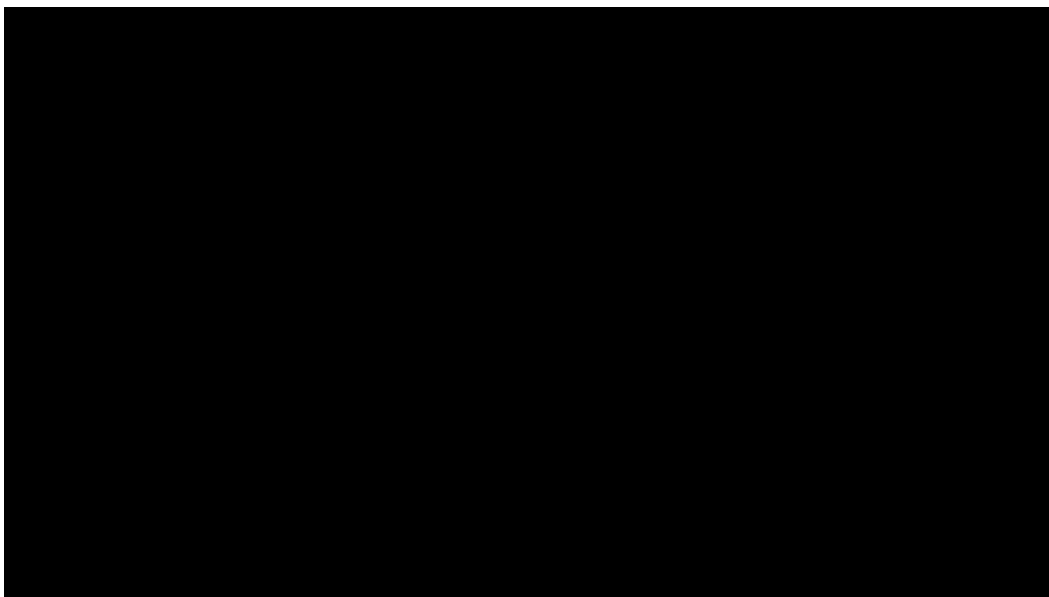


Figure 4.17 Structures of compounds isolated from the MeOH extract of *P. dulcis* cv. Toritto husks

In this way, quercetin 5-*O*- β -D-glucopyranoside (**38**), isorhamnetin 3-*O*- β -D-galactopyranoside (**42**), isorhamnetin 3-*O*- β -D-glucopyranoside (**19**) and isorhamnetin (**45**) were identified by comparison of their spectroscopic data with those reported in literature (Tamaura et al., 2002; Aquino et al., 2002; Hilbert et al., 2015; Mari et al., 2014). Isorhamnetin and quercetin glycosides, as well as their aglycones, have been widely reported for their intense antioxidant activity (Heim et al., 2002), suggesting a potential use of almond husks as a valuable source of antioxidant bioactives (Kapusta et al., 2007). Along with flavonoids, a further phenolic compound was isolated and identified as piceid (**35**), or polydatin (Fan et al., 2009). Under a chemical point of view, it is the 3-*O*- β -D-glucopyranoside derivative of resveratrol, and as this last one it has been reported for its antioxidant properties, as well as for its anticancer activity on human gastric carcinoma (Wei et al., 2013). Furthermore, two phloroglucinol derivatives were isolated and identified as 4-*O*- β -glucopyranosyl-2-*O*-methyl-phloroglucinaldehyde (**30**) and myrciaphenone A (**31**) (Sidana et al., 2013). Myrciaphenone A (**4**) showed *in vitro*

antileishmanial activity (Sidana et al., 2013). Moreover, a prenylated benzoic acid derivative was isolated and identified as malaxinic acid (**39**), previously reported in the EtOH extract of Californian almonds (Sang et al., 2002). Malaxinic acid (**39**) is structurally related to prenylated compounds exerting cytotoxic and anti-HIV activity (Xu et al., 2000; Groweiss et al., 2000). Finally, 5 triterpenes were isolated and identified as arjunolic acid (**26**), rubrajaleelol (**27**), alphaltolic acid (**46**), betulinic acid (**47**) and oleanolic acid (**48**) (Masullo et al., 2015; Akhtar et al., 2013). Arjunolic acid (**26**) has been reported for its biological properties, like antioxidant, antidiabetic, antimicrobial and anticancer (Ghosh et al., 2013), while alphaltolic acid (**46**), betulinic acid (**47**) and oleanolic acid (**48**), in particular the first one, have been reported for their antiinflammatory activity due to the capacity to inhibit iNOS expression and the NO production (Masullo et al., 2015).

To discriminate the isolated triterpenes, NMR spectroscopy resulted an elective analytical technique. As example, the structural elucidation of compounds **46**, **47** and **48** will be described.

The $^1\text{H-NMR}$ spectrum of compound **46** (Fig. 4.18) displayed signals for two protons of an isomethylene function at δ 4.60 and 4.73 (each, br s), two oxygen-bearing methine protons at δ 2.92 (d, $J = 9.1$) and 3.63 (m) and six tertiary methyl groups at δ 0.81, 0.95, 1.02, 1.03, 1.07, and 1.72 (Table 4.5). These signals along with the carbon resonances in the $^{13}\text{C-NMR}$ spectrum for the carboxyl function at δ 180.3, the two olefinic carbons at δ 109.6 and 152.5, the alcoholic functions at δ 69.5 and 84.0, and for the methyl groups at δ 15.3, 16.6, 17.3, 17.6, 19.3 and 29.1, suggested the presence of a triterpene derivative belonging to the lupane class (Table 4.5). A detailed analysis of the 2D NMR spectra (HSQC, HMBC and COSY) revealed that compound **46** was a derivate of the lup-20(29)-en-28-oic acid with two secondary alcohol functions. The HMBC (Fig. 4.20) correlations between the proton signals at δ 0.81 (Me-24) and 1.07 (Me-23) with the carbon resonance at δ 84.0 (C-3) located one secondary alcoholic function at C-3. The COSY (Fig. 4.21)

correlation between the proton signals at δ 3.63 and 2.92, along with the upfield shift of H-3 (δ 2.92), allowed us to place the further secondary alcohol function at C-2. Thus, compound **46** was identified as alphitolic acid (Masullo et al., 2015)

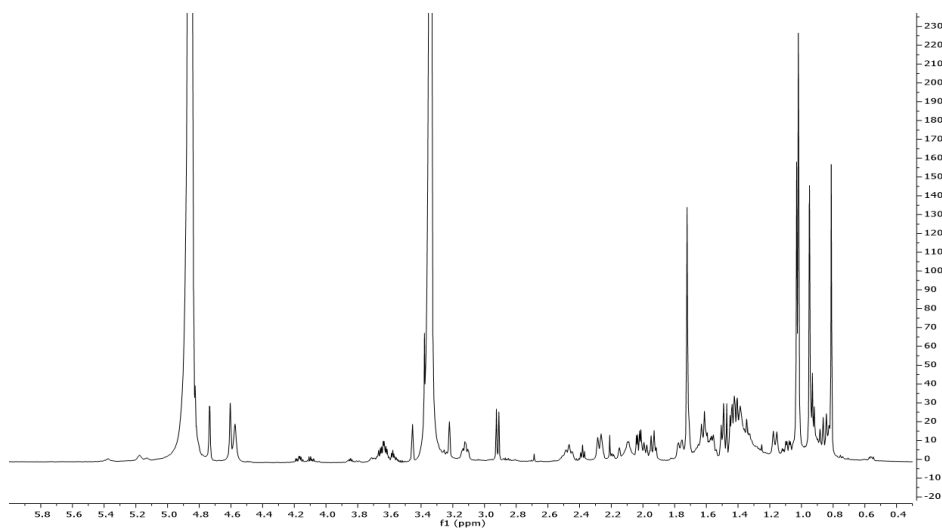


Figure 4.18 $^1\text{H-NMR}$ spectrum of compound **46**

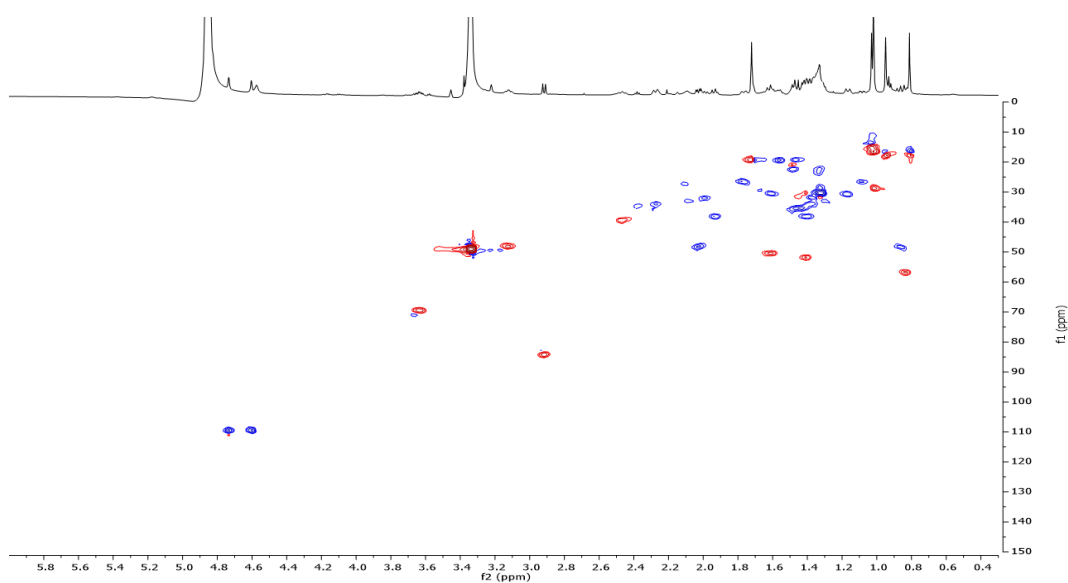


Figure 4.19 HSQC spectrum of compound **46**

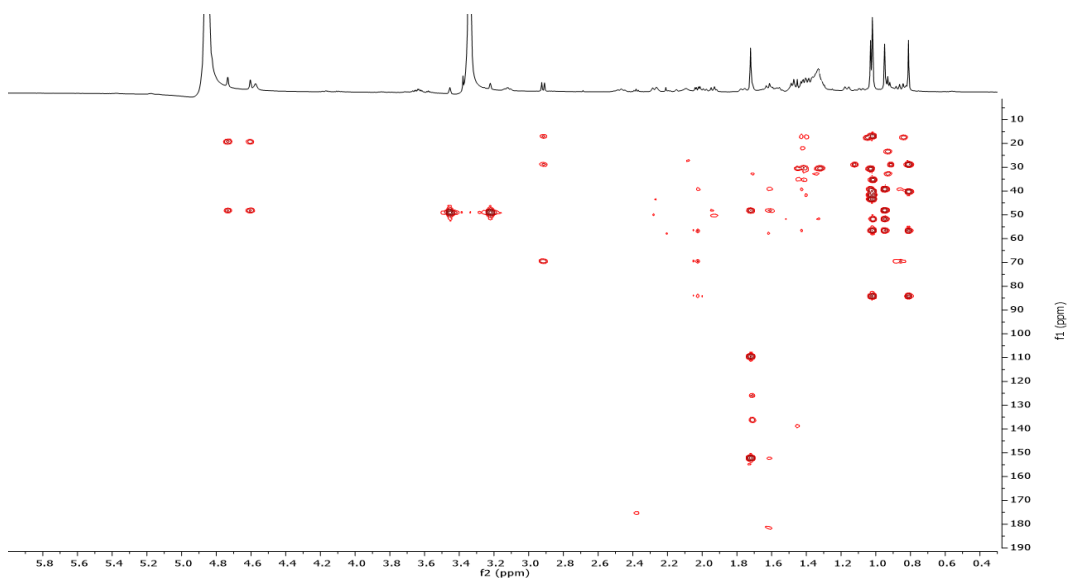


Figure 4.20 HMBC spectrum of compound 46

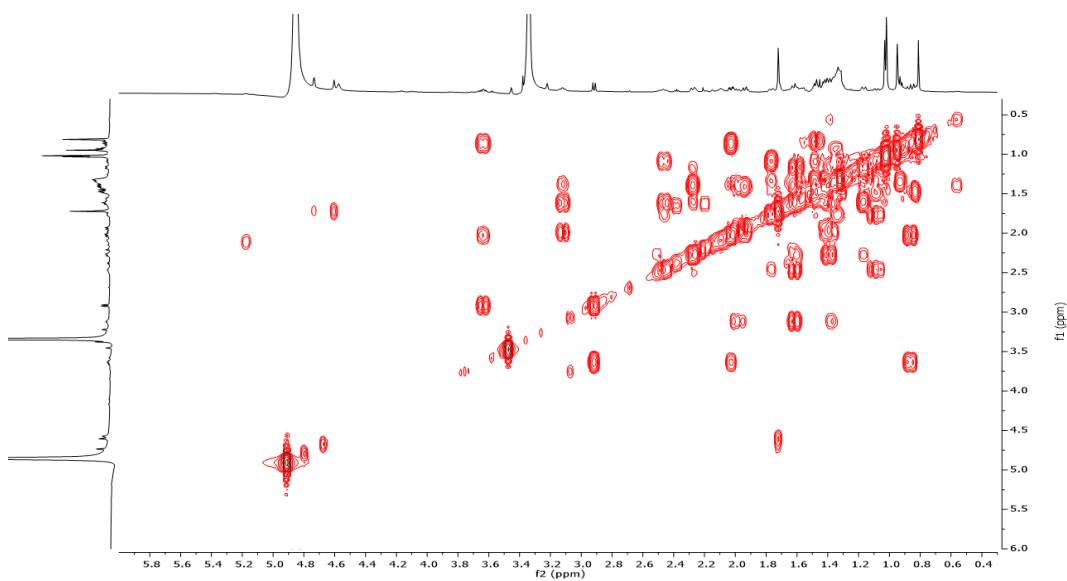


Figure 4.21 COSY spectrum of compound 46

The NMR data of compound 47 (Fig. 4.22) were almost superimposable to that of compound 46, except for the absence of a secondary alcoholic group. In detail,

in the ^1H -NMR spectrum one signal ascribable to an oxygen-bearing methine proton at δ 3.18 (dd, $J = 11.5, 4.6$ Hz) was evident. The HMBC correlations between the proton signal at δ 3.18 with the carbon resonances at δ 15.9 (C-24) and 28.4 (C-23) located the alcoholic function at C-3. Therefore, compound **47** was identified as betulinic acid (Masullo et al., 2015)

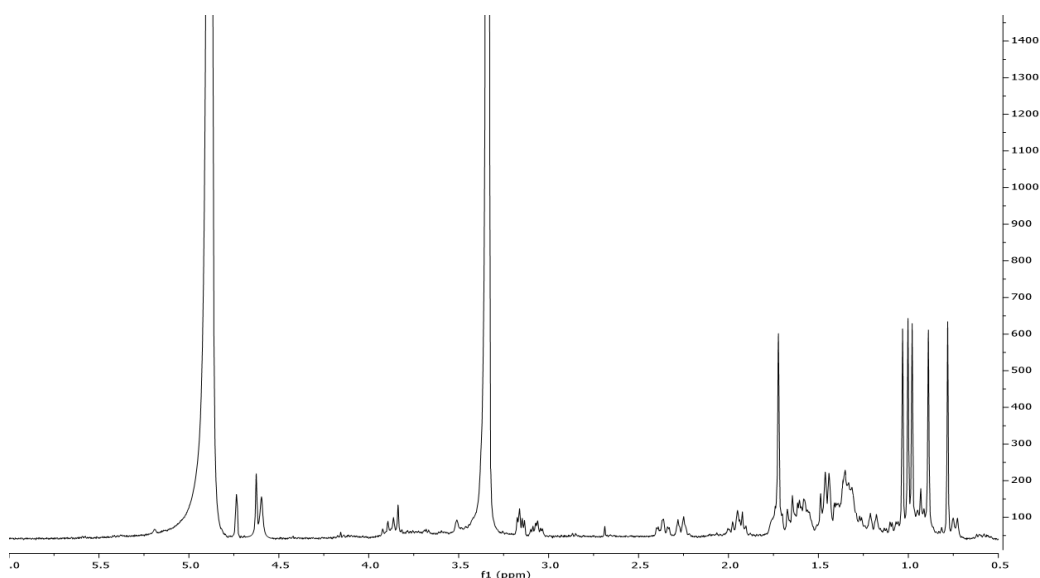


Figure 4.22 ^1H -NMR spectrum of compound **47**

The ^1H -NMR spectrum of compound **48** (Fig. 4.23) displayed signals for seven tertiary methyl groups at δ 0.81, 0.86, 0.93, 0.97 (6H), 1.00, and 1.19, for an olefinic proton at δ 5.26 (t, $J = 3.4$ Hz), and one oxygen-bearing methine proton at δ 3.18 (dd, $J = 11.6, 4.5$ Hz, H-3) (Table 4.5). These signals along with the carbon resonances in the ^{13}C -NMR spectrum for a carboxyl function at δ 180.8, the two olefinic carbons at δ 122.7, 144.0, for the methyl groups at δ 15.7, 16.1, 17.5, 23.4, 26.3, 28.6 and 33.1 suggested that compound **48** was an oleanene derivative. A detailed analysis of the 2D NMR (HSQC spectrum Fig. 4.24, HMBC spectrum Fig.

4.25, COSY spectrum Fig. 4.26) data allowed us to establish the structure of compound **48** as oleanolic acid (Masullo et al., 2015).

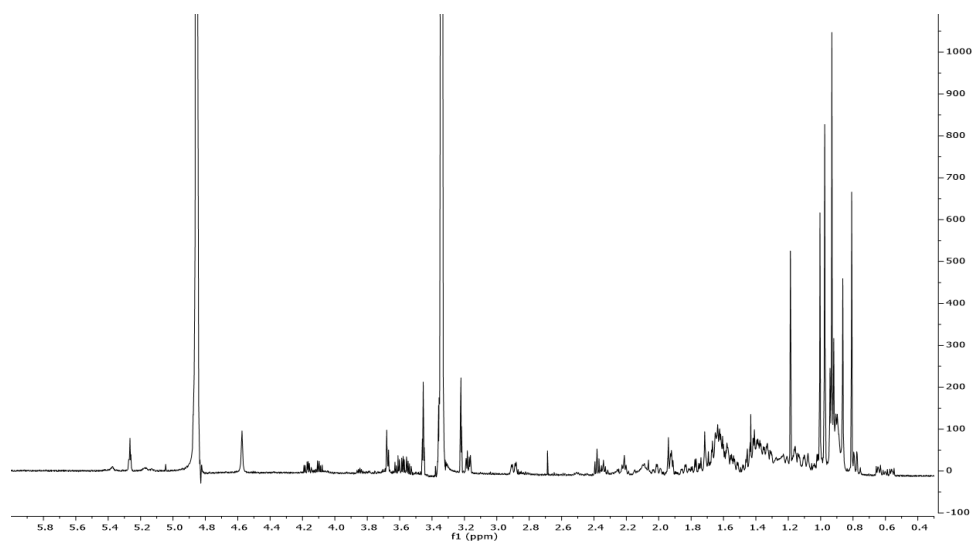


Figure 4.23 ^1H -NMR spectrum of compound **48**

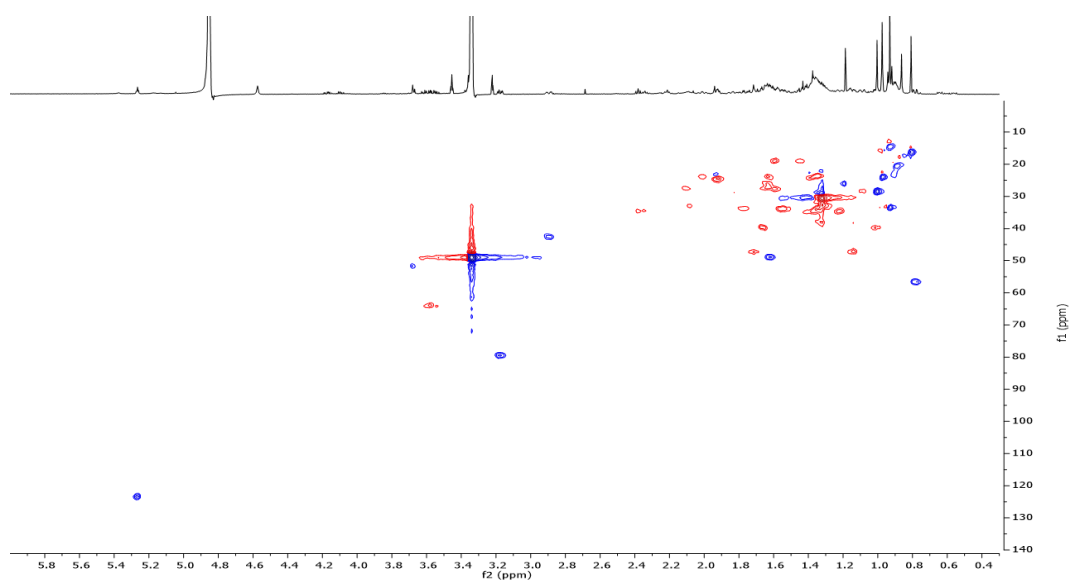


Figure 4.24 HSQC spectrum of compound **48**

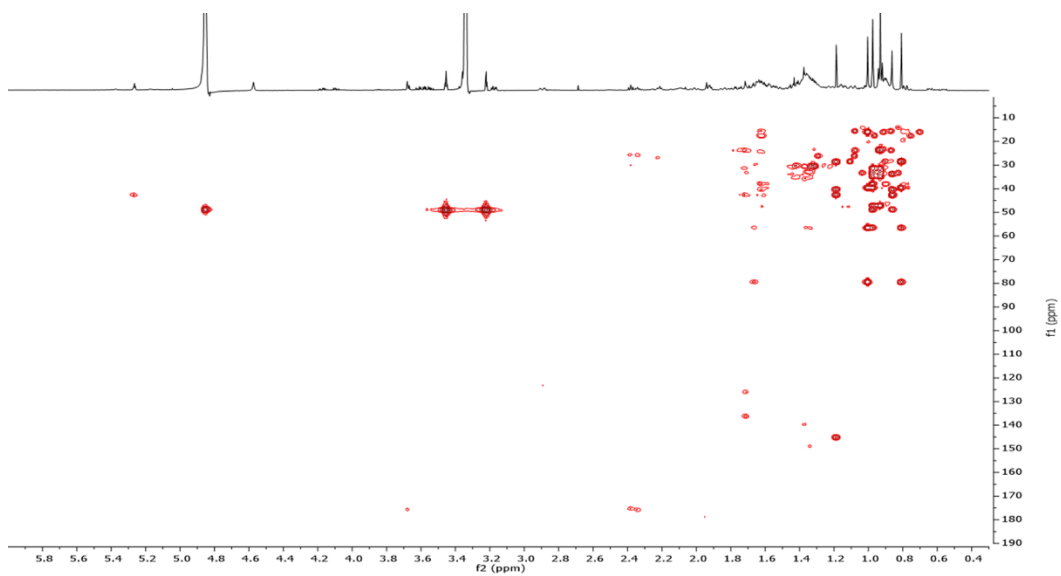


Figure 4.25 HMBC spectrum of compound 48

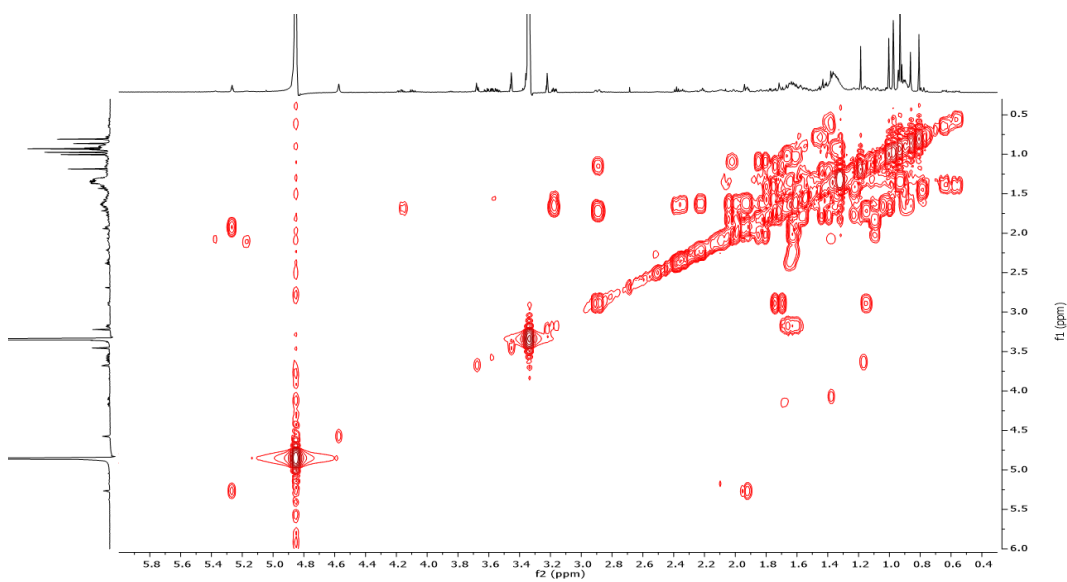


Figure 4.26 COSY spectrum of compound 48

Table 4.5 ^1H (600 MHz) and ^{13}C (150 MHz) NMR spectral data of compounds **46-48**

	46		47		48	
	δ_{C}	δ_{H} (J in Hz)	δ_{C}	δ_{H} (J in Hz)	δ_{C}	δ_{H} (J in Hz)
1	48.2	0.85, 2.02, m	40.1	0.91, 1.69, m	39.3	1.01, 1.65, m
2	69.5	3.63, m	27.6	1.61, m	27.3	1.67, 1.89, m
3	84.0	2.92, d(9.1)	79.8	3.18, dd(4.6, 11.5)	79.4	3.18, dd(4.5, 11.6)
4	40.3	-	39.7	-	40.1	-
5	57.1	0.83, m	56.8	0.90, m	56.6	0.78, m
6	19.6	1.46, 1.56, m	19.1	1.39, 1.48, m	19.4	1.45, 1.59, m
7	35.2	1.40, m	35.6	1.48, m	34.8	1.55, 1.77, m
8	43.3	-	43.5	-	41.2	-
9	52.2	1.74, m	52.3	1.71, m	48.7	1.61, m
10	38.5	-	39.2	-	37.9	-
11	22.1	1.14, m	22.1	1.30, 1.39, m	24.5	1.93, m
12	26.5	1.11, dd(11.9, 7.6)	26.4	1.08, dd(12.8, 8.1)	122.7	5.26, t(3.4)
13	39.5	2.17, td(11.6, 3.8)	39.1	2.19, td(12.4, 3.6)	144.0	-
14	42.1	-	41.9	-	42.3	-
15	30.8	1.28, dt(13.1, 2.3)	30.4	1.26, dt(13.4, 2.4)	28.6	1.08, 1.67, m
16	30.9	1.46, 2.31, m	30.8	1.44, 2.38, m	23.4	1.63, 2.02, m
17	58.1	-	58.7	-	47.6	-
18	50.8	1.66, t(10.8)	51.0	1.64, t(11.2)	42.6	2.89, d(11.0)
19	48.2	3.00, td(11.0, 5.5)	47.9	3.06, td(11.2, 5.6)	47.1	1.55, 2.77, m
20	152.5	-	153.3	-	31.2	-
21	31.5	1.47, 20.3, m	32.2	1.48, 2.06, m	33.3	1.23, 1.40, m
22	33.4	0.99, 1.82, m	34.6	0.94, 1.84, m	33.9	1.46, 1.53, m
23	29.1	1.07, s	28.4	1.06, s	28.6	1.00, s
24	17.3	0.81, s	15.9	0.84, s	16.1	0.81, s
25	17.6	0.95, s	16.7	0.96, s	15.7	0.97, s
26	16.6	1.02, s	16.9	1.04, s	17.5	0.86, s
27	15.3	1.03, s	14.7	1.00, s	26.3	1.19, s
28	180.3	-	180.5	-	180.8	-
29	109.6	4.73, br s 4.60, br s	109.2	4.71, br s 4.57, br s	33.1	0.93, s
30	19.3	1.72, s	19.4	1.73, s	23.4	0.97, s

In MeOH- d_4

In the LC-ESI/LTQOrbitrap/MS profile of the MeOH extract of *P. dulcis* (cv. Toritto) husks (Figure 4.16) further compounds not isolated from the extract were evident. These compounds were tentatively identified by comparing the pseudomolecular ions accurate mass and their typical fragmentation pattern with data reported in literature (Wu et al., 2012; Weckerle et al., 2002; Yoshikawa et al.,

2002; Chen et al., 2014; Gao et al., 2017), as well as by comparison with online databases (FoodDB).

Compounds **28** and **29** showed in their fragmentation spectra a common product ion at m/z 293 due to the loss of the (iso)pentyl moieties, and a fragment ion at m/z 149 related to a deprotonated pentose moiety; since the observed fragmentation patterns were the same for both compounds, as well as the accurate mass and the molecular formula, established as $C_{16}H_{28}O_{11}$, it was possible to assess that the detected compounds were structural isomers, and tentatively identified as (iso)pentyl pentoside hexoside (**28**, **29**) (Weckerle et al., 2002) (Table 4.4).

Compound **33** (m/z 295.1192) showed in the MS/MS spectrum a fragment ion at m/z 133, due to the loss of the hexose moiety and a product ion at m/z 161 related to the ion corresponding to the dehydrated hexose; the molecular formula was established in HRMS as $C_{15}H_{20}O_6$, and compound **33** was tentatively identified as chavicol hexoside (Yoshikawa et al., 2002) (Table 4.4).

Compound **11** (m/z 385.2942) showed in the fragmentation pattern a base peak at m/z 223 originated by the neutral loss of a dehydrated hexose moiety, together with a product ion at m/z 179, ascribable to the hexose ion. Hence, also according to the molecular formula established in HRMS as $C_{19}H_{30}O_8$, compound **11** was tentatively identified as asicariside B1, previously isolated from the leaves of *P. dulcis*, as reported in paragraph 4.2.1.1 (Wu et al., 2012) (Table 4.4).

Moreover, compound **34** (m/z 523.2194) showed in the MS/MS spectrum a product ion at m/z 361 ascribable to the loss of a dehydrated hexose moiety, followed by the loss of a water molecule (m/z 343); molecular formula was established as $C_{26}H_{36}O_{11}$, and compound **34** was tentatively identified as secoisolariciresinol hexoside (Chen et al., 2014) (Table 4.4).

Compound **41** (m/z 521.0670) exhibited in the tandem mass spectrum the neutral loss of a dehydrated hexose moiety at m/z 359, and the further loss of a water molecule at m/z 341, along with a signal at m/z 179 ascribable to a hexose ion;

molecular formula was established as C₂₆H₃₄O₁₁ and identity tentatively assigned as isolariciresinol hexoside (Chen et al., 2014) (Table 4.4).

Compound **43** was observed in HRMS as formate adduct [M-H+HCOOH]⁻ at *m/z* 417.1406, exhibiting in the MS/MS spectrum a product ion at *m/z* 209 due to the loss of a dehydrate hexose moiety, with a successive loss of water (*m/z* 191). Molecular formula was established as C₁₇H₂₄O₉, and compound **43** tentatively identified as syringin (Kirmizibekmez et al., 2008) (Table 4.4).

Finally, compound **44** (*m/z* 319.0465) exhibited in the MS/MS spectrum a diagnostic product ion at *m/z* 193 ascribable to the loss of a trihydroxyphenyl moiety; molecular formula was established as C₁₅H₁₂O₈, and putatively attributed as ampelopsin (Gao et al., 2017) (Table 4.4).

4.3.1.2 LC-ESI/LTQOrbitrap/MS based comparison of different extraction procedures

With the aim to assess the extraction selectivity of cheap and relatively non-toxic solvents, the dried husks of *P. dulcis* cv. Toritto were extracted by maceration employing EtOH 96% and EtOH:H₂O (1:1, v/v) solution. The obtained extracts were analyzed by LC/ESI/LTQOrbitrap/MS experiments and the profiles compared with the MeOH extract profile.

The comparison of the LC-HRMS profiles of the different extracts (Figure 4.27) highlighted clear differences among the extracts. In the EtOH extract profile it was possible to note a substantial intensity lowering of the peaks related to the most polar compounds, especially the two alkylated disaccharides (**28**, **29**), as well as the most polar phenolics and terpenes, while there were no relevant variations of the remaining peaks. On the other hand, in the profile of the EtOH:H₂O extract, the peaks related to the most polar compounds showed a significant increase (**28**, **29**), with an intensity reduction of the remaining peaks with a complete disappearance of those related to compounds **26**, **27**, **44-48**. The above results showed that the “eco-friendly” extraction protocols possess a discreet selectivity in extracting only

certain classes of compounds, suggesting a potential employment of the almond husks as a source for a targeted extraction of bioactives.

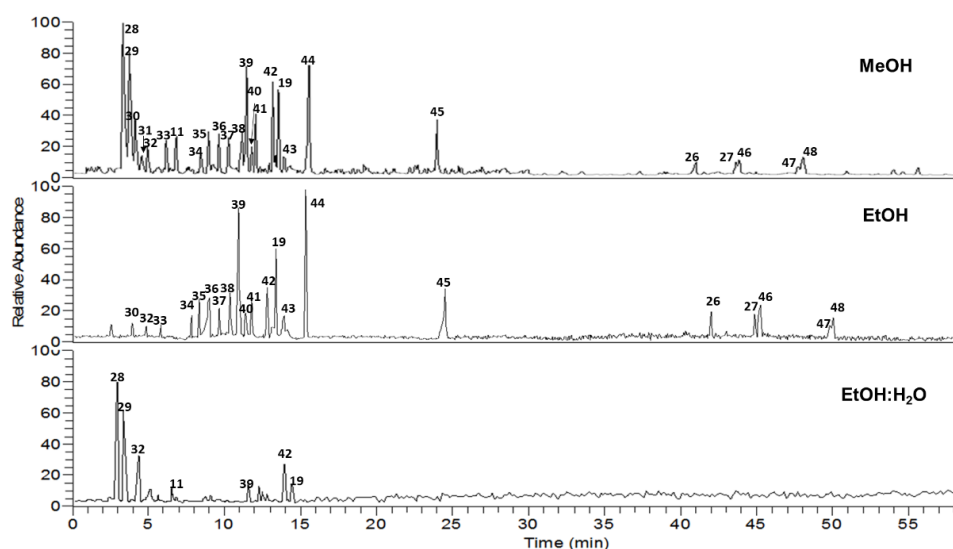


Figure 4.27 Comparison of the LC-HRMS profiles of the MeOH, EtOH and EtOH:H₂O extracts of *P. dulcis* cv. Toritto husks, in negative ion mode.

4.3.1.3 Metabolite profile comparison of *P. dulcis* husks originating from different geographical areas

Soil composition, temperature and precipitations represent some of the main environmental features affecting the growth of a plant. Aiming at evaluating if different conditions may affect the metabolome of a plant species, the husks of *P. dulcis* cvs. Fascionello, Pizzuta and Romana were extracted following the same procedures employed for the Apulian cv. The obtained extracts were analyzed by LC-ESI/LTQOrbitrap/MS experiments and the LC-HRMS profiles compared (Fig. 4.28).

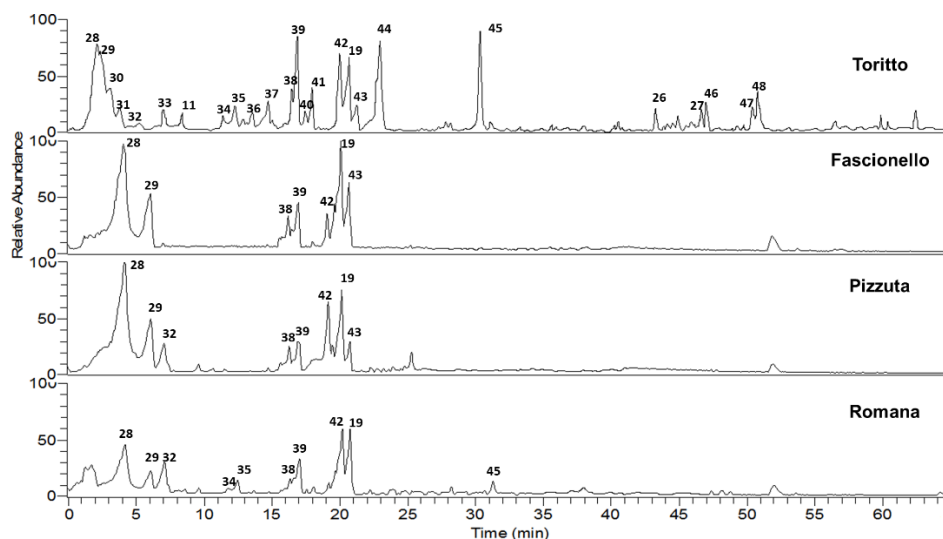


Figure 4.28 Comparison of the LC-HRMS profiles of the MeOH extracts of *P. dulcis* cvs. Toritto and Avola (Fascionello, Pizzuta and Romana) husks, in negative ion mode.

By comparing the MeOH extracts of the analyzed cultivars remarkable differences among their metabolome were observed. The profiles of the three Sicilian cvs. showed as predominant peaks those related to compounds **19**, **28**, **29**, **38**, **39** and **42** with slight intensity differences among them: peak related to compound **32** was detected in cultivars Pizzuta and Romana, but not in Fascionello, while peak related to compound **43** was detected in cultivars Fascionello and Pizzuta, but not in Romana. Moreover, peaks related to compounds **34**, **35** and **45** were detected only in cultivar Romana. The obtained results highlighted that different growing conditions (based on geographical area) may really affect the metabolome of a plant species; in this case notable differences have been observed not only between cultivars Toritto and Avola, but also among the three different Avola cultivars.

4.3.1.4 Total phenolic content and antioxidant activity of *P. dulcis* husks cvs. Toritto, Fascionello, Pizzuta and Romana

All the extracts of Apulian and Sicilian *P. dulcis* husks were submitted to Folin-Ciocalteu assay to determine the total phenolic content, and to DPPH• and ABTS^{•+} assays to evaluate the radical scavenging activity (Table 4.6).

The EtOH:H₂O extracts showed the highest phenolic content, in particular those of the Sicilian cvs. Similarly, the EtOH:H₂O extracts exerted the strongest scavenging activity towards both DPPH• and ABTS^{•+} radicals, specially those of the Sicilian cvs. Interestingly, the results achieved from the colorimetric assays highlighted clear differences among the Apulian and the Sicilian cvs. extracts, further suggesting the influence of different geographical origins on the metabolite profile of a plant species.

Table 4.6 Total phenolic content, DPPH• and ABTS^{•+} radical scavenging activity of the extracts of *P. dulcis* cvs. Toritto and Avola (Fascionello, Pizzuta and Romana) husks

Sample	Total phenolic content		DPPH•		ABTS ^{•+}	
	GAE ^a	SD ^d	IC ₅₀ ^b	SD ^d	TEAC ^c	SD ^d
TORITTO MeOH	21.43	± 1.40	60.21	± 3.21	0.10	± 0.07
TORITTO EtOH	22.54	± 0.32	81.91	± 2.75	0.05	± 0.02
TORITTO EtOH/H ₂ O	28.46	± 1.79	71.77	± 4.56	0.37	± 0.05
FASCIONELLO MeOH	45.50	± 6.94	81.96	± 4.12	0.37	± 0.09
FASCIONELLO EtOH	73.28	± 7.69	148.56	± 7.64	0.48	± 0.18
FASCIONELLO EtOH/H ₂ O	141.06	± 9.69	54.79	± 2.84	1.65	± 0.07
PIZZUTA MeOH	42.35	± 7.66	57.01	± 2.58	0.71	± 0.07
PIZZUTA EtOH	71.06	± 3.09	49.78	± 1.68	1.64	± 0.07
PIZZUTA EtOH/H ₂ O	137.72	± 6.41	19.41	± 1.21	1.59	± 0.06
ROMANA MeOH	40.13	± 5.48	34.83	± 1.98	0.89	± 0.15
ROMANA EtOH	68.83	± 2.55	80.54	± 3.67	1.63	± 0.09
ROMANA EtOH/H ₂ O	112.54	± 5.67	21.74	± 0.96	1.62	± 0.11
Vit. C			5.16	± 0.11		
Quercetin					1.87	± 0.08

^aValues are expressed as gallic acid equivalents (GAE) mg/g of dried extract. ^bValues are expressed as µg/mL. ^cValues are expressed as concentration (mM) of a standard Trolox solution exerting the same antioxidant activity of a 1 mg/mL solution of the tested extract. ^dStandard Deviation of three independent experiments.

4.4 LC-ESI/LTQOrbitrap/MS/MS profiling highlights *P. dulcis* (cv. Toritto and Avola) shells as a rich source of phenolics with multiple biological activities

Prunus dulcis Mill. shells



The shells are the endocarp of the drupe, the fruit of *P. dulcis*. It is a wooden and hard envelop, with a porous surface, and a color varying from bright to dark brown, mainly constituted by lignin, celluloses and hemicelluloses, whose main purpose is to protect the edible seed. Actually they represent one of the principal wastes deriving from almond productions, mostly used as alternative fuel for stoves or employed for mulching.

4.4.1 Results and discussion

4.4.1.1 Liquid chromatography high resolution mass spectrometry based putative identification of the MeOH extract of *P. dulcis* cv. Toritto shells

To explore the metabolite profile of *P. dulcis* cv. Toritto shells, with particular interest towards polar constituents, the MeOH extract was submitted to LC-ESI/LTQOrbitrap/MS experiments in negative ionization mode, allowing to achieve a preliminary overview on its chemical composition. A deep analysis of the LC-HRMS profile (Fig. 4.29) suggested the presence of twentytwo phenolic compounds, corresponding to caffeoylquinic acid (7), catechin (49), a phenolic glycoside (50), a prenylated benzoic acid glycoside (39), glycosylated flavonoids (15, 16, 19, 21, 61), lignans (34, 54, 58) and neolignans (53, 55, 57, 59-60, 62-66) (Table 4.7).

Table 4.7 Compounds identified and putatively identified in the MeOH extract of *P. dulcis* cv. Toritto shells

N°	R _t	Calculated Mass	[M-H] ⁻	Δppm	MS ² (%)	Molecular formula	Compound
7	4.66	354.0970	353.0875	0.26	191(100), 179(42), 135(23)	C ₁₆ H ₁₈ O ₉	3- <i>O</i> -caffeoylquinic acid
49	6.33	290.0790	289.0709	0.96	245(100), 205(46), 179(18)	C ₁₅ H ₁₄ O ₆	(+)-catechin ³
50	6.85	402.1526	401.1440	1.54	269(100), 161(53), 107(24)	C ₁₈ H ₂₆ O ₁₀	benzyl hexoside pentoside
51	9.14		585.2172		377(100), 329(25)		unknown
52	9.92		585.2174		377(100), 329(25)		unknown
53	10.86	540.2206	539.2123	1.32	521 (20), 491(100), 377(18), 343(42), 329(12), 195(26), 165(19)	C ₂₆ H ₃₆ O ₁₂	guaiacylglycerol dihydroconiferyl ether hexoside
54	11.54	582.2312	581.2227	0.95	566(16), 419(100), 401(19), 386(4), 247(13)	C ₂₈ H ₃₈ O ₁₃	lyoniresinol hexoside
55	11.74	540.2206	539.2117	0.55	521(17), 491(100), 377(35), 343(42), 329(14), 195(13), 165(17)	C ₂₆ H ₃₆ O ₁₂	guaiacylglycerol dihydroconiferyl ether hexoside
56	12.16	684.2629	683.2543		521(100), 359(34)	C ₃₂ H ₄₄ O ₁₆	unknown
34	12.77	524.2257	523.2173	-1.64	505(13), 493(17), 361(100), 343(36), 179(8), 165(24)	C ₂₆ H ₃₆ O ₁₁	secoisolariciresinol hexoside
57	13.98	522.2101	567.1071 ¹	1.22	521(26), 359(163), 341(94), 329(100), 223(12), 205(8)	C ₂₆ H ₃₄ O ₁₁	dihydrodehydrodiconiferyl alcohol hexoside
15	16.17	464.0954	463.0867	0.23	301(100), 179(12), 151(8)	C ₂₁ H ₂₀ O ₁₂	quercetin 3- <i>O</i> -β-D-galactopyranoside ²
39	16.18	368.1471	413.1442 ¹	1.00	367(100), 205(39)	C ₁₈ H ₂₄ O ₈	malaxinic acid ³
16	16.41	464.0954	463.0871	0.32	301(100), 179(16), 151(11)	C ₂₁ H ₂₀ O ₁₂	quercetin 3- <i>O</i> -β-D-glucopyranoside ²
58	16.58	552.2206	551.2119	1.65	536(23), 521(10), 503(11), 389(100), 371(34), 341(19), 235(4)	C ₂₇ H ₃₆ O ₁₂	methoxyisolariciresinol hexoside
59	16.84	522.2101	567.1264 ¹	0.33	521(24), 359(100), 341(84), 329(36), 223(13), 205(6)	C ₂₆ H ₃₄ O ₁₁	dihydrodehydrodiconiferyl alcohol 9- <i>O</i> -β-D-glucopyranoside ²
60	17.78	572.2257	571.2169	0.47	553(12), 541(3), 523(100), 375(12), 357(41), 345(89), 209(19), 195(5)	C ₃₀ H ₃₆ O ₁₁	alutaceuol
21	17.89	448.1005	447.0922	0.45	285(100), 151(9)	C ₂₁ H ₂₀ O ₁₁	kaempferol 3- <i>O</i> -β-D-glucopyranoside ²
61	18.68	624.1690	623.1602	0.96	315(100), 300(27), 151(14)	C ₂₈ H ₃₂ O ₁₆	isorhamnetin 3- <i>O</i> -β-D-rutinoside ²
19	19.03	478.1111	477.1023	0.41	315(100), 314(64), 151(11)	C ₂₂ H ₂₂ O ₁₂	isorhamnetin 3- <i>O</i> -β-D-glucopyranoside ²
62	19.84	748.2942	747.2851	1.15	729(4), 699(5), 585(12), 567(6), 519(43), 371(100), 356(11), 341(7), 223(4)	C ₃₇ H ₄₈ O ₁₆	acernikol hexoside
63	20.49	746.2785	745.2697	0.41	727(12), 715(40), 683(10), 583(46), 565(100), 547(16), 535(31), 503(12), 369(46), 354(8)	C ₃₇ H ₄₆ O ₁₆	buddlenol B hexoside
64	21.20	748.2942	747.2855	1.00	729(3), 699(6), 585(12), 567(8), 519(21), 371(100), 356(9), 341(13), 223(8)	C ₃₇ H ₄₈ O ₁₆	acernikol hexoside
65	22.30	746.2785	745.2700	0.69	727(15), 715(55), 583(9), 565(100), 547(21), 535(38), 503(24), 369(46), 354(5)	C ₃₇ H ₄₆ O ₁₆	buddlenol B hexoside
66	22.72	586.2414	585.2327	0.82	567(16), 555(6), 537(100), 371(22), 359(26), 223(11), 195(34)	C ₃₁ H ₃₈ O ₁₁	acernikol

¹Observed as formate adduct. ²The identification of this compound was corroborated by isolation and NMR spectra analysis.³The identification of this compound was corroborated by comparison with standard solution

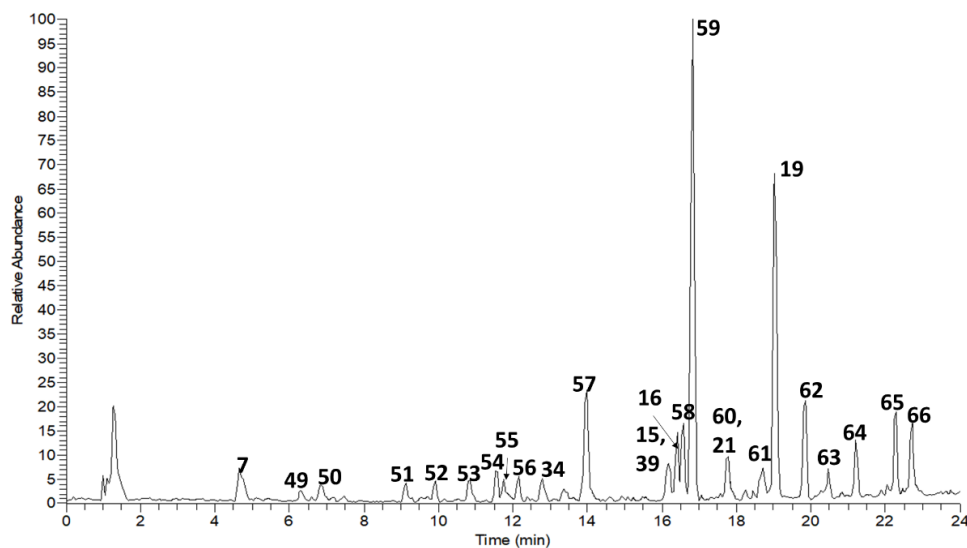


Figure 4.29 LC-HRMS profile in negative ion mode of the MeOH extract of *P. dulcis* cv. Toritto shells

The MeOH extract of *P. dulcis* cv. Toritto shells was fractionated by combined chromatographic techniques in order to isolate the main polar constituents. In Fig. 4.30 the compounds isolated and characterized by 1D and 2D NMR experiments are reported.

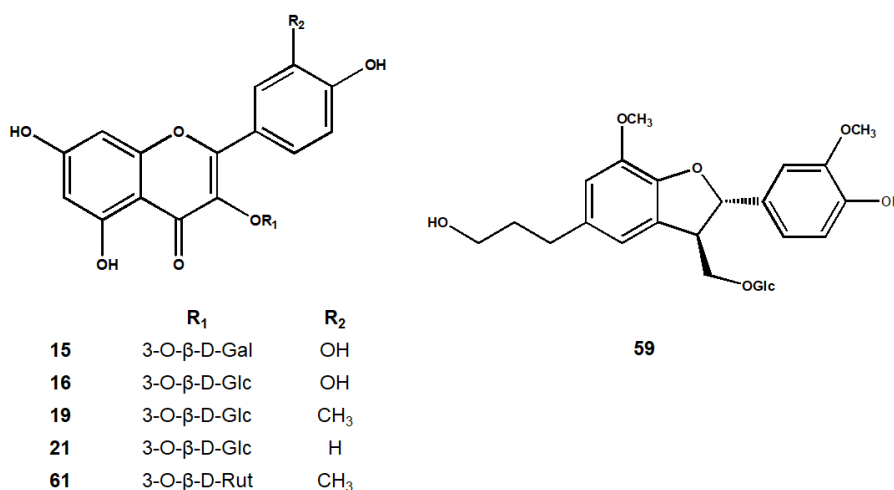


Figure 4.30 Compounds isolated from the MeOH extract of *P. dulcis* cv. Toritto shells

Besides glycosylated flavonoids, a neolignan was identified as dihydrodehydrodiconiferyl alcohol 9-*O*- β -D-glucopyranoside (**59**), also reported in the seeds of *P. tomentosa* (Liu et al., 2014).

However, the LC-HRMS profile showed the occurrence of further phenolics, mainly lignans and neolignans. Hence, an exhaustive analysis of the MS/MS spectra of the not isolated compounds was carried out.

The putative identification of the detected phenolic derivatives was carried out by determining their accurate *m/z* values, molecular formulae and characteristic fragmentation patterns, comparing the obtained information with data reported in scientific literature, online databases (KnapSack, FoodB, PubChem, ChemSpider, KEGG) and by incorporating the fragmentation spectra in online database-assisted prediction tools (MetFrag). To allow such operation, during the LC-ESI/LTQOrbitrap/MS/MS experiments the “data dependent scan” mode was employed, enabling the MS software to select the precursor ion as the most intense peak in the LC-MS spectrum.

Compound **7** (*m/z* 353.0875) showed in the MS/MS spectrum an intense ion at *m/z* 191 related to the loss of the caffeic acid moiety, together with two other product ions at *m/z* 179 and 135, originated from the loss of the quinic acid moiety and the subsequent decarboxylation (-44 Da), respectively. Moreover, the evaluation of the fragment ions relative abundance in the MS/MS spectrum allowed to determine the binding site of the caffeic acid on the quinic acid moiety at position 3. In addition, the molecular formula was established as C₁₆H₁₈O₉, in accordance with the identity putatively assigned to compound **7** as 3-*O*-caffeoylquinic acid (Clifford et al., 2003) (Table 4.7).

Compound **50** showed in the HRMS spectrum a pseudomolecular ion [M-H]⁻ at *m/z* 401.1440 and the molecular formula was established as C₁₈H₂₆O₁₀, while its fragmentation spectrum was characterized by a base peak at *m/z* 269, due to the loss of a dehydrated pentose unit, along with a fragment ion at *m/z* 107 due to the further

loss of a dehydrated hexose unit, and related to a benzyl moiety. In accordance to the achieved information, compound **50** was putatively identified as benzyl hexoside pentoside (Xu et al., 2018) (Table 4.7).

A formic acid adduct $[M-H+HCOOH]^-$ was observed in HRMS for compound **39** at m/z 413.1442, showing in the MS/MS spectrum an intense ion $[M-H-HCOOH]^-$ at m/z 367, together with a fragment ion $[M-H-HCOOH-162]^-$ at m/z 205 ascribable to the loss of a dehydrated hexose moiety; molecular formula was established as $C_{18}H_{24}O_8$. In accordance to the results obtained from the phytochemical investigation carried out on *P. dulcis* cv. Toritto husks, and considering both fragmentation spectrum and molecular formula, compound **39** was identified as malaxinic acid (Sang et al., 2002) (Table 4.7).

The peak with R_t 6.33 min showed in the HRMS spectrum a pseudomolecular ion $[M-H]^-$ at m/z 289.0709, corresponding to the molecular formula $C_{15}H_{14}O_6$. The related fragmentation pattern, along with the comparison of the R_t with standard solution, allowed to identify compound **49** as (+)-catechin (Rubilar et al., 2007) (Table 4.7).

4.4.1.2 Lignans

Lignans are a group of natural compounds occurring in several plant species, mostly reported in cereals and in the Pinaceae family. From a chemical point of view, lignans present a core made up of two phenylpropanoid units (C6-C3), mostly sinapyl, coniferyl and *p*-coumaryl alcohols, linked each other by a β - β -linkage, also described as C8-C8'. From this junction, depending on the rearrangements occurring during the biosynthetic processes, different classes of lignans may originate, as furanolignans, dibenzylbutyrolactone lignans, dibenzylbutanediol lignans, furofuranolignans and aryltetralindiol lignans. Moreover, the further coupling of *p*-coumaryl, coniferyl and syringyl alcohols leads to the formation of

p-hydroxyphenyl glycerols, guaiacyl glycerols and syringyl glycerols, respectively, which may contribute to the structure elongation.

Interest has grown towards this class of compounds because of the several biological effects they showed to possess, like anticancer properties, intense antioxidant activity, reduction of cardiovascular and diabetes diseases, and reduction of menopause symptoms (Chen et al., 2015). Hence, the ongoing research for lignans in plant matrices has increased in the last years with a consequent development of different methods for their identification.

Liquid chromatography coupled to tandem mass spectrometry demonstrated to be a sensitive and quick analytical technique for structural elucidation of lignans, also supported by a rich scientific literature background, allowing to overcome the problem of difficult isolation procedures from complex matrices.

Lignans show in ESI/HRMS/MS analysis characteristic and highly diagnostic fragment ions, which can provide key information about their chemical structure. Typical fragments are related to neutral losses of water (-18 Da), methyl radical (-15 Da), formaldehyde (-30 Da), carbon dioxide (-44 Da), acetaldehyde (-44 Da) and a combined loss of water and formaldehyde (-48 Da). In addition, neutral losses of 166, 196 and 226 Da may be observed due to the neutral loss of *p*-hydroxyphenyl, guaiacyl and syringyl glycerols, respectively (Hiroe et al., 2004).

Compound **34** (m/z 523.2173) showed in the MS/MS spectrum (Fig. 4.31) a base peak at m/z 361 yielded from the loss of a dehydrated hexose moiety; moreover, characteristic lignan fragment ions due to the loss of formaldehyde (-30 Da) and water (-18 Da) were observed for both the glycosylated and the aglycone ions. In the low m/z region of the spectrum two fragment ions ascribable to the β - β -bond cleavage were visible at m/z 179 and 165. The molecular formula was established as C₂₆H₃₆O₁₁, and compound **34** putatively identified as secoisolariciresinol hexoside (Eklund et al., 2008) (Table 4.7).

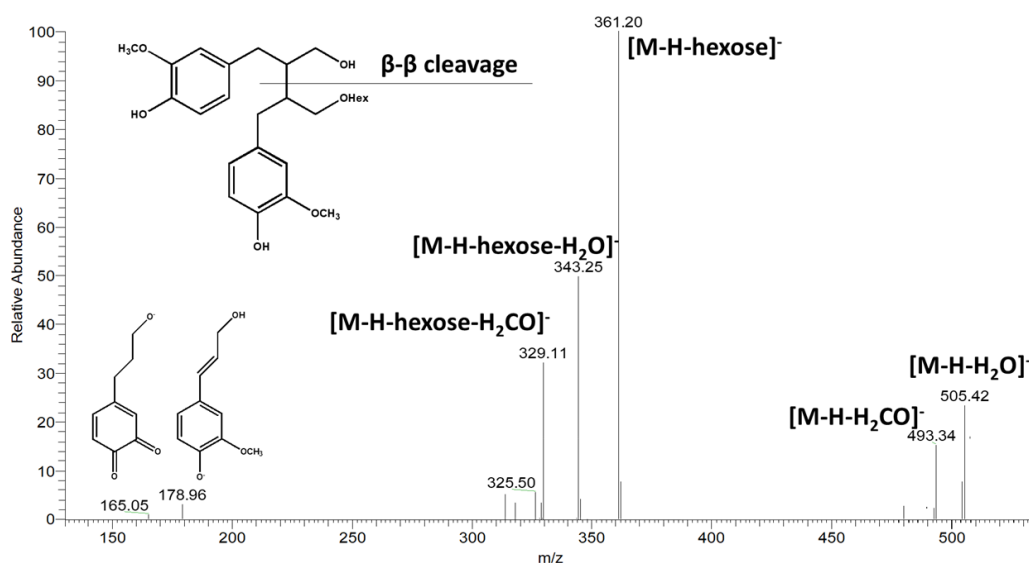


Figure 4.31 ESI/MS/MS spectrum of compound **34** in negative ion mode

Compound **54** (m/z 581.2227), whose molecular formula was established as $C_{28}H_{38}O_{13}$, exhibited a fragmentation pattern (Fig. 4.32) characterized by a fragment ion at m/z 566 due to the loss of a methyl radical, and a base peak at m/z 419 originated from the loss of the hexose moiety, followed by the loss of a water molecule (m/z 401), corresponding to the rearrangement of the diol into a furan ring, and a further methyl radical (m/z 386). In addition, a fragment ion [M-H-162-18-154]⁻ at m/z 247 was observed, elucidated by the reasonable neutral loss of the 3',5'-dimethoxy-4'-hydroxyphenyl ring. Hence, compound **54** was putatively identified as lyoniresinol hexoside (Wang et al., 2016; Chen et al., 2014) (Table 4.7).

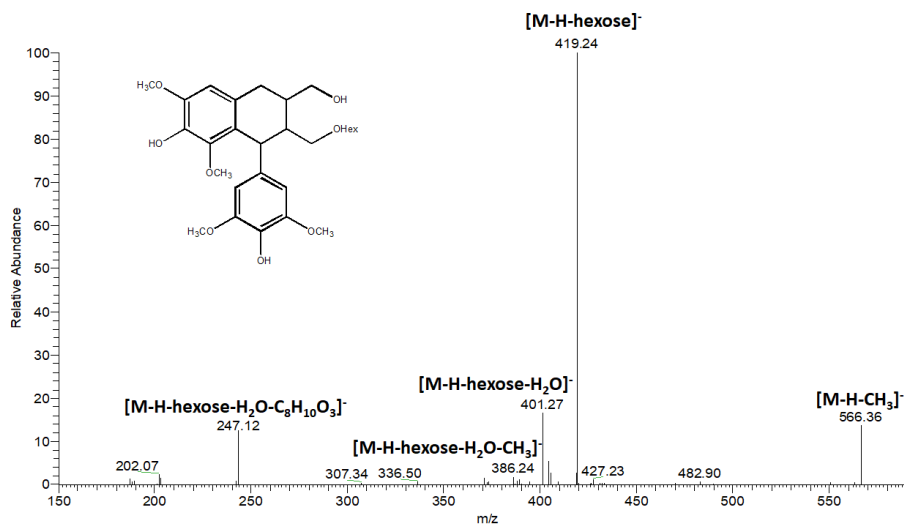


Figure 4.32 ESI/MS/MS spectrum of compound **54** in negative ion mode

Compound **58** showed a fragmentation pattern (Fig. 4.33) similar to that observed for compound **54**, with a pseudomolecular ion detected in HRMS at m/z 551.2119 (with a decrease of -30 Da respect to **54**), suggesting the absence of a methoxy group; furthermore, a product ion at m/z 235 generated from the loss of the 3',5'-dimethoxy-4'-hydroxyphenyl moiety from the aglycone (m/z 419), was observed. For compound **58** molecular formula was established as C₂₇H₃₆O₁₂, in accordance with the identity putatively attributed as methoxyisolariciresinol hexoside (Chen et al., 2014) (Table 4.7).

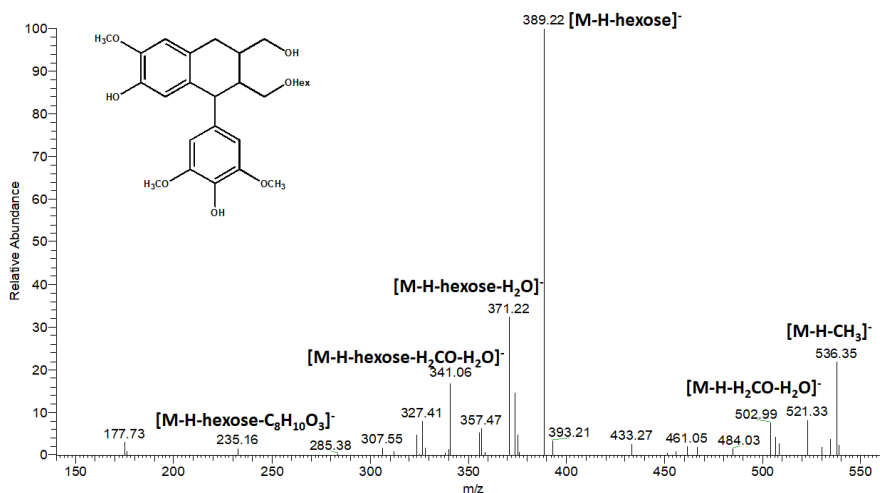


Figure 4.33 ESI/MS/MS spectrum of compound **58** in negative ion mode

4.4.1.3 Neolignans

Neolignans are characterized by bonds different from β - β -linkages. Most commonly 8-*O*-4 couplings occur, originating β -aryl ethers if the 4-site donor is a *p*-coumaryl/coniferyl alcohol, or benzodioxane lignans, if the 4-site donor is a sinapyl alcohol, together with 8-5 couplings originating phenylcoumarans (²Morreel et al., 2010).

A growing number of scientific reports highlight several biological properties possessed by neolignans, as cytotoxic effects, antibacterial, antifungal and antiproliferative activities and neuroprotective effects, as well as their conclamate antioxidant properties (Luis et al., 2002).

As well as for lignans, mass spectrometry has been widely employed for an immediate structural characterization of neolignans detected in plant matrices, thanks to the large number of obtainable information with short analysis times.

In ESI/MS/MS experiments (Fig. 4.34) compounds **53** and **55** showed similar MS/MS spectra. They exhibited a fragment ion at *m/z* 521 due to the loss of a water molecule, and the base peak at *m/z* 491 related to the sequential loss of water and formaldehyde; moreover, a fragment ion observed at *m/z* 377 was generated from the loss of the dehydrated hexose moiety, followed by the loss of water and

formaldehyde (-48 Da) at m/z 329. In addition, the product ion at m/z 343 could be attributed to the neutral loss of a guaiacylglycerol moiety, whose presence was confirmed by the fragment ion at m/z 195 (corresponding to the deprotonated guaiacylglycerol ion), with a following fragment ion at m/z 165 due to the loss of formaldehyde.

Both compounds showed superimposable MS/MS spectra, differing slightly in the fragments intensities, suggesting conceivable differences in the stereochemistry of the guaiacylglycerol stereocenters. Finally, molecular formula was established as $C_{26}H_{36}O_{12}$, in accordance to the identity putatively attributed to compounds **53** and **55** as guaiacylglycerol dihydroconiferyl ether hexoside (¹Morreel et al., 2010) (Table 4.7).

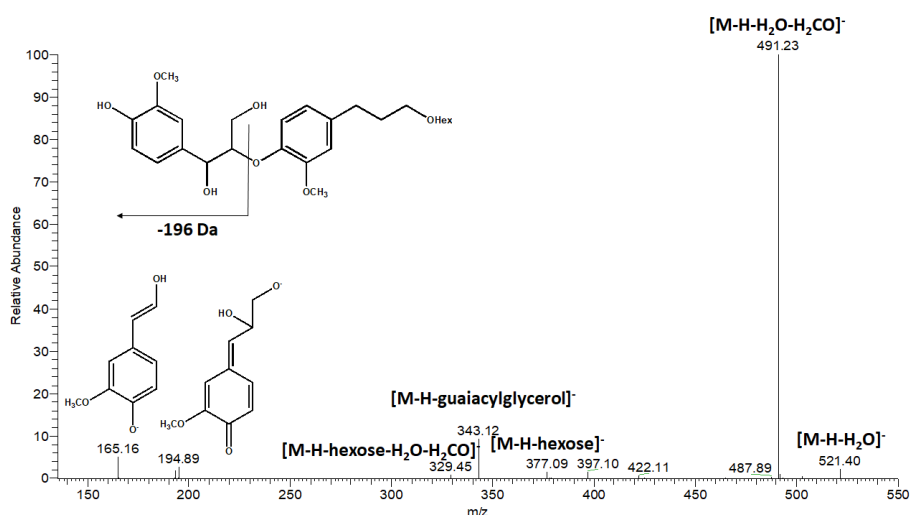


Figure 4.34 ESI/MS/MS spectrum of compound **53** in negative ion mode

Compound **57** was detected as a formate adduct $[M-H+HCOOH]^-$ at m/z 567.2071. The MS/MS spectrum (Fig. 4.35) showed a product ion at m/z 521 related to the loss of formic acid (-46 Da), while the fragment ions at m/z 359 and 341 were ascribable to the loss of the hexose moiety (-162 Da) and the further loss of a water molecule (-18 Da), while the base peak at m/z 329 was attributed to the loss of formaldehyde (-30 Da) from the aglycone ion. Moreover, the low m/z fragment ions

suggested the identity of the aglycone as phenylcoumaran with a saturated alkyl chain, since the fragment ion at m/z 223 was ascribable to the aliphatic end, which undergoes to the loss of a water molecule generating the fragment ion at m/z 205. Molecular formula was established as $C_{26}H_{34}O_{11}$. Thus, compound **57** was putatively identified as dihydrodehydrodiconiferyl alcohol hexoside (¹Morreel et al., 2010) (Table 4.7).

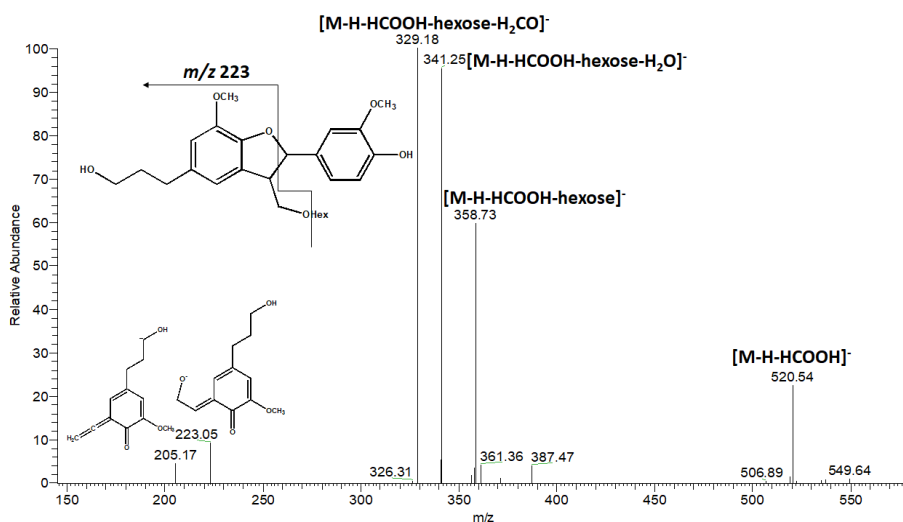


Figure 4.35 ESI/MS/MS spectrum of compound **57** in negative ion mode

Compound **60** (m/z 571.2169) showed a neolignan characteristic pattern in MS/MS spectrum (Fig. 4.36): the product ions at m/z 553 and 541 were related to the loss of a water molecule (-18 Da) and formaldehyde (-30 Da), respectively, while the base peak observed at m/z 523 was ascribable to the concurrent loss of water and formaldehyde (-48 Da). In addition, the signal at m/z 375, followed by the loss of water (m/z 357) or formaldehyde (m/z 345), suggested the presence of a guaiacylglycerol moiety (-196 Da), confirmed by the presence of the fragment ion at m/z 195. Moreover, the product ion at m/z 209 suggested the aglycone moiety as a phenylcoumaran derivative. Molecular formula was established as $C_{30}H_{36}O_{11}$. Thus, compound **60** was putatively identified as alutaceuol (Hanhineva et al., 2012) (Table 4.7).

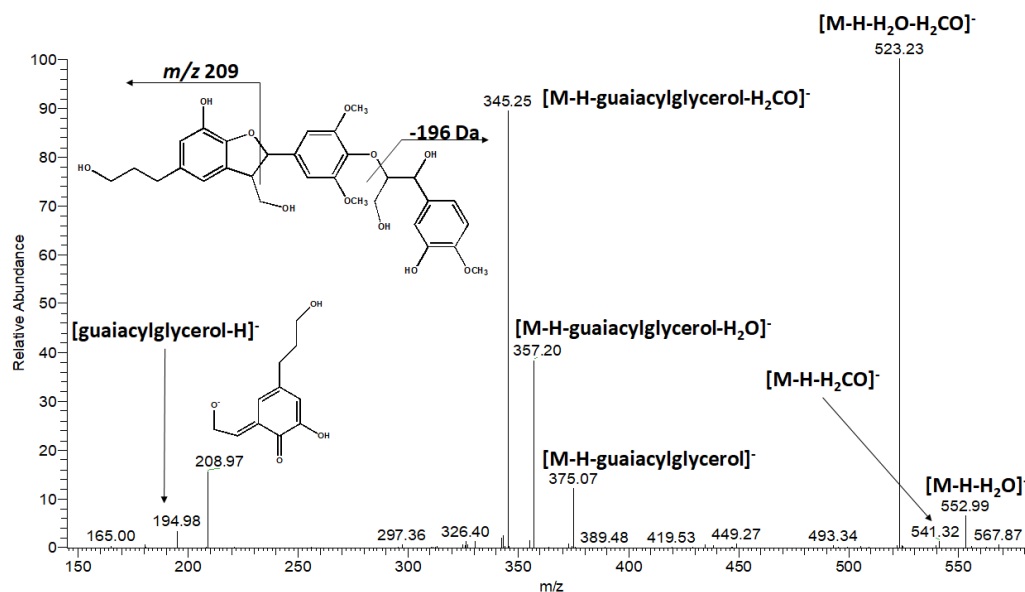


Figure 4.36 ESI/MS/MS spectrum of compound 60 in negative ion mode

Compounds 62 and 64, as well, exhibited identical MS/MS spectra (Fig. 4.37), showing slight dissimilarities only in the relative abundance of the product ions. The informative fragmentation pattern evidenced daughter ions due to the loss of a water molecule (m/z 729) and the loss of water and formaldehyde (m/z 699); in addition, the fragment ion at m/z 585 could be attributed to the loss of the hexose moiety, with the subsequent loss of water (m/z 567), and the loss of a guaiacylglycerol moiety (-196 Da). Furthermore, the product ion at m/z 223, also observed in the MS/MS spectrum of compound 57 and 59, was ascribable to the aliphatic chain of a phenylcoumaran moiety. The molecular formula for both compounds was established as C₃₇H₄₈O₁₆, in accordance to the identity putatively attributed to compounds 62 and 64 as acernikol hexoside (Hanhineva et al., 2012; Morreel et al., 2010) (Table 4.7).

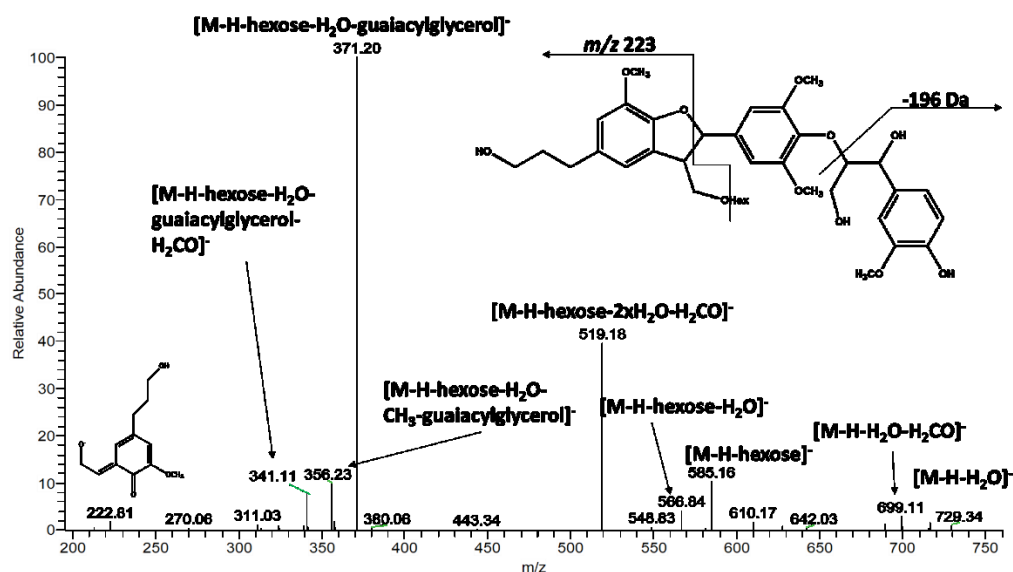


Figure 4.37 ESI/MS/MS spectrum of compound **62** in negative ion mode

Suchlike behaviour was observed for compounds **63** and **65**, with parallel fragmentation patterns. The MS/MS spectra (Fig. 4.38) showed characteristic losses of a water molecule (-18 Da) and formaldehyde (-30 Da) for both pseudomolecular ion and aglycone (m/z 583, generated by the loss of a dehydrated hexose moiety of 162 Da from the pseudomolecular ion). In addition, the fragment ion at m/z 369 could be attributed to the simultaneous loss from the aglycone of both water and a guaiacylglycerol moiety, followed by a further loss of a methyl radical (m/z 354). Moreover, the similarity with the MS/MS spectra of compounds **62** and **64**, with the difference of -2 Da for the pseudomolecular ion and for all fragment ions, presumed the presence of an unsaturation on the alkyl chain of the phenylcoumaran moiety. Molecular formula was established as $C_{37}H_{46}O_{16}$, suitable with the identity tentatively attributed to compounds **63** and **65** as buddlenol B hexoside (Hanhineva et al., 2012; ¹Morreel et al., 2010) (Table 4.7).

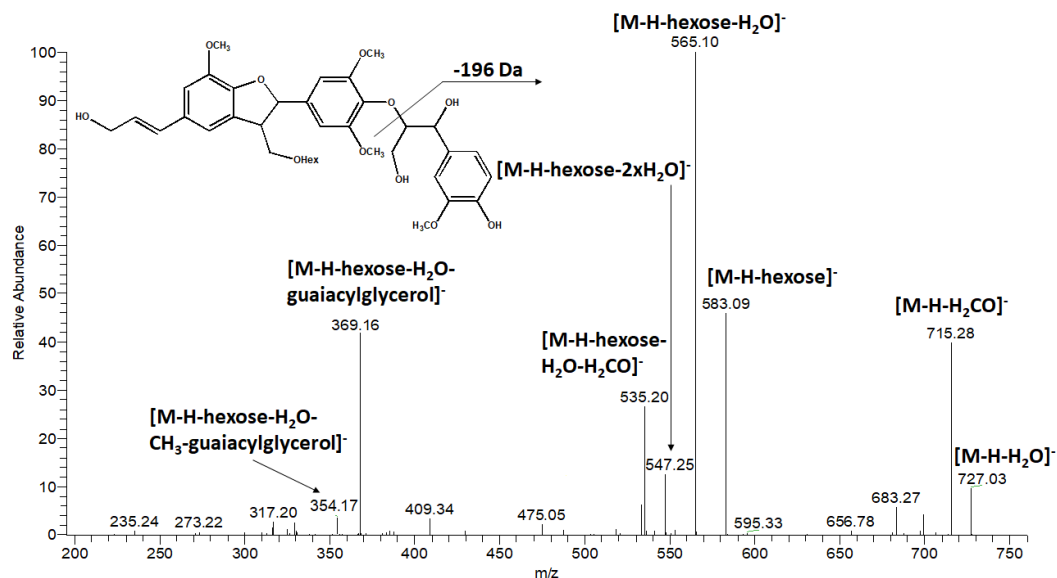


Figure 4.38 ESI/MS/MS spectrum of compound **63** in negative ion mode

Finally, compound **66** (m/z 585.2327), whose molecular formula was established as $C_{31}H_{38}O_{11}$, showed in the MS/MS spectrum (Fig. 4.39) separated losses of water (-18 Da) and formaldehyde (-30 Da), as well as their jointed loss (-48 Da). Moreover, the first two fragment ions exhibited a further loss of a guaiacylglycerol moiety at m/z 371 and 359, respectively, whose presence in the molecule was confirmed by the fragment ion at m/z 195. Furthermore, the product ion at m/z 223, also observed for previous compounds, suggested the existence of a phenylcoumaran moiety with a saturated alkyl chain, thus allowing to putatively identify compound **66** as acernikol (¹Morreel et al., 2010; ²Morreel et al., 2010) (Table 4.7).

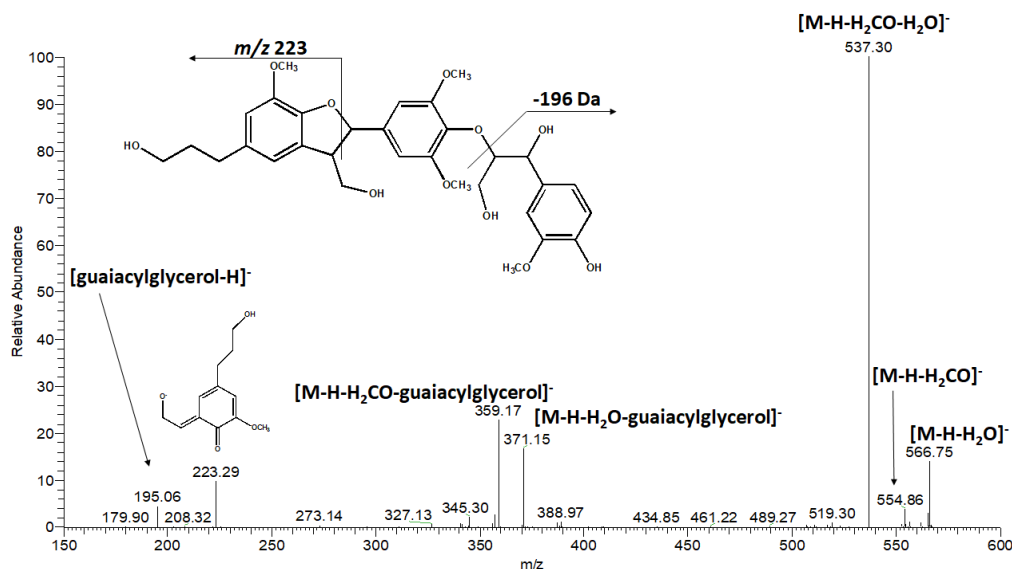


Figure 4.39 ESI/MS/MS spectrum of compound **66** in negative ion mode

4.4.1.4 “Eco-friendly” extracts comparison by LC-ESI/LTQOrbitrap/MS experiments

The phytochemical investigation of the MeOH extract of *P. dulcis* cv. Toritto shells highlighted the presence of several phenolics reported in scientific literature for their noteworthy biological activities, especially lignans and neolignans. Hence, aiming at extracting certain classes of compounds by employing solvents and methods suitable for secondary applications, different extracts were prepared by maceration using as solvents EtOH 96% and an EtOH:H₂O (1:1, v/v) solution. The obtained extracts were successively submitted to LC-ESI/LTQOrbitrap/MS experiments and the profiles compared with MeOH extract (Fig. 4.40).

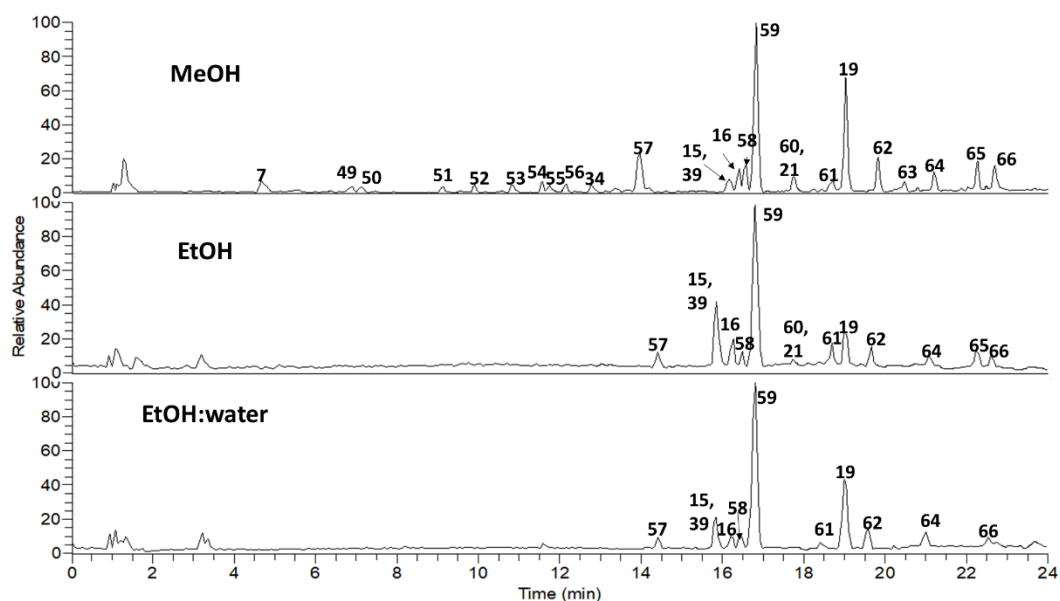


Figure 4.40 LC-HRMS profile in negative ion mode of the MeOH, EtOH and EtOH:H₂O extracts of *P. dulcis* cv. Toritto shells

“Eco-friendly” extraction methods showed good selectivity towards glycosylated flavonoids and the most apolar lignans and neolignans, rather than the most polar and minor constituents. This evidence pointed out a potential employment of “green” solvents for targeted extractions of phytochemicals, for an exhaustive exploitation of biomasses mostly considered as wastes of manufacturing processes.

4.4.1.5 LC-ESI/LTQOrbitrap/MS analysis of MeOH extracts obtained from the shells of different cultivars (Toritto and Avola)

Looking at evaluating if different growing conditions may affect the metabolome of a plant species, the MeOH extract of *P. dulcis* cv. Toritto shells was compared with the MeOH extracts of *P. dulcis* cvs. Avola shells by LC-ESI/LTQOrbitrap/MS experiments. Comparing the obtained LC-HRMS profiles (Fig. 4.41) no significant dissimilarities were detected: cv. Romana was characterized by the absence of the most polar constituents and of the peak related to compound **64**, also observed for

cv. Pizzuta, while for all the Sicilian cvs. a common absence of the peak related to compound **63** was observed.

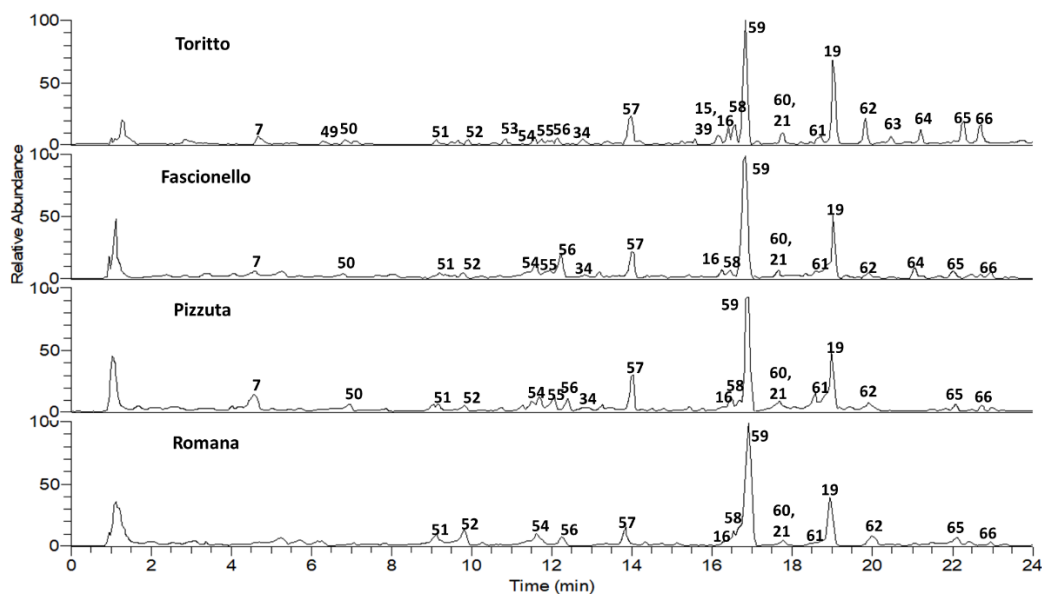


Figure 4.41 Comparison of the LC-HRMS profiles of the MeOH extracts of *P. dulcis* cv. Toritto and cvs. Avola (Fascionello, Pizzuta and Romana) shells, in negative ion mode.

4.4.1.6 Total phenolic content and radical scavenging activity of the different extract typologies of *P. dulcis* shells (cvs. Toritto and Avola)

Total phenolic content was evaluated by Folin-Ciocalteu assay, which highlighted how EtOH extracts possessed the highest phenolic content if compared to the other extracts. Moreover, the radical scavenging activity was evaluated by DPPH \cdot and ABTS $^{*\cdot}$ assays, showing a moderate activity if compared to quercetin.

Table 4.8 Total phenolic content, DPPH• and ABTS^{•+} radical scavenging activity of the extracts of *P. dulcis* cvs. Toritto and Avola (Fascionello, Pizzuta and Romana) shells

Sample	Total phenolic content		DPPH•		ABTS ^{•+}	
	GAE ^a	SD ^d	IC ₅₀ ^b	SD ^d	TEAC ^c	SD ^d
TORITTO MeOH	88.69	± 7.56	61.52	± 2.64	0.57	± 0.04
TORITTO EtOH	75.32	± 4.32	164.68	± 12.25	0.40	± 0.04
TORITTO EtOH/H ₂ O	56.80	± 4.24	175.52	± 11.78	0.20	± 0.02
FASCIONELLO MeOH	60.32	± 8.67	74.28	± 2.37	0.32	± 0.06
FASCIONELLO EtOH	100.69	± 6.12	53.06	± 4.21	0.51	± 0.04
FASCIONELLO EtOH/H ₂ O	58.53	± 7.36	88.30	± 4.73	0.35	± 0.06
PIZZUTA MeOH	53.46	± 1.95	84.15	± 4.85	0.42	± 0.06
PIZZUTA EtOH	82.72	± 7.84	73.09	± 3.54	0.75	± 0.10
PIZZUTA EtOH/H ₂ O	41.43	± 5.79	99.74	± 3.19	0.18	± 0.03
ROMANA MeOH	64.02	± 4.79	90.62	± 3.67	0.25	± 0.02
ROMANA EtOH	73.46	± 5.34	57.02	± 2.97	0.46	± 0.08
ROMANA EtOH/H ₂ O	64.22	± 1.11	83.02	± 2.52	0.11	± 0.01
Vit. C			5.16	± 0.11		
Quercetin					1.87	± 0.08

^aValues are expressed as gallic acid equivalents (GAE) mg/g of dried extract. ^bValues are expressed as µg/mL. ^cValues are expressed as concentration (mM) of a standard Trolox solution exerting the same antioxidant activity of a 1 mg/mL solution of the tested extract. ^dStandard Deviation of three independent experiments.

4.5 Conclusions

This phytochemical investigation carried out on the leaves, husks and shells of *P. dulcis*, the last two considered the main by-products deriving from almonds manufacturing, highlighted the occurrence of several classes of secondary metabolites. The “eco-friendly” extraction methods showed a good selectivity towards certain classes of compounds. The comparison of the LC-MS profiles, occasionally supported by multivariate statistical analysis, pointed out evident dissimilarities in the chemical composition of the investigated *P. dulcis* cvs., suggesting an influence of different growing conditions on the metabolome of a plant species. Moreover, the tested extracts showed to possess a good phenolic

content, in particular the “eco-friendly” extracts, as well as an interesting radical scavenging activity. Thus, the non-edible parts of *P. dulcis* may represent a potential source of bioactives with beneficial effects for human health.

4.6 Experimental section

Plant material

P. dulcis Mill. leaves, husks and shells of the cv. Toritto were provided by “La Fattoria della Mandorla”, Toritto, Italy, in October 2015. *P. dulcis* Mill. leaves of the cvs. Fascionello, Pizzuta and Romana were provided by “The consortium of the Mandorla d’Avola” in November 2015, while husks and shells were provided in September 2016.

General experimental procedures

Column chromatography was performed on Sephadex LH-20 (Pharmacia). HPLC-RI separations were performed on instrument described in general experimental procedures, using a Knauer Eurospher 100-10 C-18 column (300 x 8 mm, 10 μ m) or a μ Bondapak C-18 (300 x 8 mm, 10 μ m). HPLC-UV/Vis separations were performed on instrument described in general experimental procedures, using a Phenomenex (Torrance, CA, USA) Synergi Hydro RP-80A column (250 x 10 mm, 10 μ).

LC-ESI/LTQOrbitrap/MS/MS and LC-ESI/LTQOrbitrap/MS procedures

LC-HRMS experiments were carried out on instrument reported in general experimental procedures. LC separations were performed on a Phenomenex (Torrance, CA, USA) Kinetex C-18 column (100 x 2.10 mm, 2.6 μ m), at a flow rate of 0.2 μ l/min. Employed mobile phases were (A) water and (B) acetonitrile, both acidified 0.1% formic acid. Injection volume was 10 μ L, keeping column at room temperature.

The ESI source parameters were set as following: source voltage at 5.0 kV, capillary voltage at -12 V, tube lens offset at -121.47 V, capillary temperature at 280 °C, sheath gas at 30 (arbitrary units) and auxiliary gas at 5 (arbitrary units).

- *LC-ESI/LTQOrbitrap/MS/MS gradient conditions for the leaves extracts.*
Elution gradient: 0 min 10% B, 8 min 30% B, 20 min 30% B, 25 min 90% B, 35 min 90% B, returning to start conditions in 7 min. Only for leaves, spectra were acquired in positive ion mode too. The ESI source parameters were set as following: source voltage at 3kV, capillary voltage at 49 V, tube lens offset at 120 V, capillary temperature at 280°C, auxiliary gas flow at 10 (arbitrary unit) and sheat gas at 30 (arbitrary unit). Additionally, only for leaves a different B eluent was employed, constituted by a MeOH:acetonitrile (1:1, v/v) solution with 0.1% formic acid.
- *LC-ESI/LTQOrbitrap/MS/MS gradient conditions for the husks extracts.*
Elution gradient: 0 min 10% B, 25 min 34%, 35 min 34% B, 50 min 100% B, held for 8 min, returning to start conditions in 7 min.
- *LC-ESI/LTQOrbitrap/MS/MS gradient conditions for the shells extracts.*
Elution gradient: 0 min 10% B, 24 min 34% B, returning to start conditions in 7 min.

Extraction and purification of the MeOH extract of P. dulcis cv. Toritto leaves, and preparation of “eco-friendly” extracts

1.4 kg of air-dried leaves of *P. dulcis* cv. Toritto were extracted by maceration using petroleum ether (1.5 L, three times for three days), chloroform (1.5 L, three times for three days), and with MeOH (1.5 L, three times for three days), yielding 130.20 g of crude MeOH extract.

The leaves of *P. dulcis* cvs. Avola (Fascionello, Pizzuta and Romana) were extracted in the same way, but using a lower amount of sample (3 g) and of solvent (50 mL), obtaining 0.44 g, 0.31 g and 0.37 g of crude MeOH extract, respectively.

Moreover, the leaves of the cvs. Toritto and Avola (3 g) were extracted by maceration using EtOH 96% (50 mL, three times for three days) and a EtOH:H₂O (1:1, v/v) solution (50 mL, three times for three days). The leaves were also extracted by decoction, adding cold water (50 mL) to the leaves (3 g) and warming till boiling point, keeping boiling for 15 min, cooling to room temperature and then filtering, and by infusion, adding boiling water (50 mL) to the leaves (3 g), leaving in contact for 15 min and then filtering.

About 3.5 g of the MeOH extract of the cv. Toritto leaves were dissolved in 8 mL of MeOH and fractionated on a Sephadex LH-20 (Pharmacia) column (100 x 5 cm), using MeOH as mobile phase, affording 80 fractions (8 mL each) which were monitored by TLC. Fractions 5-15 (747.2 mg) were chromatographed by RP-HPLC-UV-Vis using as solvents (A) water-formic acid (99.9:0.1, v/v) and (B) MeOH-acetonitrile-formic acid (49.95:49.95:0.1, v/v), flow rate was 2 mL/min, selected wavelengths were 254 and 330 nm, the gradient conditions were: 0 min 10% B, 5 min 25% B, 60 min 55% B, 70 min 100% B; this led to the isolation of compounds **5** (2.2 mg, $R_t=13.2$ min), **11** (2.4 mg, $R_t=18.3$ min), **13** (3.2 mg, $R_t=22.1$ min), **20** (2.6 mg, $R_t=25.5$ min), **26** (2.8 mg, $R_t=46.8$ min) and **27** (2.6 mg, $R_t=47.1$ min). Fractions 16-20 (207.1 mg) were chromatographed by RP-HPLC-RI using MeOH:H₂O (3:7, v/v) as mobile phase (flow rate 2.0 mL/min) to yield compound **6** (2.3 mg, $R_t=9.1$ min). Fractions 25-29 (101.2 mg) were chromatographed by RP-HPLC-RI using MeOH:H₂O (2:3, v/v) as mobile phase (flow rate 2.0 mL/min) to yield compounds **14** (3.5 mg, $R_t=23.1$ min), **24** (10.9 mg, $R_t=39.6$ min). Fractions 30-34 (92.5 mg) were chromatographed by RP-HPLC-RI using MeOH:H₂O (9:11, v/v) as mobile phase (flow rate 2.0 mL/min) to yield compounds **16** (4.6 mg, $R_t=16.3$ min), **17** (3.1 mg, $R_t=22.3$ min), **18** (6.1 mg, $R_t=31.8$ min), **21** (3.1 mg, $R_t=51.7$ min) and **23** (2.9 mg, $R_t=52.1$ min). Fractions 35 and 36 were chromatographed by RP-HPLC-RI using MeOH:H₂O (9:11, v/v) as mobile phase (flow rate 2.0 mL/min) to yield compound **19** (5.0 mg, $R_t=34.8$ min). Fractions 37-

40 were chromatographed by RP-HPLC-RI using MeOH:H₂O (1:1, v/v) as mobile phase (flow rate 2.0 mL/min) to yield compound **15** (4.7 mg, R_t=10.6 min). Fractions 45-49 were chromatographed by RP-HPLC-RI using MeOH:H₂O (1:1, v/v) as mobile phase (flow rate 2.0 mL/min) to yield compound **22** (3.2 mg, R_t=4.2 min).

Extraction and purification of the MeOH extract of P. dulcis cv. Toritto husks, and preparation of “eco-friendly” extracts

Husks of *P. dulcis* cv. Toritto were air-dried until they turned from green to brown. Successively, 2.4 Kg of dried husks were extracted by maceration using solvents with increasing polarity, in particular with *n*-hexane (5.0 L, three times for three days), chloroform (5.0 L, three times for three days) and MeOH (5.0 L, three times for three days), yielding 321.50 g of MeOH crude extract. The husks of the three Sicilian cvs. Fascionello, Pizzuta and Romana were extracted in the same way, employing a lower amount of samples (30 g) and of solvent (100 mL), affording 2.76 g, 3.18 g and 0.94 g of crude MeOH extract, respectively. Furthermore, the husks of the four cultivars (30 g) were extracted by maceration employing EtOH 96% (100 mL, three times for three days), and an EtOH:H₂O (1:1, v/v) solution (100 mL, three times for three days). To remove the sugars detected in the MeOH extract by TLC, about 5 g of the MeOH extract were submitted to a BuOH:H₂O liquid-liquid extraction, yielding 1.41 g of BuOH crude extract.

About 3.5 grams of MeOH extract of cv. Toritto husks were dissolved in 8 mL of MeOH and fractionated on a Sephadex LH-20 (Pharmacia) column (100 x 5 cm), employing MeOH as mobile phase, affording 91 fractions (8 mL each), which were monitored by TLC. Fractions 19-24 (245.1 mg) were chromatographed by RP-HPLC-RI using MeOH:H₂O (3:7, v/v) as mobile phase (flow rate 2 mL/min) and the Knauer C-18 column to yield compound **30** (2.3 mg, R_t=34 min). Fractions 25-29 (100.6 mg) were chromatographed by RP-HPLC-RI using MeOH:H₂O (3:7, v/v)

as mobile phase (flow rate 2 mL/min) and the Knauer C-18 column to yield compound **31** (4.2 mg, $R_t = 10.2$ min). Fractions 42-48 (31.4 mg) were chromatographed by RP-HPLC-RI using MeOH:H₂O (3:1, v/v) as mobile phase (flow rate 2 mL/min) and the μ Bondapak C-18 column to yield compound **45** (2.8 mg, $R_t = 6.1$ min). Fractions 33-41 (97.4 mg) were chromatographed by RP-HPLC-RI using MeOH:H₂O (9:11, v/v) as mobile phase (flow rate 2 mL/min) and the μ Bondapak C-18 column to yield compounds **35** (3.6 mg, $R_t = 6.8$ min), **42** (4.1 mg, $R_t = 25.8$ min) and **19** (4.4 mg, $R_t = 26.1$ min). Fractions 12-16 (646.1 mg) were chromatographed by RP-HPLC-RI using MeOH:H₂O (39:11, v/v) as mobile phase (flow rate 2 mL/min) and the Knauer C-18 column to yield compound **26** (3.6 mg, $R_t = 4.2$ min). Fractions 17-18 (342.3 mg) were chromatographed by RP-HPLC-UV-Vis, (elution gradient was: 0 min 10% B, 30 min 100% B, held for 15 minutes, flow rate 2 mL/min, wavelength 254 nm) to yield compounds **39** (2.7 mg, $R_t = 15.8$ min), **27** (2.9 mg, $R_t = 25.5$ min), **46** (3.1 mg, $R_t = 32.2$ min), **47** (3.0 mg, $R_t = 38.9$ min), and **48** (2.8 mg, $R_t = 40.4$ min).

Extraction and purification of the MeOH extract of P. dulcis cvs. Toritto and Avola shells, and preparation of “eco-friendly” extracts

1.8 Kg of the *P. dulcis* cv. Toritto shells were extracted by maceration using solvents with increasing polarity: *n*-hexane (3.2 L, three times for three days), chloroform (3.0 L, three times for three days), MeOH (3.1 L, three times for three days), obtaining 21.25 g of crude MeOH extract. The shells of the Sicilian cvs. Fascionello, Pizzuta and Romana were extracted by adopting the same protocol, with a lower amount of samples (10 g) and solvent (100 mL), yielding 0.12 g, 0.22 g and 0.09g of crude MeOH extracts, respectively. Furthermore, the shells of all the cultivars were extracted by maceration (10 g) employing EtOH 96% (100 mL, three times for three days), and an EtOH:H₂O (1:1, v/v) solution (100 mL, three times for three days).

About 3.5 grams of crude MeOH extract were dissolved in 8 mL of MeOH and fractionated on Sephadex LH-20 (100 x 5 cm) column, affording 90 fractions (8 mL each), monitored by TLC. Fractions 15-17 were chromatographed by RP-HPLC-UV/Vis (elution gradient: 0 min 10% B held for 5 min, 10 min 25% B, 30 min 40% B, 35 min 100% B held for 10 min; wavelength: 285 nm), yielding compounds **57** (1.8 mg, R_t =15.0 min) and **59** (1.5 mg, R_t =18.3 min). Fractions 18-24 were chromatographed by RP-HPLC-UV/Vis (elution gradient: 0 min 10% B, 40 min 70% B, 50 min 100% B held for 10 min; wavelength: 280 nm), yielding compounds **15** (2.3 mg, R_t =12.3 min), **16** (2.6mg, R_t =13.5 min), **61** (1.9 mg, R_t =17.9 min), **21** (2.6 mg, R_t =20.5 min) and **19** (2.1 mg, R_t =21.8 min).

Chemometrics

Data analysis

Before undergoing data analysis, the raw data acquired by LC-ESI/LTQOrbitrap/MS experiments were filtered by employing MZmine 2.21 software. In particular, paying attention to preserve the variance of the compounds contained in the LC-MS spectra, baseline correction, gap filling, data reduction, noise elimination, peak detection, as well as the discard of m/z values due to in-source fragmentation events, were carried out; the filtered data were processed in order to obtain a data matrix successively employed for the multivariate data analysis. Moreover, the identification of the metabolites was carried out by comparing the m/z values and the related R_t reported in the data matrix with those of the compounds previously elucidated. Samples were analyzed in duplicate.

Multivariate data analysis

To identify the differences among the analyzed *P. dulcis* cultivars, the data obtained from the LC-MS experiments were submitted to chemometric analyses, in particular Principal Component Analysis (PCA) and Partial Least Square Discriminant Analysis (PLS-DA). Principal Component Analysis (PCA) is a powerful unsupervised method to detect relevant patterns related to environmental and genetic factors that combined with PLS-DA, a supervised chemometric model, may be helpful in discriminating varieties originating from different regions (D'Urso et al., 2016).

The chromatograms obtained from the LC-MS analyses were evaluated using the free software package MZmine (<http://mzmine.sourceforge.net/>), and the resulting data were processed employing SIMCA-P+ software 12.0 (Umetrics AB, Umea, Sweden). Pareto scaling was applied to all data from the matrix. To define homogeneous clusters of samples, the whole data matrix (20 samples x 343 signals obtained by a pretreatment of raw data with MZmine) was first analyzed by PCA. Score and loading plots of PCA were generated for the entire dataset in order to visualize the clustering of the leaves of the analyzed almond varieties. The known clusters confirmed by PCA were used as Y classes in Partial Least Square Discriminant Analysis. Data were modeled as well by PLS-DA as a supervised approach to visualize clustering relationship.

Analyses were performed in duplicate. All the models were validated by cross-validation techniques and permutation tests according to standardized good practice to minimize false discoveries and to obtain robust statistical models. T^2 of Hotellings and $R^2(x)$ values were used to evidence the robustness of the statistical method.

Total phenolic content

As reported in general experimental procedures.

DPPH• radical scavenging activity

As reported in general experimental procedures.

ABTS^{•+} radical scavenging activity

As reported in general experimental procedures.

NMR analysis

As reported in general experimental procedures.

Statistical analysis

The statistical analysis was performed by several tests. In order to eliminate uncertain data, the Q-Dixon test was performed. All the values in this work were expressed as mean \pm SD. The statistical analysis was performed with one-way ANOVA for repeated measurements. The statistically significant differences were also assessed by applying the paired Student's t-test.

4.7 References

Akhtar, N.; Saleem, M.; Riaz, N.; Ali, M. S.; Yaqoob, A.; Nasim, F.-u.-H.; Jabbar, A. Isolation and characterization of the chemical constituents from *Plumeria rubra*, *Phytochem. Lett.* **2013**, 6, 291-298.

Alipieva, K.; Kokubun, T.; Taskova, R.; Evstatieva, L.; Handjieva, N. LC-ESI-MS analysis of iridoid glucosides in *Lamium* species. *Biochem. Syst. Ecol.* **2006**, 35, 17-22.

Aquino, R.; Morelli, S.; Tomaino, A.; Pellegrino, M.; Saija, A.; Grumetto, L.; Puglia, C.; Ventura, D.; Bonina, F. Antioxidant and photoprotective activity of a

crude extract of *Culcitium reflexum* HBK leaves and their major flavonoids. *J Ethnopharmacol* **2002**, 79, 183-191.

Chen, J. J.; Li, M.; Wu, X. D. High-Throughput Structural Elucidation of Lignans in Flaxseed by High-Performance Liquid Chromatography Coupled with Electrospray Ionization Mass Spectrometry. *Anal Lett* **2014**, 47, 556-567.

Chen, X. Y.; Wang, H.-Q.; Zhang, T.; Liu, C.; Kang, J.; Chen, R.-Y.; Yu, D.-Q. Aromatic Glucosides from the Seeds of *Prunus davidiana*, *J. Nat. Prod.* **2013**, 76, 1528-1534.

Chen, Y.; Yu, H.; Wu, H.; Pan, Y.; Wang, K.; Jin, Y.; Zhang, C. Characterization and Quantification by LC-MS/MS of the Chemical Components of the Heating Products of the Flavonoids Extract in *Pollen Typhae* for Transformation Rule Exploration. *Molecules* **2015**, 20, 18352-18366.

Clifford, M. N.; Johnston, K. L.; Knight, S.; Kuhnert, N. Hierarchical scheme for LC-MS identification of chlorogenic acid. *J. Agr. Food Chem.* **2003**, 51, 2900-2911.

D'Urso, G.; Maldini, M.; Pintore, G.; d'Aquino, L.; Montoro, P.; Pizza, C, Characterisation of *Fragaria vesca* fruit from Italy following a metabolomics approach through integrated mass spectrometry techniques *LWT-Food Sci.Technol.* **2016**, 74, 387-395.

D'Andrea, G.; Quercetin: A flavonol with multifaceted therapeutic applications?, *Fitoterapia.* **2015**, 106, 256-271.

Deep, M. K.; Siddqui, A. A. Isolation and characterization of some pharmaceutical active flavonoids from *Cichorium intybus* plant (Kasini), *J. Ultra Chem.* **2012**, 8, 125-134.

Eklund, P. C.; Backman, M. J.; Kronberg, L. A.; Smeds, A. I.; Sjöholm, R. E. Identification of lignans by liquid chromatography-electrospray ionization ion-trap mass spectrometry. *J. Mass Spec.* **2008**, 43, 97-107.

Fan, P. H.; Marston, A., Hay, A. E., Hostettmann, K. Rapid separation of three glucosylated resveratrol analogues from the invasive plant *Polygonum cuspidatum* by high-speed countercurrent chromatography. *J Sep Sci* **2009**, 32, 2979-2984.

Gao, Q. P.; Ma, R. Y.; Chen, L.; Shi, S. Y.; Cai, P.; Zhang, S. H.; Xiang, H. Y. Antioxidant profiling of vine tea (*Ampelopsis grossedentata*): Off-line coupling heart-cutting HSCCC with HPLC-DAD-QTOF-MS/MS. *Food Chem* **2017**, 225, 55-61.

Ghosh, J.; Sil, P. C. Arjunolic acid: A new multifunctional therapeutic promise of alternative medicine. *Biochimie* **2013**, 95, 1098-1109.

Gleadow, R. M; Woodrow, I. E. Constraints on effectiveness of cyanogenic glycosides in herbivore defense. *J. Chem. Ecol.* **2002**,28, 1301-13.

Groweiss, A.; Cardellina, J. H.; Boyd, M. R. HIV-Inhibitory prenylated xanthenes and flavones from *Maclura tinctoria*. *J Nat Prod* **2000**, 63, 1537-1539.

Hanhineva, K.; Rogachev, I.; Aura, A.; Aharoni, A.; Poutanen, K.; Mykkaˆnen, H. Identification of novel lignans in the whole grain rye bran by non-targeted LC-MS metabolite profiling. *Metabolomics* **2012**, 8, 399-409.

Heim, K. E.; Tagliaferro, A. R.; Bobilya, D. J. Flavonoid antioxidants: chemistry, metabolism and structure-activity relationships. *J Nutr Biochem* **2002**, 13, 572-584.

Hilbert, G.; Tamsamani, H.; Bordenave, L; Pedrot, E.; Chaher, N.; Cluzet, S.; Delaunay, J, C., Ollat, N.; Delrot, S.; Merillon, J. M.; Gomes, E.; Richard, T. Flavonol profiles in berries of wild *Vitis accessions* using liquid chromatography coupled to mass spectrometry and nuclear magnetic resonance spectrometry. *Food Chem* **2015**, 169, 49-58.

Hiroe, K., Shin-Ichi, K.; Naoko, F.; Asuka, A.; Kumi, K.; Yuka, Y.; Takahiko, M.; Nobuji, N. Abscisic Acid Related Compounds and Lignans in Prunes (*Prunus domestica* L.) and Their Oxygen Radical Absorbance Capacity (ORAC). *J. Agric. Food Chem.* **2004**, 52, 344-349.

Hisamoto, M.; Kikuzaki, H.; Nakatani, N. Constituents of the leaves of *Peucedanum japonicum* Thunb. and their biological activity. *J. Agric. Food Chem.* **2004**, *52*, 445-450.

Ieri, F.; Innocenti, M.; Possieri, L.; Gallori, S.; Mulinacci, N. Phenolic composition of “bud extracts” of *Ribes nigrum* L., *Rosa canina* L. and *Tilia tomentosa* M. *J. Pharm. Biomed. Anal.* **2015**, *115*, 1-9.

Iwanaga, A.; Kusano, G.; Warashina, T.; Miyase, T. Phenolic constituents of the aerial parts of *Cimicifuga simplex* and *Cimicifuga japonica*, *J. Nat. Prod.* **2010**, *73*, 609-612.

Jiao, Q. S.; Xu, L. L.; Zhang, J. Y.; Wang, Z. J.; Jiang, Y. Y.; Liu, B. Rapid Characterization and Identification of Non-Diterpenoid Constituents in *Tinospora sinensis* by HPLC-LTQ-Orbitrap MSⁿ. *Molecules* **2018**, *23*.

Jiménez-López, J.; Ruiz-Medina, A.; Ortega-Barrales, P.; ELlorent-Martínez, J. *Rosa rubiginosa* and *Fraxinus oxycarpa* herbal teas: characterization of phytochemical profiles by liquid chromatography-mass spectrometry, and evaluation of antioxidant activity. *New J. Chem.* **2017**, *41*, 7681-7688.

Juanjuan, C.; Min, L.; Xiaodan, W. High-Throughput Structural Elucidation of Lignans in Flaxseed by High-Performance Liquid Chromatography Coupled with Electrospray Ionization Mass Spectrometry. *Analytical Letters.* **2014**, *47*, 556–567.

Kapusta, I.; Janda, B.; Szajwaj, B.; Stochmal, A.; Piacente, S.; Pizza, C.; Franceschi, F.; Franz, C.; Oleszek, W. Flavonoids in horse chestnut (*Aesculus hippocastanum*) seeds and powdered waste water by-products. *J Agr Food Chem* **2007**, *55*, 8485-8490.

Kazuma, K.; Noda, N.; Suzuki, M. Malonylated flavonol glycosides from the petals of *Clitoria ternatea*, *Phytochem.* **2003**, *62*, 229-237.

Kim, S. K.; Kim, H. J.; Choi, S. E.; Park, K. H.; Choi, H. K.; Lee, M. W. Antioxidative and inhibitory activities on nitric oxide (NO) and prostaglandin E2

(COX-2) production of flavonoids from seeds of *Prunus tomentosa* Thunberg, *Arch. Pharmacol Res.* **2008**, 31, 424-428.

Kim, Y. H.; Yang, H. E.; Park, B. K.; Heo, M. Y.; Jo, B. K.; Kim, H. P. The extract of the flowers of *Prunus persica*, a new cosmetic ingredient, protects against solar ultraviolet-induced skin damage in vivo. *J. Cosmet. Sci.* **2002**, 53, 27-34.

Kirmizibekmez, H.; Bassarello, C.; Piacente, S.; Calis, I. Phenylethyl glycosides from *Globularia alypum* growing in Turkey. *Helv Chim Acta* **2008**, 91, 1525-1532.

Kris, M.; Hoon, K.; Fachuang, L.; Oana, D.; Takuya, A.; Ruben, V.; Claudiu, N.; Geert, G.; Dirk, I.; Eric, M.; Ralph, J.; Wout, B. Mass Spectrometry-Based Fragmentation as an Identification Tool in Lignomics. *Anal. Chem.* **2010**, 82, 8095–8105.

Kumar, K.; Yadav, A. N.; Kumar, V.; et al. Food waste: a potential bioresource for extraction of nutraceuticals and bioactive compounds. *Bioresour. Bioprocess.* **2017**, 4, 18.

Lima, E.; de Sousa Filho, P. T.; Bastida, J.; Schmeda-Hirschmann, G. Saponins from *Cariniana rubra* (Lecytidaceae), *Bol. Soc. Chil. Quím.* **2002**, 47.

Liu, Q.; Huang, X.; Bai, M.; Chang, X.; Yan, X.; Zhu, T.; Zhao, W.; Peng, Y.; Song, S. Antioxidant and antiinflammatory active dihydrobenzofuran neolignans from the seeds of *Prunus tomentosa* *J. Agric. Food Chem.* **2014**, 62, 7796–7803.

Luis, J.; Rosa, R.; Giner, M.; Prieto, M. New findings on the bioactivity of lignans. *Studies Nat. Prod. Chem.* **2002**, 26, 183-292

Mann, A.; Ibrahim, K.; Oyewale, A. O.; Amupitan, J. O.; Fatope, M. O.; Okogun, J. I. Isolation and elucidation of three triterpenoids and its antimycobacterial activity of *Terminalia avicennioides*. *Am. J. Org. Chem.* **2012**, 2, 14-20.

Mari, A.; Napolitano, A.; Masullo, M.; Pizza, C.; Piacente, S. Identification and quantitative determination of the polar constituents in *Helichrysum italicum* flowers and derived food supplements. *J. Pharm. Biomed. Anal.* **2014**, 96, 249-255.

Masullo, M.; Montoro, P.; Autore, G.; Marzocco, S.; Pizza, C.; Piacente, S. Quail-quantitative determination of triterpenic acids of *Ziziphus jujuba* fruits and evaluation of their capability to interfere in macrophages activation inhibiting NO release and iNOS expression. *Food Res Int* **2015**, *77*, 109-117.

Miyase, T.; Ueno, A.; Takizawa, N.; Kobayashi, H.; Oguchi, H. Studies on the glycosides of *Epimedium grandiflorum* Morr. var. *thunbergianum* (Miq.) Nakai. II. *Chem. Pharm. Bull.* **1987**, *35*, 3713-3719.

¹Morreel, K.; Kim, H.; Lu, F.; Dima, O.; Akiyama, T.; et al. Mass spectrometry-based fragmentation as an identification tool in lignomics. *Anal. Chem.* **2010**, *82*, 8095-8015.

²Morreel, K.; Dima, O.; Kim, H.; Lu, F.; Niculaes, C.; Vanholme, R.; Dauwe, R.; Goeminne, G.; Inze, D.; Messens, E.; Ralph, J.; Boerjan, W. Mass Spectrometry-Based Sequencing of Lignin Oligomers. *Plant Physiology.* **2010**, *153*, 1464–1478.

Murata, T.; Miyase, T.; Yoshizaki, F. New phenolic compounds from *Meehanian urticifolia*, *J. Nat. Med.* **2011**, *65*, 385-390.

Nascimento, A. M.; Maria-Ferreira, D.; Dal Lin, F. T.; Kimura, A.; de Santana-Filho, A. P.; Werner, M. F. d. P.; Iacomini, M.; Sasaki, G. L.; Cipriani, T. R.; de Souza, L. M. Phytochemical analysis and antiinflammatory evaluation of compounds from an aqueous extract of *Croton cajucara* Benth, *J. Pharm. Biomed. Anal.* **2017**, *145*, 821-830.

Nguyen Ngoc, H.; Nghiem, D. T.; Pham, T. L. G.; Stuppner, H.; Ganzera, M. Phytochemical and analytical characterization of constituents in *Urceola rosea* (Hook. & Arn.) D.J. Middleton leaves. *J. Pharm. Biomed. Anal.* **2018**, *149*, 66-69.

Oshimi, S.; Zaima, K.; Matsuno, Y.; Hirasawa, Y.; Iizuka, T., Studiawan, H.; Indrayanto, G.; Zaini, N. C.; Morita, H. Studies on the constituents from the fruits of *Phaleria macrocarpa*. *J. Nat. Med.* **2008**, *62*, 207-210.

Otsuka, H.; Hirata, E.; Shinzato, T.; Takeda, Y. Stereochemistry of megastigmane glucosides from *Glochidion zeylanicum* and *Alangium premnifolium*, *Phytochem.* **2003**, 62, 763-768.

Qingfeng, M. S.; Liua, Z. J.; Yi, L.; Zhongdong, L.; Xiaojin, S.; Wenjian, W.; Bin, W.; Mingkang, Z. Chemical profiling of San-Huang decoction by UPLC–ESI-Q-TOF-MS. *J. Pharm. Biomed. Anal.* **2016**, 131, 20–32.

Rubilar, M.; Pinelo, M.; Shene, C.; Sineiro, J.; José Nuñez, M. Separation and HPLC-MS Identification of Phenolic Antioxidants from Agricultural Residues: Almond Hulls and Grape Pomace. *J. Agric. Food Chem.* **2007**, 55, 10101–10109.

Sang, S. M.; Lapsley, K.; Rosen, R. T.; Ho, C. T. New prenylated benzoic acid and other constituents from almond hulls (*Prunus amygdalus* Batsch). *J Agr Food Chem* **2002**, 50, 607-609.

Santos Pimenta, L. P.; Schilthuizen, M.; Verpoorte, R.; Choi, Y. H. Quantitative analysis of amygdalin and prunasin in *Prunus serotina* Ehrh. using ¹H-NMR spectroscopy, *Phytochem. Anal.* **2014**, 25, 122-126.

Sendker, J.; Ellendorff, T.; Hoelzenbein, A. Occurrence of benzoic acid esters as putative catabolites of prunasin in senescent leaves of *Prunus laurocerasus*. *J. Nat. Prod.* **2016**, 79, 1724-1729.

Sidana, J.; Neeradi, D.; Choudhary, A.; Singh, S.; Foley, W. J.; Singh I. P. Antileishmanial polyphenols from *Corymbia maculata*. *J. Chem. Sci.* **2013**, 125, 765-775.

Song, Z.; Xu, X. Advanced research on antitumor effects of amygdalin. *J. Cancer Res. Ther.* **2014**, 10, 3-7.

Tamura, Y.; Nakajima, K.; Nagayasu, K.; Takabayashi, C. Flavonoid 5-glucosides from the cocoon shell of the silkworm. *Bombyx mori*. *Phytochemistry* **2002**, 59, 275-278.

Tang, G.; Zhao, C., Liu, Q.; Feng, X.; Xu, X.; Cao, S.; Meng, X.; Li, S.; Gan, R.; Li, H. Potential of grape wastes as a natural source of bioactive compounds. *Molecules*. **2018**, *23*, 2598.

Tomas, F. Isolation and identification of quercetin-3-galactoside in the *Prunus amygdalus* leaf, *Rev. Agroquim. Tecnol. Aliment.* **1977**, *17*, 281-284.

Wang, L.; Liu, S.; Zhang, X.; Xing, J.; Liu, Z.; Song, F. A strategy for identification and structural characterization of compounds from *Gardenia jasminoides* by integrating macroporous resin column chromatography and liquid chromatography-tandem mass spectrometry combined with ion-mobility spectrometry. *J. Chrom. A* **2016**, *1452*, 47-57.

Wang, S.; Liu, L.; Wang, L.; Hu, Y.; Zhang, W.; Liu, R. Structural characterization and identification of major constituents in Jitai tablets by high-performance liquid chromatography/diode-array detection coupled with electrospray ionization tandem mass spectrometry. *Molecules* **2012**, *17*, 10470-10493.

Wang, Y.; Zhu, H.; Wang, D.; Cheng, R.; Yang, C.; Xu, M.; Zhang, Y. A new phloroglucinol glucoside from the whole plants of *Glochidion eriocarpum*. *Bull. Korean Chem. Soc.* **2014**, *35*, 631-634.

Weckerle, B.; Gati, T.; Toth, G.; Schreier, P. 3-Methylbutanoyl and 3-methylbut-2-enoyl disaccharides from green coffee beans (*Coffea arabica*). *Phytochemistry* **2002**, *60*, 409-414.

Wei, X. H.; Yang, S. J.; Liang, N.; Hu, D. Y.; Jin, L. H.; Xue, W.; Yang, S. Chemical Constituents of *Caesalpinia decapetala* (Roth) Alston. *Molecules* **2013**, *18*, 1325-1336.

Wu, H.; Hu, X.; Zhang, X.; Chen, S.; Yang, J.; Xu, X. Isolation and chemotaxonomic significance of megastigmane-type sesquiterpenoids from *Sarcandra glabra*. *J. Med. Plant Res.* **2012**, *6*, 4501-4504.

Xu, Y. J.; Chiang, P. Y.; Lai, Y. H.; Vittal, J. J.; Wu, X. H.; Tan, B. K. H.; Imiyabir, Z.; Goh, S. H. Cytotoxic prenylated depsidones from *Garcinia parvifolia*. *J Nat Prod* **2000**, 63, 1361-1363.

Xu, Y.; Cai, H.; Cao, G.; Duan, Y.; Pei, K.; Tu, S.; Zhou, J.; Xie, L.; et al. Profiling and analysis of multiple constituents in Baizhu Shaoyao San before and after processing by stir-frying using UHPLC/Q-TOF-MS/MS coupled with multivariate statistical analysis. *J. Chrom. B: Anal. Tech Biomed. Sci.* **2018**, 1083, 110-123.

Yoshikawa, M.; Murakami, T.; Ishiwada, T.; Morikawa, T.; Kagawa, M., Higashi, Y.; Matsuda, H. New flavonol oligoglycosides and polyacylated sucroses with inhibitory effects on aldose reductase and platelet aggregation from the flowers of *Prunus mume*. *J Nat Prod* **2002**, 65, 1151-1155.

Zhang, J.; Xu, X.; Xu, W.; Da-yuan, J. H.; Xiao-Hui. Z. Rapid Characterization and Identification of Flavonoids in *Radix Astragali* by Ultra-High-Pressure Liquid Chromatography Coupled with Linear Ion Trap-Orbitrap Mass Spectrometry. *J. Chrom. Sci.* **2015**, 53, 945–952.

Chapter 5
**Polar constituents, multi-class polar lipids and free
fatty acids profiling of pistachios (*Pistacia vera* cv.
Napoletana) by
LC-ESI/HRMS/MS and GC-FID**

5.1 Introduction

Pistachio (*P. vera* L.) is one of the most requested nuts on world market. Usually it is consumed roasted and salted, occasionally fresh; however, due to recent culinary trends, pistachios have been more often employed in cookery for the preparation of innovative recipes, following the “nouvelle cuisine” claims. Therefore, ingredients with specific organoleptic features, as shape, color, taste and fragrance are more and more yearned. Among such sophisticated ingredients, the Italian PDO “Pistacchio di Bronte” was widely counted. Peculiar characteristics of this pistachio variety are the intense green color and the enveloping violet/purple integument, along with its intense taste and flavour.

The nutritional features have been since long assessed, also for other varieties, as well as the fatty acid composition (Hernandez-Alonso et al., 2016). Nevertheless, little is known about the polar constituents, due to a lack of exhaustive information in scientific literature, and so for the main non-fatty acids non-polar constituents, for which even less has been reported.

For these reasons, a phytochemical investigation was carried out on both polar and non-polar fractions of *P. vera* cv. Napoletana seeds, aiming at achieving a complete overview on the metabolite profile of the most appreciated Italian pistachio variety.

In this chapter the following topics will be discussed:

- LC-ESI/LTQOrbitrap/MS/MS metabolite profiling of *P. vera* seeds, focusing on the polar fraction;
- comparison of “eco-friendly” extracts by LC-ESI/LTQOrbitrap/MS experiments;
- evaluation of total phenolic content and radical scavenging activity of the prepared extracts;
- quantitative analysis of the main compounds of interest;

- LC-ESI/QToF/MS/MS metabolite profiling of the non-polar fraction of *P. vera* seeds;
- GC-FID quali-quantitative analysis of the oily fraction.

5.2 LC-ESI/HRMS/MS analysis of the polar fraction of *P. vera* cv. Neapolitana seeds

Pistacia vera L. seeds



The seeds show an intense green color, and are enveloped by a thin integument usually violet. They are characterized by a distinctive flavor, and represent one of the most requested nuts on the market.

5.2.1 Results and discussion

5.2.1.1 LC-ESI/HRMS/MS profiling of pistachios

Aiming at defining the metabolite profile of the polar fraction of *P. vera* seeds, the MeOH extract was submitted to LC-ESI/LTQOrbitrap/MS/MS experiments, in negative ion mode. The LC-HRMS profile (Fig. 5.1) showed several peaks with m/z values ascribable to phenolic compounds. In particular, they could be grouped as gallic acid derivatives (1, 3, 5, 10, 13, 17), catechins (2, 6, 7, 9), proanthocyanidins (4), flavonoids (11, 12, 14-16, 18-20, 22, 23), neolignans (21), and anacardic acids (24-26) (Table 5.1).

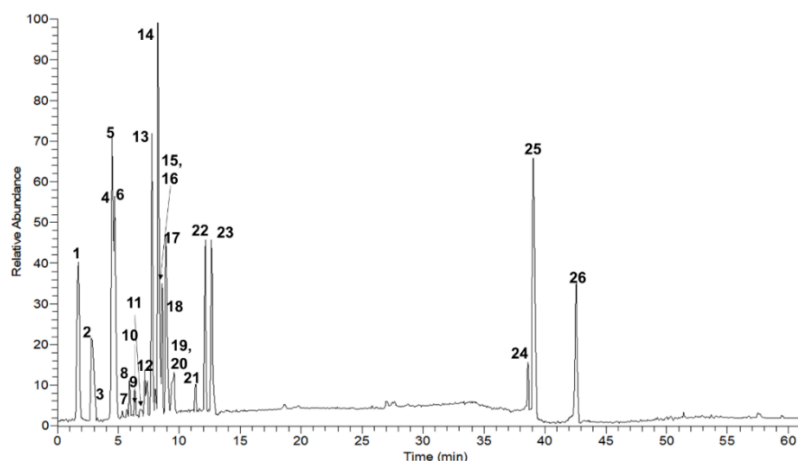


Figure 5.1 LC-HRMS profile in negative ion mode of the MeOH extract of *P. vera* seeds

Table 5.1 Compounds identified and putatively identified in *P. vera* seeds

N°	R _t	Calculated Mass	[M-H] ⁻	Δppm	MS ² (%)	Molecular formula	Compound
1	1.76	170.0215	169.0140	-0.84	125(100)	C ₇ H ₆ O ₅	gallic acid ¹
2	2.84	306.0739	305.0659	1.24	261(49), 221(87), 219(76), 179(100), 165(35), 125(24)	C ₁₅ H ₁₄ O ₇	(epi)gallocatechin
3	3.19	154.0266	153.0187	1.02	109(100)	C ₇ H ₆ O ₄	protocatechuic acid ¹
4	4.32	578.1424	577.1339	-0.57	451(29), 425(100), 407(49), 289(27), 287(26)	C ₃₀ H ₂₆ O ₁₂	EC-EC
5	4.37	184.0371	183.0293	0.69	168(98), 124(100)	C ₈ H ₈ O ₅	methyl gallate ¹
6	4.52	290.0790	289.0709	-1.36	245(100), 205(44), 179(26)	C ₁₅ H ₁₄ O ₆	(+)-catechin ¹
7	5.48	290.0790	289.0712	0.84	245(100), 205(44), 179(26)	C ₁₅ H ₁₄ O ₆	(-)-epicatechin ¹
8	5.70	450.1162	449.1076	0.62	287(100), 269(42), 259(49)	C ₂₁ H ₂₂ O ₁₁	eriodictyol hexoside
9	6.10	458.0849	457.0764	0.74	331(38), 305(100), 169(57)	C ₂₂ H ₁₈ O ₁₁	(epi)gallocatechin gallate
10	6.58	198.0528	197.0450	0.96	169(100)	C ₉ H ₁₀ O ₅	ethyl gallate ¹
11	6.99	480.0903	479.0820	-1.22	316(100), 317(54)	C ₂₁ H ₂₀ O ₁₃	myricetin 3- <i>O</i> -β-D-glucopyranoside ¹
12	7.53	450.1162	449.1077	-0.43	343(12), 287(100)	C ₂₁ H ₂₂ O ₁₁	aromadendrin hexoside
13	7.75	788.1072	787.0984	1.58	617(100), 393(27)	C ₃₄ H ₂₈ O ₂₂	1,2,3,6-tetra- <i>O</i> -galloyl-β-D-glucopyranoside ¹
14	7.82	464.0954	463.0869	1.07	301(100), 300(62)	C ₂₁ H ₂₀ O ₁₂	quercetin 3- <i>O</i> -β-D-glucopyranoside ¹
15	8.04	448.1005	447.0917	0.71	285(100)	C ₂₁ H ₂₀ O ₁₁	kaempferol 3- <i>O</i> -β-D-galactopyranoside ¹
16	8.35	450.1162	449.1073	-0.66	343(16), 287(100)	C ₂₁ H ₂₂ O ₁₁	aromadendrin hexoside
17	8.66	940.1181	939.1091	1.69	769(93), 617(21), 393(100), 169(35)	C ₄₁ H ₃₂ O ₂₆	1,2,3,4,6-penta- <i>O</i> -galloyl-β-D-glucopyranoside ¹
18	8.87	434.1213	433.1130	1.42	271(100)	C ₂₁ H ₂₂ O ₁₀	naringenin hexoside
19	9.14	432.1056	431.0972	-1.00	371(48), 341(62), 311(39), 269(100)	C ₂₁ H ₂₀ O ₁₀	vitexin
20	9.34	448.1005	447.0920	0.56	285(100)	C ₂₁ H ₂₀ O ₁₁	kaempferol 3- <i>O</i> -β-D-glucopyranoside ¹
21	11.09	586.2414	585.2325	0.80	567(4), 537(100), 371(29), 359(22), 195(3)	C ₃₁ H ₃₈ O ₁₁	acernikol
22	11.85	288.0633	287.0552	1.44	151(100)	C ₁₅ H ₁₂ O ₆	eriodictyol
23	12.34	286.0477	285.0395	-0.99	243(58), 241(100), 217(62), 199(91), 175(77), 151(34)	C ₁₅ H ₁₀ O ₆	luteolin ¹
24	38.65	320.2351	319.2285	1.31	275(100), 106(29)	C ₂₀ H ₃₂ O ₃	(13:0)-anacardic acid ¹
25	39.18	346.2507	345.2427	1.87	301(100), 106(14)	C ₂₂ H ₃₄ O ₃	(15:1)-anacardic acid ¹
26	42.71	374.2820	373.2739	1.11	329(100), 106(19)	C ₂₄ H ₃₈ O ₃	(17:1)-anacardic acid ¹

¹The identification of this compound was corroborated by comparison with standard solution. EC = (epi)catechin

Some of the detected compounds were identified by comparing the experimental R_t observed in the LC-MS profile with standard solutions analyzed in the same

experimental conditions. Most of the standards used were isolated from *P. vera* leaves and husks. This identification approach allowed to unambiguously attribute the following constituents: gallic acid (**1**), protocatechuic acid (**3**), methyl gallate (**5**), (+)-catechin (**6**), (-)-epicatechin (**7**), ethyl gallate (**10**), myricetin 3-*O*- β -D-glucopyranoside (**11**), 1,2,3,6-tetra-*O*-galloyl- β -D-glucopyranoside (**13**), quercetin 3-*O*- β -D-glucopyranoside (**14**), kaempferol 3-*O*- β -D-galactopyranoside (**15**), 1,2,3,4,6-penta-*O*-galloyl- β -D-glucopyranoside (**17**), kaempferol 3-*O*- β -D-glucopyranoside (**20**), luteolin (**23**), (13:0)-anacardic acid (**24**), (15:1)-anacardic acid (**25**) and (17:1)-anacardic acid (**26**).

For the other constituents, they were putatively identified by accurate m/z values determination, along with the interpretation of their fragmentation patterns, and comparing the obtained information with data reported in scientific literature, online databases (KnapSack, FoodB, PubChem, ChemSpider, KEGG) and by incorporating the fragmentation spectra in online database-assisted prediction tools (MetFrag). To acquire the MS/MS spectra, during the LC-ESI/LTQOrbitrap/MS/MS experiments, “data dependent scan” mode was employed, allowing the MS software to select the precursor ion as the most intense peak in the LC-MS spectrum.

Compound **2** (m/z 305.0659) showed in the MS/MS experiments (Fig. 5.2) a base peak at m/z 179, originating from the loss of a trihydroxyphenyl moiety, a product ion at m/z 261 generated from the loss of an acetaldehyde molecule (- 44 Da), along with a diagnostic ion at m/z 125 due to a Heteronuclear Ring Fission (HRF) occurring on the C-ring as well. Moreover, the product ion at m/z 221 was likely corresponding to the neutral loss of a 1,3-cyclobutadien-1,3-diol as a consequence of a ring size reduction rearrangement occurring at the C-ring. Molecular formula was established as C₁₅H₁₄O₇. The achieved information, together with data reported in literature, allowed to assess compound **2** as (epi)galocatechin (Callemien et al., 2008) (Table 5.1).

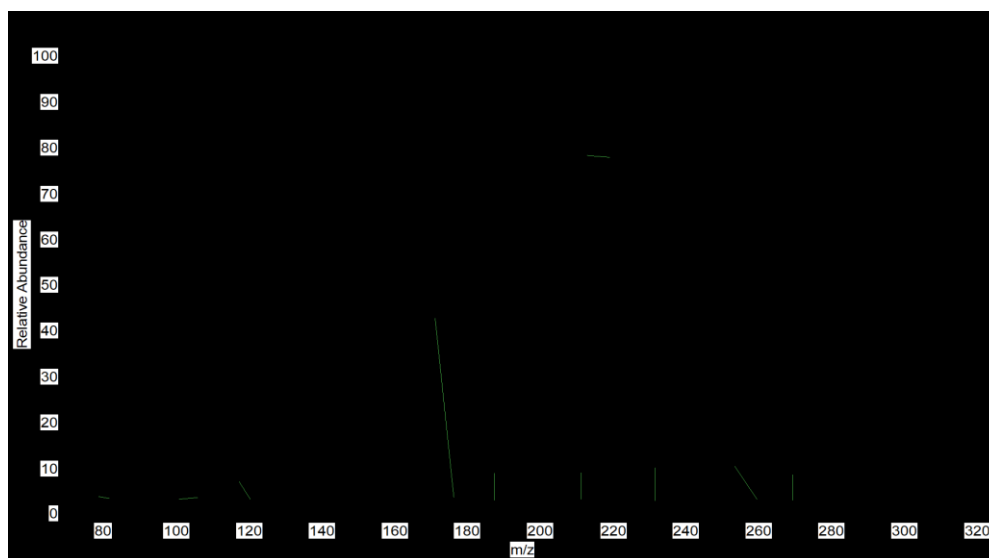


Figure 5.2 ESI/MS/MS spectrum of compound **2** in negative ion mode

Compound **4** (m/z 577.1339) exhibited in the fragmentation spectrum a base peak at m/z 425 originated by a Retro Diels-Alder (RDA) reaction occurring on the C-ring, while a HRF reaction yielded the product ion at m/z 451; in addition, two informative signals were observed at m/z 289 and 287, suggesting the occurrence of two (epi)catechin moieties bonded by a B-type linkage. According to the achieved structural information, matched with online databases (FoodB) and scientific literature, compound **4** was putatively identified as B-type (epi)catechin dimer (Lin et al., 2014) (Table 5.1).

Compound **9** (m/z 457.0764) yielded a MS/MS spectrum (Fig. 5.3) exhibiting a base peak at m/z 305, originating from the neutral loss of a dehydrated gallic acid (-152 Da), whose presence was confirmed by the signal at m/z 169, while the loss of the B-ring produced the fragment ion at m/z 331. Molecular formula was established as $C_{22}H_{18}O_{11}$. Similarities observed with the fragmentation pathway of compound **2** and comparison with online databases (FoodB) allowed to putatively identify compound **9** as (epi)gallocatechin gallate (Table 5.1).

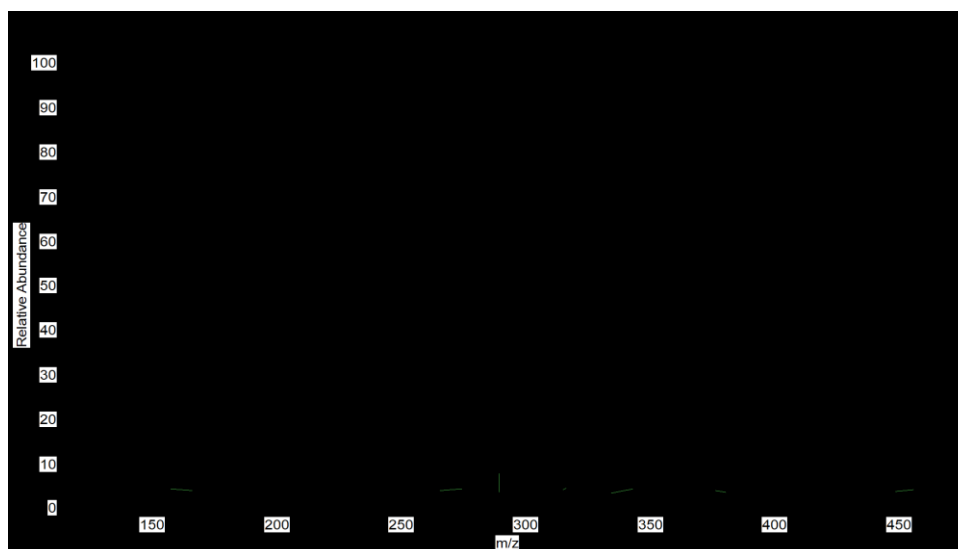


Figure 5.3 ESI/MS/MS spectrum of compound **9** in negative ion mode

Compounds **8**, **12**, **16** and **18**, showing in HRMS pseudomolecular ions $[M-H]^-$ at m/z 449.1076, 449.1077, 449.1073 and 433.1130, respectively, exhibited a common behaviour in tandem mass experiments, producing a base peak originated from the neutral loss of a hexose moiety (-162 Da). For compound **8** a product ion at m/z 269 was observed, generated by a $^{0,4}A$ fission occurring at the C-ring, while compounds **12** and **16** showed a fragment ion at m/z 343 generated from a $^{1,2}A$ fission occurring at the C-ring. The structural information provided by the MS/MS spectra, together with the accurate m/z values and comparison with online databases (FoodB) allowed to putatively identify the analyzed compounds as eriodictyol hexoside (**8**), aromadendrin hexoside (**12**), aromadendrin hexoside (isomer) (**16**) and naringenin hexoside (**18**) (Table 5.1).

Compound **19** (m/z 431.0972) showed a characteristic fragmentation pattern of a C-glycoside flavonoid, featured by neutral losses of 60, 90 and 120 Da, due to cleavages $^{0,4}A$, $^{0,3}A$ and $^{0,2}A$, respectively, occurring at the sugar ring, and a signal at m/z 269, corresponding to the deprotonated aglycone. Molecular formula was established as $C_{21}H_{20}O_{10}$. According to the structural information achieved, and

supported by data reported in scientific literature, compound **19** was putatively identified as vitexin (Belguith-Hadrichea et al., 2017) (Table 5.1).

Furthermore, the fragmentation spectrum of compound **22** was characterized by the single base peak at m/z 151, originated from the $^{1,3}A$ cleavage occurring at the C-ring. Along with the accurate m/z value, determined in HRMS as 287.0552 ($C_{15}H_{12}O_6$), and matching with online databases (FoodB), compound **22** was putatively assessed as eriodictyol (Table 5.1).

Finally, compound **21** (m/z 585.2325) showed a totally different behaviour in tandem mass experiments: the fragmentation pattern exhibited neutral losses of 18 (water) and 48 (water + formaldehyde) Da originating ions at m/z 567 and 537, respectively, which further exhibited a neutral loss of 196 Da, corresponding to a dehydrated guaiacylglycerol moiety. Molecular formula was established as $C_{31}H_{38}O_{11}$. A successive comparison with scientific reports and free databases allowed to putatively identify compound **21** as acernikol (Li et al., 2010) (Table 5.1).

Some of the above described constituents (**1**, **6**, **7**, **22**, **23**), have been identified in *P. vera* cv. Napoletana seeds representing the “Pistacchio di Bronte”, by comparison with standard solutions employing a HPLC-UV/Vis device (Tomaino et al., 2010). In addition, seeds and skins were used to produce extracts showing *in vitro* good antioxidant and photoprotective properties (Martorana et al., 2013).

The cited reports, together with the results achieved from the present phytochemical investigation, highlighted the occurrence of antioxidant phenolics, claiming the benefits that pistachio consumption may exert on human health (Terzo et al., 2017).

5.2.1.2 “Eco-friendly” extractions

In order to propose simple and quick extraction protocols, employing “green” solvents suitable with human consumption, *P. vera* seeds were extracted by maceration using EtOH 96% and an EtOH:H₂O (1:1, v/v) solution. The obtained

extracts were successively submitted to LC-ESI/LTQOrbitrap/MS experiments, followed by a comparison of the yielded profiles (Fig. 5.4).

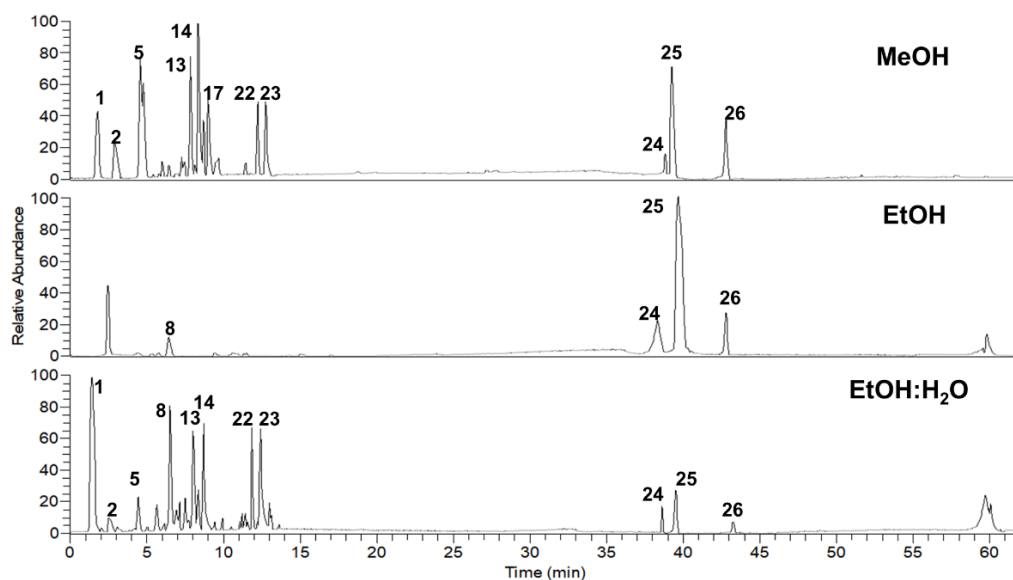


Figure 5.4 LC-HRMS profiles of the MeOH, EtOH and EtOH:H₂O extracts of *P. vera* seeds

The matching of the LC-MS profiles pointed out the efficacy and high selectivity of EtOH in extracting mainly anacardic acids, also detected in the EtOH:H₂O extract, but as minor constituents, since the hydroalcoholic solution proved to be more effective in extracting compounds possessing higher polarity, like flavonoids and gallic acid derivatives.

5.2.1.3 Total phenolic content and radical scavenging activity

The extracts prepared from *P. vera* seeds were tested in order to assess the phenolic content, as well as the radical scavenging activity (Table 5.2).

The Folin-Ciocalteu assay results pointed out the highest phenolic content of the MeOH extract if compared to the “eco-friendly” extracts, also exerting the strongest antioxidant activity; for the EtOH extract no considerable results were observed.

Table 5.2 Total phenolic content, DPPH• and ABTS^{•+} radical scavenging activity of the extracts of *P. vera* seeds

Sample	Total phenolic content		DPPH•		ABTS ^{•+}	
	GAE ^a	SD ^d	IC ₅₀ ^b	SD ^d	TEAC ^c	SD ^d
Seeds MeOH	163.09	± 15.41	74.7	± 8.47	0.63	± 0.09
Seeds EtOH	33.65	± 3.68	N/A	± -	N/A	± -
Seeds EtOH/H ₂ O	104.39	± 11.28	83.47	± 7.61	0.50	± 0.07
Vit. C			5.16	± 0.11		
Quercetin					1.87	± 0.08

^a Values are expressed as gallic acid equivalents (GAE) mg/g of dried extract. ^b Values are expressed as µg/mL. ^c Values are expressed as concentration (mM) of a standard Trolox solution exerting the same antioxidant activity of a 1 mg/mL solution of the tested extract. ^d Standard Deviation of three independent experiments.

5.2.1.4 Quantification of anacardic acids by Multiple Reaction Monitoring (MRM) approach

To quantify the anacardic acids detected in the LC-MS profiles of the extracts of *P. vera* seeds (Fig. 5.4), LC-ESI/QTrap/MS/MS experiments were carried out by a MRM approach, as successively described in paragraph 6.5.

The obtained results (Table 5.3) evidenced (15:1)-anacardic acid (**26**) as the most abundant, although, if compared to the other parts of *P. vera*, the seeds showed a sensibly lower concentration of anacardic acids.

Table 5.3 Concentrations (µg/mg of dried extract) of main anacardic acids identified in the different extracts of *P. vera* seeds.

	AA (13:0)	SD*	AA (15:1)	SD*	AA (17:1)	SD*
MeOH	0.16	± 0.01	0.55	± 0.03	0.29	± 0.03
EtOH	<LoQ	-	0.85	± 0.05	0.35	± 0.04
EtOH:H ₂ O	0.15	± 0.01	0.38	± 0.03	0.17	± 0.01

AA = Anacardic Acid; Results expressed as mean of three independent experiments. *Standard Deviation of three independent experiments.

5.3 LC-ESI/QToF/MS/MS multi-class polar lipids profiling of *P. vera* seeds

5.3.1 Results and discussion

5.3.1.1 LC-ESI/QToF/MS/MS analysis of the polar lipids of “Pistacchio di Bronte”

To assess the main polar lipids occurring in *P. vera* seeds, pistachios were extracted and submitted to LC-ESI/QToF/MS/MS experiments as described in paragraph 3.3.1.3.

As result, different classes of phospholipids were detected, varying for their polar head group, as well as for the number of fatty acyl side chains, characterized by various length and unsaturation degree, along with diacylglycerols and triacylglycerols.

Identification of the detected compounds was carried out by determination of the accurate m/z values, together with an exhaustive analysis of their MS/MS spectra acquired by tandem mass experiments. In addition, fragmentation spectra were incorporated in online database-assisted prediction tools (MetFrag), and the achieved information further compared with scientific literature and online databases (FoodB, Lipid Maps) (Song et al., 2018; Holčapek et al., 2003).

5.3.1.2 Phospholipids identification

Analysis and interpretation of the MS/MS spectra, acquired by performing tandem mass spectrometry experiments in positive and negative ion mode, was carried out according to observations described in paragraph 3.3.1.4.

As result, the occurrence of 22 phospholipids (3 1-PCs, 9 PCs, 3 PEs, 5 PIs, 2 PGs) was pointed out (Table 5.4). The identified compounds have been reported in Chinese pistachios (Song et al., 2018), while no data were found for Italian

varieties, suggesting a persistent lack of information about the polar lipids composition of *P. vera* seeds.

The achieved results may contribute to extend the knowledge about the metabolite profile of the “Pistacchio di Bronte”, highlighting the occurrence of non-polar constituents reported for their capacity to reduce cholesterol levels in plasma, as well as for their neuroprotective effects (Keller et al., 2013; Nagai, K., 2012)

Table 5.4 Phospholipids putatively identified in Italian *P. vera* seeds

N°	Compound	R _t	m/z	Ion	Ion Mode	Molecular Formula	MS/MS
27	LPC(18:2)	4.1	520.3357	[M+H] ⁺	+	C ₂₆ H ₅₀ NO ₇ P	337, 184
28	LPC(16:0)	5.0	520.3357	[M+H] ⁺	+	C ₂₆ H ₅₀ NO ₇ P	313, 184
29	LPC(18:1)	5.2	522.3554	[M+H] ⁺	+	C ₂₆ H ₅₂ NO ₇ P	339, 184
30	PC(16:0/16:0)	10,2	730.5351	[M+H] ⁺	+	C ₄₀ H ₈₀ NO ₈ P	551, 313, 184
31	PC(16:0/18:1)	12,6	760.5864	[M+H] ⁺	+	C ₄₂ H ₈₂ NO ₈ P	577, 339, 313, 184
32	PC(16:0/18:2)	11,6	758.5686	[M+H] ⁺	+	C ₄₂ H ₈₀ NO ₈ P	575, 337, 313, 184
33	PC(16:1/18:2)	10,2	756.5535	[M+H] ⁺	+	C ₄₂ H ₇₈ NO ₈ P	573, 337, 311, 184
34	PC(18:0/18:1)	14,2	788.6166	[M+H] ⁺	+	C ₄₄ H ₈₆ NO ₈ P	605, 341, 339, 184
35	PC(18:0/18:2)	13,8	786.5995	[M+H] ⁺	+	C ₄₄ H ₈₄ NO ₈ P	603, 341, 337, 184
36	PC(18:1/18:1)	12,6	786.6025	[M+H] ⁺	+	C ₄₄ H ₈₄ NO ₈ P	603, 339, 184
37	PC(18:1/18:2)	11,6	784.5848	[M+H] ⁺	+	C ₄₄ H ₈₂ NO ₈ P	601, 339, 337, 184
38	PC(18:2/18:2)	10,7	782.5693	[M+H] ⁺	+	C ₄₄ H ₈₀ NO ₈ P	599, 337, 184
39	PE(16:0/18:2)	10.4	716.5205	[M+H] ⁺	+	C ₃₉ H ₇₄ NO ₈ P	575, 337, 313
40	PE(18:1/18:2)	10.7	742.5342	[M+H] ⁺	+	C ₄₁ H ₇₆ NO ₈ P	601, 339, 337
41	PE(18:2/18:2)	11.2	740.5169	[M+H] ⁺	+	C ₄₁ H ₇₄ NO ₈ P	599, 337
42	PI(16:0/18:1)	5.8	835.5363	[M-H] ⁻	-	C ₄₃ H ₈₁ O ₁₃ P	281, 255, 241, 153
43	PI(16:0/18:2)	5.3	833.5218	[M-H] ⁻	-	C ₄₃ H ₇₉ O ₁₃ P	279, 255, 241, 153
44	PI(18:0/18:1)	6.0	863.5653	[M-H] ⁻	-	C ₄₅ H ₈₅ O ₁₃ P	283, 281, 241, 153
45	PI(18:0/18:2)	5.6	861.5498	[M-H] ⁻	-	C ₄₅ H ₈₃ O ₁₃ P	283, 279, 241, 153
46	PI(18:0/18:3)	5.3	859.5359	[M-H] ⁻	-	C ₄₅ H ₈₁ O ₁₃ P	283, 277, 241, 153
47	PG(16:0/18:1)	6.0	747.5194	[M-H] ⁻	-	C ₄₀ H ₇₇ O ₁₀ P	673, 281, 255, 171
48	PG(16:0/18:2)	5.8	745.5038	[M-H] ⁻	-	C ₄₀ H ₇₅ O ₁₀ P	671, 279, 255, 171

LPC = lysophosphatidylcholine, PC = phosphatidylcholine, PE = phosphatidylethanolamine, PI = phosphatidylinositol, PG = phosphatidylglycerol,

5.3.1.3 Diacylglycerols and triacylglycerols identification

Along with phospholipids, diacylglycerols and triacylglycerols were detected. The identity assignment was carried out as previously described in paragraph 3.3.1.5.

As result, five diacylglycerols and two triacylglycerols were identified in *P. vera* seeds (Table 5.5). Also in this case a triacylglycerol derivative (**54**) with a side chain possessing an odd number of carbons was detected.

Aside from their primary function as energy storage, triacylglycerols and diacylglycerols showed to play an important role in metabolic pathways at epidermal levels, mainly affecting the permeability barrier function of skin (Radner & Fischer, 2014).

Table 5.5 Glycerides putatively identified in *P. vera* seeds

N°	Compound	R _t	m/z	Ion	Ion Mode	Molecular Formula	MS/MS
49	DG(16:0/18:1)	13,3	612.5576	[M+NH ₄] ⁺	+	C ₃₇ H ₇₀ O ₅	577, 339, 313
50	DG(18:1/18:1)	13,4	638.5732	[M+NH ₄] ⁺	+	C ₃₉ H ₇₂ O ₅	603, 339, 265
51	DG(18:1/18:2)	12,6	636.5573	[M+NH ₄] ⁺	+	C ₃₉ H ₇₀ O ₅	601, 339, 337, 263
52	DG(18:2/18:2)	11,9	634.5413	[M+NH ₄] ⁺	+	C ₃₉ H ₆₈ O ₅	599, 337
53	DG(20:1/22:4)	15,6	716.5949	[M+NH ₄] ⁺	+	C ₄₅ H ₇₈ O ₅	429, 413, 375, 357
54	TG(18:1/18:1/19:1)	17,0	916.7954	[M+NH ₄] ⁺	+	C ₅₈ H ₁₀₆ O ₆	617, 603
55	TG(18:2/18:2/18:3)	17,1	894.7539	[M+NH ₄] ⁺	+	C ₅₇ H ₉₆ O ₆	597, 577, 339, 337, 263, 261

DG = diacylglycerol, TG = triacylglycerol

5.3.1.4 Free fatty acids identification

Along with phospholipids and glycerides, fatty acids were detected. In the MS/MS spectra they exhibited the same behaviour observed in paragraph 3.3.1.6, allowing their putative identification as palmitic acid (**56**), stearic acid (**57**), oleic acid (**58**) and linoleic acid (**59**) (Table 5.6).

Free fatty acids are widely reported in nuts, and their effects on human health have been exhaustively described. In particular, dietary fatty acids showed to be able to modulate plasma lipids, and polyunsaturated fatty acids resulted effective in reducing hematic cholesterol levels (Howard et al., 1995; Fernandez & West, 2005).

Table 5.6 Free fatty acids putatively identified in *P. vera* seeds

N°	Compound	R _t	m/z	Ion	Ion Mode	Molecular Formula	MS/MS
56	Palmitic acid	6.2	255.2339	[M-H] ⁻	-	C ₁₆ H ₃₂ O ₂	237, 209
57	Stearic acid	6.9	283.2653	[M-H] ⁻	-	C ₁₈ H ₃₆ O ₂	265, 237
58	Oleic acid	6.4	281.2511	[M-H] ⁻	-	C ₁₈ H ₃₄ O ₂	263, 235
59	Linoleic acid	5.9	279.2339	[M-H] ⁻	-	C ₁₈ H ₃₂ O ₂	261, 233

5.4 Free fatty acids GC-FID quali-quantitative analysis of *P. vera* seeds

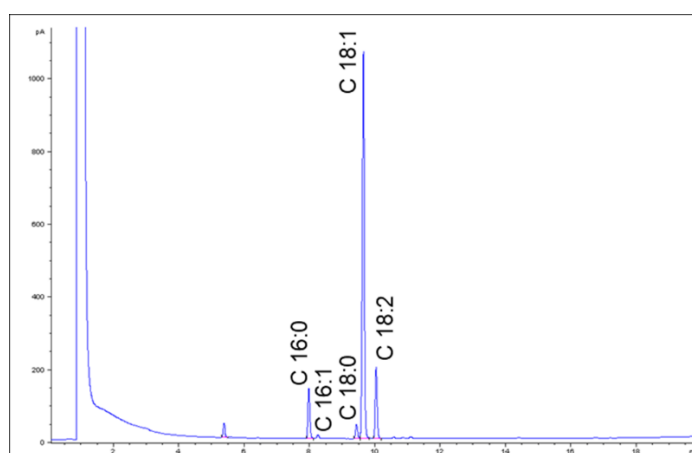
5.4.1 Results and discussion

5.4.1.1 Fatty acids extraction and fatty acid methyl esters (FAMES) synthesis

To allow free fatty acids quali-quantitative analyses, pistachios were extracted by following the same procedure described in paragraph 3.4.1.2, also reporting the protocol for derivatization into methyl esters, suitable with gaschromatography.

5.4.1.2 Identification and quantification of the major free fatty acids

Identification of the free fatty acids detected in the GC-FID experiments was carried out as shown in paragraph 3.4.1.3.

**Figure 5.3** GC-FID profile of the oily fraction of *P. vera* seeds

Successively, adopting the same workflow previously described in paragraph 3.4.1.3, the main constituents of the oily fraction were quantified (Table 5.7).

Table 5.7 Amount of the main fatty acids quantified in the oily fraction of *P. vera* seeds

C 16:0	C16:1	C 18:0	C 18:1	C 18:2
5.98 ± 0.12	1.09 ± 0.08	2.89 ± 0.09	70.61 ± 1.18	19.43 ± 0.43

Results expressed as percentage of the total amount of the detected free fatty acids.
Standard Deviation of three independent experiments.

The achieved results were in accordance with previous scientific reports assessing the free fatty acids content in “Pistacchio di Bronte” (Pantano et al., 2016). As shown in Figure 5.3, oleic acid (C 18:1, **58**) represented the major constituent; such compound has been reported for *in vitro* antioxidant activity, as well as motility stimulant activity in human extravillous trophoblast cells (Wei et al., 2016; Yang et al., 2017). In addition, it has been demonstrated that free fatty acids possess antibacterial activity, suggesting a potential enteroprotective effect against pathogenic enterobacteria (Desbios & Smith, 2010).

5.5 Conclusions

Phytochemical investigation carried out on the polar fraction of *P. vera* cv. Napoletana seeds highlighted the occurrence of different phenolic constituents, mainly flavonoids and gallic acid derivatives. The employment of “green” solvents pointed out the effectiveness of EtOH in extracting anacardic acids, while colorimetric assays evidenced a discreet phenolic content; furthermore, the quantitative analysis assessed in the MeOH extract the highest concentration of anacardic acids.

Moreover, non-polar fraction investigation performed by a LC-ESI/HRMS/MS approach highlighted the presence of several classes of phospholipids, along with di-/triacylglycerols and free fatty acids. These last ones were also identified and

quantified by GC-FID experiments, putting in evidence oleic acid as major constituent.

According to the achieved results, the “Pistacchio di Bronte” showed to possess a diversified metabolome, made up of compounds mainly reported for their antioxidant and cholesterol lowering properties, suggesting that a regular and moderate intake may afford concrete benefits to human health, as body weight and glycemetic control, also supporting to counteract the onset of cardiovascular diseases (Terzo et al., 2017).

5.6 Experimental section

Plant material

P. vera cv. Napoletana seeds were collected in August 2017, and provided by “Aromaticilia”, Bronte, Sicily, Italy.

Extraction of polar constituents

413.5 g of seeds were extracted with increasing polarity solvents: *n*-hexane (600 mL, three times for three days), chloroform (600 mL, three times for three days) and MeOH (600 mL, three times for three days), affording 16.1 g of crude MeOH extract. A small amount (3.0 g) of the crude MeOH extract was then submitted to a liquid-liquid extraction process, by using *n*-hexane and MeOH (three times), in order to remove fats eventually still present. A successive liquid-liquid extraction by using BuOH and H₂O (three times) was performed, in order to remove the high content of sugars, detected by TLC analysis, and 224.0 mg of BuOH extract were obtained. In addition, the seeds were extracted by maceration using EtOH 96% and an EtOH:H₂O (1:1, v/v) solution: 100 mL of solvent were poured to 10 g of seeds, and extracted three times for three days, yielding 949.2 mg of EtOH extract and 595.1 mg of EtOH:H₂O extract.

LC-ESI/LTQOrbitrap/MS/MS and LC-ESI/LTQOrbitrap/MS analysis of polar constituents

LC-HRMS experiments were carried out on instrument reported in general experimental procedures. LC separation was performed on a Phenomenex (Torrance, CA, USA) Kinetex EVO C-18 column (100 x 2.1 mm, 5 µm) at a flow rate of 0.2 ml/min. Employed mobile phases were (A) water and (B) acetonitrile both acidified 0.1% formic acid. Elution gradient was: 0 min 10% B, 40 min 100%

B, held for 10 min, returning to start conditions in 7 min. Injection volume was 5 μ L, keeping column at room temperature.

The ESI source parameters were set as following: source voltage at 5.0 kV, capillary voltage at -12 V, tube lens offset at -121.47 V, capillary temperature at 280 °C, sheath gas at 30 (arbitrary units) and auxiliary gas at 5 (arbitrary units).

LC-ESI/QTrap/MS/MS quantitative analysis

Quantitative analysis was carried out on instrument reported in general experimental procedures. LC separation was performed on a Phenomenex (Torrance, CA, USA) Kinetex EVO C-18 column (100 x 2.1 mm, 5 μ m). The mobile phases were (A) water-formic acid (99.9:0.1, v/v) and (B) acetonitrile-formic acid (99.9:0.1, v/v). Gradient conditions: 0 min 10% B, 40 min 100% B, held for 10 min, returning to start conditions in 7 min. Source temperature was set at 349°C, column temperature was 40°C, flow rate was 0.2 mL/min and injection volume 2 μ L.

Polar lipids extraction

As reported in general experimental procedures.

LC-ESI/QToF/MS/MS and LC-ESI/QToF/MS analysis of polar lipids

As reported in general experimental procedures.

Free fatty acids extraction

As reported in general experimental procedures. Extraction procedures yielded 14.19 g of oily extract.

Fatty acids methyl esters (FAME) synthesis

As reported in general experimental procedures.

GC-FID quali-quantitative analysis of free fatty acids

As reported in general experimental procedures.

Total phenolic content

As reported in general experimental procedures.

DPPH• radical scavenging activity

As reported in general experimental procedures.

ABTS⁺ radical scavenging activity

As reported in general experimental procedures.

5.6 References

Abdelmoneim, H. A.; Xiaoqiang, Z.; Sherif, M. A.; Sameh, A. K.; Qingzhe, J.; Xingguo, W. Natural phospholipids: occurrence, biosynthesis, separation, identification, and beneficial health aspects. *Critical Rev. Food Sci. Nutr.* **2017**, *18*, 1-23.

Ballistreri, G.; Arena, E.; Fallico, B. Pistachios as a source of health-promoting substances. *Acta Horticulturae* **2011**, *912*, 837-842.

Belguith-Hadrichea, O.; Ammarb, S.; Contrerasc, M. M.; Fetouie, H.; Segura-Carreteroc, A.; El Fekia, A; Bouazizb, M. HPLC-DAD-QTOF-MS profiling of phenolics from leaf extracts of two Tunisian fig cultivars: Potential as a functional food. *Biomed. & Pharmacotherapy.* **2017**, *89*, 185–193.

Bligh, E. G.; Dyer, W. J. A rapid method of total lipid extraction and purification. *Canad. J. Biochem. Phys.* **1959**, *37*, 911-917.

Callemien, D.; Collin, S. Use of RP-HPLC-ESI/HRMS/MS to differentiate various proanthocyanidin isomers in lager beer extracts. *J. Amer. Soc. Brewing Chemists*. **2008**, 66, 109-115.

Desbios, A. P.; Smith, V. J. Antibacterial free fatty acids: activities, mechanisms of action and biotechnological potential. *Appl Microbiol Biotechnol*. **2010**, 85, 1629-42.

Fernandez, M. L.; West, K. L. Mechanisms by which dietary fatty acids modulate plasma lipids. *J. Nutr*. **2005**, 19, 2075-2078.

Grace, M. H.; Esposito, D.; Timmers, M. A.; Xiong, J.; Yousef, G.; Komarnytsky, S.; Lila, M. A. *In vitro* lipolytic, antioxidant and antiinflammatory activities of roasted pistachio kernel and skin constituents. *Food Funct*. **2016**, 7, 4285–4298.

Henrandez-Alonso, P.; Bullò, M.; Salas-Salvadò, J. Pistachios for health, what do we know about this multifaceted nut? *Nutr Today*. **2016**, 51, 133–138.

Holčapek, M.; Jandera, P.; Zderadička, P.; Hrubà, L. Characterization of triacylglycerol and diacylglycerol composition of plant oils using high-performance liquid chromatography–atmospheric pressure chemical ionization mass spectrometry. *J. Chrom. A*. **2003**, 1010, 195–215.

Howard, B. V.; Hannah, J. S.; Heiser, C. C.; Jablonski, K. A.; Paidi, M. C.; Alarif, L.; Robbins, D. C.; Howard, W. J. Polyunsaturated fatty acids result in greater cholesterol lowering and less triacylglycerol elevation than do monounsaturated fatty acids in a dose-response comparison in a multiracial study group. *Am J Clin Nutr*. **1995**, 62, 392-402.

Ichihara, K.; Fukubayashi, Y. Preparation of fatty acid methyl esters for gas-liquid chromatography. *J. Lipid Res*. **2010**, 51, 635–640.

Keller, S. A.; Malarski, C.; Reuther, R.; Kertscher, M.; Kiehntopf, G. Milk phospholipid and plant sterol-dependent modulation of plasma lipids in healthy volunteers. *Eur. J. Nutr*. **2013**, 52, 1169–79.

Li, L.; Seeram, N. P. Maple syrup phytochemicals include lignans, coumarins, a stilbene, and other previously unreported antioxidant phenolic compounds. *J Agric Food Chem.* **2010**, 58, 11673–11679.

Lin, L.; Sun, J.; Chen, P.; Monagas, M. J.; Harnly, J. M. UHPLC-PDA-ESI/HRMSⁿ profiling method to identify and quantify oligomeric proanthocyanidins in plant products. *J. Agric. Food Chem.* **2014**, 62, 9387–9400.

Martorana, M.; Arcoraci, T.; Rizza, L.; Cristani, M.; Bonina, F. P.; Saija, A.; Trombetta, D.; Tomaino, A. *In vitro* antioxidant and *in vivo* photoprotective effect of pistachio (*Pistacia vera* L., variety Bronte) seed and skin extracts. *Fitoterapia.* **2013**, 85, 41-48.

Nagai, K. Bovine milk phospholipid fraction protects Neuro2a cells from endoplasmic reticulum stress via PKC activation and autophagy. *J. Biosci. Bioeng.* **2012**, 114, 466–71.

Pantano, L.; Lo Cascio, G.; Alongi, A.; Cammilleri, G.; Vella, A.; Macaluso, A.; Cicero, N.; Migliazzo, A.; Ferrantelli, V. Fatty acids determination in Bronte pistachios by gas chromatographic method. *Nat. Prod. Res.* **2016**.

Pulfer, M.; Murphy, R. C. Electrospray mass spectrometry of phospholipids. *Mass Spectrometry Reviews.* **2003**, 22, 332–364.

Radner, F. P.; Fischer, J. The important role of epidermal triacylglycerol metabolism for maintenance of the skin permeability barrier function. *Biochim. Biophys. Acta.* **2014**, 1841, 409-415.

Song, S.; Cheong, L.; Wang, H.; Man, Q.; Pang, S.; Li, Y.; Ren, B.; Wang, Z.; Zhang, J. Characterization of phospholipid profiles in six kinds of nut using HILIC-ESIIT-TOF-MS system. *Food Chem.* **2018**, 240, 1171–1178.

Terzo, S.; Baldassano, S.; Caldara, G. F.; Ferrantelli, V.; Lo Dico, G.; Mulè, F.; Amato, A. Health benefits of pistachios consumption. *Nat Prod Res.* **2017**, 15, 1-12.

Tomaino, A.; Martorana, M.; Arcoraci, T.; Monteleone, D.; Giovinazzo, C.; Saija, A. Antioxidant activity and phenolic profile of pistachio (*Pistacia vera* L., variety Bronte) seeds and skins. *Biochimie*. **2010**, 92, 1115-1122.

Wei, C.; Yen, P.; Chang, S.; Cheng, P.; Lo, Y.; Liao, V. H. Antioxidative activities of both oleic acid and *Camellia tenuifolia* seed oil are regulated by the transcription factor DAF-16/FOXO in *Caenorhabditis elegans*, *PLoS One*. **2016**, 11.

Yang, C.; Lim, W.; Bazer, F. W.; Song, G. Oleic acid stimulation of motility of human extravillous trophoblast cells is mediated by stearoyl-CoA desaturase-1 activity, *MHR: Basic Sci. Reprod. Med.* **2017**, 23, 755–770.

Chapter 6
Analysis of polar constituents of *Pistacia vera* (cv. Napoletana) biomasses

6.1 Introduction

Pistacia vera L. (Anacardiaceae) is a tree native of Central Asia, and widely cultivated for the production of its edible seeds, known as pistachios. It possesses wide obovate dark green leaves, while the pink-violet flowers are unisexual, apetalous and borne in panicles. The fruit is a drupe, constituted by a soft and thin husk, usually green and violet, enveloping a beige colored bivalve thin shell, containing the edible seed, characterized by an intense green color, covered by a fine purple integument.

Pistachio manufacturing represents one of the most intensive nuts productions. In 2016, according to FAOSTAT data, world pistachio production was about 1.1 million tonnes, with United States as major producer (about 405 000 tonnes), followed by Iran (about 315 000 tonnes) and Turkey (about 170 000 tonnes) (FAOSTAT, 2018). Also considering that the final product represents about 40% of the total fruit weight, an intensive pistachio production leads to a massive amount of by-products, mainly represented by husks and shells. However, due to the increasing automation of the harvesting techniques based on the tree shaking, leaves have become an additional by-product deriving from pistachio production. The disposal of the collateral biomasses represents a concrete problem, since the related costs bare on farmers finances, with direct backlash on the final prize. In addition, *P. vera* is a tree with biennial fruiting cycle: usually it is possible to assist to a rich pistachio production during the “fruiting years”, alternating to a reduced or totally absent production during the “non-fruiting years”; due to the influence of climatic conditions affecting the fruiting, there is no guarantee of a constant production over the years, with a direct affection on the final prize.

To overcome the disposal costs, farmers are used to employ discarded husks for fertilization, while shells are usually sold as cheap fuel for stoves; on the contrary, leaves find no applications. However, during last years scientific literature has reported a growing number of studies supporting the potential value of biomasses

discarded from agricultural manufacturing as a source of bioactive compounds, finalized to applications in fields like cosmetics and nutraceuticals (Tang et al., 2018; Hamaio et al., 2016; Kumar et al., 2017).

Therefore, aiming at valorizing the main by-products deriving from pistachio production as a potential source of bioactives, leaves, husks and shells of *P. vera* were submitted to phytochemical investigations. Interest was shown for the by-products deriving from the manufacturing of the most appreciated Italian pistachio variety, the “Pistacchio di Bronte” cv. Napoletana, awarded with the Protected Origin Designation (PDO) label.

In this chapter, the following topics will be discussed:

- isolation and characterization of the main polar constituents detected in the LC-ESI/LTQOrbitrap/MS profiles of the leaves, husks and shells MeOH extracts;
- preparation of extracts by using “green” solvents and different protocols, with subsequent comparison of their LC-ESI/LTQOrbitrap/MS profiles;
- evaluation of radical scavenging activity by DPPH· and ABTS^{•+} assays, as well as total phenolic content determination by Folin-Ciocalteu assay;
- LC-ESI/LTQOrbitrap/MS profiles comparison of the leaves extracts collected during the “fruiting” and “non-fruiting” years;
- compounds of interest quantitative analysis by MRM approach.

6.2 Analysis of the leaves of *P. vera* polar fraction

Pistacia vera L. leaves



The leaves of *P. vera* are obovate, deciduous and with a pinnate arrangement, characterized by a lively green color, and a yellowish edge, with parallel veins.

6.2.1 Results and discussion

6.2.1.1 LC-ESI/LTQOrbitrap/MS/MS metabolite profiling of the MeOH extract of *P. vera* “non-fruiting year” leaves

The MeOH extract of *P. vera* “non-fruiting year” leaves was submitted to LC-ESI/LTQOrbitrap/MS/MS experiments, in negative ion mode, in order to achieve preliminary information about the chemical composition. The peaks observed in the LC-HRMS profile (Fig. 6.1) showed accurate m/z values ascribable to phenolic constituents, mainly flavonoids with several glycoside moieties (**4-8**, **10-15**, **18**, **19**, **21**, **22**), a quercetin (**23**), catechin (**1**), gallic acid derivatives (**9**, **16**, **17**, **20**), a glycosylated monoacylglycerol (**24**), as well as two compounds (**2**, **3**) supposed as glycosylated megastigmanes (Table 6.1).

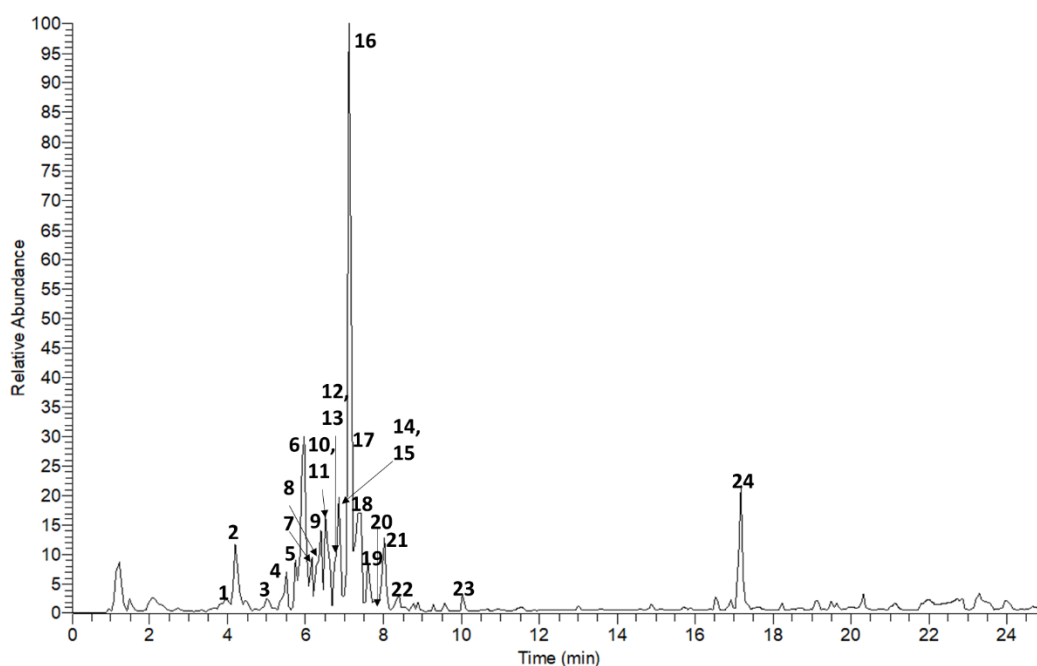


Figure 6.1 LC-HRMS profile in negative ion mode of the MeOH extract of *P. vera* "non-fruiting year" leaves

Table 6.1 Compounds identified and putatively identified in the MeOH extract of *P. vera* "non-fruiting year" leaves

Nº	R _t	Calculated Mass	[M-H] ⁻	Δppm	MS ² (%)	Molecular formula	Compound
1	3.94	290.0790	289.0720	0.542	245(100), 205(36), 179(17)	C ₁₅ H ₁₄ O ₆	(+)-catechin ¹
2	4.19	432.1995	431.1926	1.269	385(100), 269(54), 179(59)	C ₂₀ H ₃₂ O ₁₀	megastigmane hexoside
3	5.00	388.2097	387.2027	0.684	225(100)	C ₁₉ H ₃₂ O ₈	megastigmane hexoside
4	5.50	632.1013	631.0949	0.991	479(100)	C ₂₈ H ₂₄ O ₁₇	myricetin 3- <i>O</i> -β-D-galloyl)-β-D-glucopyranoside ¹
5	5.73	626.1483	625.1419	1.165	317(51), 316(100)	C ₂₇ H ₃₀ O ₁₇	myricetin 3- <i>O</i> -β-D-rutinoside ¹
6	5.97	480.0903	479.0838	1.646	317(39), 316(100)	C ₂₁ H ₂₀ O ₁₃	myricetin 3- <i>O</i> -β-D-glucopyranoside ¹
7	6.15	494.0696	493.0679	0.456	317(100)	C ₂₁ H ₁₈ O ₁₄	myricetin 3- <i>O</i> -β-D-glucuronide ¹
8	6.28	616.1064	615.0999	0.351	463(100)	C ₂₈ H ₂₄ O ₁₆	quercetin 3- <i>O</i> -(6"- <i>O</i> -galloyl)-β-D-glucopyranoside ¹
9	6.39	788.1072	787.1013	0.465	617(100)	C ₃₄ H ₂₈ O ₂₂	1,2,3,6-tetra- <i>O</i> -galloyl-β-D-glucopyranoside ¹
10	6.48	450.0798	449.0728	1.654	316(100)	C ₂₀ H ₁₈ O ₁₂	myricetin 3- <i>O</i> -β-D-xylopyranoside ¹
11	6.51	610.1533	609.1470	1.843	301(100)	C ₂₇ H ₃₀ O ₁₆	quercetin 3- <i>O</i> -β-D-rutinoside ¹
12	6.51	450.0798	449.0728	1.113	316(100)	C ₂₀ H ₁₈ O ₁₂	myricetin 3- <i>O</i> -α-L-arabinofuranoside ¹

13	6.60	464.0954	463.0882	1.080	301(100)	C ₂₁ H ₂₀ O ₁₂	quercetin 3- <i>O</i> -β-D-galactopyranoside ¹
14	6.75	464.0954	463.0882	0.461	301(100)	C ₂₁ H ₂₀ O ₁₂	quercetin 3- <i>O</i> -β-D-glucopyranoside ¹
15	6.86	478.0747	477.0680	0.731	301(100)	C ₂₁ H ₁₈ O ₁₃	quercetin 3- <i>O</i> -β-D-glucuronide ¹
16	7.10	940.1181	939.1124	0.941	787(9), 769(100), 617(18)	C ₄₁ H ₃₂ O ₂₆	1,2,3,4,6-penta- <i>O</i> -galloyl-β-D-glucopyranoside ¹
17	7.27	336.0481	335.0413	1.413	183(100)	C ₁₅ H ₁₂ O ₉	methyl digallate
18	7.41	434.0849	433.0780	1.463	300(100)	C ₂₀ H ₁₈ O ₁₁	quercetin 3- <i>O</i> -α-L-arabinofuranoside ¹
19	7.57	448.1005	447.0936	1.846	301(100)	C ₂₁ H ₂₀ O ₁₁	quercetin 3- <i>O</i> -α-L-rhamnoside ¹
20	7.82	1092.1291	1091.1231	1.210	939(100), 787(32)	C ₄₈ H ₃₆ O ₃₀	hexagalloyl hexoside
21	8.01	586.0958	585.0894	0.216	301(100)	C ₂₇ H ₂₂ O ₁₅	quercetin 3- <i>O</i> -(5"- <i>O</i> -galloyl)-α-L-arabinofuranoside ¹
22	8.40	448.2308	447.2239	0.898	285(100)	C ₂₁ H ₃₆ O ₁₀	kaempferol 3- <i>O</i> -β-D-glucopyranoside ¹
23	10.03	302.0426	301.0357	0.463	179(100), 151(84)	C ₁₅ H ₁₀ O ₇	quercetin ¹
24	17.18	676.3670	675.3604	1.448	513(22), 397(100), 277(12)	C ₃₃ H ₅₆ O ₁₄	DGMG (18:3)
25	30.28	290.1881	289.1812	1.941	245(100), 106(45)	C ₁₈ H ₂₆ O ₃	(11:1)-anacardic acid
26	32.13	316.2038	315.1970	1.156	271(100), 106(36)	C ₂₀ H ₂₈ O ₃	(13:2)-anacardic acid
27	34.03	292.2038	291.1968	1.684	247(100), 106(34)	C ₁₈ H ₂₈ O ₃	(11:0)-anacardic acid
28	34.39	360.2664	359.2232	1.198	315(100), 106(51)	C ₂₃ H ₃₆ O ₃	(16:1)-anacardic acid
29	35.38	318.2194	317.2130	0.321	273(100), 106(44)	C ₂₀ H ₃₀ O ₃	(13:1)-anacardic acid
30	37.19	370.2507	369.2440	1.169	325(100), 106(33)	C ₂₄ H ₃₄ O ₃	(17:3)-anacardic acid
31	38.12	320.2351	319.2285	1.465	275(100), 106(29)	C ₂₀ H ₃₂ O ₃	(13:0)-anacardic acid
32	38.62	346.2507	345.2441	0.694	301(100), 106(37)	C ₂₂ H ₃₄ O ₃	(15:1)-anacardic acid
33	39.26	372.2664	371.2596	0.961	327(100), 106(42)	C ₂₄ H ₃₆ O ₃	(17:2)-anacardic acid
34	39.48	372.2664	371.2592	0.846	327(100), 106(39)	C ₂₄ H ₃₆ O ₃	(17:2)-anacardic acid
35	41.24	348.2664	347.2598	0.466	303(100), 106(45)	C ₂₂ H ₃₆ O ₃	(15:0)-anacardic acid
36	41.38	374.2820	373.2754	1.321	329(100), 106(36)	C ₂₄ H ₃₈ O ₃	(17:1)-anacardic acid
37	43.92	376.2977	375.2908	1.145	331(100), 106(42)	C ₂₄ H ₄₀ O ₃	(17:0)-anacardic acid

¹The identification of this compound was corroborated by isolation and NMR spectra analysis

The following interpretation of the MS/MS spectra, acquired by tandem mass spectrometry experiments performed in data dependent scan mode, allowed to putatively determine the identity of the detected compounds and to attribute the

different glycoside moieties linked to flavonoids. However, to achieve an univocal identification of the main constituents detected in the LC-HRMS profile, purification of the MeOH extract was carried out, followed by NMR-based structural elucidation.

6.2.1.2 Isolation and characterization

The MeOH extract of *P. vera* “non-fruiting year” leaves was at first fractionated by size-exclusion chromatography performed on a Sephadex LH-20 column; the obtained fractions were further purified by RP-HPLC. The isolated compounds were finally submitted to 1D and 2D NMR experiments, comparing the obtained data with scientific literature, allowing an unambiguous identification of compounds (Fig. 6.2) (Tourè et al., 2018; Braca et al., 2003; Duan et al., 2004; Bottone et al., 2018; Madikizela et al., 2013).

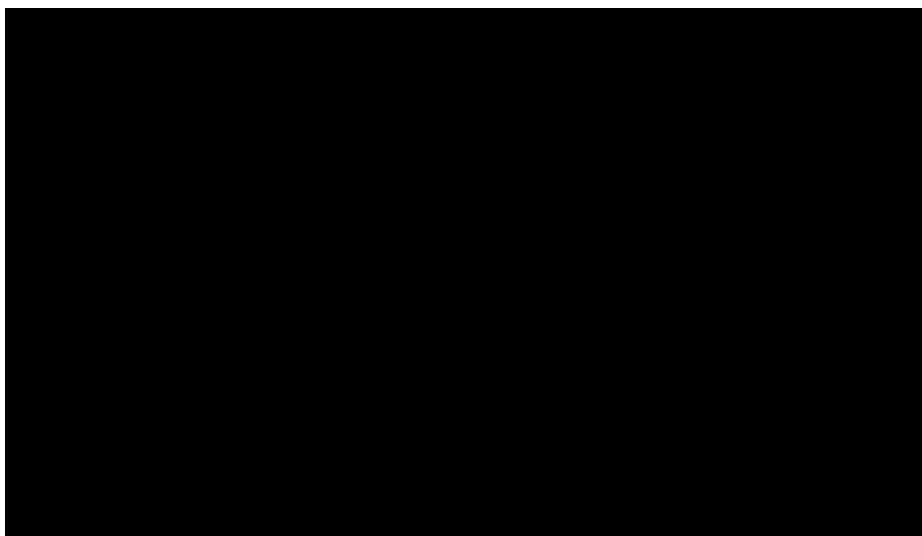


Figure 6.2 Structures of the main constituents isolated from the MeOH extract of *P. vera* "non-fruiting year" leaves

The main isolated constituents were represented by flavonoids, whose aglycones were myricetin, quercetin and kaempferol, with different glycoside moieties, as hexosides and pentosides, occasionally identified as furanosides and pyranosides, as well as their related acidic form, and in some cases esterified with gallic acid.

Flavonoid constituents were identified as myricetin 3-*O*-(6"-*O*-galloyl)- β -D-glucopyranoside (4), myricetin 3-*O*- β -D-rutinoside (5), myricetin 3-*O*- β -D-glucopyranoside (6), myricetin 3-*O*- β -D-glucuronide (7), quercetin 3-*O*-(6"-*O*-galloyl)- β -D-glucopyranoside (8), myricetin 3-*O*- β -D-xylopyranoside (10), quercetin 3-*O*- β -D-rutinoside (11), myricetin 3-*O*- α -L-arabinofuranoside (12), quercetin 3-*O*- β -D-galactopyranoside (13), quercetin 3-*O*- β -D-glucopyranoside (14), quercetin 3-*O*- β -D-glucuronide (15), quercetin 3-*O*- α -L-arabinofuranoside (18), quercetin 3-*O*- α -L-rhamnoside (19), quercetin 3-*O*-(5"-*O*-galloyl)- α -L-arabinofuranoside (21), kaempferol 3-*O*- β -D-glucopyranoside (22), quercetin (23).

Flavonoids have been exhaustively investigated over the years for their several biological activities, mainly antioxidant and antiinflammatory. However, they showed to possess further interesting activities like anticancer, antiviral, antibacterial, cardioprotective and antidiabetic, highlighting a multi-tasking nature, proving the beneficial effects for human health (Wang et al., 2018).

Most of the identified flavonoids have been reported in the aerial parts and fruits of Sardinian *P. terebinthus* and *P. lentiscus*, whose aqueous extracts showed *in vitro* inhibitory effects on pancreatic lipase, α -amylase and α -glucosidase, suggesting a potential application in therapeutic treatment of diseases like atherosclerosis, diabetes, obesity and dyslipidemia (Foddai et al., 2015). In addition, also in Egyptian *P. chinensis*, *P. khinjuk* and *P. lentiscus* leaves, most of the isolated flavonoids were identified in the EtOH extracts, showing *in vitro* cytotoxicity towards different cancer cells lines like PC3 prostate cancer cells, MCF7 breast cancer cells and A549 lung cancer cells (Kirolos et al., 2018).

In addition to glycosylated flavonoids, (+)-catechin (1) was isolated. This flavan-3-ol showed to possess interesting antioxidant properties, able to counteract human plasma oxidation (Lotito et al., 1999; Holloway et al., 2015). Furtherly, catechins represent the main constituents occurring in green tea (*Camellia sinensis*),

whose extracts exert *in vitro* a good antimicrobial activity against enteropathogens (Archana et al., 2011).

Along with flavonoid-like compounds, two galloyl hexosides were isolated and identified as 1,2,3,6-tetra-*O*-galloyl- β -D-glucopyranoside (**9**) and 1,2,3,4,6-penta-*O*-galloyl- β -D-glucopyranoside (**16**) (Cho et al., 2010). Both compounds have been identified in *P. atlantica* fruits, as well as compounds **11**, **14**, **15**, and **22** (Khalloukia et al., 2017). Compound **16**, isolated from Tunisian *P. lentiscus* fruits, showed antioxidant properties and transcript-modulator activity on human K562 cells treated with H₂O₂ (Abdelwahed et al., 2007). In addition, compound **16** proved to possess antidiabetic properties, inhibitory effects on angiogenesis, while in pulmonary fibroblasts under inflammation conditions it increased elastin deposition by decreasing Reactive Oxygen Species (ROS) and matrix metalloproteinases, suggesting its effectiveness in arresting emphysema progression (Ren et al., 2006; Cryan et al., 2013; Parasaram et al., 2018). Furtherly, both tetra- and pentagalloyl glucosides (**9**, **16**) isolated from *Galla chinensis*, exerted inhibitory activity towards Hepatitis C Virus (HCV) NS3 protease (Duan et al., 2004).

Matching the isolated compounds with LC-MS/MS results highlighted the occurrence of additional constituents not afforded by isolation procedures. Therefore, the remaining compounds were characterized by determining their accurate *m/z* values and studying their fragmentation spectra, comparing the achieved data with scientific literature and online databases (FoodB, KnapSack).

Compounds **2** and **3** showed in HRMS pseudomolecular ions [M-H]⁻ at *m/z* 431.1926 and 387.2027, respectively. Both shared in their MS/MS spectra a signal ascribable to the loss of a hexose moiety (-162 Da); the comparison of their molecular formulae, determined as C₂₀H₃₂O₁₀ and C₁₉H₃₂O₈, respectively, with data reported in literature suggested a megastigmane aglycone moiety. Unfortunately, no further information were achieved from the analysis of their fragmentation spectra to carry out a satisfying structural elucidation, so that compounds **2** and **3**

were tentatively identified as megastigmane hexosides (Wang et al., 2009; Jia et al., 2017).

On the other hand, compound **17** (m/z 335.0413) showed a base peak in MS/MS at m/z 183, due to the loss of a dehydrated gallic acid moiety (-152 Da). Molecular formula was established as $C_{15}H_{12}O_9$, suggesting two conjugated gallic acid moieties with an additional methyl group; however, it was not possible to determine the location of the methyl group as well as the linking site of the gallic acid units, leading to tentatively identify compound **17** as methyl digallate (Ersan et al., 2016).

Moreover, pseudomolecular ion of compound **20** showed a higher m/z value if compared to the others (m/z 1091.1231), and its fragmentation spectrum presented two consecutive losses of 152 Da, observed at m/z 939 and 787, which were the nominal m/z values of the pseudomolecular ions corresponding to compounds **16** and **9**, respectively, suggesting the occurrence of an additional gallic acid unit; on the basis of the achieved information, compound **20** was putatively identified as hexagalloyl hexoside (FoodB).

Finally, compound **24** (m/z 675.3604), displayed a different behaviour in the MS/MS spectrum: a fragment ion at m/z 513 suggested the neutral loss of a dehydrated hexose moiety (-162 Da), while the base peak at m/z 397 was ascribable to the loss of a C 18:3 fatty acyl side chain (-278 Da), confirmed by the signal observed at m/z 277. Molecular formula was established in HRMS as $C_{33}H_{56}O_{14}$, in agreement with the identity putatively assigned to compound **24** as diglycoside monoacylglycerol 18:3 (DGMG 18:3) (FoodB).

*6.2.1.3 Extraction of *P. vera* “non-fruiting year” leaves by employing “green” solvents and protocols, with subsequent LC-ESI/LTQOrbitrap/MS analysis*

With the purpose to suggest alternative extraction protocols, characterized by a quick and simple performance, and by the employment of cheap and easily available solvents showing a good safety utilization level, *P. vera* “non-fruiting

year” leaves were submitted to sperimentally adapted extraction protocols, in particular by maceration using as solvents EtOH 96% and an EtOH:H₂O (1:1, v/v) solution, as well as by infusion and decoction using only water.

The obtained extracts were submitted to LC-ESI/LTQOrbitrap/MS experiments, and the achieved profiles compared with the MeOH one (Fig. 6.3).

“Eco-friendly” extraction protocols showed a significant class-specific selectivity, mainly due to the employed solvent rather than the extraction method. Indeed, LC-HRMS profiles of infusion and decoction (Fig. 6.3) were characterized by several peaks related to phenolics previously detected and identified in the MeOH extract. On the other hand, EtOH and EtOH:H₂O extracts (Fig. 6.3) showed in their LC-HRMS profiles peaks not observed in the MeOH extract. By a successive structural elucidation based on the determination of the accurate *m/z* values and the analysis of the fragmentation spectra, followed by comparison with data reported in scientific literature and online databases, the major peaks detected in the LC-HRMS profiles of the EtOH and EtOH:H₂O extracts were attributed to anacardic acids (**25-37**), differing for side chains length and unsaturation degree. However, it is possible to observe that some peaks ascribable to anacardic acids were detected also in decoction, suggesting a potential role of high temperature in extracting in water a discreet amount of less polar constituents; on the contrary, no significant peaks related to anacardic acids were detected in infusion, probably due to milder extraction conditions.

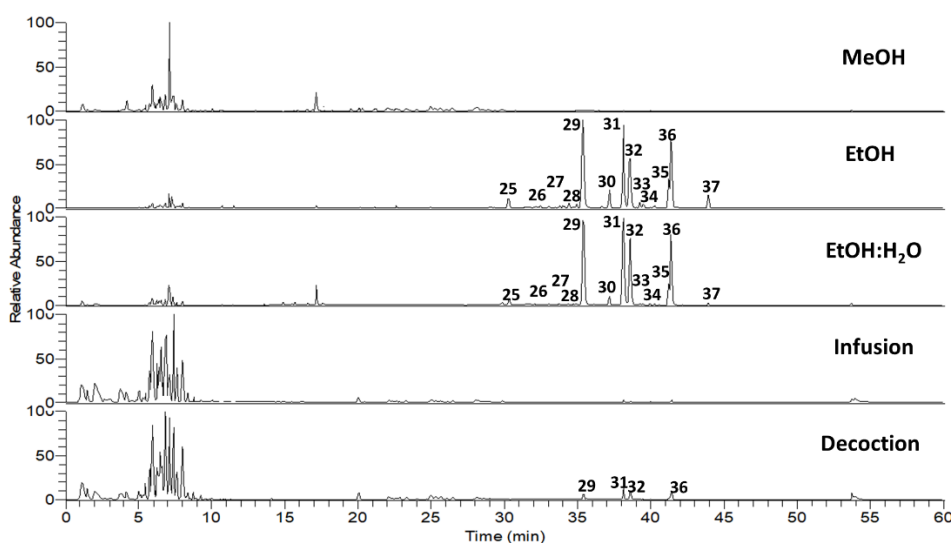


Figure 6.3 LC-HRMS profiles in negative ion mode of the MeOH, EtOH, EtOH:H₂O extracts, Infusion and Decoction of *P. vera* "non-fruited year" leaves

Such evidences may suggest a potential use of EtOH and EtOH:H₂O for a selective extraction of anacardic acids, highly interesting compounds reported for their several biological activities.

6.2.1.4 Anacardic acids

Anacardic acids are salicylic acid derivatives, with an additional aliphatic side

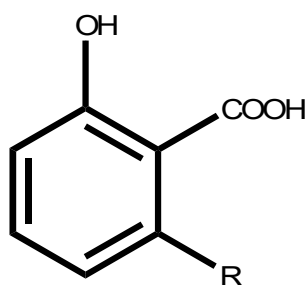


Figure 6.4 Chemical structure of generic anacardic acid. R represents the aliphatic side chain, varying for length and unsaturation degree

chain, varying for carbon number and unsaturation degree (Fig. 6.4). Interesting feature of this class of compounds is that differently from fatty acids, which usually show an even number of carbon atoms, the alkyl side chain is usually made up of an odd number of carbons. A growing interest has been shown for anacardic acids, because of the several biological activities they proved to possess. They showed a remarkable antioxidant activity exerted by inhibiting enzymes involved in ROS production and by chelating

bivalent metal ions as Cu²⁺ and Fe²⁺, known for their role in oxidant processes

(Kubo et al., 2006). Moreover, they resulted effective against bacteria showing antibiotic resistance, in particular against *Staphylococcus aureus*, and *Streptococcus mutans* as well (Kubo et al., 2004; Rathi et al., 2014). However, the most interesting activity resulted their high efficacy in inhibiting Hystone Acetyl Transferase (HAT), an enzyme playing an important role in a multitude of biological pathways involved in morbidities. As example, they resulted effective *in vitro* in sensitize cancer cells to ionizing radiations (Sun et al., 2006), as well as suppressing the expression of gene products regulated by NF- κ B involved in cell survival, invasion and proliferation (Sung et al., 2008). In addition, an *in vitro* promising activity has been shown against *Plasmodium falciparum* (Cui et al., 2008). Such experimental evidences about their potential role in pharmacological applications attracted interest of several medicinal chemistry research groups; as result, a growing number of anacardic acids derivatives was synthesized, like analogues with mixed activator/inhibitor activity for HATs, able to potentiate PCAF HATs and inhibit p300/CBP HATs, suggesting a perspective employment in anticancer therapies (Sbardella et al., 2008).

Structural elucidation of the detected anacardic acids was carried out by determining their accurate m/z values and their typical fragmentation patterns, comparing the achieved information with data reported in literature and databases. All compounds showed in their MS/MS spectra a common base peak originated from the loss of the carboxylic group as carbon dioxide (-44 Da); in addition, product ions at m/z 106 were ascribable to the phenolic ring possessing a methylene group deriving from the aliphatic side chain fragmentation. Accurate m/z values allowed to determine the alkyl side chains length and number of unsaturations (Table 6.1); unfortunately no further information was obtained from the analysis of the MS/MS spectra, hence it was not possible to establish the position of eventual unsaturations, although it has been reported that usually they occur on Δ^8 , $\Delta^{8,11}$ and

$\Delta^{8,11,14}$ positions in mono-, di- and triunsaturated derivatives, respectively (Morais et al., 2017; Carvalho et al., 2013).

6.2.1.5 Comparison of the “non-fruiting year” and “fruiting year” *P. vera* leaves

Some fruit trees, like apple (*Malus domestica*) and pecan (*Carya illinoensis*), show an alternate year bearing, with a massive fruit production during one year and a reduced production in the next one. In some cases, during bearing years farmers don't collect all the produced fruits, leading to an almost constant production over the years. However, in other cases all the produced fruits are collected, leading to an intensive bearing only during the “fruiting” year, as happens for *P. vera* (Rosenstock et al., 2010).

Inducing alternate years bearing may cause a stress in plant species, with a consequent alteration in metabolic pathways. Therefore, aiming at evaluating a possible correlation between human operations and the metabolome of a plant species, the leaves of “non-fruiting year” and “fruiting year” of *P. vera* were compared. For this purpose, “fruiting year” leaves were extracted following the same procedures employed for “non-fruiting year” leaves; the obtained extracts were submitted to LC-ESI/LTQOrbitrap/MS experiments, and the profiles compared.

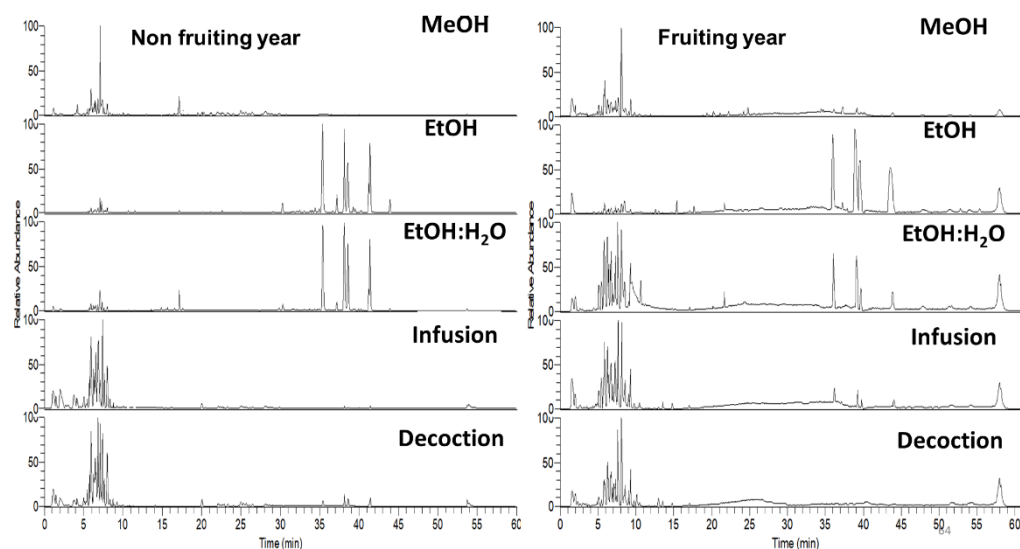


Figure 6.5 LC-HRMS profiles in negative ion mode of the different extracts of *P. vera* "non-fruiting year" and "fruiting year" leaves

No remarkable differences were observed among the LC-HRMS profiles (Fig. 6.5) of the leaves collected in different periods, suggesting no significant changes in the metabolome of *P. vera* cv. *Napoletana* during the years.

6.2.1.6 *P. vera* leaves as promising source of antioxidants

To complete our investigation on *P. vera* cv. *Napoletana* leaves, all the produced extracts were submitted to Folin-Ciocalteu assay to determine the total phenolic content, and to DPPH \cdot and ABTS $^{+\cdot}$ assays to evaluate their radical scavenging activity (Table 6.2).

A noteworthy phenolic content was observed for all the prepared extracts, with the MeOH extracts showing the highest (440.50 ± 21.67 and 347.91 ± 31.44 GAE mg/g dried extract for "fruiting year" and "non-fruiting year" leaves, respectively). In addition, all the extracts showed a significant radical scavenging activity towards DPPH \cdot , with the highest activity exerted by the MeOH extract of the "fruiting year" leaves ($IC_{50} = 6.34 \pm 0.85$ μ g/mL), confirmed by the results achieved from ABTS $^{+\cdot}$ assay, where the MeOH extracts exhibited once again their notable radical

scavenging activity (1.68 ± 0.18 and 1.54 ± 0.15 TEAC mM, for “fruiting year” and “non-fruiting year” leaves, respectively).

The obtained results highlighted *P. vera* leaves as a valuable source of phenolics exerting a noteworthy antioxidant activity, suggesting perspective employments for secondary applications.

Table 6.2 Total phenolic content, DPPH• and ABTS⁺ radical scavenging activity of the extracts of *P. vera* “non-fruiting year” and “fruiting year” leaves

Sample	Total phenolic content		DPPH•			ABTS ⁺	
	GAE ^a	SD ^d	IC ₅₀ ^b	SD ^d	TEAC ^c	SD ^d	
“Non-fruiting year” MeOH	347.91	± 31.44	12.56	± 0.62	1.54	± 0.15	
“Non-fruiting year” EtOH	208.28	± 38.92	16.84	± 2.85	1.35	± 0.11	
“Non-fruiting year” EtOH/H ₂ O	205.87	± 17.92	15.55	± 1.11	1.37	± 0.13	
“Non-fruiting year” DECOCTION	293.46	± 39.98	18.35	± 1.24	0.75	± 0.04	
“Non-fruiting year” INFUSION	167.72	± 27.50	17.40	± 3.21	0.53	± 0.07	
“Fruiting year” MeOH	440.50	± 21.67	6.34	± 0.85	1.68	± 0.18	
“Fruiting year” EtOH	232.54	± 18.67	15.99	± 1.65	1.29	± 0.11	
“Fruiting year” EtOH/H ₂ O	385.87	± 26.00	12.90	± 0.56	1.68	± 0.23	
“Fruiting year” DECOCTION	261.24	± 30.76	17.87	± 2.26	1.26	± 0.16	
“Fruiting year” INFUSION	245.32	± 22.92	18.96	± 2.36	1.22	± 0.17	
Vit. C			5.16	± 0.11			
Quercetin					1.87	± 0.08	

^a Values are expressed as gallic acid equivalents (GAE) mg/g of dried extract. ^b Values are expressed as µg/mL. ^c Values are expressed as concentration (mM) of a standard Trolox solution exerting the same antioxidant activity of a 1 mg/mL solution of the tested extract. ^d Standard Deviation of three independent experiments.

6.3 Phenolic constituents of *P. vera* cv. *Napoletana* husks

Pistacia vera L. husks



The husks may be differently colored according to the variety; usually they are brownish or green with a red/purple coloration on the summit, with a surface scattered by tiny green dots. It is thin and with a soft consistency, easily removable at complete ripening

6.3.1 Results and discussion

6.3.1.1 Preliminary LC-ESI/LTQOrbitrap/MS/MS analysis of the MeOH extract of *P. vera* husks

MeOH extract of the husks was at first analyzed by LC-ESI/LTQOrbitrap/MS/MS, achieving preliminary information about the chemical composition. Sundry peaks were observed in the LC-HRMS profile (Fig. 6.6), which showed mass spectra with related m/z of pseudomolecular ions values ascribable to phenolic compounds. A further analysis of the acquired fragmentation spectra allowed a tentative identification of 14 gallic acid derivatives (**38-41**, **44**, **46**, **47**, **50**, **53**, **54**, **56-58**), 2 aminoalkaloids (**43**, **48**), 11 flavonoids (**6**, **8**, **14**, **15**, **18**, **22**, **45**, **49**, **51**, **52**, **55**), diglycoside monoacylglycerol (**24**), an aromatic disaccharide (**42**), and 7 anacardic acids (**25**, **29**, **30**, **31**, **32**, **35**, **36**) (Table 6.3).

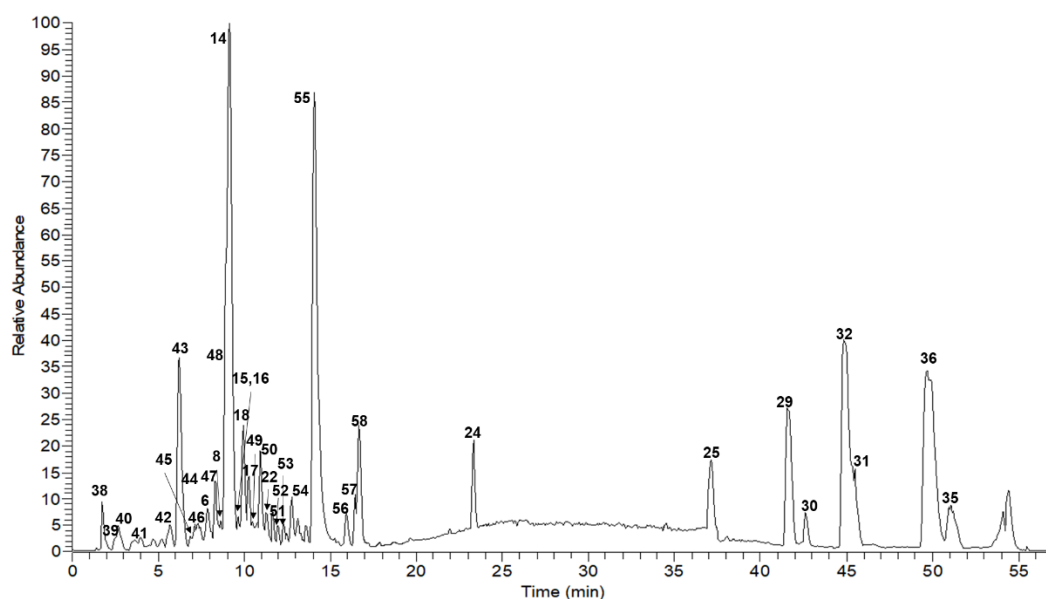


Figure 6.6 LC-HRMS profile in negative ion mode of the MeOH extract of *P. vera* husks

Table 6.3 Compounds identified and putatively identified in the MeOH extract of *P. vera* husks

N°	R _t	Calculated Mass	[M-H] ⁻	Δppm	MS ² (%)	Molecular formula	Compound
38	1.75	332.0743	331.0661	-0.54	271(62), 169(100)	C ₁₃ H ₁₆ O ₁₀	gallic acid 4- <i>O</i> -β-D-glucopyranoside ¹
39	2.49	170.0215	169.0140	1.24	125(100)	C ₇ H ₆ O ₅	gallic acid
40	2.68	326.0637	325.0558	-1.38	169(100), 125(18)	C ₁₄ H ₁₄ O ₉	galloyl shikimic acid
41	3.65	404.1318	403.1236	0.57	313(100), 271(31), 169(75)	C ₁₇ H ₂₄ O ₁₁	gallic acid derivative
42	5.67	402.1526	401.1444	0.39	269(100), 161(18)	C ₁₈ H ₂₆ O ₁₀	benzyl hexoside pentoside
43	6.18	305.0535	304.0455	-0.86	286(8), 260(100), 166(61), 153(38), 150(59), 122(31)	C ₁₄ H ₁₁ NO ₇	4,5,4'-trihydroxy-3,3'-iminobenzoic acid ¹
44	6.29	154.0266	153.0187	-0.92	109(100)	C ₇ H ₆ O ₄	protocatechuic acid ¹
45	7.31	406.1839	405.1758	1.45	273(100), 149(52), 131(20)	C ₁₈ H ₃₀ O ₁₀	unknown
46	7.46	184.0371	183.0293	0.64	168(100), 124(97)	C ₈ H ₈ O ₅	methyl gallate ¹
6	7.86	480.0903	479.0820	-0.99	316(100), 317(52)	C ₂₁ H ₂₀ O ₁₃	myricetin 3- <i>O</i> -β-D-glucopyranoside ¹
47	8.21	198.0528	197.0450	-1.05	169(100)	C ₉ H ₁₀ O ₅	ethyl gallate ¹
8	8.29	616.1064	615.0979	-1.18	463(100), 301(18)	C ₂₈ H ₂₄ O ₁₆	quercetin 3- <i>O</i> -(6''- <i>O</i> -galloyl)-β-D-glucopyranoside ¹
48	8.93	289.0586	288.0506	-1.54	270(32), 244(100), 200(26), 150(28), 137(19), 106(15), 93(14)	C ₁₄ H ₁₁ NO ₆	4,4'-dihydroxy-3,3'-imino-di-benzoic acid ¹
14	9.18	464.0954	463.0873	0.84	301(100)	C ₂₁ H ₂₀ O ₁₂	quercetin 3- <i>O</i> -β-D-glucopyranoside ¹
16	9.58	940.1181	939.1124	0.69	787(9), 769(100), 617(18)	C ₄₁ H ₃₂ O ₂₆	1,2,3,4,6-penta- <i>O</i> -galloyl-β-D-glucopyranoside ³
15	9.60	478.0747	477.0663	-1.15	301(100)	C ₂₁ H ₁₈ O ₁₃	quercetin 3- <i>O</i> -β-D-glucuronide ¹

18	9.96	434.0849	433.0765	1.28	300(100), 301(63)	C ₂₀ H ₁₈ O ₁₁	quercetin 3- <i>O</i> - α -L-arabinofuranoside ¹
17	10.21	336.0481	335.0402	0.64	183(100)	C ₁₅ H ₁₂ O ₉	methyl digallate
49	10.27	448.1005	447.0922	0.69	285(100), 284(36), 327(21)	C ₂₁ H ₂₀ O ₁₁	kaempferol 3- <i>O</i> - β -D-galactopyranoside ¹
50	10.96	484.0853	483.0794	-0.35	331(100), 313(18), 169(21), 125(20)	C ₂₀ H ₂₀ O ₁₄	digallate hexoside
22	11.31	448.1005	447.0921	1.59	285(100), 284(36), 327(21)	C ₂₁ H ₂₀ O ₁₁	kaempferol 3- <i>O</i> - β -D-glucopyranoside ¹
51	11.96	478.1107	477.1027	-1.63	315(100)	C ₂₂ H ₂₂ O ₁₂	isorhamnetin 3- <i>O</i> - β -D-galactopyranoside ¹
52	12.22	478.1107	477.1024	1.27	315(100)	C ₂₂ H ₂₂ O ₁₂	isorhamnetin 3- <i>O</i> - β -D-glucopyranoside ¹
53	12.46	484.0853	483.0791	0.69	331(100), 313(16), 169(34), 125(22)	C ₂₀ H ₂₀ O ₁₄	digallate hexoside
54	12.78	484.0853	483.0790	-0.64	331(100), 313(19), 169(29), 125(24)	C ₂₀ H ₂₀ O ₁₄	digallate hexoside
55	14.10	286.0477	285.0397	1.44	267(18), 257(26), 243(59), 241(100), 217(74), 213(22), 201(23), 199(81), 197(23), 175(78), 151(41), 133(14)	C ₁₅ H ₁₀ O ₆	luteolin ¹
56	15.92	468.1267	467.1187	0.83	313(100), 169(42), 125(12)	C ₂₁ H ₂₄ O ₁₂	gallic acid derivative
57	16.43	468.1267	467.1193	-1.67	313(100), 169(39), 125(14)	C ₂₁ H ₂₄ O ₁₂	gallic acid derivative
58	16.67	468.1267	467.1196	-0.36	313(100), 169(33), 125(21)	C ₂₁ H ₂₄ O ₁₂	gallic acid derivative
24	23.32	676.3670	675.3585	0.49	513(26), 397(100), 277(14)	C ₃₃ H ₅₆ O ₁₄	DGMG (18:3)
59	34.53	362.2457	361.2370	-1.47	317(100), 299(75), 219(41), 203(27)	C ₂₂ H ₃₄ O ₄	2-(pentadecen-1-yl)-dihydroxybenzoic acid
25	37.12	290.1881	289.1801	0.32	245(100), 106(18)	C ₁₈ H ₂₆ O ₃	(11:1)-anacardic acid ²
60	38.05	390.2770	389.2678	0.44	345(100), 327(95), 247(49), 231(52)	C ₂₄ H ₃₈ O ₄	2-(heptadecen-1-yl)-dihydroxybenzoic acid
61	39.11	390.2770	389.2680	-0.74	345(100), 327(52), 219(32), 203(19)	C ₂₄ H ₃₈ O ₄	2-(heptadecen-1-yl)-dihydroxybenzoic acid (isomer)
29	41.58	318.2194	317.2115	-1.01	273(100), 106(19)	C ₂₀ H ₃₀ O ₃	(13:1)-anacardic acid ²
30	42.58	370.2507	369.2425	1.67	325(100), 106(23)	C ₂₄ H ₃₄ O ₃	(17:3)-anacardic acid ²
62	43.13	388.2613	387.2525	-0.22	343(100)	C ₂₄ H ₃₆ O ₄	2-(heptadecen-2-yl)-dihydroxybenzoic acid
32	44.86	346.2507	345.2427	0.96	301(100), 106(22)	C ₂₂ H ₃₄ O ₃	(15:1)-anacardic acid ²
31	45.51	320.2351	319.2271	1.58	275(100), 106(20)	C ₂₀ H ₃₂ O ₃	(13:0)-anacardic acid ²
36	49.71	374.2820	373.2739	1.33	329(100), 106(23)	C ₂₄ H ₃₈ O ₃	(17:1)-anacardic acid ²
35	51.08	348.2664	347.2582	-0.71	303(100), 106(21)	C ₂₂ H ₃₆ O ₃	(15:0)-anacardic acid ²

¹The identification of this compound was corroborated by isolation and NMR spectra analysis. ²The identification of this compound was corroborated by isolation and ESI/HRMS/MS analysis. ³The identification of this compound was corroborated by comparison with standard solution

For an unambiguous attribution of the hypothesized constituents, the MeOH extract was submitted to chromatographic purification steps, and the main isolated compounds were characterized by 1D and 2D NMR experiments.

6.3.1.2 Isolation and characterization

The MeOH extract was fractionated by size-exclusion chromatography on a Sephadex LH-20 column, the obtained fractions were further purified by RP-HPLC, and the structural elucidation of the isolated compounds was performed by interpreting the experimental spectra achieved by heteronuclear (HSQC and HMBC) NMR experiments. Finally, the obtained data were compared with scientific literature (de Souza Santos et al., 2017; Tourè et al., 2018; Braca et al., 2003; Duan et al., 2004; Amer et al., 2012).

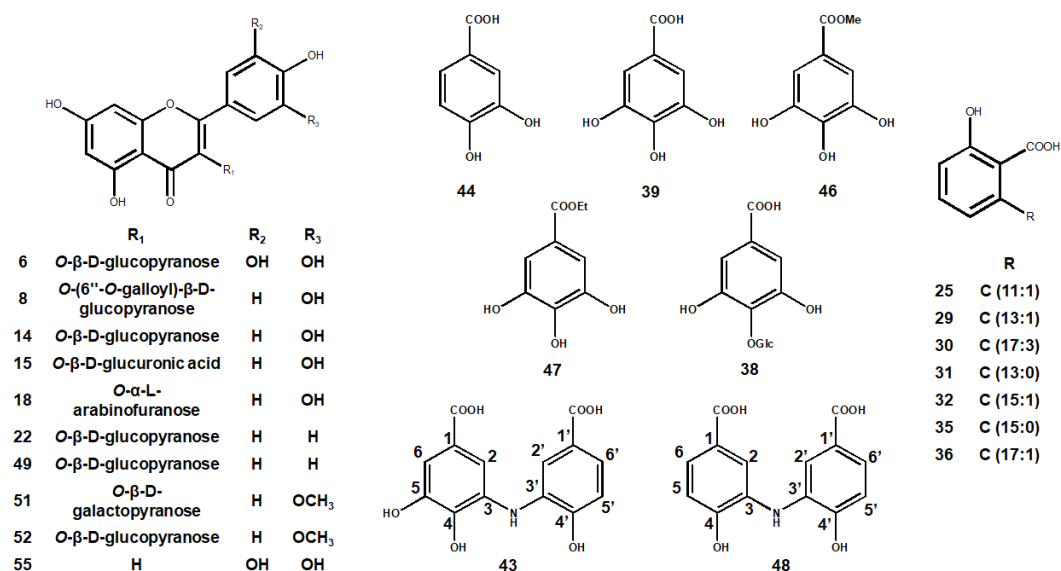


Figure 6.7 Structures of the compounds isolated from the MeOH extract of *P. vera* husks

Gallic acid (**39**) and its derivatives, like methoxy- (**46**) and ethoxy- (**47**) gallates, gallic acid 4-*O*-β-D-glucopyranoside (**38**), jointly with protocatechuic acid (**44**), showed to be recurrent secondary metabolites in *Pistacia* genus, as well as in the Anacardiaceae family (Ersan et al., 2016; de Souza Santos et al., 2017; Al Sayed et al., 2010). Gallic acid (**39**), and so several of its analogues, showed to possess intense antioxidant properties, together with anticancer and antiinflammatory activities, and resulted effective against *Pseudomonas* strains often found in

contaminated foodstuffs (Locatelli et al., 2013; Sorrentino et al., 2018). Due to the multiplicity of the exerted biological activities, over the last years interest has grown towards gallic acid (**39**), suggesting a future employment as lead compound in drug development (Nayeem et al., 2016).

In addition to gallic acid (**39**) and its derivatives, several glycosylated flavonoids were isolated, along with luteolin (**55**), and identified as myricetin 3-*O*- β -D-glucopyranoside (**6**), quercetin 3-*O*-(6''-*O*-galloyl)- β -D-glucopyranoside (**8**), quercetin 3-*O*- β -D-glucopyranoside (**14**), quercetin 3-*O*- β -D-glucuronide (**15**), quercetin 3-*O*- α -L-arabinofuranoside (**18**), kaempferol 3-*O*- β -D-galactopyranoside (**49**), kaempferol 3-*O*- β -D-glucopyranoside (**22**), isorhamnetin 3-*O*- β -D-galactopyranoside (**51**), kaempferol 3-*O*- β -D-glucopyranoside (**52**).

The accurate *m/z* values determined for pseudomolecular ion $[M-H]^-$ of compounds **43** and **48** (304.0455 and 288.0506, respectively), suggested the presence of an odd number of nitrogen atoms, while their fragmentation patterns suggested for compound **43** a structure constituted by a *p*-hydroxybenzoic acid bonded to a protocatechuic acid, and for compound **48** two linked *p*-hydroxybenzoic acid moieties. Compounds **43** and **48** on the basis of *m/z* values and fragmentation patterns have been identified as trihydroxyiminobenzoic acid and dihydroxyiminodibenzoic acid, respectively (Amer et al., 2012; Klika et al., 2014). However, for an unambiguous assessment of the amino-bridge position, both compounds were submitted to 1D (Fig. 6.8 for **43**, Fig. 6.11 for **48**) and 2D (HSQC: Fig. 6.9 for **43**, Fig. 6.12 for **48**; HMBC: Fig. 6.10 for **43**, Fig. 6.13 for **48**) NMR experiments.

The $^1\text{H-NMR}$ spectrum of compound **43** (Fig. 6.8) showed signals ascribable to H-5' at δ 6.83 (d, $J = 9.2$ Hz) and to H-6' at δ 7.42 (dd, $J = 1.9, 9.2$ Hz), with overlapped signals at δ 7.16-7.17, corresponding to H-2' [δ 7.17 (d, $J = 1.9$ Hz)], and to H-2,6 at δ 7.16-7.17 (s). Signals at δ 7.16 (H-2, s) and 7.17 (H-6, s) showed in the HMBC spectrum (Fig. 6.10) a correlation with C-4 at δ 139.4 and $\underline{\text{COOH}}$ at

δ 169.9, suggesting the presence of a gallic acid-like subunit. On the other hand, signal at δ 7.17 (H-2') and δ 7.42 (H-6') correlated in the HMBC spectrum (Fig. 6.10) with C-4' at δ 151.2 and COOH at δ 170.8, while the signal at δ 6.83 (H-5') showed correlation with C-1' at δ 121.9 and C-3' at δ 134.4, suggesting the presence of a protocatechuic acid like moiety. Interestingly, for C-3' (δ 134.4) a lower δ was observed, if compared with NMR spectroscopic data reported for protocatechuic acid, usually about δ 144.8, suggesting a linkage with an heteroatom different from oxygen. A following comparison of the experimental spectral data with scientific literature allowed to unambiguously determine compound **43** as 4,5,4'-trihydroxy-3,3'-iminobenzoic acid (Amer et al., 2012).

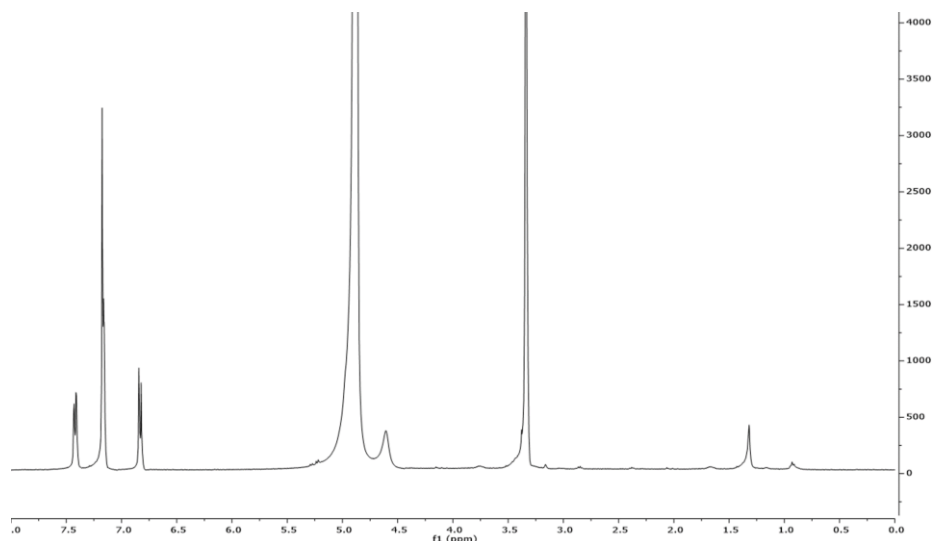
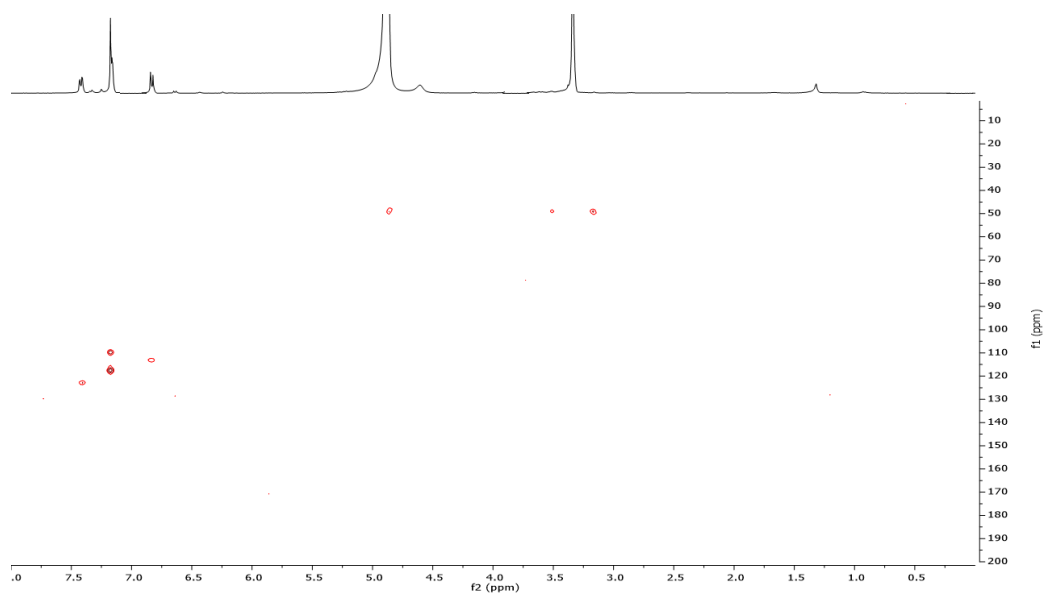
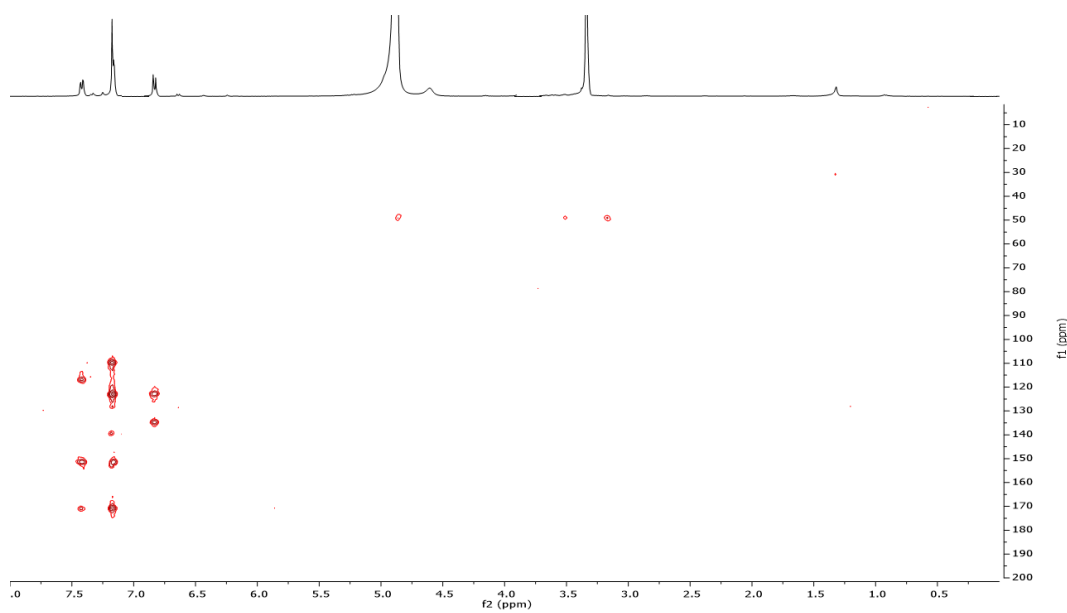


Figure 6.8 ^1H -NMR spectrum of compound **43**

Figure 6.9 HSQC spectrum of compound **43**Figure 6.10 HMBC spectrum of compound **43**

On the other hand, the ^1H -NMR spectrum of compound **48** (Fig. 6.11) showed signals ascribable to H-2,2' at δ 7.89 (d, $J = 1.8$ Hz), to H-5,5' at δ 6.91 (d, $J = 8.5$

Hz) and to H-6,6' at δ 7.54 (dd, $J = 1.8, 8.5$ Hz). The observed multiplicity suggested the occurrence of a 1,3,4-trisubstituted aromatic ring. The signal at δ 7.89 (C-2,2', δ 115.9) showed in the HMBC spectrum (Fig. 6.13) correlation with C-6,6' at δ 123.9 and C-4,4' at δ 151.3, this last one observed also for signal at δ 7.54 (C-6,6', δ 123.9) which additionally correlated with C-2,2' at δ 115.9. The signal at δ 6.91 (C-5,5', δ 113.4) correlated in the HMBC spectrum with C-1,1' at δ 122.0 and C-3,3' at δ 134.2. The carbon chemical shift observed for C-3,3' exhibited a value as in compound **43**, suggesting an heteroatom different from oxygen. Moreover, HRMS showed a m/z value higher than expected for a single trisubstituted aromatic ring, while the occurrence of only three signals in the $^1\text{H-NMR}$ spectrum suggested compound **48** as a symmetric molecule. The achieved information, along with data reported in scientific literature, allowed to univocally identify compound **48** as 4,4'-dihydroxy-3,3'-iminodibenzoic acid (Klika et al., 2014).

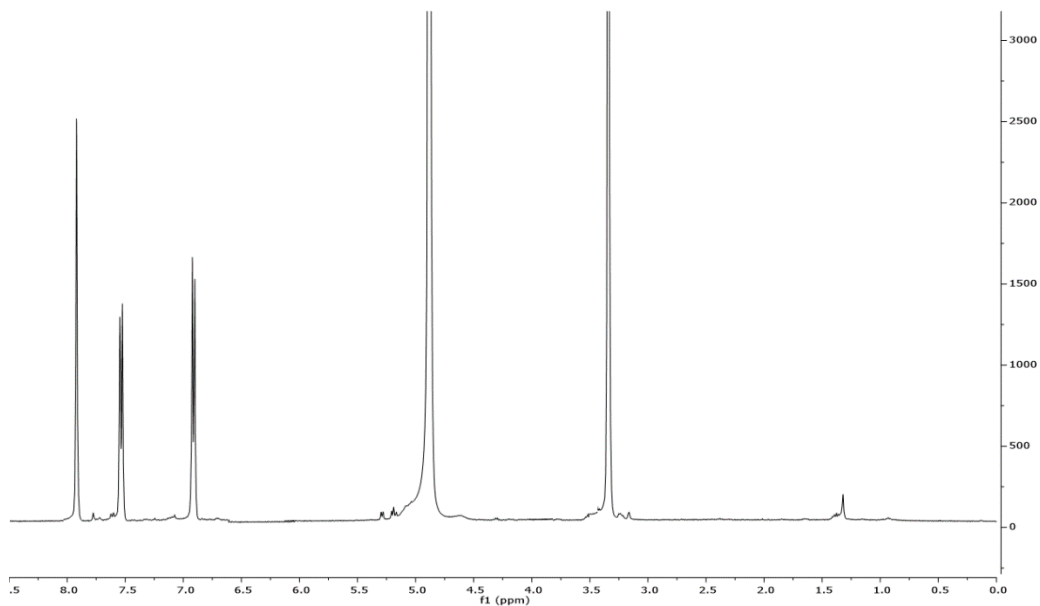


Figure 6.11 $^1\text{H-NMR}$ spectrum of compound **48**

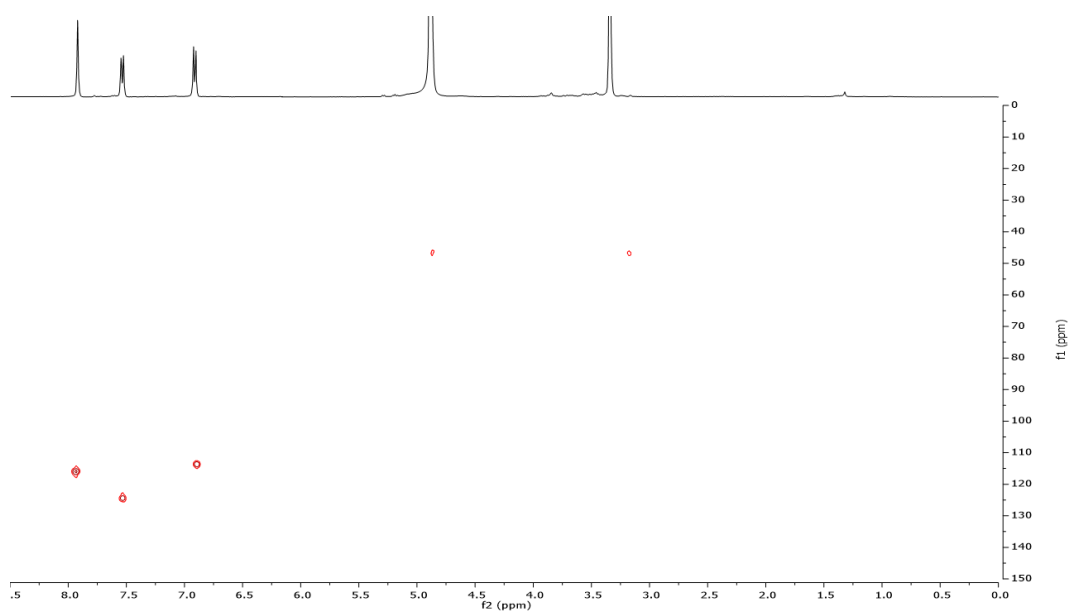


Figure 6.12 HSQC spectrum of compound 48

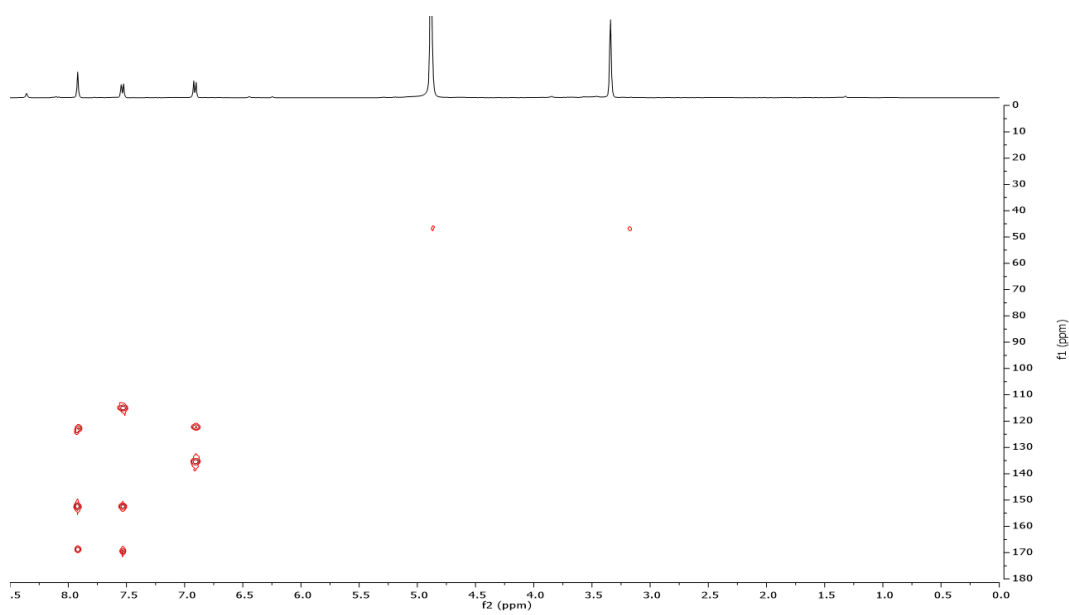


Figure 6.13 HMBC spectrum of compound 48

Table 6.4 ^1H (600 MHz) and ^{13}C (150 MHz) NMR spectral data of compounds **43** and **48**

	43		48	
	δ_{C}	δ_{H} (J in Hz)	δ_{C}	δ_{H} (J in Hz)
1	122.7	-	122.0	-
2	109.5	7.16, s	115.9	7.89, d(1.8)
3	132.2	-	134.2	-
4	139.4	-	151.3	-
5	143.7	-	113.4	6.91, d(8.5)
6	109.9	7.17, s	123.9	7.54, dd(1.8, 8.5)
<u>COOH</u>	169.9	-	169.7	-
1'	121.9	-	122.0	-
2'	116.6	7.17, d(1.9)	115.9	7.89, d(1.8)
3'	134.4	-	134.2	-
4'	151.2	-	151.3	-
5'	113.2	6.83, d(9.2)	113.4	6.91, d(8.5)
6'	122.4	7.42, dd(1.9, 9.2)	123.9	7.54, dd(1.8, 8.5)
<u>COOH</u>	170.8	-	169.7	-
NH	-	exchange	-	exchange

In MeOH- d_4

Finally, since in the LC-HRMS profile (Fig. 6.6) the peaks related to anacardic acids were observed, they were isolated by direct purification of the MeOH extract by semi-preparative RP-HPLC-UV/Vis. So far the isolation of compounds **25**, **29**, **30**, **31**, **32**, **35** and **36** was performed; their structural elucidation was carried out by ESI/HRMS/MS experiments in negative ion mode, allowing to determine their accurate m/z values and to acquire their characteristic fragmentation patterns. The obtained information allowed to confirm the identity of the isolated compounds as anacardic acids, and to assess the side chains length and unsaturation degree. Detected compounds were identified as (11:1)-anacardic acid (**25**), (13:1)-anacardic acid (**29**), (17:3)-anacardic acid (**30**), (13:0)-anacardic acid (**31**), (15:1)-anacardic acid (**32**), (15:0)-anacardic acid (**35**) and (17:1)-anacardic acid (**36**). However, also performing MS^n experiments the achieved information were not exhaustive enough to define the position of the unsaturations.

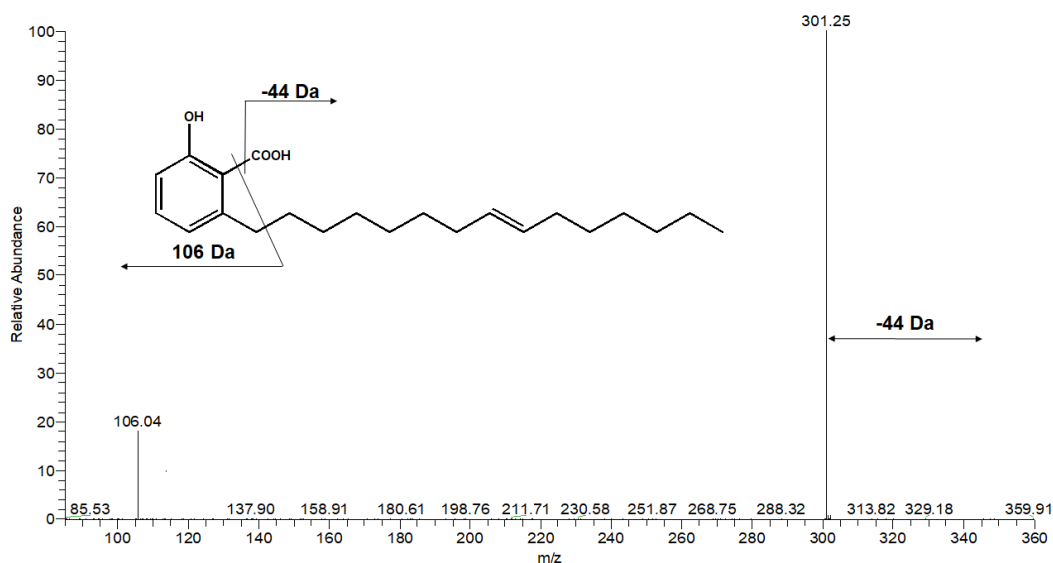


Figure 6.14 ESI/MS/MS spectrum of compound **32** in negative ion mode

Notwithstanding, a subsequent matching among the isolated compounds and those reported in Table 6.3 evidenced constituents not isolated from the husks MeOH extract. Such compounds were putatively identified by comparing the accurate m/z values and the MS/MS spectra with data reported in scientific literature, as well as with online databases specific on mass spectra of natural products (FoodB). Where possible, identification of not isolated constituents was assessed by comparing the R_t observed in the LC-HRMS profile (Fig. 6.6) with R_t of reference standard solutions analyzed in the same experimental conditions (it is the case of compound **16**, identified as 1,2,3,4,6-penta-*O*-galloyl- β -D-glucopyranoside).

Compound **40** (m/z 325.0558) exhibited in the fragmentation spectrum a product ion at m/z 169, ascribable to a deprotonated gallic acid, which underwent to a neutral loss of the carboxylic group as carbon dioxide (-44 Da), generating a fragment ion at m/z 125. Molecular formula was established as $C_{14}H_{14}O_9$. On the basis of scientific literature, it was possible to putatively identify compound **40** as galloyl shikimic acid (Ersan et al., 2016).

Compounds **41**, **56-58** exhibited in their tandem mass spectra a common base peak at m/z 313, ascribable to a glycosylated gallic acid moiety, and fragment ions at m/z 169 corresponding to a deprotonated gallic acid. Unfortunately the achieved information did not allow a more accurate structural elucidation of the detected compounds, tentatively identified as gallic acid derivatives (Ersan et al., 2016).

Compound **17** (m/z 335.0402) produced in MS/MS experiments a base peak at m/z 183, originating from the loss of a dehydrated gallic acid from parent ion and ascribable to a deprotonated gallic acid methyl ester ion, supporting a putative identification as methyl digallate (Ersan et al., 2016).

Furthermore, compounds **50**, **53** and **54** showed in their MS/MS spectra a common fragmentation pattern for this class of molecules, characterized by a base peak at m/z 331 due to the neutral loss of a dehydrated hexose moiety (-162 Da), and diagnostic product ions at m/z 169, related to a deprotonated gallic acid ion, and m/z 125, originated by a subsequent decarboxylation (-44 Da). The comparison of the obtained data with scientific reports suggested compounds **50**, **53** and **54** as digallate hexosides (Ersan et al., 2016).

In addition, compound **42** (m/z 401.1444) showed in MS/MS experiments a base peak at m/z 269 originating from the neutral loss of a dehydrated pentoside (-132 Da), along with a fragment ion at m/z 161 ascribable to a deprotonated dehydrated hexose ion. Molecular formula was established as $C_{18}H_{26}O_{10}$. According to the achieved information, it was possible to tentatively assess the identity of compound **42** as benzyl hexoside pentoside (Amessis-Ouchemoukh et al., 2017).

Finally, compound **24** (m/z 675.3585) exhibited in its fragmentation spectrum a base peak at m/z 397 originating from the loss of a C (18:3) fatty acyl chain (-278 Da), whose occurrence was confirmed by the signal observed at m/z 277; in addition, a product ion at m/z 513 suggested the loss of a dehydrated hexose moiety (-162 Da). Matching the experimental MS/MS spectrum with online databases

(LipidMaps) allowed to putatively identify compound **24** as DGMG (18:3), previously detected in the leaves.

6.3.1.3 “Eco-friendly” extraction methods show class-specific selectivity

In the frame of a sustainable and “green” chemistry, along with the purpose to suggest simple and quick extraction methods by using solvents with reduced costs and toxicity, *P. vera* husks were extracted employing EtOH 96% and a hydroalcoholic solution (EtOH:H₂O, 1:1, v/v); the extracts were successively submitted to LC-ESI/LTQOrbitrap/MS experiments in negative ion mode, and the profiles compared with the MeOH extract profile obtained in the same experimental conditions (Fig. 6.15).

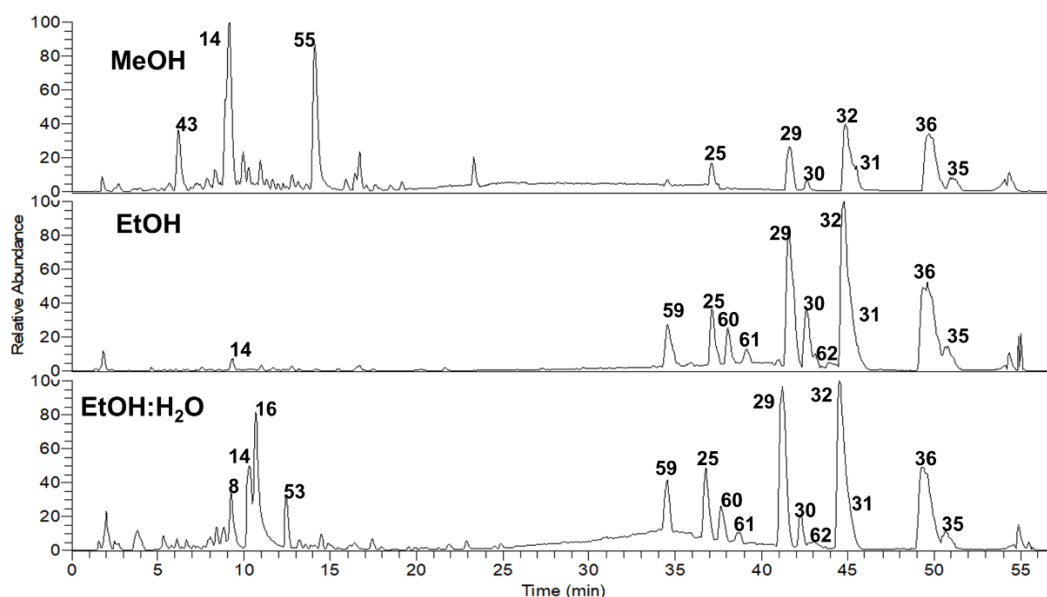


Figure 6.15 LC-HRMS profiles in negative ion mode of the MeOH, EtOH and EtOH:H₂O extracts of *P. vera* husks

As previously observed for the leaves (Fig. 6.2), also in this case EtOH and EtOH:H₂O solution exhibited selectivity towards certain classes of compounds: the former proved to be highly effective and specific in extracting anacardic acids, while the latter showed a good selectivity also towards some of the more polar constituents.

Noteworthy is the occurrence of additional peaks (**59**, **60**, **61**, **62**) in the LC-HRMS profiles of the “eco-friendly” extracts, not detected in the MeOH extract profile. Therefore, to assign the identity of the new spotted compounds, tandem mass spectrometry experiments in data dependent scan mode were performed. This operation returned MS/MS spectra featured by a common base peak ascribable to the loss of a carboxylic group as carbon dioxide (-44 Da), as observed for anacardic acids. Moreover, an integrative determination of the accurate m/z values and comparison with scientific literature led to the putative identification of compounds **59**, **60**, **61**, **62** as 2-(pentadecen-1-yl)-dihydroxybenzoic acid (**59**), 2-(heptadecen-1-yl)-dihydroxybenzoic acid (**60**), 2-(heptadecen-1-yl)-dihydroxybenzoic acid (isomer) (**61**) and 2-(heptadecen-2-yl)-dihydroxybenzoic acid (**62**). Such compounds have been reported as gentisic acid derivatives in *Micronychia tsiramiramy* (Anacardiaceae), showing *in vitro* a moderate antiplasmodial activity against a chloroquine-resistant *Plasmodium falciparum* strain, as well as a discreet cytotoxicity against human cervix carcinoma cell line KB-3-1 (Razakariny et al., 2016).

6.3.1.4 Antioxidant activity of the extracts of *P. vera* husks

To estimate the phenolic content of the different prepared extracts, Folin-Ciocalteu assay was carried out; in addition, radical scavenging activity was evaluated by DPPH• and ABTS^{•+} assays (Table 6.5).

Among the employed solvents, MeOH resulted the most effective in extracting phenolics (411.98 ± 28.39 GAE mg/g dried extract). Due to the highest phenolic content, MeOH extract exerted the strongest radical scavenging activity towards DPPH• ($IC_{50} = 6.62 \pm 0.41$ μ g/mL) and ABTS^{•+} (1.69 ± 0.06 mM) if compared to the other extracts.

Table 6.5 Total phenolic content, DPPH• and ABTS^{•+} radical scavenging activity of the extracts of *P. vera* husks

Sample	Total phenolic content		DPPH•		ABTS ^{•+}	
	GAE ^a	SD ^d	IC ₅₀ ^b	SD ^d	TEAC ^c	SD ^d
Husks MeOH	411.98	± 28.39	6.62	± 0.41	1.69	± 0.06
Husks EtOH	219.57	± 38.79	23.59	± 2.14	1.23	± 0.05
Husks EtOH/H ₂ O	274.57	± 27.31	18.86	± 1.36	1.32	± 0.05
Vit. C			5.16	± 0.11		
Quercetin					1.87	± 0.08

^a Values are expressed as gallic acid equivalents (GAE) mg/g of dried extract. ^b Values are expressed as µg/mL. ^c Values are expressed as concentration (mM) of a standard Trolox solution exerting the same antioxidant activity of a 1 mg/mL solution of the tested extract. ^d Standard Deviation of three independent experiments.

6.4 Phenolic-based metabolite profile of *P. vera* shells extracts

Pistacia vera L. shells



Thin, beige colored and totally enveloped by the husk, initially intact they tear by ripening advancing, turning into a bivalve shell and showing the inner edible seed.

6.4.1 Results and discussion

6.4.1.1 LC-ESI/LTQOrbitrap/MS/MS of the MeOH extract of *P. vera* shells

The MeOH extract of *P. vera* shells was initially submitted to LC-ESI/LTQOrbitrap/MS/MS experiments, in negative ion mode, aiming at gaining inceptive information about the chemical composition. The LC-HRMS profile (Fig. 6.16) exhibited several peaks with m/z values suggesting the occurrence of different classes of phenolics.

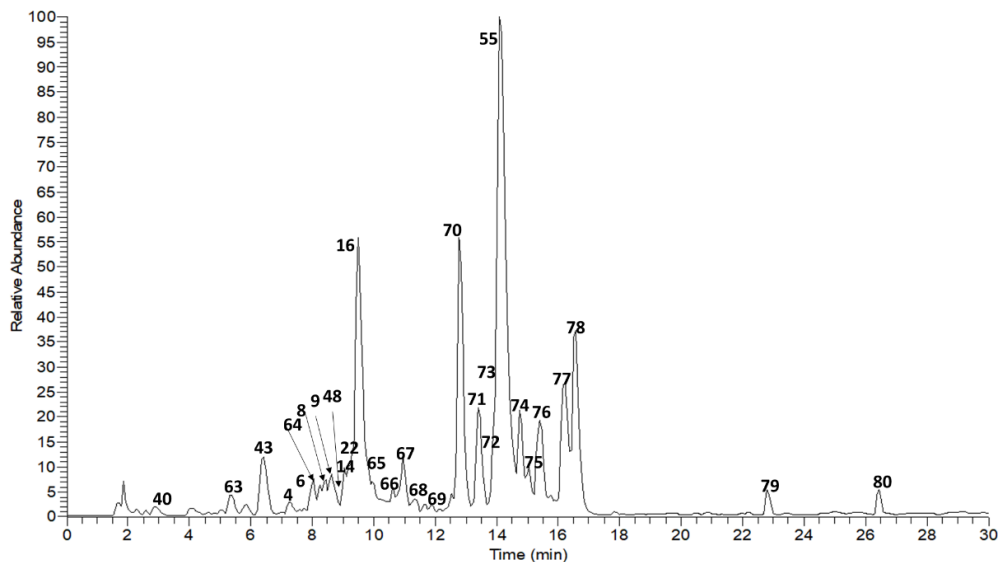


Figure 6.16 LC-HRMS profile in negative ion mode of the MeOH extract of *P. vera* shells

In agreement with the initial achieved information and an exhaustive research in scientific literature, it was possible to tentatively identify the detected compounds

as gallic acid derivatives (**9**, **16**, **40**, **63**, **64**), amino alkaloids (**43**, **48**), phenolic acids (**69**), fatty acids (**80**), flavonoids (**4**, **6**, **8**, **14**, **22**, **55**, **65-67**, **77**, **78**), lignans (**68**, **73**, **74**, **76**), neolignans (**70**, **71**, **75**) and anacardic acids (**29**, **31**, **32**, **36**) (Table 6.6).

Table 6.6 Compounds identified and putatively identified in the MeOH extract of *P. vera* shells

N°	R _t	Calculated Mass	[M-H] ⁻	Δppm	MS ² (%)	Molecular formula	Compound
40	2.85	326.0637	325.0557	0.38	169(100), 125(10)	C ₁₄ H ₁₄ O ₉	galloyl shikimic acid
63	5.37	454.1111	453.1027	-0.47	327(62), 313(100), 301(46), 169(24)	C ₂₀ H ₂₂ O ₁₂	hydroxymethoxyphenyl galloyl hexoside
43	6.4	305.0535	304.0456	1.54	260(100), 166(61), 153(38), 150(59), 122(31)	C ₁₄ H ₁₁ NO ₇	4,5,4'-trihydroxy-3,3'-iminobenzoic acid ¹
4	7.24	632.1013	631.0930	1.63	479(100), 317(5)	C ₂₈ H ₂₄ O ₁₇	myricetin 3- <i>O</i> -(6'- <i>O</i> -galloyl)-β-glucopyranoside ¹
6	7.97	480.0903	479.0821	-1.27	317(54), 316(100)	C ₂₁ H ₂₀ O ₁₃	myricetin 3- <i>O</i> -β-D-glucopyranoside ¹
64	8.23	498.1373	497.1288	0.99	327(89), 313(100), 183(29), 169(13)	C ₂₂ H ₂₆ O ₁₃	trimethoxyphenyl galloyl hexoside
8	8.38	616.1064	615.0979	0.84	463(100), 301(18)	C ₂₈ H ₂₄ O ₁₆	quercetin 3- <i>O</i> -(6'- <i>O</i> -galloyl)-β-glucopyranoside ¹
9	8.62	788.1072	787.0982	0.62	635(28), 617(100), 465(12)	C ₃₄ H ₂₈ O ₂₂	1,2,3,6-tetra- <i>O</i> -galloyl-β-D-glucopyranoside ²
48	9.03	289.0586	288.0506	0.74	270(32), 244(100), 200(26), 150(28), 137(19), 106(15), 93(14)	C ₁₄ H ₁₁ NO ₆	4,4'-dihydroxy-3,3'-imino-di-benzoic acid ²
14	9.15	464.0954	463.0871	-1.11	301(100)	C ₂₁ H ₂₀ O ₁₂	quercetin 3- <i>O</i> -β-D-glucopyranoside ¹
22	9.28	448.1005	447.0923	0.77	285(100)	C ₂₁ H ₂₀ O ₁₁	kaempferol 3- <i>O</i> -β-D-glucopyranoside ¹
16	9.47	940.1181	939.1103	0.96	787(15), 769(100), 617(11), 599(9), 393(81), 317(24), 169(28)	C ₄₁ H ₃₂ O ₂₆	1,2,3,4,6-penta- <i>O</i> -galloyl-β-D-glucopyranoside ¹
65	9.95	304.0583	303.0502	1.58	285(100), 177(10), 125(6)	C ₁₅ H ₁₂ O ₇	taxifolin
66	10.63	432.1056	431.0972	1.23	311(5), 269(100)	C ₂₁ H ₂₀ O ₁₀	apigenin hexoside
67	10.95	462.1162	461.1078	1.47	446(89), 299(100)	C ₂₂ H ₂₂ O ₁₁	chrysoeriol hexoside
68	11.6	434.1576	433.1489	-1.20	418(16), 403(62), 385(16), 373(100), 181(15)	C ₂₂ H ₂₆ O ₉	hydroxysyringaresinol
69	11.94	360.0845	359.0760	0.53	197(25), 179(19), 161(100)	C ₁₈ H ₁₆ O ₈	rosmarinic acid
70	12.79	586.2414	585.2328	0.88	567(12), 537(100), 371(29), 359(26), 356(15), 195(15), 165(8)	C ₃₁ H ₃₈ O ₁₁	acernikol
71	13.39	586.2414	585.2331	-1.48	567(11), 537(100), 371(29), 359(26), 356(15), 195(15), 165(7)	C ₃₁ H ₃₈ O ₁₂	acernikol (isomer)

72	13.6	492.1056	491.0967	0.39	311(100)	C ₂₆ H ₂₀ O ₁₀	unknown
73	13.86	644.2468	643.2384	1.42	625(15), 613(26), 595(100), 565(8), 417(48), 401(12), 387(21), 225(17), 195(18)	C ₃₃ H ₄₀ O ₁₃	buddlenol D
55	14.07	286.0477	285.0399	-1.01	267(21), 257(35), 243(70), 241(100), 217(74), 199(95), 175(88), 151(36), 133(18)	C ₁₅ H ₁₀ O ₆	luteolin ¹
74	14.75	810.3098	809.3009	0.66	791(100), 773(91), 761(75), 743(76), 713(48), 667(27), 613(40), 595(26), 565(52), 417(12), 195(24), 181(12)	C ₄₂ H ₅₀ O ₁₆	hedyotisol A
75	15.03	582.2101	581.2017	0.59	533(25), 385(100), 370(9), 195(6)	C ₃₁ H ₃₄ O ₁₁	buddlenol A
76	15.4	810.3098	809.3010	0.46	791(95), 773(42), 761(100), 743(51), 713(36), 667(38), 619(11), 613(80), 595(62), 565(84), 417(39), 195(21), 181(13)	C ₄₂ H ₅₀ O ₁₆	hedyotisol A (isomer)
77	16.22	270.0528	269.0447	-1.42	225(100), 201(31), 183(23), 151(29), 149(49)	C ₁₅ H ₁₀ O ₅	apigenin
78	16.57	300.0633	299.0553	1.09	285(5), 284(100)	C ₁₆ H ₁₂ O ₆	chrysoeriol
79	22.81	714.2676	713.2585	1.42	698(12), 537(100), 519(26), 505(86), 369(34)	C ₄₀ H ₄₂ O ₁₂	unknown
80	26.42	316.2613	315.2533	-0.49	297(100), 279(19), 171(36), 155(15), 141(12), 127(10)	C ₁₈ H ₃₆ O ₄	9,10-Dihydroxystearic acid
29	41.19	318.2194	317.2110	0.35	273(100)	C ₂₀ H ₃₀ O ₃	(13:1)-anacardic acid ²
32	45.29	346.2507	345.2424	0.47	301(100)	C ₂₂ H ₃₄ O ₃	(15:1)-anacardic acid ²
31	45.51	320.2351	319.2269	0.95	275(100)	C ₂₀ H ₃₂ O ₃	(13:0)-anacardic acid ²
36	50.15	374.2820	373.2734	-0.48	329(100)	C ₂₄ H ₃₈ O ₃	(17:1)-anacardic acid ²

¹The identification of this compound was corroborated by isolation and NMR spectra analysis. ²The identification of this compound was corroborated by comparison with standard solution.

However, for an unambiguous attribution of the main constituents detected in the LC-HRMS profile, the MeOH extract was purified by employing chromatographic techniques, and the structural elucidation of the isolated compounds was carried out by NMR experiments.

6.4.1.2 Isolation and characterization

A starting size-exclusion chromatography step was carried out on the MeOH extract of *P. vera* shells, and the achieved fractions further purified by RP-HPLC.

Isolated compounds were submitted to 1D and 2D NMR experiments, and the obtained data compared with scientific literature.

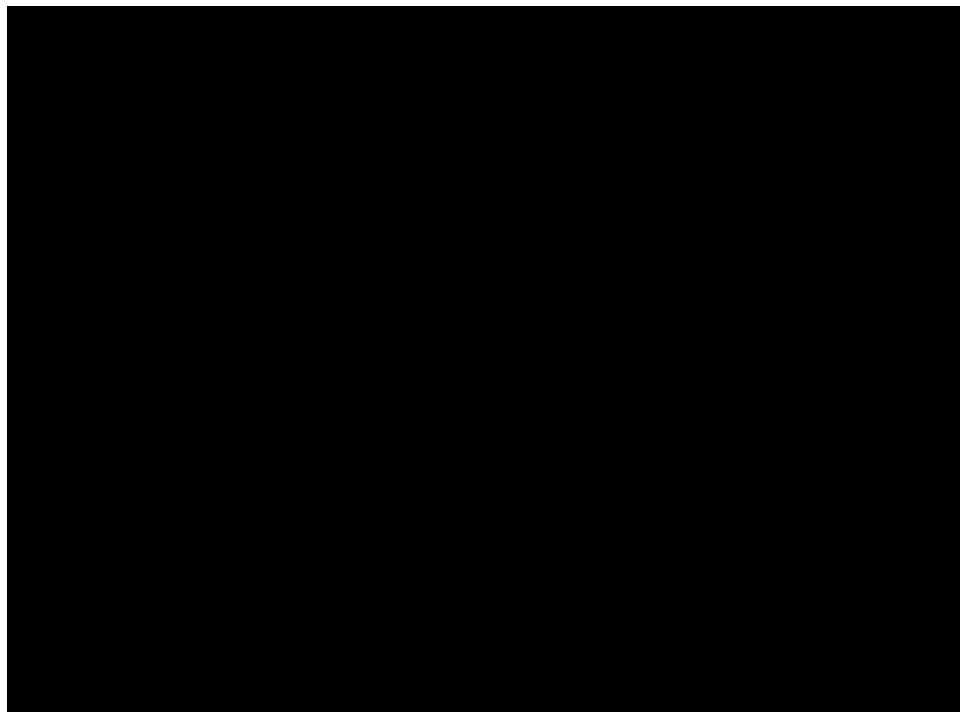


Figure 6.17 Compounds isolated from the MeOH extract of *P. vera* shells

As result, compound **16** was identified as 1,2,3,4,6-penta-*O*-galloyl- β -D-glucopyranoside, a gallic acid derivative which showed to possess antibacterial activity against a broad spectrum of both Gram-positive and Gram-negative bacteria, including antibiotic resistant strains (Cho et al., 2010).

In addition, isolated flavonoids were identified as myricetin 3-*O*-(6''-*O*-galloyl)- β -D-glucopyranoside (**4**), myricetin 3-*O*- β -D-glucopyranoside (**6**), quercetin 3-*O*-(6''-*O*-galloyl)- β -D-glucopyranoside (**8**), quercetin 3-*O*- β -D-glucopyranoside (**14**), kaempferol 3-*O*- β -D-glucopyranoside (**22**) and luteolin (**55**) (Vitek et al., 2017; Bottone et al., 2018). Besides the characteristic antioxidant properties, flavonoids have been also reported for their anticancer activity, like compound **8**, which reduced *in vitro* cell viability of leukemic CCRF-CEM cells (Vitek et al., 2017).

Furtherly, compound **43** was identified as 4,5,4'-trihydroxy-3,3'-iminobenzoic acid, previously reported in *P. vera* husks.

However, not all the compounds detected in the LC-HRMS profile (Fig. 6.16) were isolated. Nevertheless, the identification of the other constituents was performed by different approaches. For compounds **9**, **29**, **31**, **32**, **36** and **48**, attribution was carried out by comparing their R_t with reference standard solutions. Otherwise, for the other constituents structural elucidation was carried out through interpretation of the MS/MS spectra acquired by tandem mass spectrometry experiments, along with determination of accurate m/z values, followed by comparison with data reported in scientific reports and online databases (FoodB, MetFrag).

Compound **40** (at m/z 325.0557) exhibited in the MS/MS spectrum a base peak at m/z 169, related to a deprotonated gallic acid ion, along with a product ion at m/z 125, generated by a subsequent loss of the carboxylic group as carbon dioxide (-44 Da). Molecular formula was established as $C_{14}H_{14}O_9$. As previously reported in the *P. vera* husks, compound **40** was putatively identified as galloyl shikimic acid (Ersan et al., 2016) (Table 6.6).

Compound **63** (m/z 453.1027) yielded in MS/MS experiments a base peak at m/z 313, ascribable to a deprotonated galloyl dehydrohexoside ion, originated from the loss of a hydroxymethoxyphenol moiety; moreover, the product ion observed at m/z 301 was generated by the loss of a dehydrated gallic acid (-152 Da), whose occurrence was confirmed by the signal at m/z 169. Molecular formula was established as $C_{20}H_{22}O_{12}$. Hence, in accordance with scientific literature, compound **63** was putatively identified as hydroxymethoxyphenyl galloyl hexoside (de Souza Santos et al., 2017) (Table 6.6).

Similar behaviour was observed in the fragmentation pattern of compound **64**, (m/z 497.1288), also characterized by a base peak at m/z 313, related to a deprotonated galloyl dehydrohexoside resulting ion, generated from the neutral loss

of a trimethoxyphenyl moiety. Molecular formula was established as $C_{22}H_{26}O_{13}$. Therefore, it was possible to putatively assess compound **64** as trimethoxyphenyl galloyl hexoside, in accordance with data reported in literature (Slaghenaufi et al., 2016) (Table 6.6).

Moreover, compound **69** (m/z 359.0760) showed in the fragmentation spectrum a base peak at m/z 161 ascribable to a caffeic acid anion, together with a product ion at m/z 179 due to the loss of a caffeic acid moiety, and molecular formula established as $C_{18}H_{16}O_8$, allowing a putative identification of compound **27** as rosmarinic acid (Boudiar et al., 2018) (Table 6.6).

Differently, compound **65** (m/z 303.0502) showed in the MS/MS spectrum a base peak at m/z 285 originating from the loss of a water molecule (-18 Da), along with a product ion at m/z 177 generated by the further loss of the B-ring, and an additional fragment ion at m/z 125 originated from a $^{1,4}A$ cleavage occurred at the C-ring. Molecular formula was established as $C_{15}H_{12}O_7$. Supported by the matching with online database (FoodB), compound **65** was putatively identified as taxifolin (Table 6.6).

On the other hand, compounds **66** and **67** exhibited similar fragmentation pathways, characterized by the neutral loss of a hexose moiety (-162 Da). On the basis of the accurate m/z value of the precursor ions determined in HRMS and comparison with online database (FoodB), it was possible to putatively identify compound **66** as apigenin hexoside and compound **67** as chrysoeriol hexoside (Table 6.6). Interestingly, for both compounds the corresponding aglycones were detected in the LC-HRMS profile at R_t 16.22 min (m/z 269.0447, **77**) and 16.57 min (m/z 299.0553, **78**), respectively, and putatively identified by comparing their experimental fragmentation patterns with online database (FoodB) as well (Table 6.6).

Compound **80** showed in HRMS a pseudomolecular ion $[M-H]^-$ at m/z 315.2533, suggesting a fatty acid structure presenting two hydroxy groups; submitted to

tandem mass spectrometry experiments, it yielded a base peak at m/z 297, originated from the loss of a carboxylic group as carbon dioxide (-44 Da), in addition with product ions at m/z 171 and 141 which allowed to determine the position of the hydroxy groups on the aliphatic chain. In agreement with data reported in literature, compound **80** was identified as 9,10-dihydroxystearic acid (Moe et al., 2004) (Table 6.6).

Finally, as observed in the shells of *P. dulcis*, the LC-HRMS profile of the MeOH extract of *P. vera* shells showed peaks characterized by pseudomolecular ions at m/z values suggesting the occurrence of lignans and neolignans.

Compound **68** (m/z 433.1489) showed in the MS/MS spectrum (Fig. 6.18) peculiar neutral losses of a methyl radical (-15 Da), formaldehyde (-30 Da), with a base peak at m/z 373 originated from the loss of two formaldehyde molecules (-60 Da); in addition, the signal at m/z 181 was ascribable to a deprotonated syringaldehyde ion, produced by a $^{2,5}X^-$ cleavage. Molecular formula was established as $C_{22}H_{26}O_9$. Supported by data reported in literature, compound **68** was putatively identified as hydroxysyringaresinol (Hanhineva et al., 2012) (Table 6.6).

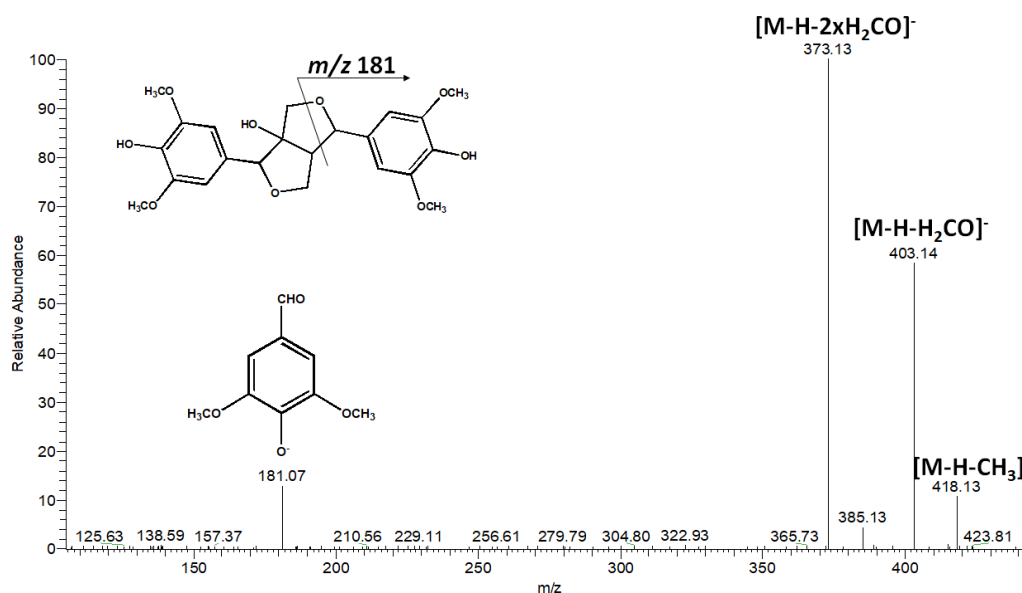


Figure 6.18 ESI/MS/MS spectrum of compound **68** in negative ion mode

Fragmentation spectra of compounds **70** and **71** (Fig. 6.19) were characterized by fragment ions deriving from neutral losses of water (-18 Da) and formaldehyde (-30 Da), single, or combined (-48 Da); in addition, diagnostic product ions originated from the loss of a guaiacylglycerol moiety (-196 Da) were observed, together with a fragment ion at m/z 223 ascribable to the $^{1,2}\text{B}^-$ ion of the aliphatic end. Relying on data reported in literature, compound **70** and **71** were putatively identified as acernikol and acernikol isomer (Morreel et al., 2010) (Table 6.6).

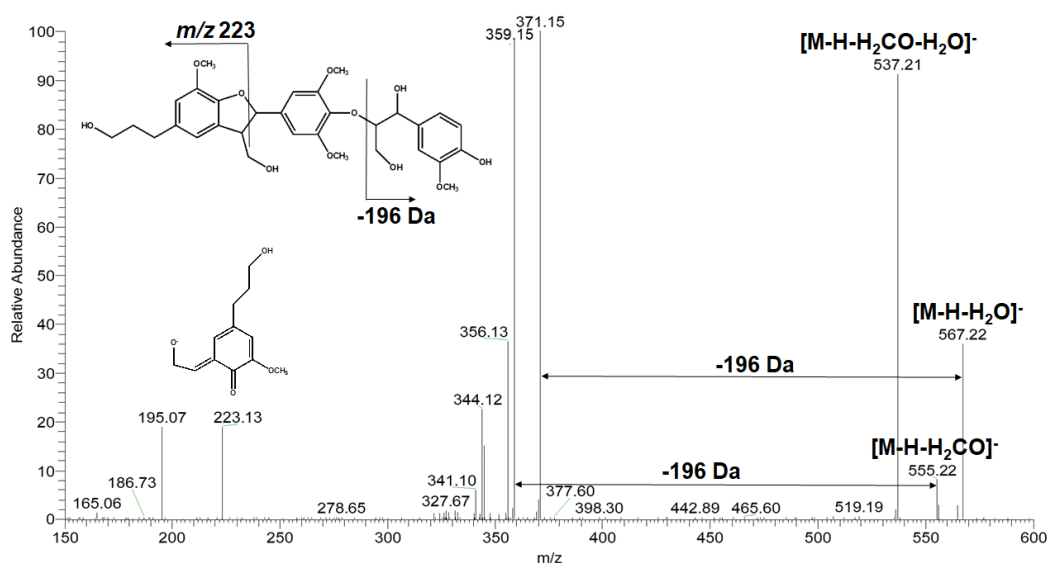


Figure 6.19 ESI/MS/MS spectrum of compound **70** in negative ion mode

Compound **73** (m/z 643.2384) exhibited in the MS/MS profile (Fig. 6.20) a base peak at m/z 595 originated from the contemporary loss of water and formaldehyde (-48 Da), a fragment ion at m/z 417 generated from the neutral loss of a dehydrated syringoylglycerol (-226 Da), confirmed by the signal at m/z 225, and a diagnostic fragment ion at m/z 181 already observed for compound **68**, corresponding to a deprotonated syringaldehyde ion deriving from a $^{2,5}\text{X}^-$ cleavage. Molecular formula was established as $\text{C}_{33}\text{H}_{40}\text{O}_{13}$. By comparing achieved information with scientific literature, compound **73** was putatively identified as buddlenol D (Hanhineva et al., 2012) (Table 6.6).

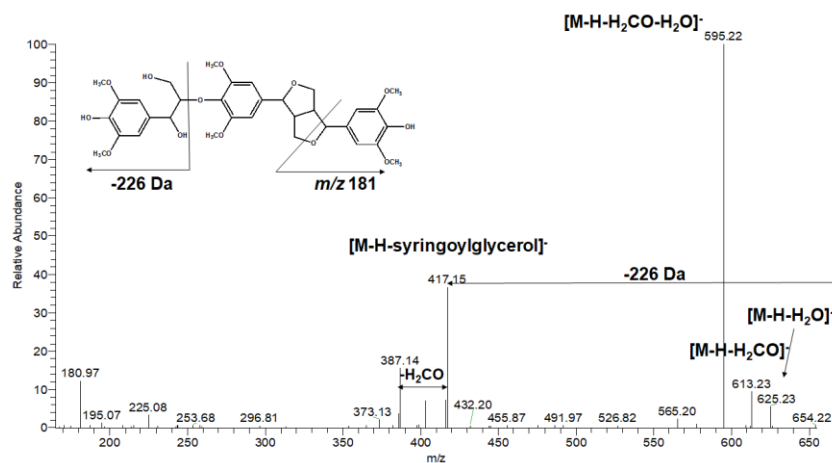


Figure 6.20 ESI/MS/MS spectrum of compound **73** in negative ion mode

Compounds **74** and **76** showed in their MS/MS spectra (Fig. 6.21) informative neutral losses of water (-18 Da) and formaldehyde (-30 Da), single or combined, characteristic of lignans. In addition, two consecutive neutral losses of dehydrated guaiacylglycerol moieties (-196 Da) were observed at m/z 613 and 417. At lower m/z values, the signal at m/z 195 was ascribable to a deprotonated guaiacylglycerol ion, while a deprotonated syringaldehyde ion was observed at m/z 181. A further matching with scientific reports supported the identity putatively assessed for compounds **74** and **76** as hedyotisol A and hedyotisol A isomer (Hanhineva et al., 2012) (Table 6.6).

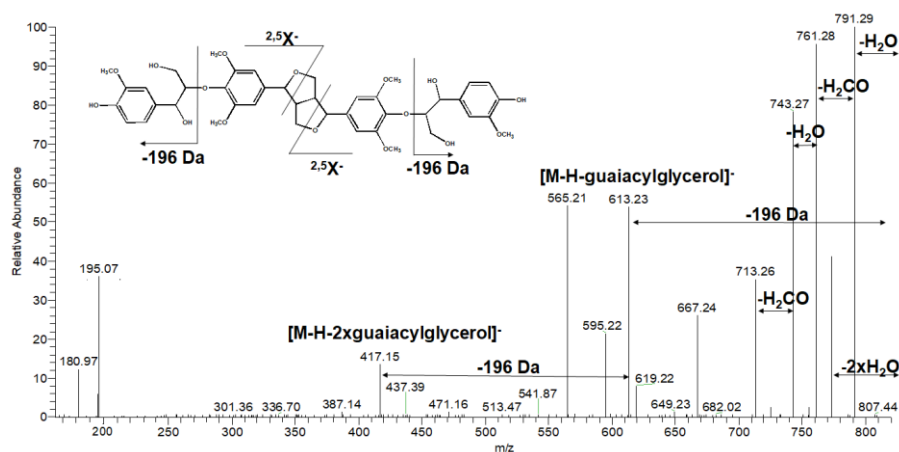


Figure 6.21 ESI/MS/MS spectrum of compound **74** in negative ion mode

Finally, the fragmentation spectrum of compound **75** (m/z 581.2017) (Fig. 6.22) exhibited a product ion at m/z 533 originated from the contemporary neutral loss of water and formaldehyde (-48 Da), and a base peak at m/z 385 yielded by the neutral loss of a dehydrated guaiacylglycerol moiety (-196 Da); moreover, the diagnostic signal at m/z 219, originated by the $^{1,2}X^-$ cleavage, suggested the occurrence of a phenylcoumaran backbone with two unsaturations on the aliphatic chain. Molecular formula was established as $C_{31}H_{34}O_{11}$. It was therefore possible to putatively assess compound **75** as buddlenol A (Li et al., 2013; Hanhineva et al., 2012) (Table 6.6).

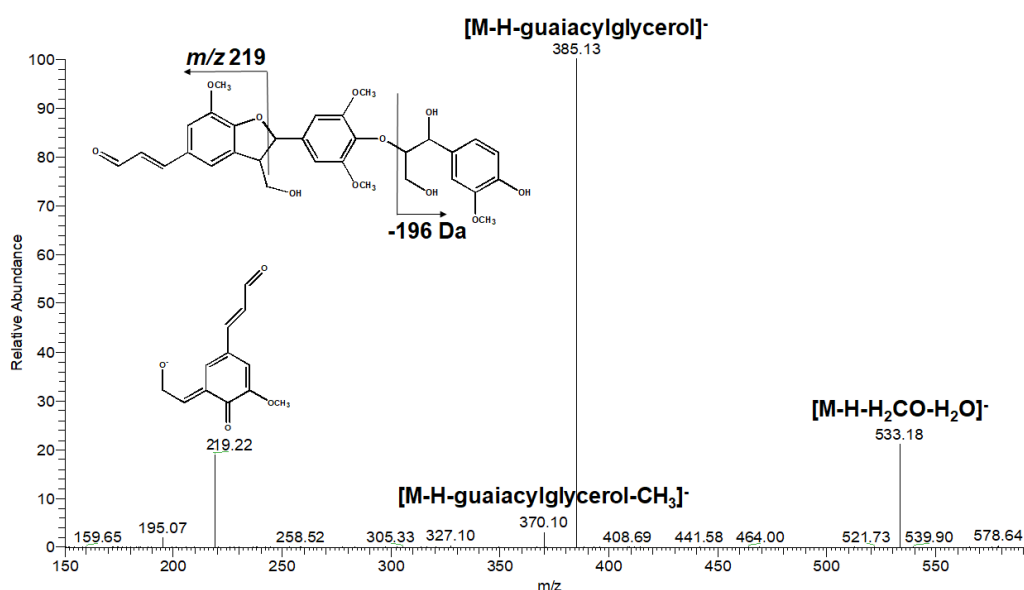


Figure 6.22 ESI/MS/MS spectrum of compound **75** in negative ion mode

6.4.1.3 “Eco-friendly” extracts and comparison by LC-ESI/LTQOrbitrap/MS

To propose alternative extraction protocols with a reduced environmental impact, thanks to the employment of “green” solvents, *P. vera* shells were extracted by maceration with EtOH 96% and an EtOH:H₂O (1:1, v/v) solution. The obtained extracts were successively analyzed by LC-ESI/LTQOrbitrap/MS experiments, and the profiles, including the MeOH extract profile, compared (Fig. 6.23).

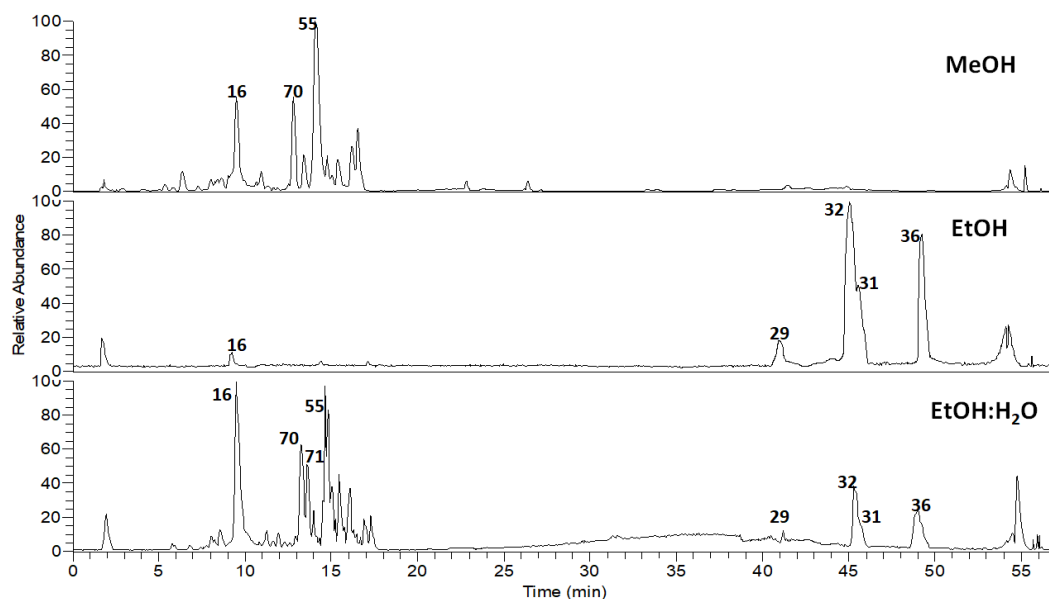


Figure 6.23 LC-HRMS profiles, in negative ion mode, of the MeOH, EtOH, EtOH:H₂O extracts of *P.vera* shells

The comparison of the LC-HRMS profiles of the prepared extracts pointed out noticeable differences in their chemical composition, since in the EtOH extracts the main constituents were represented by compounds **29**, **31**, **32** and **36**, corresponding to anacardic acids formerly isolated and identified in the husks; in EtOH:H₂O such compounds were detected as well, even if as minor constituents. Such evidences highlighted a class-specific selectivity of EtOH, resulted the most effective solvent in extracting anacardic acids.

6.4.1.4 Phenolic content and radical scavenging activity of *P. vera* shells extracts

Prompted by the occurrence of different phenolics identified in the extracts of *P. vera* shells, their total content was assessed by Folin-Ciocalteu assay. The MeOH extract showed the highest phenolic content (340.69 ± 33.15 GAE mg/g dried extract) if compared to EtOH and EtOH:H₂O extracts, as well as the best antioxidant activity, as evidenced by the results of DPPH• ($IC_{50} = 14.28 \pm 1.24$ µg/mL) and

ABTS^{•+} (1.69 ± 0.11 mM) assays, even if the “eco-friendly” extracts exhibited good radical scavenging activity as well (Table 6.7).

Table 6.7 Total phenolic content, DPPH• and ABTS^{•+} radical scavenging activity of the extracts of *P. vera* shells

Sample	Total phenolic content		DPPH•		ABTS ^{•+}	
	GAE ^a	SD ^d	IC ₅₀ ^b	SD ^d	TEAC ^c	SD ^d
Shells MeOH	340.69	± 33.15	14.28	± 1.24	1.69	± 0.11
Shells EtOH	123.09	± 4.74	26.64	± 1.98	1.28	± 0.08
Shells EtOH/H ₂ O	140.13	± 13.97	23.92	± 2.84	1.55	± 0.09
Vit. C			5.16	± 0.11		
Quercetin					1.87	± 0.08

^a Values are expressed as gallic acid equivalents (GAE) mg/g of dried extract. ^b Values are expressed as $\mu\text{g/mL}$. ^c Values are expressed as concentration (mM) of a standard Trolox solution exerting the same antioxidant activity of a 1 mg/mL solution of the tested extract. ^d Standard Deviation of three independent experiments.

6.5 LC-ESI/QTrap/MS/MS quantitative determination of the main anacardic acids by Multiple Reaction Monitoring (MRM) analysis

Due to their occurrence in most of the investigated extracts of *P. vera* cv. *Napoletana* parts, as well as to the growing interest shown by scientific research towards such compounds with promising biological activities, the main identified anacardic acids were quantified by LC-ESI/QTrap/MS/MS experiments working in MRM mode.

At first, a LC-ESI/QTrap/MS/MS method was developed in order to achieve accurate results; in particular, standard solutions of the compounds of interest were initially submitted to ESI/MS and ESI/MS/MS experiments, directly injecting them in the ESI source of the mass spectrometer, and the main transitions observed during the tandem mass experiments were used to optimize the instrument tuning settings (in particular, DP declustering potential, EP entrance potential, CE collision energy, CXP collision cell exit potential) for each analyzed compound, allowing the

development of a selective MRM method, in which for each compound a specific transition precursor/product ion was monitored (Table 6.8).

Table 6.8 Instrument settings used for the quantitative analysis of the main anacardic acids of *P. vera* parts extracts

Compound	[M-H] ⁻	MS/MS	DP	EP	CE	CXP
(11:1)-anacardic acid (25)	289.2	245.1	-68	-9.90	-35	-16
(13:1)-anacardic acid (29)	317.2	273.1	-68	-9.90	-35	-16
(17:3)-anacardic acid (30)	369.2	325.1	-60	-9.90	-35	-16
(13:0)-anacardic acid (31)	319.1	275.1	-68	-9.90	-35	-16
(15:1)-anacardic acid (32)	345.3	301.1	-68	-9.90	-37	-16
(15:0)-anacardic acid (35)	347.2	303.1	-68	-9.90	-36	-16
(17:1)-anacardic acid (36)	373.3	329.1	-68	-9.90	-39	-16

DP Declustering Potential, EP Entrance Potential, CE Collision Energy, CXP Collision Cell Exit Potential

Successively, standard solutions were used to prepare standard mixtures at different concentrations, and analyzed by LC-ESI/MS/MS experiments in order to assess the calibration curves for each compound of interest. The results were expressed as mean of three experiments, and the calibration curves were generated by plotting the peak areas in function of the reported concentrations. Finally, a diluted solution of each extract was analyzed in triplicate by using the same operating conditions.

Aiming at ensuring a correct workflow, the reproducibility of the experiments and of the obtained results, the LC-ESI/QTrap/MS/MS method used for the quantitative analyses was validated according to the European Medicine Agency guidelines (EMA Quality guidelines ICH Q2). In particular, all experiments were performed in triplicate, accuracy was determined by analyzing random standard solutions after calibration curves were assessed, while precision was evaluated by analyzing the same concentration in standard in triplicate, and repeating the experiments in different days. Moreover, a satisfactory linearity was observed in the quantification concentrations range of all analytes, with a correlation coefficient (R^2) between 0.995 and 0.999 (Table 6.9).

Table 6.9 Quantitative data of *P. vera* parts extracts, (MRM, negative ion mode). Seven-point calibration, with seven standards. LOQ (Limit of quantification) and LOD (Limit of detection) expressed in ng/mL

Compound	R ²	Regression line	LOQ (ng/mL)	LOD (ng/mL)
(11:1)-anacardic acid (25)	0.9999	y=864x-210	13.0	1.0
(13:1)-anacardic acid (29)	0.9992	y=452x+25.1	9.0	1.0
(17:3)-anacardic acid (30)	0.9983	y=686x+1800	23.0	3.0
(13:0)-anacardic acid (31)	0.9986	y=3560x+544	15.0	4.0
(15:1)-anacardic acid (32)	0.9952	y=724x+69.1	14.0	1.5
(15:0)-anacardic acid (35)	0.9980	y=12200x+161	19.0	1.0
(17:1)-anacardic acid (36)	0.9971	y=12800x-738	13.5	1.0

The obtained results (Table 6.10) highlighted compounds **25**, **30**, **31**, **32** and **36** as the most abundant anacardic acids. In addition, it was observed that in some extracts of *P. vera* parts it was not possible to assess the concentration of certain compounds, in particular in the MeOH extract of the “non-fruiting year” leaves. On the other hand, all the husks extracts represented the highest concentration of all quantified analytes, mainly MeOH and EtOH extracts. Therefore, it is possible to hypothesize a potential employment of *P. vera* husks as a rich source of anacardic acids.

Table 6.10 Concentration ($\mu\text{g}/\text{mg}$ dried extract) of the main anacardic acids in the extracts of *P. vera* different parts

	AA (11:1)	SD	AA (13:1)	SD	AA (17:3)	SD	AA (13:0)	SD
NFL M	<LoQ	-	<LoQ	-	<LoQ	-	<LoQ	-
NFL E	4.04	± 0.12	1.90	± 0.07	14.06	± 1.02	5.14	± 0.37
NFL EH	2.56	± 0.11	0.86	± 0.04	2.12	± 0.14	1.31	± 0.11
NFL I	<LoQ	-	0.14	± 0.01	1.38	± 0.09	<LoQ	-
NFL D	0.61	± 0.04	0.19	± 0.01	8.48	± 1.11	0.01	± 0.01
FL M	0.87	± 0.09	0.43	± 0.03	4.02	± 0.18	0.58	± 0.07
FL E	5.30	± 0.27	3.04	± 0.14	1.46	± 0.13	6.46	± 0.24
FL EH	2.34	± 0.14	1.13	± 0.07	3.46	± 0.09	1.54	± 0.09
FL I	1.63	± 0.14	0.42	± 0.03	2.44	± 0.07	0.29	± 0.02
FL D	0.69	± 0.05	0.14	± 0.01	<LoQ	-	<LoQ	-
H M	34.02	± 2.13	8.32	± 0.42	15.16	± 1.35	46.05	± 2.41
H E	32.80	± 2.01	7.88	± 0.67	6.36	± 0.41	50.43	± 2.22
H EH	18.90	± 1.36	3.90	± 0.11	13.32	± 1.22	23.01	± 1.04
SH M	1.69	± 0.13	0.28	± 0.04	16.01	± 1.16	0.69	± 0.07
SH E	1.16	± 0.08	0.31	± 0.03	17.10	± 1.31	2.82	± 0.16
SH EH	1.38	± 0.08	0.36	± 0.03	15.50	± 1.23	2.18	± 0.11
	AA (15:1)	SD	AA (15:0)	SD	AA (17:1)	SD		
NFL M	<LoQ	-	<LoQ	-	<LoQ	-		
NFL E	1.28	± 0.08	0.55	± 0.07	3.08	± 0.19		
NFL EH	0.32	± 0.02	0.14	± 0.01	0.83	± 0.12		
NFL I	<LoQ	-	<LoQ	-	<LoQ	-		
NFL D	<LoQ	-	0.04	± 0.01	0.37	± 0.04		
FL M	0.08	± 0.01	0.13	± 0.01	0.73	± 0.08		
FL E	2.42	± 0.14	1.16	± 0.05	5.34	± 0.28		
FL EH	0.37	± 0.04	0.16	± 0.02	0.87	± 0.11		
FL I	0.12	± 0.02	<LoQ	-	0.49	± 0.03		
FL D	<LoQ	-	<LoQ	-	0.25	± 0.02		
H M	36.20	± 2.06	7.62	± 0.21	32.41	± 1.96		
H E	39.61	± 1.89	8.44	± 0.43	35.20	± 1.57		
H EH	19.83	± 1.41	2.90	± 0.18	15.06	± 0.39		
SH M	0.65	± 0.07	0.09	± 0.01	0.74	± 0.07		
SH E	1.78	± 0.11	0.48	± 0.03	2.20	± 0.12		
SH EH	1.98	± 0.16	0.36	± 0.02	2.44	± 0.14		

NFL = "non-fruiting year" leaves; FL = "fruiting year" leaves; H = husks; SH = shells.

M = MeOH; E = EtOH; EH = EtOH:H₂O; I = Infusion; D = Decoction;

AA = Anacardic Acid.

Results expressed as mean of three independent experiments.

Standard Deviation of three independent experiments.

6.6 Conclusions

The phytochemical investigation carried out on different parts of *P. vera*, mainly considered as by-products deriving from pistachio manufacturing processes, pointed out a metabolome mostly constituted by phenolic derivatives. "Eco-friendly" extraction methods resulted effective in extracting such metabolites, in particular, EtOH showed a high class-specific selectivity towards anacardic acids, compounds of great interest in scientific research. Moreover, all the prepared

extracts showed in preliminary colorimetric assays a good phenolic content, as well as a noteworthy radical scavenging activity. Finally, quantitative analyses carried out on all the prepared extracts of the investigated *P. vera* parts pointed out a good content of certain anacardic acids, highlighting the husks as the richest source.

Therefore, the obtained results may contribute to afford an added value to the leaves, husks and shells of *P. vera* cv. *Napoletana*, considered the main collateral biomasses originating from pistachio production workflow, as potential sources of bioactive compounds with a perspective employment in secondary applications.

6.7 Experimental section

Plant material

All the plant parts were provided by “Aromaticilia”, Bronte, Sicily, Italy. Leaves of “non-fruiting year” were collected in August 2016, while leaves of the “fruiting year”, husks and shells were collected in August 2017.

General experimental procedures

Column chromatography was carried out on Sephadex LH-20 (Pharmacia). HPLC-RI separations were performed on instrument described in general experimental procedures, using a Supelco (Bellefonte, PA, USA) Supelcosil LC-18 column (250 x 10 mm, 5 μ m). HPLC-UV/Vis separations were performed on instrument described in general experimental procedures, using a Supelco (Bellefonte, PA, USA) Supelcosil LC-18 column (250 x 10 mm, 5 μ m).

LC-ESI/LTQOrbitrap/MS/MS and LC-ESI/LTQOrbitrap/MS procedures

Qualitative LC-HRMS experiments were performed on instrument reported in general experimental procedures. For LC separation a C18 reversed-phase (RP) column was employed, at a flow rate of 0.2 ml/min. Employed mobile phases were (A) water and (B) acetonitrile, both acidified 0.1% formic acid. Injection volume was 5 μ L, keeping column at room temperature.

The ESI source parameters were set as following: source voltage at 5.0 kV, capillary voltage at -12 V, tube lens offset at -121.47 V, capillary temperature at 280 °C, sheath gas at 30 (arbitrary units) and auxiliary gas at 5 (arbitrary units).

- *LC-ESI/LTQOrbitrap/MS/MS gradient conditions for the leaves extracts.* A Phenomenex (Torrance, CA, USA) Kinetex C-18 column (100 \times 2.10 mm, 2.6 μ m) was used. Elution gradient was: 0 min 10% B, 10 min 40% B, 30

min 70% B, 40 min 100% B, held for 10 min, returning to start conditions in 7 min.

- *LC-ESI/LTQOrbitrap/MS/MS gradient conditions for the husks extracts.* A Waters (Milford, MA, USA) Symmetry C-18 column (150 x 201 mm, 5 μ m) was used. Elution gradient was: 0 min 10% B, 40 min 100% B, held for 10 min, returning to start conditions in 7 min.
- *LC-ESI/LTQOrbitrap/MS/MS gradient conditions for the shells extracts.* A Waters (Milford, MA, USA) Symmetry C-18 column (150 x 201 mm, 5 μ m) was used. Elution gradient was: 0 min 10% B, 30 min 70% B, returning to start conditions in 7 min.

Extraction and purification of the MeOH extract of P. vera leaves, and preparation of “eco-friendly” extracts

1.5 kg of air-dried *P. vera* “non-fruiting year” leaves were extracted with *n*-hexane (3.5 L, three times for three days), chloroform (3.5 L, three times for three days) and MeOH (3.5 L, three times for three days), yielding 36.1 g of crude MeOH extract. *P. vera* “fruiting year” leaves were extracted at the same way, but employing a lower amount of sample (3 g) and solvent (50 mL), yielding 0.12 g of crude MeOH extract. Moreover, the leaves of both years (3 g) were extracted by maceration using as solvent EtOH 96% (50 mL, three times for three days) and an EtOH:H₂O solution (1:1, v/v) (50 mL, three times for three days), yielding 0.12 g and 0.79 g of crude extract, respectively, for the “non-fruiting year” leaves, 0.46 g and 0.91 g of crude extract, respectively, for “fruiting year” leaves. In addition, the leaves were extracted by infusion and decoction as well. Infusion was performed by pouring boiling water (50 mL) to the leaves (3 g), leaving in contact for 15 min and successively filtering, yielding 0.31 g and 0.34 g of crude extract for “non-fruiting year” and “fruiting year” leaves, respectively. For decoction, leaves (3 g) were submerged in cold water (50 mL) and heated till boiling point, keeping boiling

for 15 min, followed by final filtration, allowing to obtain 0.29 g and 0.26 g of crude extract for “non-fruiting year” and “fruiting year” leaves, respectively.

About 3.5 g of crude MeOH extract of the “non-fruiting year” leaves were dissolved in MeOH (8 mL) and fractionated on a Sephadex LH-20 (Pharmacia) column (100 x 5 cm), using MeOH as mobile phase, affording 92 fractions (8 mL each) which were monitored by TLC.

Fractions 7-15 (537.6 mg) were chromatographed by RP-HPLC-UV/Vis (elution gradient: 0 min 10% B, 10 min 40% B, 30 min 70% B, 40 min 100% B, held for 10 min; wavelength was 254 nm) yielding compound **22** (2.1 mg, $R_t = 17.4$ min). Fractions 16-25 (269.8 mg) were chromatographed by RP-HPLC-UV/Vis (elution gradient: 0 min 10% B, 10 min 40% B, 30 min 70% B, 40 min 100% B, held for 10 min; wavelength was 310 nm) yielding compound **11** (2.1 mg, $R_t = 14.3$ min). Fractions 26-33 (198.8 mg) were chromatographed by RP-HPLC-UV/Vis (elution gradient: 0 min 10% B, 5 min 25% B, 20 min 58% B, 32 min 100% B, held for 10 min; wavelength was 254 nm) yielding compound **1** (2.4 mg, $R_t = 13.6$ min). Fractions 34-40 (53.3 mg) were chromatographed by RP-HPLC-UV/Vis (elution gradient: 0 min 10% B, 10 min 40% B, 30 min 70% B, 40 min 100% B, held for 10 min; wavelength was 310 nm) yielding compounds **4** (1.9 mg, $R_t = 11.5$ min), **14** (2.1 mg, $R_t = 15.6$ min), **18** (2.6 mg, $R_t = 17.3$ min) and **19** (2.2 mg, $R_t = 19.9$ min). Fractions 41-51 (58.7 mg) were chromatographed by RP-HPLC-UV/Vis (elution gradient: 0 min 10% B, 10 min 40% B, 30 min 70% B, 40 min 100% B, held for 10 min; wavelength was 310 nm) yielding compounds **8** (2.5 mg, $R_t = 12.8$ min), **10** (2.3 mg, $R_t = 13.2$ min), **12** (2.6 mg, $R_t = 14.2$ min), **13** (2.4 mg, $R_t = 15.9$ min) and **16** (2.0 mg, $R_t = 21.2$ min). Fractions 52-66 (105.2 mg) were chromatographed by RP-HPLC-UV/Vis (elution gradient: 0 min 10% B, 30 min 100% B, held for 10 min; wavelength was 254 nm) yielding compounds **5** (2.6 mg, $R_t = 10.0$ min), **6** (2.4 mg, $R_t = 12.2$ min), **7** (2.0 mg, $R_t = 13.9$ min), **15** (2.8 mg, $R_t = 14.9$ min), **21** (2.5 mg, $R_t = 16.1$) and **23** (2.1 mg, $R_t = 19.4$). Fractions 67-92 (190.6 mg) were

chromatographed by RP-HPLC-UV/Vis (elution gradient: 0 min 10% B, 10 min 40% B, 25 min 70% B, 35 min 100% B, held for 10 min; wavelength was 310 nm) yielding compound **9** (2.7 mg, R_t = 14.1 min).

Extraction and purification of MeOH extract of P. vera husks, and preparation of “eco-friendly” extracts

365.6 g of dried husks were extracted with increasing polarity solvents: *n*-hexane (1.8 L, three times for three days), chloroform (1.8 L, three times for three days) and MeOH (1.8 L, three times for three days), affording 69.1 g of crude MeOH extract. By monitoring the extract profile by TLC, a remarkable amount of sugars was detected. Therefore about 3 g of MeOH extract were submitted to BuOH:H₂O liquid/liquid extraction, yielding 833.0 mg of BuOH extract monitored by TLC, until no more sugars were detected. In addition, husks were extracted by maceration using EtOH 96% and an EtOH:H₂O (1:1, v/v) solution: 100 mL of solvent were poured to 3 g of dried husks, and extracted three times for three days, yielding 386.7 mg of EtOH extract and 1.056 g of EtOH:H₂O extract.

About 3.5 g of crude BuOH extract were dissolved in 8 mL of MeOH and fractionated by size-exclusion chromatography on a Sephadex LH-20 (Pharmacia) column (100 x 5 cm), using MeOH as mobile phase, affording 54 fractions (8 mL each) monitored by TLC.

Fractions 12-16 (464.5 mg) were chromatographed by RP-HPLC-UV/Vis (elution gradient: min 10% B, 30 min 100% B, held for 10 min; wavelength was 290 nm) yielding compounds **39** (2.8 mg, R_t = 9.8 min), **44** (2.9 mg, R_t = 11.9 min), **46** (3.1 mg, R_t = 13.7 min) and **47** (2.9 mg, R_t = 15.5 min). Fractions 17-18 (170.6 mg) were chromatographed by RP-HPLC-UV/Vis (elution gradient: min 10% B, 30 min 100% B, held for 10 min; wavelength was 270 nm) yielding compounds **6** (2.6 mg, R_t = 11.6 min), **8** (2.3 mg, R_t = 15.2 min) and **15** (2.7 mg, R_t = 20.0 min). Fractions 19-23 (91.7 mg) were chromatographed by RP-HPLC-UV/Vis (elution

gradient: min 10% B, 30 min 100% B, held for 10 min; wavelength was 254 nm) yielding compounds **38** (2.9 mg, $R_t = 9.7$ min), **14** (2.8 mg, $R_t = 14.9$ min), **48** (2.4 mg, $R_t = 15.4$ min), **51** (3.1 mg, $R_t = 15.9$ min) and **52** (2.6 mg, $R_t = 17.1$ min). Fractions 24-28 (133.1 mg) were chromatographed by RP-HPLC-UV/Vis (elution gradient: 0 min 10% B, 10 min 40% B, 40 min 70% B, 50 min 100% B, held for 10 min; wavelength was 254 nm) yielding compound **43** (2.7 mg, $R_t = 13.4$ min). Fractions 29-36 (97.7 mg) were chromatographed by RP-HPLC-UV/Vis (elution gradient: min 10% B, 30 min 100% B, held for 10 min; wavelength was 254 nm) yielding compounds **18** (2.3 mg, $R_t = 13.1$ min), **49** (2.6 mg, $R_t = 14.5$ min), **22** (1.9 mg, $R_t = 15.0$ min) and **55** (2.9 mg, $R_t = 19.1$).

The BuOH extract was chromatographed by RP-HPLC-UV/Vis (elution gradient: min 10% B, 30 min 100% B, held for 35 min; wavelength was 254 nm) yielding compounds **25** (2.4 mg, $R_t = 36.9$ min), **29** (2.6 mg, $R_t = 42.0$ min), **30** (1.9 mg, $R_t = 43.1$ min), **32** (3.1 mg, $R_t = 48.2$ min), **31** (3.3 mg, $R_t = 49.3$ min), **36** (3.6 mg, $R_t = 59.5$ min) and **35** (2.5 mg, $R_t = 62.8$ min).

Extraction and purification of the MeOH extract of P. vera shells, and preparation of “eco-friendly” extracts

765.1 g of milled shells were extracted with *n*-hexane (1.8 L, three times for three days), chloroform (1.8 L, three times for three days) and MeOH (1.8 L, three times for three days), yielding 13.5 g of crude MeOH extract. To remove sugars, about 1.0 g of MeOH extract was submitted to BuOH:H₂O liquid/liquid extraction until no more sugars were detected, yielding 357.5 mg of BuOH extract. In addition, the shells were extracted by using EtOH 96% and EtOH:H₂O (1:1, v/v) solution, by pouring 100 mL of extraction solvent to 5 g of milled shells, yielding 5.5 mg and 15.7 mg of crude extracts, respectively.

About 3.0 g of crude BuOH extract were dissolved in 8 mL of MeOH and fractionated by size-exclusion chromatography on a Sephadex LH-20 (Pharmacia)

column (100 x 5 cm), using MeOH as mobile phase, affording 76 fractions (8 ml each) monitored by TLC.

Fractions 10-13 (218.5 mg) were chromatographed by RP-HPLC-RI using MeOH:H₂O (4:6, v/v) as mobile phase (flow rate was 2 mL/min) yielding compound **22** (3.8 mg, R_t = 9.1 min). Fractions 14-18 (96.5 mg) were chromatographed by RP-HPLC-RI using MeOH:H₂O (9:11, v/v) as mobile phase (flow rate was 2 mL/min) yielding compound **16** (3.0 mg, R_t = 12.6 min). Fractions 23-29 (46.3 mg) were chromatographed by RP-HPLC-RI using MeOH:H₂O (9:11, v/v) as mobile phase (flow rate was 2 mL/min) yielding compounds **43** (2.4 mg, R_t = 8.0 min), **4** (2.6 mg, R_t = 11.4 min) and **14** (3.1 mg, R_t = 13.2 min). Fractions 35-45 (70.4 mg) were chromatographed by RP-HPLC-UV/Vis (elution gradient: 0 min 10% B, 30 min 100% B, held for 10 min; wavelength was 270 nm) yielding compound **55** (2.8 mg, R_t = 19.4 min). Fractions 30-34 (72.3 mg) were chromatographed by RP-HPLC-RI using MeOH:H₂O (9:11, v/v) as mobile phase (flow rate was 2 mL/min) yielding compounds **6** (2.1 mg, R_t = 9.8 min) and **8** (2.8 mg, R_t = 12.5 min).

LC-ESI/QTrap/MS/MS quantitative analysis

Instrument used for quantitative analysis is reported in general experimental procedures. For LC separation a Phenomenex (Torrance, CA, USA) Kinetex EVO C-18 column (100 x 2.1 mm, 5 μm) was used. The mobile phases were (A) water-formic acid (99.9:0.1, v/v) and (B) acetonitrile-formic acid (99.9:0.1, v/v). Gradient conditions: 0 min 10% B, 40 min 100% B, held for 10 min, returning to start conditions in 7 min. Source temperature was set at 349°C, column temperature was 40°C, flow rate was 0.2 mL/min and injection volume 2 μL.

Statistical analysis

The statistical analysis was performed by several tests. In order to eliminate uncertain data, the Q-Dixon test was performed. All the values in this work were expressed as mean \pm SD. The statistical analysis was performed with one-way ANOVA for repeated measurements. The statistically significant differences were also assessed by applying the paired Student's t-test.

Total phenolic content

As reported in general experimental procedures.

DPPH• radical scavenging activity

As reported in general experimental procedures.

ABTS^{•+} radical scavenging activity

As reported in general experimental procedures.

NMR analysis

As reported in general experimental procedures.

6.8 References

"Pistachio production in 2016, Crops/Regions/World list/Production Quantity (pick lists)". UN Food and Agriculture Organization, Corporate Statistical Database (FAOSTAT). **2018**.

Abdelwahed, A.; Bouhlel, I.; Skandrani, I.; Valenti, K.; Kadri, M.; Guiraud, P.; Steiman, R.; Mariotte, A.; Ghedira, K.; Laporte, F.; Dijoux-Franca, M.; Chekir-Ghedira, L. Study of antimutagenic and antioxidant activities of gallic acid and

1,2,3,4,6-pentagalloylglucose from *Pistacia lentiscus* confirmation by microarray expression profiling. *Chemico-Biological Interactions*. **2007**, 165, 1–13.

Al Sayed, E.; Martiskainen, O.; Sinkkonen, J.; Pihlaja, K.; Ayoub, N.; Singaba, A. N.; El-Azizia, M. Chemical composition and bioactivity of *Pleiogynium timorense* (Anacardiaceae). *Nat. Prod. Comm.* **2010**, 5, 1-6.

Amer, B.; Ole Juvik, J. O.; Dupont, F., Francis, G. W.; Fossen, T. Novel aminoalkaloids from European mistletoe (*Viscum album* L.). *Phytochem. Lett.* **2012**, 5, 677–681.

Amessis-Ouchemoukh, N.; Abu-Reidah, I. M.; Quirantes-Piné, R., Rodríguez-Pérez, C.; Madani, K.; Fernández-Gutiérrez, A.; Segura-Carretero, A. tentative characterisation of iridoids, phenylethanoid glycosides and flavonoid derivatives from *Globularia alypum* L. (Globulariaceae) leaves by LC-ESI-QTOF-MS. *Phytochem. Anal.* **2014**, 25, 389–398.

Archana, S.; Jayanthi, A. Comparative analysis of antimicrobial activity of leaf extracts from fresh green tea, commercial green tea and black tea on pathogens. *J. App. Pharm. Sci.* **2011**, 1, 149-152.

Bottone, A.; Montoro, P.; Masullo, M.; Pizza, C.; Piacente, S. Metabolomics and antioxidant activity of the leaves of *Prunus dulcis* Mill. (Italian cvs. Toritto and Avola). *J. Pharm. Biom. Anal.* **2018**, 158, 54–65.

Boudiar, T.; Lozano-Sanchez, J.; Harfi, B.; del Mar Contreras-G'mez, M.; Segura-Carretero, A. Phytochemical characterization of bioactive compounds composition of *Rosmarinus eriocalyx* by RP-HPLC-ESI-QTOF-MS. *Nat. Prod. Res.* **2018**, Ahead of Print.

Braca, A.; Politi, M.; Sanogo, R.; Sanou, H.; Morelli, I.; Pizza, C.; De Tommasi, N. Chemical composition and antioxidant activity of phenolic compounds from wild and cultivated *Sclerocarya birrea* (Anacardiaceae) leaves. *J. Agric. Food Chem.* **2003**, 51, 6689-6695.

Cho, J.; Sohn, M.; Lee, J., Kim. W. Isolation and identification of pentagalloylglucose with broad-spectrum antibacterial activity from *Rhus trichocarpa* Miquel. *Food Chem.* **2010**, 123, 501–506.

Cryan, L. M.; Bazinet, L.; Habeshian, K. A.; Cao, S.; Clardy, J.; Christensen, K. A.; Rogers, M. S. 1,2,3,4,6-penta-*O*-galloyl- β -D-glucopyranose (PGG) inhibits angiogenesis via inhibition of CMG2. *J Med Chem.* **2013**, 56, 1940–1945.

Cui, L., Miao, J.; Furuya, T.; Fan, Q., Li, X., Rathod, P. K.; Su, X. Z.; Cui, L. Histone acetyltransferase inhibitor anacardic acid causes changes in global gene expression during in vitro *Plasmodium falciparum* development. *Eukaryotic Cell* **2008**, 7, 1200-1210.

De Souza Santos, C. C.; Masullo, M.; Cerulli, A.; Mari, A.; Dos Santos Estevam, C.; Pizza, C.; Piacente, S. Isolation of antioxidant phenolics from *Schinopsis brasiliensis* based on a preliminary LC-MS profiling. *Phytochemistry* **2017**, 140, 45-51.

Duan, D.; Li, Z.; Luo, H.; Zhang, W.; Chen, L.; Xu, X. Antiviral compounds from traditional chinese medicines *Galla Chinese* as inhibitors of HCV NS3 protease. *Bioorganic & Medicinal Chemistry Letters* **2004**, 14, 6041–6044.

Erşan, S.; Üstündağ, O. G.; Carle, R.; Schweiggert, R. M. Identification of phenolic compounds in red and green pistachio (*Pistacia vera* L.) hulls (Exo- and Mesocarp) by HPLC-DAD-ESI-(HR)-MSⁿ. *J. Agric. Food Chem.* **2016**, 64, 5334–5344.

Foddai, M.; Kasabri, V.; Afifi, F. U.; Azara, E., Petretto, G. L.; Pintore, G. In vitro inhibitory effects of Sardinian *Pistacia lentiscus* L. and *Pistacia terebinthus* L. on metabolic enzymes: Pancreatic lipase, α -amylase, and α -glucosidase. *Starch/Stärke* **2015**, 67, 204–212.

Hamaio, C.; Delgado, O.; Fleuri, L F. Orange and mango by-products: agro-industrial waste as source of bioactive compounds and botanical versus commercial description—A review. *Food Rev. Int.* **2016**, 32, 1–14.

Hanhineva, K.; Rogachev, I.; Aura, A., Aharoni, A., Poutanen, K.; Mykkanen, H. Identification of novel lignans in the whole grain rye bran by non-targeted LC–MS metabolite profiling. *Metabolomics* **2012**, 8, 399–409.

Holloway, A. C.; Mueller-Harvey, I.; Gould, S. W. J.; Fielder, M. D.; Naughton, D. P.; Kelly, A. F. Heat treatment enhances the antimicrobial activity of (+)-Catechin when combined with copper sulphate. *Letters in Applied Microbiology* **2015**, 61, 381-389.

Jia, C.; Zhu, Y.; Zhang, J.; Yang, J.; Xu, C.; Mao, D. Identification of glycoside compounds from tobacco by high performance liquid chromatography/electrospray ionization linear ion-trap tandem mass spectrometry coupled with electrospray ionization orbitrap mass spectrometry. *J. Bras. Chem. Soc.* **2017**, 28, 629-640.

Khalloukia, F.; Breuera, A.; Meriemec, E.; Ulricha, C. M.; Owena, R. W. Characterization and quantitation of the polyphenolic compounds detected in MeOH extracts of *Pistacia atlantica* Desf. fruits from the Guelmim region of Morocco. *J. Pharm. Biom. Anal.* **2017**, 134, 310–318.

Kirollos, F. N.; Elhawary, S. S.; Salama, O. M.; Elkhawas, Y. A. LC-ESI/HRMS/MS and cytotoxic activity of three *Pistacia* species. *Nat Prod Res.* **2018**, 28, 1-4.

Klika, K. D.; Khallouki, F.; Owenc, R. W. Amino phenolics from the fruit of the argan tree *Argania spinosa* (Skeels L.). *Z. Naturforsch.* **2014**, 69, 363-367.

Kubo, I.; Masuoka, N.; Joung, T.; Tsujimoto, H. K. Antioxidant activity of anacardic acids. *Food Chemistry* **2006**, 99, 555-562.

Kubo, I.; Nihei, K.; Kazuo, T. Antibacterial action of anacardic acids against methicillin resistant *Staphylococcus aureus* (MRSA). *J. Agr. Food Chem.* **2004**, 51, 7624-8.

Kumar, K.; Yadav, A. N.; Kumar, V.; et al. Food waste: a potential bioresource for extraction of nutraceuticals and bioactive compounds. *Bioresour. Bioprocess.* **2017**, 4, 18.

Li, L. Z.; Peng, Y.; Niu, C.; Gao, P. Y.; Huang, X. X.; Mao, X. L.; Song, S. J. Isolation of cytotoxic compounds from the seeds of *Crataegus pinnatifida*. *Chin J Nat Med.* **2013**, 11, 411-4.

Locatelli, C.; Filippin-Monteiro, F. B.; Centa, A.; Crezinsky-Pasa, T. B. Antioxidant, antitumoral and antiinflammatory activities of gallic acid. *Handbook on Gallic Acid* **2013**, 215-230.

Lotito, S. B.; Fraga, C. G. (+)-Catechin as antioxidant: mechanisms preventing human plasma oxidation and activity in red wines. *Biofactors.* **1999**, 10, 125-30.

Madikizela, B.; Aderogba, M. A.; Van Staden, J. Isolation and characterization of antimicrobial constituents of *Searsia chirindensis* L. (Anacardiaceae) leaf extracts. *J. Ethnopharm.* **2013**, 150, 609–613.

Moe, M. K.; Jensen, E. Structure elucidation of unsaturated fatty acids after vicinal hydroxylation of the double bonds by negative ion electrospray ionisation low-energy tandem mass spectrometry. *Eur. J. Mass Spectrom.* **2004**, 10, 47–55.

Morais, S. M.; Silva, K. A.; Araujo, H.; Vieira, I. G. P.; Alves, D. R.; Fontenelle, R. O. S.; Silva, A. M. S. Anacardic acid constituents from cashew nut shell liquid: NMR characterization and the effect of unsaturation on its biological activities. *Pharmaceuticals.* **2017**, 10, 31.

Morreel, K.; Dima, O.; Kim, H.; Lu, F.; Niculaes, C.; Vanholme, R.; Dauwe, R.; Goeminne, G.; Inze, D.; Messens, E.; Ralph, J.; Boerjan, W. Mass spectrometry-based sequencing of lignin oligomers. *Plant Physiology.* **2010**, 153, 1464–1478.

Nayeem, N.; Asdaq, S. M. B.; Salem, H.; Alfqy, S. Gallic Acid: A Promising lead molecule for drug development. *J. App. Pharm.* **2016**, 8, 213.

Nicoletti Carvalho, A. N.; Annoni, R.; Lobo Torres, L. H.; Amer, B.; Juvik, O. J.; Dupont, F.; Francis, G. W.; Fossen, T. Novel aminoalkaloids from European mistletoe (*Viscum album* L.). *Phyto. Letters* **2012**, 5, 677–681.

Parasaram, V.; Nosoudi, N.; Chowdhury, A.; Vyavahare, N. Pentagalloyl glucose increases elastin deposition, decreases reactive oxygen species and matrix

metalloproteinase activity in pulmonary fibroblasts under inflammatory conditions. *Biochem Biophys Res Commun.* **2018**,499, 24-29.

Rathi, M. D.; Sousa, D. L.; Lima, R., Oliveira, P., Rodrigues, L.; Duarte, S. Antimicrobial activity of anacardic acid against mature *Streptococcus mutans* biofilm. **2014**, Conference paper.

Razakarivony, A. A.; Lenta, B. N.; Andriamihaja, B.; Michalek, C.; Razanamahefa, B.; Razafimahefa, D. R.; Rakotondramanga, M. F.; Randrianasolo, R.; Lannang, A. M.; Randriamiamisaina, R.; Boyom, F. F.; Rosenthal, P. J.; Sewald, N. Long-chain alkyl-substituted gentisic acid and benzoquinone derivatives from the root of *Micronychia tsiramiramy* (Anacardiaceae). *Z. Naturforsch.* **2016**, 71, 297–303.

Ren, Y.; Himmeldirk, K.; Chen, X. Synthesis and structure–activity relationship study of antidiabetic penta-*O*-galloyl-*D*-glucopyranose and its analogues. *J. Med. Chem.* **2006**, 49, 2829–2837.

Rosenstock, T. S.; Rosa, U. A., Plant, R. E.; Brown, P. H. A reevaluation of alternate bearing in pistachio. *Scientia Horticulturae* **2010**, 124, 149-152.

Santos Durão, A. C. C.; et al. Anacardic acids from cashew nuts ameliorate lung damage induced by exposure to diesel exhaust particles in mice. *Evidence-Based Complementary and Alternative Medicine.* **2013**, 9, 13-25.

Sbardella, G.; Castellano, S.; Vicidomini, C.; Rotili, D.; Nebbioso, A.; Miceli, M.; Altucci, L.; Mai, A. Identification of long chain alkylidenemalonates as novel small molecule modulators of histone acetyltransferases. *Bioorg. Med. Chem. Lett.* **2008**, 18, 2788-92.

Slaghenaufi, D.; Franca, C.; Morac, N., Marchandab, S., Perello, M. C.; deRevel, G. Quantification of three galloylglucoside flavour precursors by liquid chromatography tandem mass spectrometry in brandies aged in oak wood barrels. *J.Chrom. A* **2016**, 1442, 26-32.

Sorrentino, E.; Succi, M.; Tipaldi, L.; Pannella, G.; Maiuro, L.; Sturchio, M.; Coppola, R.; Tremonte, P. Antimicrobial activity of gallic acid against food-related *Pseudomonas* strains and its use as biocontrol tool to improve the shelf life of fresh black truffles. *Int. J. Food Microbio.* **2018**, 266, 183-189.

Sun, Y.; Jiang, X.; Chen, S.; Price, B. D. Inhibition of histone acetyltransferase activity by anacardic acid sensitizes tumor cells to ionizing radiation. *FEBS Letters* **2006**, 580, 4353-4356.

Sung, B.; Pandey, M. K.; Ahn, K S.; Yi, T.; Chaturvedi, M. M.; Liu, M.; Aggarwal, B. B. Anacardic acid (6-nonadecyl salicylic acid), an inhibitor of histone acetyltransferase, suppresses expression of nuclear factor- κ B-regulated gene products involved in cell survival, proliferation, invasion, and inflammation through inhibition of the inhibitory subunit of nuclear factor- κ B α kinase, leading to potentiation of apoptosis. *Blood* **2008**, 111, 4880-4891.

Tang, G.; Zhao, C., Liu, Q.; Feng, X.; Xu, X.; Cao, S.; Meng, X.; Li, S.; Gan, R.; Li, H. Potential of grape wastes as a natural source of bioactive compounds. *Molecules.* **2018**, 23, 2598.

Touré, A.; Kablan, A.; Landry, C.; Kabran, A.; Faustin, A.; Marcelline, K.; et al. Isolation of (+)-catechin and (-)-epicatechin from the leaves of *Amaranthus cruentus* L. (Amaranthaceae). *Int. J. Chem. Studies* **2018**, 6, 3697-3700.

Vitek, R.; de Novais, L. M. R.; Torquato, H. F. V.; Paredes-Gamero, E. J.; de Carvallho, M. G.; de Sousa Jr., P. T.; Jacinto, M. J.; da Silva, V. C. Chemical constituents and antileukemic activity of *Eugenia dysenterica*. *Nat. Prod. Res.* **2017**, 31, 1930–1934.

Wang, T.; Li, Q.; Bi, K. Bioactive flavonoids in medicinal plants: Structure, activity and biological fate. *Asian J. Pharm. Sci.* **2018**, 13, 12-23.

Wang, G.; Cui, N.; Hao, H. Universal method for rapid detection and structure determination of complicated ingredients of traditional Chinese medicine. *Faming Zhuanli Shenqing.* **2009**.

General experimental procedures

Reagents

Extraction and HPLC-grade solvents were purchased by VWR International PBI (Milano, Italy). LC-MS grade water, acetonitrile, MeOH and formic acid were purchased by Merck (Darmstadt, Germany). 2,2-diphenyl-1-picrylhydrazyl (DPPH•), Folin-Ciocalteu reagent, 2,2'-azino-bis(3-ethylbenzothiazoline-6-sulphonic acid) (ABTS), potassium persulfate (K₂S₂O₈), phosphate-buffered saline (PBS) solution, Trolox, MeOH-d₄ 99.95% and gallic acid were purchased by Sigma-Aldrich (Darmstadt, Germany).

Chromatographic method

Analytical Thin Layer Chromatography (TLC) in direct phase was performed with sheets of silica gel laminated on glass 60 F254 of 0.25 mm (Merck). The revelation was carried out both with UV light at 254 and 365 nm and with the following solution: saturated solution of cerium sulphate in 65% sulfuric acid, followed by heating at 100°C for 15 minutes.

For Molecular Exclusion Chromatography a resin of Sephadex LH-20 (25-100 mm Pharmacia) was used, eluting with MeOH at constant flow of 1.2 mL/min. The size of the used column was 100 x 5 cm.

HPLC-RI separations were performed on a Waters 590 (Waters, Milford, MA, USA) system equipped with a Waters R401 refractive index detector and a Rheodyne injector, employing as mobile phase a MeOH:H₂O solution. HPLC-UV/Vis separations were performed on an Agilent Technologies (Santa Clara, CA, USA) 1260 Bin Pump VL system, equipped with a 1260 MWD VL UV-Vis detector, a 1260 μ -Degasser and a Rheodyne injector. Employed mobile phases were (A) water and (B) acetonitrile both acidified 0.1% formic acid, at a flow rate of 2 mL/min and injection volume of 5 μ L.

ESI-HRMS, LC-ESI/HRMS and LC-ESI/HRMS/MS analyses

LC-ESI/HRMS spectra were carried out using a Thermo Scientific Accela HPLC system (Thermo Scientific, San Jose, CA) coupled to a LTQOrbitrap XL mass spectrometer, operating in negative and positive ion mode. The Orbitrap mass analyzer was calibrated according to the manufacturer's directions using a mixture of caffeine, methionine-arginine-phenylalanine-alanine-acetate (MRFA), sodium dodecyl sulfate, sodium taurocholate and Ultramark 1621. Data were collected and analyzed using the software provided by the manufacturer. In full LC-ESI/LTQOrbitrap/MS experiments Total Ion Current (TIC) profile was produced by monitoring the intensity of all the ions produced and acquired in every scan during the chromatographic run. In order to get structural information, Data Dependent experiments were performed. For the data-dependent scan, the first and the second most intense ions from the HRMS scan event were selected, in order to offer their tandem mass (MS^2) product ions with a normalization collision energy at 30%, a minimum signal threshold at 250, and an isolation width at 2.0. The scan was collected in the Orbitrap at a resolution of 30 000 in a m/z range of 150–1600 Da. The m/z of each identified compound was calculated to 4 decimal places and measured with a mass accuracy < 2 ppm.

By using a syringe pump (flow rate 10 μ L/min) each isolated compound was dissolved in a MeOH:H₂O (1:1, v/v) solution and infused in the ESI source. ESI/HRMS/MS analyses were performed using the same conditions described for LC-HRMS/MS analysis.

Quantitative analyses

Quantitative LC-ESI/QTrap/MS/MS analyses were performed in negative ion mode by MRM approach, using a Shimadzu LC30AD UHPLC system (Shimadzu Corporation, Kyoto, Japan) connected to a Shimadzu SIL30AC autosampler with a

Shimadzu CTO20A column oven, coupled to a QTrap 6500 (Sciex, Foster City, CA, USA) mass spectrometer. Before executing the quantification of the compounds of interest, the values of declustering potential (DP), entrance potential (EP), collision energy (CE) and collision cell exit potential (CXP) were optimized for each standard by introducing them directly in the ESI source.

Method validation for quantitative analysis

LC-ESI/QTrap/MS/MS method was validated according to the European Medicines Agency (EMA) guidelines relating to the validation of analytical methods, in particular precision, specificity, linearity, limit of quantification (LOQ) and limit of detection (LOD) were determined. Precision was evaluated at five and seven concentrations for each compound through triplicate intra-day assays and inter-day assays over 3 days. Specificity was defined as the non-interference by other analytes detected in the region of interest. Linearity was evaluated by correlation values of calibration curves. The limit of quantification (LOQ; equivalent to sensitivity), defined as the lowest concentration of analyte that could be quantified with acceptable accuracy and precision, was estimated by injecting a series of increasingly diluted standard solutions until the signal-to-noise ratio was reduced to 10. The limit of detection (LOD) is defined as the concentration of analyte required to give a signal equal to the background (blank) plus three times the standard deviation of the blank.

Reagents for polar lipids and fatty acids analysis

Ultrapure water was obtained by purifying demineralized water in a Direct-Q 3 UV-R system (Merck Millipore, Darmstadt, Germany). LC-MS grade MeOH, acetonitrile, isopropanol, as well as HPLC grade chloroform, formic acid >99%, ammonium formate >95%, and sodium hydroxide >99% were purchased from Carl Roth (Karlsruhe, Germany). Hexakis (2,2-difluoroethoxy) phosphazene, used as

lock mass in the LC-MS/MS and LC-MS experiments, was purchased from Santa Cruz Biotechnology (Dallas, TX, USA). Fatty acids methyl esters standard solution was purchased by Sigma Aldrich (St. Louis, MO, USA). HCl 37 % (v/v), MeOH and *n*-hexane used for free fatty acids analysis, all HPLC grade, were purchased by VWR International GmbH (Darmstadt, Germany).

Polar lipids extraction

The extraction of polar lipids was performed according to the method described by Bligh & Dyer, with slight modifications (Bligh & Dyer, 1959). In brief, 30 g of frozen seeds were ground (140 s, 4000 U/min) with an equal weight of dry ice by employing a Grindomix GM 300 knife mill (Retsch, Haan, Germany). The obtained homogenized powder was freeze-dried. 50 mg of the freeze-dried samples were put into a 1.5 mL eppendorf tube and 0.75 mL of a MeOH:CHCl₃ solution (2:1, v/v) were added. Successively, two steel balls (3 mm diameter) were added and ball milling (1 min, 3 m/s) was executed by using a Bead Ruptor 24 (Biolabproducts, Beverly, Germany) equipped with a 1.5 mL microtube carriage kit. After milling, 0.25 mL of CHCl₃ were added to the samples, vortexed for 1 minute, then 0.5 mL H₂O were added and finally milled again (2 min, 3 m/s). For phase separation, eppendorf tubes were centrifuged at 14700 rpm for 20 minutes. Lower phase was used for the LC-MS analysis, after filtration with Rotilabo PTFE syringe filters, pore diameter 0.45 µm (Carl Roth, Karlsruhe, Germany).

LC-ESI/QToF/MS/MS and LC-ESI/QToF/MS analysis of polar lipids

Spectra were acquired both in negative and in positive ion mode, on a Dionex Ultimate 3000 UHPLC system (Dionex, Idstein, Germany), constituted by a binary pump (UltiMate 3000 RS pump), a degasser (UltiMate 3000 degasser), an autosampler (UltiMate 3000 Autosampler WPS-3000) and a column compartment (UltiMate 3000 Column Compartment TCC-3000), equipped with a RP C-18 (150

x 2.1 mm, 1.7 μm) column (Phenomenex, Aschaffenburg, Germany), coupled to an ultrahigh resolution quadrupole-time-of-flight mass spectrometer with an electrospray ionization source (maXis, Bruker Daltonics, Bremen, Germany). End plate offset was -500 V, capillary voltage was +4500 V in positive ion mode and -4500 V in negative ion mode, nebulizer pressure was set at 4.0 bar, dry gas at 9.0 L/min at a temperature of 200°C. The employed mobile phases were (A) water and (B) acetonitrile:isopropanol (1:3, v/v), both 10 mM ammonium formate for positive ion mode analyses and 10 mM ammonium acetate for negative ion mode analyses; the gradient conditions used for LC separation were as following: 0 min 55% B (held for 2 min), 4 min 75% B, 18 min 100% B (held for 7 minutes), 26 min 55% B (held for 4 min). Flow rate was 0.300 mL/min, injection volume was 4 μL , column was kept at a temperature of 50°C, while the samples were kept at 5°C in the autosampler during the analyses. Experiments were performed in triplicate, with collision energy values of 20, 40 and 60 eV. The calibration of the mass spectrometer was performed externally, using sodium formate clusters with a solution of formic acid:1 M NaOH water solution:isopropanol (0.1:1:100, v/v/v). Moreover, sodium formate (for positive ion mode) and ammonium acetate (for negative ion mode) cluster solutions were automatically injected in the end of each experiment by employing a 6-port divert valve to allow internal mass calibration. An isopropanol Hexakis (2,2-difluoroethoxy) phosphazene solution (1 mg/mL) (Santa Cruz Biotechnology Dallas, TX, USA) was used for lock-mass calibration, which was applied on a support material located in the source; the solution was constantly released by vaporization and hence detected during the experiments. Data were acquired with a spectra rate of 1 Hz and a mass range 80-1300 m/z . MS/MS data were acquired in Data-Depending Scan experiments, selecting the precursor ion as the most intense peak during the LC-MS analyses.

Free fatty acids extraction

For the extraction of free fatty acids, 50 g of freeze-dried seeds were extracted with 200 mL of *n*-hexane, by continuous stirring, three times for three days. Solvent was removed from the extracts by vacuum drying, and successively by gurgling with nitrogen till constant weight.

Fatty acids methyl esters (FAME) synthesis

Prior to GC-FID analysis, free fatty acids were converted into their respective methyl ester derivatives. For this operation, the acid-catalyzed esterification procedure described by Ichihara & Fukubayashi was employed, after suitable modifications (Ichihara & Fukubayashi, 2010). In brief, 150 μ L of oil sample were dissolved in 10 mL of *n*-hexane; of this solution, 1 mL was transferred in a glass tube and 250 μ L of a 2 M HCl MeOH solution were added, followed by the addition of 4 mL of *n*-hexane. The solution was stirred vigorously and kept in the dark for 16 hours. Finally, samples were centrifuged for 30 min at 14700 rpm, and 50 μ L of the supernatant were carefully removed and further dissolved in 950 μ L of *n*-hexane, prior to GC analysis.

GC-FID quali-quantitative analysis of free fatty acids

For the GC analysis, an Agilent 7820A GC System (Agilent Technologies, Santa Clara, CA, USA) was employed, equipped with a DB-624 (30 m x 0.250 mm, 1.40 μ m) column, and a FID detector. Injection volume was 1 μ L, temperature of injection port was set at 250°C with a split ratio 1:10. Nitrogen was used as carrier gas at a flow rate of 2 mL/min. Temperature program was the following: 0 min 100°C (held for 2 min), 12 min 180°C, 16 min 200°C, 20 min 240°C. Detector temperature was set at 250°C. The identification of the Fatty Acids Methyl Esters (FAMES) was performed by comparing their retention time with those of the constituents of a standard mixture.

Quantification was carried out on the basis of GC-FID peak areas using integration data. Results were expressed as percentage amount of total detected free fatty acids. Experiments were performed in triplicate. BHT was used as reference standard, and the observed peaks aligned to it.

Folin-Ciocalteu assay for total phenolic content determination

Folin-Ciocalteu assay was employed to determine the total phenolic content of the extracts (Masullo et al., 2017). In brief, 62.5 μL of a 0.5 mg/mL solution of the extracts were put into an eppendorf tube and then an equal volume of Folin-Ciocalteu reagent was added and stirred vigorously. After 5 min, 125 μL of a 0.1 M solution of Na_2CO_3 and 1 mL of water were added. The samples were stirred vigorously for 10 seconds and incubated in the dark at room temperature for 2 hours. Incubated samples were finally centrifuged at 13400 rpm for 90 seconds and the supernatant was transferred into 1 mL cuvettes and the absorbance was measured at 760 nm using a Thermo Scientific Evolution 201 UV-Visible Spectrophotometer (Thermo Scientific, Germany). A blank was prepared using MeOH instead of the extract. Gallic acid was used as standard reference. For the calibration curve, 5, 10, 20, 30, 40, 50 $\mu\text{g/mL}$ solutions of gallic acid were prepared and submitted to the assay following the same procedure used for the extracts. The calibration curve equation for gallic acid was $y = 0.0054x + 0.0201$ ($R^2 = 0.996$). All the experiments were performed in triplicate and results expressed as mean of Gallic Acid Equivalents (GAE, mg/g dried extract).

DPPH• assay for radical scavenging activity evaluation

Radical scavenging activity of the extracts was evaluated by DPPH• assay (Masullo et al., 2017). In brief, DPPH• solution was prepared by dissolving 3.6 mg of solid DPPH• in 100 mL of MeOH, and further diluting till an absorbance value of 0.900 ± 0.020 , measured at 517 nm. Stock solutions (1 mg/mL) of the of the

extracts were used to prepare six different concentrations: 5, 10, 25, 50, 75, 100, 150 $\mu\text{g/mL}$; of each solution, 0.5 mL were put into an eppendorf tube and 0.5 mL of a 0.1 mM MeOH DPPH \cdot solution were added. The samples were stirred vigorously for 10 seconds and kept in the dark for 30 min, they were then transferred into a 1 mL cuvette and the absorbance was measured at 517 nm using a Thermo Scientific Evolution 201 UV-Visible Spectrophotometer (Thermo Scientific, Germany). A control solution was prepared replacing the tested extracts with MeOH. Vitamin C was used for results comparison. The percentage of DPPH \cdot radical scavenging activity of the extracts was calculated as:

$$\text{DPPH}\cdot \text{ free radical scavenging activity (I\%)} = [(A_0 - A) / A_0] \times 100$$

Where A_0 is the absorbance of the control solution, and A is the absorbance of the DPPH \cdot solution containing the extract. The percentage of DPPH \cdot radical scavenging activity (%) was plotted against the extract concentration ($\mu\text{g/mL}$) to determine the IC_{50} . All the experiments were performed in triplicate.

ABTS $^{\cdot}$ assay for radical scavenging activity evaluation*

ABTS $^{*\cdot}$ assay was further carried out to test the radical scavenging activity of the extracts (Kirmizibekmez et al., 2012). The ABTS $^{*\cdot}$ radical solution was prepared by mixing 50 mL of a 2 mM ABTS solution with 0.2 mL of a 70 mM potassium persulfate solution. The obtained mixture was stored in the dark at room temperature for 16 hours, then diluted with a phosphate-buffered saline (PBS) solution (pH = 7.4) to an absorbance of 0.700 ± 0.020 measured at 734 nm.

To evaluate the radical scavenging activity, 20 μL of different concentrations of the extracts (250, 500, 750, 1000 $\mu\text{g/mL}$) were added to 1 mL of ABTS $^{*\cdot}$ radical solution, stirred, and incubated in the dark at room temperature for 6 min. The absorbance was then measured at 734 nm by employing a Thermo Scientific Evolution 201 UV-Visible Spectrophotometer (Thermo Scientific, Germany). A negative control was prepared by using MeOH instead of the extract. Trolox was

used as reference standard (0.3, 0.5, 1.0, 1.5 mM). Quercetin was used for results comparison. The TEAC value is defined as the concentration (mM) of a standard Trolox solution exerting the same antioxidant activity of a 1 mg/mL extract solution. Each determination was performed in triplicate.

NMR analysis

NMR experiments were performed on a Bruker DRX-600 spectrometer (Bruker BioSpin GmbH, Rheinstetten, Germany) equipped with a Bruker 5 mm TCI CryoProbe at 300 K. All 2D NMR spectra were acquired in MeOH-d₄, and standard pulse sequences and phase cycling were used for COSY, HSQC, and HMBC spectra. The NMR data were processed using Topspin 3.2 software.

References

- Bligh, E. G.; Dyer, W. J. A rapid method of total lipid extraction and purification. *Canad. J. Biochem. Phys.* **1959**, 37, 911-917.
- Ichihara, K.; Fukubayashi, Y. Preparation of fatty acid methyl esters for gas-liquid chromatography. *J. Lipid Res.* **2010**, 51, 635–640.
- Kirmizibekmez, H.; Ariburnu, E.; Masullo, M.; Festa, M.; Capasso, A.; Yesilada, E.; Piacente, S. Iridoid, phenylethanoid and flavonoid glycosides from *Sideritis trojana*. *Fitoterapia*. **2012**, 83, 130–136.
- Masullo, M.; Cerulli, A.; Mari, A.; de Souza Santos, C. C.; Pizza, C.; Piacente, S. LC–MS profiling highlights hazelnut (Nocciola di Giffoni PGI) shells as a byproduct rich in antioxidant phenolics. *Food Res. Int.* **2017**, 101, 180–187.

Conclusion

The main target of the present study was the definition of the chemical profile of selected Southern Italy typical agricultural productions and related by-products (*O. ficus indica* cv. Sulfarina, *F. carica* cv. Dottato, *P. dulcis* cvs. Filippo Cea, Fascionello, Pizzuta, Romana, *P. vera* cv. Napoletana), with the aim to clarify their metabolome and to highlight the occurrence of phytochemicals with health benefits.

The flowers of *O. ficus indica* cv. Sulfarina, deriving from the “scozzolatura” process, proved to be a good source of antioxidant phenolics, mainly phenylbutirric acids and glycosylated flavonoids, isolated and characterized by NMR analyses, and quantified by LC-ESI/QTrap/MS/MS experiments.

With the aim to investigate the metabolite profile of the leaves of *F. carica* cv. Dottato, a phytochemical investigation was carried out. As result, several classes of coumarins, along with C- and O-glycosylated flavonoids, were identified. Moreover, “eco-friendly” extraction methods resulted quite effective in extracting antioxidant phenolics, supporting the employment of common fig leaves as a source of bioactives.

The leaves, husks and shells of *P. dulcis* cvs. Filippo Cea, Fascionello, Pizzuta and Romana were submitted to phytochemical investigation, highlighting the occurrence of several classes of secondary metabolites, like minor phenolic acids derivatives, flavonoids, both glycosylated and aglycones, different classes of terpenes, along with lignans and neolignans. In addition, “green” solvents exhibited selectivity towards certain classes of compounds, returning extracts with a good radical scavenging activity.

Furthermore, the polar fraction of *P. dulcis* seeds was investigated, as well as the main by-products deriving from peeling processes (removed skins and blanching water), pointing out the occurrence of cyanogenic glycosides in the seeds, while integuments and blanching water resulted a rich source of antioxidant phenolics,

specially proanthocyanidins and glycosylated flavonoids. Moreover, clear differences were observed among the metabolite profiles of Apulian and Sicilian cultivars, suggesting the influence of different growing conditions on the metabolome of a plant species.

The extensive phytochemical investigation carried out on the leaves, husks and shells of *P. vera* cv. *Napoletana* evidenced a phenolics-based metabolome of the main by-products of pistachio manufacturing, with gallic acid derivatives and flavonoids as main constituents, along with anacardic acids effectively and selectively extracted by ethanol, as confirmed by the LC-ESI/QTrap/MS/MS quantitative analyses. In addition, noteworthy phenolic content and radical scavenging activity were observed for all the prepared extracts.

The LC-HRMS/MS-based metabolite profiling carried out on the polar fraction of *P. vera* cv. *Napoletana* seeds highlighted the occurrence of antioxidant constituents, chemically related to the phenolics identified in the non-edible parts.

During the PhD stage spent at the University of Hamburg, the non-polar fraction of almonds and pistachios was investigated. Several phospholipids classes, varying for head groups, side chains length and unsaturation degree, along with diacylglycerols and triacylglycerols, were assessed by LC-ESI/QToF/MS/MS analyses, while GC-FID experiments allowed quali-quantitative determinations of the main free fatty acids.

The achieved results may contribute to afford an added value to discarded and underestimated biomasses deriving from agrifood processes, which demonstrated to represent a rich source of bioactives, suggesting perspective applications for secondary uses, like their employment in cosmetics and nutraceuticals. In addition, we furtherly supported the claim of beneficial effects on human health deriving from a daily moderate almond or pistachio nuts intake. Finally, the present work highlighted LC-HRMS as a powerful analytical technique for a quick and informative preliminary metabolite profiling of plant matrices, even if NMR

spectroscopy still results essential to achieve an exhaustive and complete metabolome definition of plant species.

Publications

Bottone, A.; Masullo, M.; Montoro, P.; Pizza, C.; Piacente, S. HR-LC-ESI-Orbitrap-MS based metabolite profiling of *Prunus dulcis* Mill. (Italian cultivars Toritto and Avola) husks and evaluation of antioxidant activity. *Phytochemical Analysis*, **2019**, 1–9.

Bottone, A.; Montoro, P.; Masullo, M.; Pizza, C.; Piacente, S. Metabolomics and antioxidant activity of the leaves of *Prunus dulcis* Mill. (Italian cvs. Toritto and Avola). *Journal of Pharmaceutical and Biomedical Analysis*, **2018**, 158, 54–65.

Kılınç, H.; Masullo, M.; **Bottone, A.**; Karayıldırım, T.; Alankuş, O.; Piacente, S. Chemical constituents of *Silene montbretiana*. *Natural Product Research*, **2018**.

Shakeri, A.; Masullo, M.; **Bottone, A.**; Asili, J.; Emami, S. A.; Piacente, S.; Iranshahi, M. Sesquiterpene lactones from *Centaurea rhizantha* C.A. Meyer. *Natural Product Research*, **2018**.

Masullo, M.; Mari, A.; Cerulli, A.; **Bottone, A.**; Kontek, B.; Olas, B.; Pizza, C.; Piacente, S. Quali-quantitative analysis of the phenolic fraction of the flowers of *Corylus avellana*, source of the Italian PGI product “Nocciola di Giffoni”: Isolation of antioxidant diarylheptanoids. *Phytochemistry*, **2016**, 130, 273–281.

